

# **Deciphering the impact of *Ruminococcus gnavus* cell surface glycosylation at the mucosal interface**

**Victor Laplanche**

A thesis submitted for the degree of Doctor of Philosophy (PhD)  
To the University of East Anglia

Quadram Institute Bioscience  
Gut Microbes and Health  
Norwich Research Park  
Norwich  
NR4 7UQ  
United Kingdom

June 2023

This copy of the thesis has been supplied on condition that anyone who consults it is understood to recognise that its copyright rests with the author and that use of any information derived therefrom must be in accordance with current UK Copyright Law. In addition, any quotation or extract must include full attribution.

## Abstract

The gut microbiota plays a major role in human health and an alteration in gut microbiota structure and function has been implicated in several diseases. *Ruminococcus gnavus* is an important member of the 'normal' gut microbiota and over-represented in inflammatory bowel disease. There is therefore great interest in understanding the mechanisms underpinning its interaction and communication with the host. Here we investigated the role of cell surface glycosylation in the capacity of *R. gnavus* strains to influence host response. We first developed a flow cytometry assay to screen cell surface glycosylation of *R. gnavus* E1, ATCC 29149 and ATCC 35193 strains using a range of fluorescently labelled lectins. The lectin binding profile differed between strains and depending on the carbohydrate source in the growth medium, suggesting strain-specific differences in carbohydrate epitopes on the cell surface. These were supported by bioinformatic analyses revealing differences in *R. gnavus* biosynthetic clusters for glucorhamnan and capsular polysaccharides. To validate these findings, the polysaccharides present on *R. gnavus* E1 and ATCC 35913 strains cell surface were structurally characterised by NMR and mass spectrometry, revealing a backbone composed of four  $\alpha$ -(1,2)- and  $\alpha$ -(1,3)-linked rhamnose and sidechains composed of one  $\beta$ -(1,2)-linked glucose, which differed from the previously reported structure of ATCC 29149 glucorhamnan. We next investigated how *R. gnavus* strains and their associated glucorhamnans influenced gut barrier function and host immune response *in vitro*. The data showed that *R. gnavus* ATCC 35913 was the most immunogenic strain using both epithelium and immune cell models. While the epithelium integrity remains unchanged, the purified glucorhamnans affected the production of cytokines by mBMDCs and triggered the activation of NF- $\kappa$ B pathway in reporter cells. The cytokine profile was strain-specific and varied depending on the glucorhamnan composition. Collectively these data showed that *R. gnavus* induces pro or anti-inflammatory responses in a strain-dependent manner, and underscores the importance of investigating the role of gut microbes at the strain level. This knowledge may be used to inform the development of diagnostic or therapeutics in *R. gnavus*-associated diseases.

## **Access Condition and Agreement**

Each deposit in UEA Digital Repository is protected by copyright and other intellectual property rights, and duplication or sale of all or part of any of the Data Collections is not permitted, except that material may be duplicated by you for your research use or for educational purposes in electronic or print form. You must obtain permission from the copyright holder, usually the author, for any other use. Exceptions only apply where a deposit may be explicitly provided under a stated licence, such as a Creative Commons licence or Open Government licence.

Electronic or print copies may not be offered, whether for sale or otherwise to anyone, unless explicitly stated under a Creative Commons or Open Government license. Unauthorised reproduction, editing or reformatting for resale purposes is explicitly prohibited (except where approved by the copyright holder themselves) and UEA reserves the right to take immediate 'take down' action on behalf of the copyright and/or rights holder if this Access condition of the UEA Digital Repository is breached. Any material in this database has been supplied on the understanding that it is copyright material and that no quotation from the material may be published without proper acknowledgement.

## Acknowledgement

This project is part of the Sweet Crosstalk Innovative Training Network, financed by the Marie Skłodowska-Curie Actions within the European Framework Horizon 2020 ([sweetcrosstalk.eu/](http://sweetcrosstalk.eu/)). This work is also supported by the BBSRC Institute Strategic Programme Gut Microbes and Health BB/R012490/1.

I would like to thank Dr. Michelle Kilcoyne and Dr. Maria Traka for accepting to be the examiners of my thesis and to discuss it.

I would then like to thank Prof. Nathalie Juge for accepting me in her team, and for the help and guidance through my PhD with such a great scientific expertise, allowing me to produce the work presented in this thesis. I am grateful to have had, in addition, a particularly supportive supervisory committee, composed of Dr. Stephanie Schüller, Dr. Tanja Šuligoj, Dr. Emmanuelle Crost, Dr. Dimitrios Latousakis and Dr. Andrew Bell, who gave me guidance and training during my PhD.

During my project, I had the opportunity to work with several scientist of the QIB staff and students who helped me with their knowledge and know-how that enabled me to work in the best conditions to reach my goals during this project. I would like to thank especially Dr. Dimitra Lamprinaki for her help with flow cytometry handling, Dr. Yemane Tedros for his share on his expertise with eukaryotic cells, Dr. Sally Dreger for her help with the production of immune cells, Dr. Connor McGrath and Dr. Stephanie Schüller for the support they provided concerning cytokine analysis and epithelial cell work and George Saava for his expertise and advises with statistical analysis. Then, I would like to give courtesy to Dr. Kathryn Gotts, Dr. Catherine Booth and Dr. Tanja Šuligoj for providing the great images used in this thesis.

I am particularly grateful for having worked with external collaborators of the University of Naples, in Italy, Prof. Cristina De Castro, Ms Samantha Armiento, Dr. Anna Notaro and Dr. Immacolata Speciale, and I would like to thank them for welcoming and supervising me during my placement in their team and for caring the structural analysis associated with this project.

It also has been an honour to work in collaboration with the different members of the Sweet Crosstalk International Training Network, which provided us great trainings and organised wonderful meetings where we have been able to learn more and allowed us to have opened point of view about the glycoscience field thanks to other ITN members.

## Table of Contents

|   |    |
|---|----|
| Abstract.....   | 1  |
| Acknowledgement .....                                 | 2  |
| List of abbreviation .....                            | 7  |
| List of figures.....                                  | 11 |
| List of tables .....                                  | 13 |
| List of supplementary data .....                      | 14 |
| Chapter 1: Introduction .....                         | 15 |
| 1.1. The human gastrointestinal (GI) tract.....       | 16 |
| 1.1.1. Organisation and function .....                | 16 |
| 1.1.2. The intestinal mucus layer.....                | 18 |
| 1.2. The gut microbiota .....                         | 25 |
| 1.2.1. Structure and function .....                   | 25 |
| 1.2.2. Role in health and disease.....                | 27 |
| 1.2.3. The cell surface of gut microbes.....          | 29 |
| 1.3. The mucosal interface .....                      | 32 |
| 1.3.1. The intestinal epithelium.....                 | 32 |
| 1.3.2. Tolerogenic signalling pathway .....           | 37 |
| 1.3.3. The intestinal mucosal immune system .....     | 38 |
| 1.4. Bacterial cell surface polysaccharides.....      | 46 |
| 1.4.1. Structure and biosynthesis .....               | 46 |
| 1.4.2. Effect on gut homeostasis and immunity.....    | 51 |
| 1.5. <i>Ruminococcus gnavus</i> .....                 | 51 |
| 1.5.1. Role in health and disease .....               | 51 |
| 1.5.2. <i>R. gnavus</i> factors of colonisation ..... | 53 |
| 1.5.3. Cell surface carbohydrate composition.....     | 54 |
| 1.6. Aim and Objectives .....                         | 58 |
| 2.1. Bacterial growth assays.....                     | 60 |
| 2.1.1. Bacterial strains and growth conditions.....   | 60 |
| 2.1.2. Transmission electronic microscopy (TEM).....  | 61 |

|   |    |
|---|----|
| 2.1.3. Quality control of <i>R. gnavus</i> glycerol stocks .....                          | 61 |
| 2.1.4. Bacteria quantification by qPCR .....  | 62 |
| 2.2. <i>R. gnavus</i> gene transcription analysis .....                                   | 63 |
| 2.2.1. RNA extraction and cDNA production .....   | 63 |
| 2.2.2. Quantitative PCR analysis (qPCR) .....   | 64 |
| 2.3. Lectin binding screening by flow cytometry .....                                     | 65 |
| 2.4. Structural analysis of <i>R. gnavus</i> cell surface polysaccharide .....            | 66 |
| 2.4.1. Cell preparation .....   | 66 |
| 2.4.2. Polysaccharide extraction.....   | 67 |
| 2.4.3. Monosaccharide structure and configuration analysis .....                          | 70 |
| 2.4.4. Gas chromatography-Mass spectrometry (GC-MS) .....                                 | 71 |
| 2.4.5. Nuclear Magnetic Resonance (NMR) analysis.....                                     | 71 |
| 2.4.6. High-Performance Liquid Chromatography (HPLC) analysis .....                       | 72 |
| 2.5. Reporter cell assays.....  | 72 |
| 2.5.1. C-type lectin reporter cells .....   | 72 |
| 2.5.2. NF- $\kappa$ B reporter cells .....  | 74 |
| 2.6. Mammalian cell assays.....   | 74 |
| 2.6.1. Culture of intestinal epithelial cell models.....                                  | 74 |
| 2.6.2. Generation and culture of mBMDCs .....   | 75 |
| 2.6.3. Stimulation of mammalian cells with <i>R. gnavus</i> strains or glucorhamnan ..... | 76 |
| 2.7. Gene expression analysis .....   | 78 |
| 2.8. Protein analysis .....   | 80 |
| 2.8.1. Protein extraction.....  | 80 |
| 2.8.2. Western blot analysis .....  | 80 |
| 2.8.3. Enzyme-linked immunosorbent assay (ELISA).....                                     | 81 |
| 2.10. <i>In silico</i> analysis .....   | 84 |
| 2.11. Statistics .....  | 84 |
| 3.1. Introduction.....  | 86 |
| 3.2. Results .....  | 87 |
| 3.2.1. <i>In vitro</i> screening by flow cytometry.....                                   | 87 |

|  |     |
|--|-----|
| 3.2.2. Bioinformatics analysis .....   | 96  |
| 3.2.3. Structural characterisation of <i>R. gnavus</i> cell surface polysaccharide.....                            | 101 |
| 3.2.4. <i>R. gnavus</i> gene transcription analysis of GTs from glucorhamnan and <i>cps</i> clusters .....         | 109 |
| 3.3. Discussion.....   | 112 |
| 4.1. Introduction.....   | 117 |
| 4.2. Results .....   | 118 |
| 4.2.2. Effect of <i>R. gnavus</i> strains and glucorhamnans on gut barrier integrity .....                         | 118 |
| 4.2.1. Effect of <i>R. gnavus</i> strains and glucorhamnans on cytokine secretion.....                             | 123 |
| 4.3. Discussion .....  | 131 |
| 5.1. Introduction.....   | 135 |
| 5.2. Results .....   | 136 |
| 5.2.1. Effect of <i>R. gnavus</i> and glucorhamnan on cytokine production in mBMDCs .....                          | 136 |
| 5.2.2. Role of NF- $\kappa$ B activation pathway in the interaction between <i>R. gnavus</i> and immune cells..... | 140 |
| 5.2.3. Role of CLRs in the interaction between <i>R. gnavus</i> and immune cells .....                             | 142 |
| 5.3. Discussion.....   | 144 |
| References .....   | 158 |
| Supplementary data.....  | 196 |

## List of abbreviation

|         |   |
|---------|---|
| 2'FL    | 2'-fucosyllactose   |
| 3'FL    | 3'-fucosyllactose   |
| 3'SL    | 3'-sialyllactose  |
| AMG     | Acetylated methyl glycoside   |
| AMP     | Antimicrobial peptide   |
| ANOVA   | Analysis of Variance  |
| AOG     | Acetylated octyl glycoside  |
| APC     | Antigen-presenting cell   |
| ASC     | Apoptosis-associated speck-like protein containing a CARD           |
| AWERB   | Animal Welfare and Ethical Review Body                              |
| BHI-YH  | Brain heart infusion broth-yeast extract-haemin                     |
| BLAST   | Basic Local Alignment Search Tool                                   |
| BMDC    | Bone marrow-derived dendritic cells                                 |
| CARD    | Caspase recruitment domain  |
| CCR     | CC chemokine receptor   |
| CD      | Cluster of differentiation  |
| CLN     | Claudin   |
| CLR     | C-type lectin receptor  |
| ConA    | Concanavalin A  |
| COSY    | Correlated Spectroscopy   |
| CPRG    | Chlorophenol-red $\beta$ -D-galactopyranoside                       |
| CPS     | Capsular polysaccharide   |
| CRD     | Carbohydrate recognition domain                                     |
| Ct      | Threshold cycle   |
| CXCR    | CXC chemokine receptor  |
| DC      | Dendritic cell  |
| DC-SIGN | DC-specific intercellular adhesion molecule-3-grabbing non-integrin |
| Dectin  | Dendritic-cell-associated C-type lectin                             |
| DFL     | Difucosyllactose  |
| DMEM    | Dulbecco's Modified Eagle Medium                                    |
| DSS     | Dextran sulfate solution  |
| DTT     | Dithiothreitol  |
| ECACC   | European Collection of Authenticated Cell Cultures                  |
| EcN     | <i>Escherichia coli</i> Nissle 1917                                 |
| ELISA   | Enzyme-linked immunosorbent assay                                   |
| EPEC    | Enteropathogenic <i>Escherichia coli</i>                            |
| EPS     | Extracellular polysaccharides                                       |
| ERK     | Extracellular signal-related kinase                                 |
| Foxp3   | Forkhead box P3   |

|        |  |
|--------|--|
| FSC    | Forward scatter                                      |
| Gal    | Galactose  |
| GalA   | Galacturonic acid                                    |
| GalNAc | <i>N</i> -Acetylgalactosamine                        |
| GAPDH  | Glyceraldehyde-3-phosphate dehydrogenase             |
| GC-MS  | Gas chromatography-Mass spectrometry                 |
| GH     | Glycoside hydrolase                                  |
| GI     | Gastrointestinal                                     |
| GlcNAc | <i>N</i> -Acetylglucosamine                          |
| GNL    | <i>Galanthus nivalis</i> lectin                      |
| GRF    | Growth hormone-releasing factor                      |
| GSLI   | <i>Griffonia simplicifolia</i> lectin I isolectin B4 |
| GT     | Glycosyltransferase                                  |
| HePS   | Heteropolysaccharides                                |
| HMBC   | Heteronuclear Multiple Bond Correlation              |
| HoPS   | Homopolysaccharides                                  |
| HPLC   | High-Performance Liquid Chromatography               |
| HSQC   | Heteronuclear Single Quantum Coherence               |
| IBD    | Inflammatory bowel disease                           |
| IBS    | Irritable bowel syndrome                             |
| IEC    | Immune effector cell                                 |
| IEL    | Intraepithelial lymphocyte                           |
| IFN    | Interferon   |
| Ig     | Immunoglobulin                                       |
| IL     | Interleukin  |
| IRF    | Interferon regulatory factor                         |
| ITAM   | Immunoreceptor tyrosine-based activation motif       |
| JAM    | Junctional adhesion molecule                         |
| Lac    | Lactose  |
| LCA    | <i>Lens culinaris</i> agglutinin                     |
| LDS    | lithium dodecyl sulfate                              |
| LPL    | Lamina propria leukocyte                             |
| LPS    | Lipopolysaccharide                                   |
| LTL    | <i>Lotus tetragonolobus</i> lectin                   |
| MALT   | Mucosa-associated lymphoid tissue                    |
| MAMP   | Microbe-associated molecular pattern                 |
| MD-2   | Myeloid differentiation factor 2                     |
| Mel    | Melibiose  |
| MFI    | Mean fluorescence intensity                          |
| MHC    | Major histocompatibility complex                     |
| MIF    | Macrophage Migration Inhibitory Factor               |

|                |   |
|----------------|---|
| MPLA           | Monophosphoryl lipid A  |
| MurNAc         | <i>N</i> -acetylmuramic acid  |
| MYD88          | Myeloid differentiation primary response 88                               |
| Neu5Ac         | Sialic acid   |
| NFAT           | Nuclear factor of activated T-cells                                       |
| NF- $\kappa$ B | Nuclear Factor kappa B  |
| NLR            | NOD-like receptor   |
| NLRP3          | NOD-, LRR- and pyrin domain-containing protein 3                          |
| NMR            | Nuclear Magnetic Resonance  |
| NOD            | Nucleotide-binding and oligomerization domain                             |
| NOESY          | Nuclear Overhauser Effect Spectroscopy                                    |
| PAMP           | Pathogen-associated molecular pattern                                     |
| PBS            | Phosphate-buffered saline   |
| PCR            | Polymerase Chain Reaction   |
| PG             | Peptidoglycan   |
| PKC            | Protein kinase C  |
| PPMA           | Partially methylated acetylated alditol                                   |
| PRR            | Pattern recognition receptor  |
| PS             | Polysaccharide  |
| qPCR           | Quantitative Polymerase Chain Reaction                                    |
| Raf            | Raffinose   |
| RCAI           | <i>Ricinus communis</i> agglutinin I                                      |
| Reg3 $\gamma$  | Regenerating islet-derived protein 3 $\gamma$                             |
| ROR $\gamma$   | RAR-related orphan receptor gamma   |
| ROS            | Reactive oxygen specie  |
| RPS13          | Ribosomal Protein S13   |
| SCFA           | Short chain fatty acid  |
| Sig            | Secretory immunoglobulin  |
| SIGN-R1        | Specific intercellular adhesion molecule-3-grabbing nonintegrin-related 1 |
| SLP            | Surface layer protein   |
| SNA            | <i>Sambucus nigra</i> lectin  |
| SSC            | Side scatter  |
| Suc            | Sucrose   |
| Syk            | Spleen tyrosine kinase  |
| TEER           | Trans-epithelial electrical resistance                                    |
| TEM            | Transmission electronic microscopy  |
| TGF- $\beta$   | Transforming growth factor beta   |
| TLR            | Toll-like receptor  |
| TMB            | 3,3',5,5'-Tetramethylbenzidine  |
| TNF- $\alpha$  | Tumor necrosis factor alpha   |
| TOCSY          | Total Correlation Spectroscopy  |

|      |  |
|------|--|
| TRIF | TIR-domain-containing adapter-inducing interferon- $\beta$ |
| UEAI | <i>Ulex europaeus</i> agglutinin I                         |
| ZO   | Zonula occludens   |

## List of figures

|   |     |
|---|-----|
| Figure 1: The GI tract anatomy in human.....  | 17  |
| Figure 2: The mucus protection in small intestine and colon.....  | 20  |
| Figure 3: Representation of gut mucus both inner layer and outer layer thickness along the GI tract. ....   | 22  |
| Figure 4: Microbiota bacterial distribution through the GI tract. ....  | 26  |
| Figure 5: General representation of Gram-positive and Gram-negative cell wall composition. ....   | 31  |
| Figure 6: Intestinal tight junction proteins.....   | 34  |
| Figure 7: Schematic of potential differentiation repertoire in T helper cells (Th cells). ....  | 39  |
| Figure 8: TLRs in human immunity. ....  | 41  |
| Figure 9: Examples of PRRs on immune cells. ....  | 44  |
| Figure 10: <i>R. gnavus</i> ATCC 29149 cell surface glucorhamnan. ....  | 55  |
| Figure 11: <i>R. gnavus</i> ATCC 29149 <i>cps</i> biosynthesis cluster.....   | 56  |
| Figure 12: Polysaccharide extraction of <i>R. gnavus</i> ATCC 35913 strain. ....  | 69  |
| Figure 13: Schematic representation of Lac operon activation via recognition of the ligand by C-type lectin receptor (CLR) through the carbohydrate recognition domain (CRD)..... | 73  |
| Figure 14: Effect of <i>R. gnavus</i> strains and glucorhamnan on cytokine production by BMDCs. ....  | 77  |
| Figure 15: <i>R. gnavus</i> strains grown with Glc, Fuc, 3'FL and GlcNAc lectin binding with ConA. ....   | 89  |
| Figure 16: <i>R. gnavus</i> strains grown with Glc, Raf, Lac, 2'FL and BHI-YH lectin binding with RCAI.....   | 90  |
| Figure 17: <i>R. gnavus</i> strains grown with Glc, Fuc, 3'FL and 2'FL lectin binding with GSLI. ..   | 91  |
| Figure 18: Effect of carbohydrate source used to grow <i>R. gnavus</i> strains on binding with different lectins. ....  | 93  |
| Figure 19: Summary of <i>R. gnavus</i> lectin binding screening by flow cytometry.....  | 95  |
| Figure 20: <i>R. gnavus</i> ATCC 29149 cell surface glucorhamnan ....   | 96  |
| Figure 21: Bioinformatic analysis of glucorhamnan clusters.....   | 97  |
| Figure 22: <i>R. gnavus</i> ATCC 29149 <i>cps</i> biosynthetic gene cluster. ....   | 100 |
| Figure 23: Transmission electronic microscopy (TEM) of <i>R. gnavus</i> strains. ....   | 101 |
| Figure 24: GC-MS analysis of the pellet fraction and the aqueous phase of <i>R. gnavus</i> ATCC 35913 cell surface polysaccharide. ....   | 103 |
| Figure 25: Absolute configuration analysis of rhamnose by GC-MS of <i>R. gnavus</i> ATCC 35913 pellet fraction. ....  | 104 |
| Figure 26: Absolute configuration analysis of glucose by GC-MS of <i>R. gnavus</i> ATCC 35913 pellet fraction. ....   | 105 |
| Figure 27: GC-MS analysis of the pellet fraction from ATCC 35913 glucorhamnan purification with the PMAA method. ....   | 106 |

|   |     |
|---|-----|
| Figure 28: 2D NMR spectrum of <i>R. gnavus</i> ATCC 35913 glucorhamnan. ....  | 107 |
| Figure 29: <i>R. gnavus</i> glucorhamnan cluster GT gene expression. ....   | 111 |
| Figure 30: <i>R. gnavus</i> cps cluster GT gene expression. ....  | 112 |
| Figure 31: Structure of <i>R. gnavus</i> glucorhamnan. ....   | 113 |
| Figure 32: Polysaccharides sharing similar structures with <i>R. gnavus</i> glucorhamnan. ....  | 114 |
| Figure 33: Immunofluorescence microscopy of T84 monolayer grown with LS174T on transwell. ....  | 119 |
| Figure 34: Effect of <i>R. gnavus</i> strains and purified glucorhamnan on tight junction gene expression. ....   | 120 |
| Figure 35: Effect of <i>R. gnavus</i> strains and purified glucorhamnan on tight junction proteins in the T84 model. ....   | 121 |
| Figure 36: Effect of <i>R. gnavus</i> strains and purified glucorhamnan on tight junction proteins expression. ....   | 122 |
| Figure 37: Transepithelial electrical resistance (TEER) of T84 cells grown on transwells and effect of <i>R. gnavus</i> strains and associated purified glucorhamnans. .... | 123 |
| Figure 38: Effect of <i>R. gnavus</i> strains and purified glucorhamnans on cytokine production by intestinal cells in apical side of the T84/LS174T model. ....            | 125 |
| Figure 39: Effect of <i>R. gnavus</i> strains and purified glucorhamnans on cytokine production by intestinal cells in basolateral side of the T84/LS174T model. ....       | 126 |
| Figure 40: Effect of <i>R. gnavus</i> strains and glucorhamnan on IL-29 production by T84/LS174T cells. ....  | 127 |
| Figure 41: Effect of <i>R. gnavus</i> strains and glucorhamnan on IL-29 production by T84 cells. ....   | 128 |
| Figure 42: Effect of <i>R. gnavus</i> strains and associated glucorhamnan on cytokines gene expression. ....  | 130 |
| Figure 43: Effect of <i>R. gnavus</i> strains and purified glucorhamnan on TLR4 gene expression. ....   | 131 |
| Figure 44: Effect of <i>R. gnavus</i> strains and purified glucorhamnans on cytokine production by mBMDCs. ....   | 138 |
| Figure 45: Effect of <i>R. gnavus</i> strains and purified glucorhamnans on cytokine production by mBMDCs. ....   | 139 |
| Figure 46: Effect of <i>R. gnavus</i> strains and purified glucorhamnan on IL-10 production by mBMDCs. ....   | 140 |
| Figure 47: Effect of <i>R. gnavus</i> strains and purified glucorhamnans on the NF- $\kappa$ B pathway. ....  | 141 |
| Figure 48: Analysis of the interaction between <i>R. gnavus</i> strains and C-type lectin reporter cells. ....  | 143 |

## List of tables

|   |     |
|---|-----|
| <b>Table 1: Examples of cell surface polysaccharide structures found on commensal bacteria.</b>                         | 48  |
| <b>Table 2: List of primers used for quality control of <i>R. gnavus</i> glycerol stocks.</b>                           | 62  |
| <b>Table 3: List of primers used for <i>R. gnavus</i> gene qPCR analysis.</b>   | 65  |
| <b>Table 4: Lectins used this study.</b>  | 66  |
| <b>Table 5: List of primers used for epithelium cells gene expression analysis.</b>                                     | 79  |
| <b>Table 6: List of antibodies used for western blot analysis.</b>  | 81  |
| <b>Table 7: Antibodies used for human or mouse cytokines in ELISA or U-PLEX assays in this study.</b>                   | 82  |
| <b>Table 8: Summary of GTs present in the glucorhamnan cluster of <i>R. gnavus</i> strains.</b>                         | 99  |
| <b>Table 9: Relative quantification of monosaccharides of <i>R. gnavus</i> strains E1 and ATCC 35913 glucorhamnans.</b> | 108 |

## List of supplementary data

|   |                                     |
|---|-------------------------------------|
| <b>Supplementary data 1: Full LAB stock solutions recipes. ....</b>   | <b>196</b>                          |
| <b>Supplementary data 2: E1 and ATCC 35913 proteins homologous to proteins involved in the glucorhamnan synthesis in <i>R. gnavus</i> ATCC 29149: .....</b>                       | <b>197</b>                          |
| <b>Supplementary data 3: 1H NMR spectra of different <i>R. gnavus</i> strains glucorhamnan purification samples.....</b>  | <b>200</b>                          |
| <b>Supplementary data 4: Effect of <i>R. gnavus</i> strains and purified glucorhamnans on cytokine production by intestinal cells in apical side of the T84/LS174T model.....</b> | <b>201</b>                          |
| <b>Supplementary data 5: Effect of <i>R. gnavus</i> strains and purified glucorhamnan on tight junction gene expression. ....</b>   | <b>202</b>                          |
| <b>Supplementary data 6: Effect of <i>R. gnavus</i> strains and purified glucorhamnan on tight junction proteins expression. ....</b>   | <b>Error! Bookmark not defined.</b> |

## Chapter 1: Introduction

## 1.1. The human gastrointestinal (GI) tract

### 1.1.1. Organisation and function

The human GI tract is a complex organ which carries out vital physiological functions such as the digestion of food and absorption of nutrients, and the regulation of the host immune response. The GI tract is subdivided into two main regions: the upper tract that is composed of the mouth, the pharynx, the oesophagus and the stomach, and the lower part which is composed of the small and large intestines. The small intestine, which is approximately 7 m long, comprises the duodenum, the jejunum and the ileum; while the large intestine, which is 1.5 m long, is composed by the caecum, the colon and the rectum (Fig. 1A). The GI tract represents an exchange surface of approximately 400 m<sup>2</sup>, making it the largest mucosal surface of interaction with the external environment in the body. As a result, the GI tract is in constant contact with pathogens and antigens derived from the diet (Turner, 2009). In addition, the large intestine shelters more than 10<sup>13</sup> microbial cells (Sender et al., 2016; Thursby & Juge, 2017), ranging from less than a thousand microbial cells in the stomach up to 10<sup>12</sup> microbial cells in the colon (Fig. 1A), covering more than 1000 species making up the gut microbiota (Almeida et al., 2019). These microorganisms benefit from the conditions offered by the gut environment such as a consistent temperature and an abundance of dietary and host complex carbohydrates. In turn, the gut microbiota plays a fundamental role in the physiology of the host by contributing to nutrient metabolism, xenobiotic and drug metabolism, maintenance of structural integrity of the gut mucosal barrier, immunomodulation, and protection against pathogens (see section 1.1.2.).

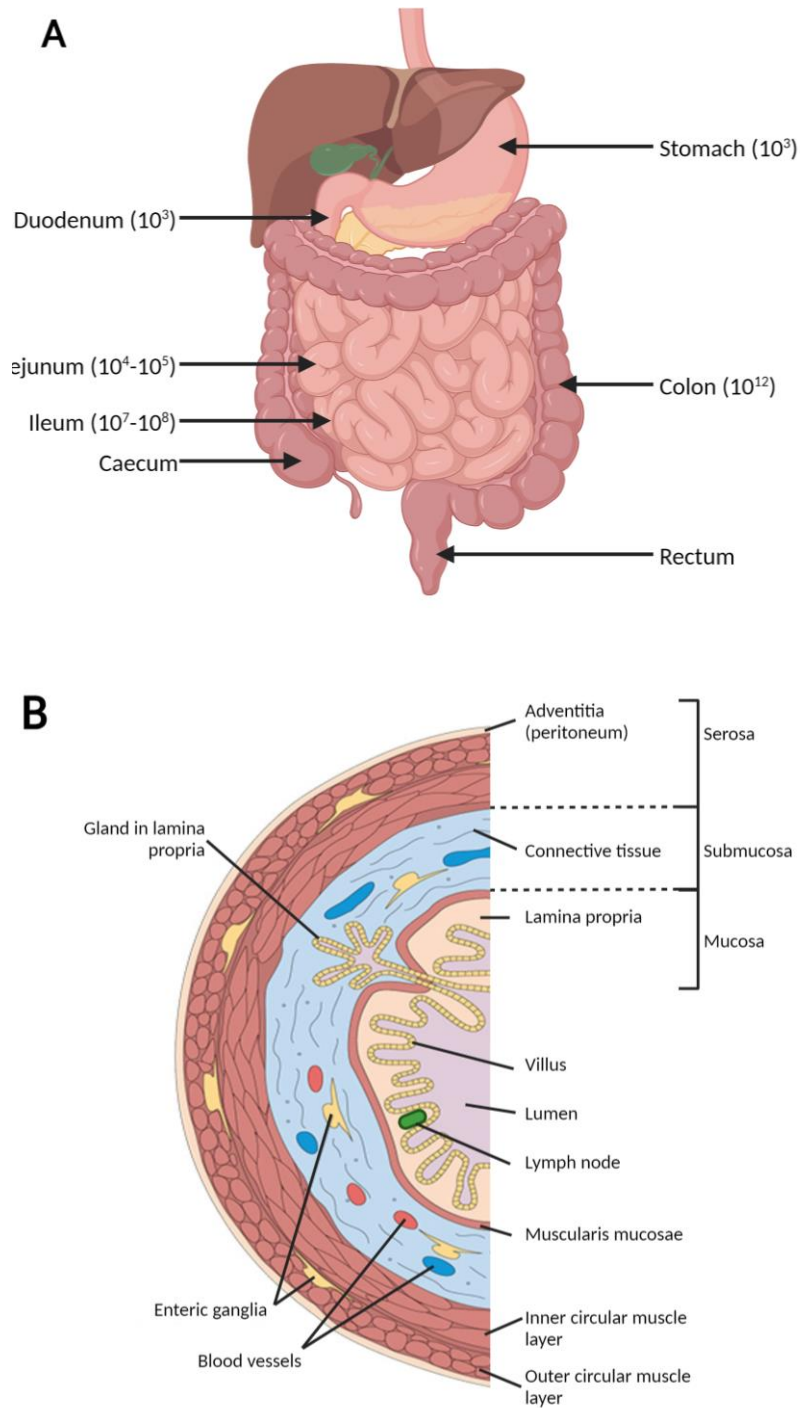


**Figure 1: The GI tract anatomy in human.**

(A) General features of the small and large intestine including the microbial density associated with each region of the GI tract. (B) Diagram showing the structure of the duodenum (in the small intestine) portion of the digestive tract, with the three main layers (the mucosa, the submucosa and the serosa) and their major components.

Throughout the GI tract, the gut wall is organised transversally by three different specialised layers as represented in Fig. 1B. The mucosa, in direct contact with the lumen, is comprised of the mucus layer and the epithelial layer that permits the uptake of nutrients and the processing of waste products (Sancho et al., 2003). The mucosa includes the glandular tissue, a lamina propria involved in the vascular supply of the epithelium and its loose connective tissue support, and the muscularis mucosae that separates the mucosa from the rest of the gut. The submucosa plays a role in distributing nutrients in the body through blood and lymphatic vessels. Finally, the serosa is involved in reducing friction related to the gut motion by secreting lubricative fluids (Liao et al., 2009) (Fig. 1B).

Defences against threats from the lumen (such as microbes, endotoxins or the digestive enzymatic activity) are organised at different levels. The first defence is composed of the mucus layer and the epithelial monolayer maintained together by a tight junction protein network. Then, the GI tract harbours a plethora of immune cell types involved in the protection against potential threats breaking through these protective layers. These elements are organised differently in the small and large intestine.

#### 1.1.2. The intestinal mucus layer

The GI tract is covered by a mucus gel which is the first line of contact between the gut microbiota and the host. It is composed by water, electrolytes, lipids and various proteins, comprising the large glycoproteins called mucins which organisation and composition vary along the gut axis. The colonic outer layer provides a habitat for microbes while the inner layer protects the epithelium from contact with these microbes (Johansson et al., 2008) (Fig. 2). The mucus barrier, which is composed of a mucin complex rich in O-glycosylation, provides nutrients and habitat for intestinal microbes but is also involved in the fight against pathogens. In turn, the gut microbiota modulates the production and secretion of mucins and stratification of the mucus layers. There is a bidirectional communication performed between the microbiota and the mucus barrier, maintaining homeostasis of the gut environment. Any

abnormalities may induce a disorder in the gut community, thereby causing inflammatory damage (Fang et al., 2021). The intestinal mucus differs in thickness along the GI tract. The mucus layer thickness can vary from around 300  $\mu\text{m}$  in the small intestine to approximately 700  $\mu\text{m}$  in the rectum in rats (Fig. 3) (Atuma et al., 2001; Juge, 2012). The organisation of the intestinal mucus system reflects the GI tract physiology. The increased thickness of mucus towards the colon is in line with the protective role of mucus against the large number of microbes present in the colon (Paone & Cani, 2020) as well as its role as lubricant for the stool (Barker, 2014) while the small intestine has a loose and penetrable mucus that allows diffusion of nutrients (Ermund et al., 2013). In the small intestine, the mucus layer is also permissive to the movement of antibodies (like IgA) and antimicrobial peptides which are small peptides involved in the inhibition of micro-organisms such as bacteria, fungi, viruses or parasites as part of the innate immunity. These molecules are secreted by Paneth cells and plasma cells respectively (Kayama et al., 2020) while it blocks the direct contact between the host epithelium cells and the bacteria present in the lumen (Duangnumsawang et al., 2021; Leal et al., 2017). The interactions between commensal microbiota and host mucins drive intestinal colonization, while at the same time, the microbiota can utilize the polysaccharides on mucins and affect the colonic mucus properties.

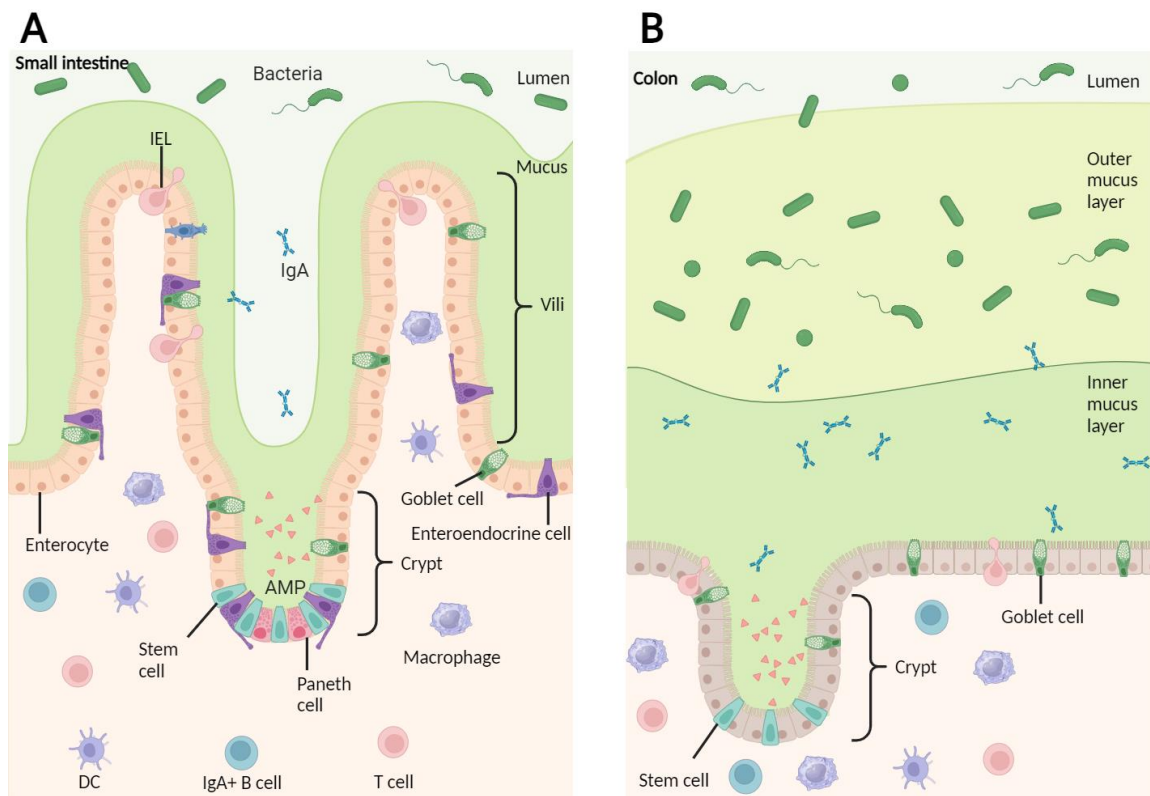


**Figure 2: The mucus protection in small intestine and colon.**

In the small intestine the mucus is not attached and forms a diffusion barrier with antibacterial products that limit penetration by bacteria. In colon bacteria are compartmentalized to the outer loose mucus layer while the inner attached layer is almost free of bacteria and protect the epithelium. AMP, antimicrobial peptides; IEL, intraepithelial lymphocyte; DC, dendritic cell; IgA, immunoglobulin- $\alpha$ .

The intestinal mucus is produced by the goblet cells (Birchenough et al., 2015), present along the GI tract, and specialised in mucin secretion. The mucus is composed of mucins, O-linked glycoproteins which constitute the structural backbone for the mucus barrier. Mucin glycosylations are composed of *N*-acetylgalactosamine (GalNAc), galactose (Gal) and *N*-acetylglucosamine (GlcNAc), usually terminated with fucose and sialic acid residues (Jensen, 2009). The proteic part of mucins contains tandem repeat units of varying length consisting of the amino acids proline, serine, and threonine, which create sites for O-glycosylation by O-linked oligosaccharides (Grondin et al., 2020). The number and type of monosaccharide added generates a broad structural variability in mucin glycoproteins and results in a range from short linear structures to more complex branched forms. In the intestine, these glycoproteins

are built from the mucin polysaccharide core 1 to 4 (Pucci et al., 2021). MUC1 and MUC4 are membrane-bound, whereas MUC2, MUC5 are secreted and present in the two layers of the mucus (Danese et al., 2018). MUC2 (Muc2 in rodents) is the main structural component of mucus in the small and large intestines. Muc2/MUC2 mucin shows region specific O-glycosylation profile (Larsson et al., 2009; Robbe et al., 2003a, 2003b) which is affected by the gut microbiota (Johansson et al., 2015) and regulated by differential expression of host glycosyltransferases (Arike et al., 2017). These mucin polysaccharides provide adhesion sites and nutrients to mucin-degrading bacteria, permitted by the use of glycoside hydrolases from the gut microbiota, but also pathogens, inhabiting the mucus niche (for a review, see Etienne-Mesmin et al., 2019). Recent studies based on mice deficient in key glycosyltransferases called polypeptidyl GalNAc transferases involved in mucin polysaccharide biosynthesis have underscored the importance of mucin O-glycosylation in mucus barrier function (for a review, see Bergstrom & Xia, 2013Bergstrom & Xia, 2013).

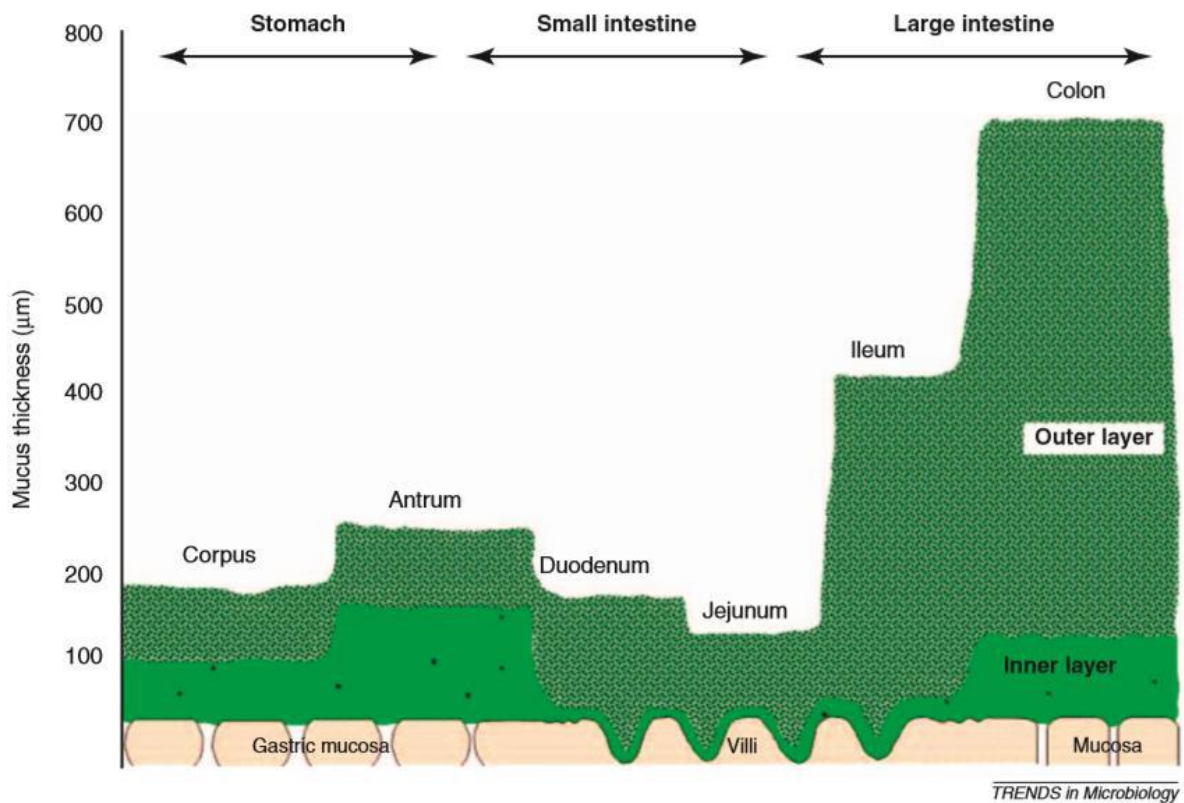


**Figure 3: Representation of gut mucus both inner layer and outer layer thickness along the GI tract.**

The GI tract epithelium is covered with an inner mucus layer, firmly adherent to the epithelial cells and an outer mucus layer, loose and inhabiting species of the gut microbiota (represented as black dots). Thickness for inner and outer layer in each GI tract region is represented. Redrawn from Atuma et al. (2001).

#### 1.1.2.1. Mucin glycosylation

Mucin glycosylation takes place throughout its production: first, the *N*-glycosylation is operated in the endoplasmic reticulum: then, the mucins are transported into the golgi apparatus where *O*-glycosylation, which represent 80% of the glycoprotein mass, occurs before transport to the membrane (Arike et al., 2017). The first stage of glycosylation of mucins is the attachment of *N*-acetylgalactosamine (GalNAc) to the hydroxyl group of serine and threonine residues by members of the GalNAc transferase (GnT) family forming the Tn antigen (Bennett et al., 2012). Core transferases then act upon this *O*-GalNAc residue in a sequential fashion to form one of the 8 core structures, with structures 1 – 4 most commonly

found in intestinal mucins (Tailford et al., 2015; Thomsson et al., 2012). Following the formation of the Tn antigen, the core 1 T-antigen is synthesised by extension with galactose. A further addition of *N*-acetylglucosamine (GlcNAc) by the core 2 GnT enzyme produces the core 2 structure. Core 3 is produced from the T-antigen by addition of GlcNAc and addition of a second GlcNAc converts the core 3 to core 4 (Fu et al., 2016). Following extension, polysaccharides are terminated by one of the numerous epitopes which are, in many cases, fucosylated, sialylated or sulphated. Like the core structures these terminal epitopes show species and regional specificity.

Several factors allow the mucin glycosylation to display a broad variability of structure, one of which is the 8 different core structure being used; then, the length of those glycosylation can vary from 1 to 20 residues and finally, there is a variability in the epitopes found attached to the polysaccharide, which can count up to 16 different structures (Tailford et al., 2015).

The distribution of core structures has been shown to vary along the GI tract in humans and mice and is influenced by specific expression patterns of the core transferases (Ariake et al., 2017). Core 3 structures are spread throughout the intestinal and gastric mucus, with core 4 structures being present in the colonic mucus of humans. Core 1 and 2 polysaccharides dominate in the gastric and duodenal mucus (Robbe et al., 2004).

These core structures are then extended by the action of a range of other glycoside transferases to add galactose, GalNAc and/or GlcNAc residues. The region-specific glycosylation is determined by the expression of glycoside transferases, which is influenced by the presence of the gut microbiota. Compared to germ-free mice, conventionally raised animals show longer polysaccharide chains, and this is proposed to give greater protection to the protein backbone from bacterial proteases (Ariake et al., 2017). In the same study, fewer enzymes responsible for O-glycan elongation were found in the small intestine, with shorter polysaccharides structures also found in the small intestine of mice.

### 1.1.2.2. Establishment of homeostasis

Mucin is an important factor of the gut microbiota homeostasis as mucins and their polysaccharides broadly modulate the microbiota composition, promoting diversity and retaining health-associated bacteria, while resisting microbial outgrowth in the presence of simple dietary sugars. Notably, recent studies indicated that MUC2 mucin plays a role in the protection of gut barrier, the regulation of microbiome homeostasis and the prevention of diseases. For example, mice fed a diet supplemented with mucin polysaccharides were shown to exhibit differences in microbial composition (Pruss et al., 2021). Also, mucus and goblet cell development are tightly regulated during early life and synchronized with microbial colonization (Pruss et al., 2021).

Glycosylation of secretory gel-forming mucins has an enormous impact on intestinal barrier function, microbial metabolism, and mucus colonization by both pathogenic and commensal microbes. Mucin O-glycans and polysaccharide-derived sugars may be degraded and used as a nutrient source and may regulate microbial gene expression and virulence. Short-chain fatty acids, produced as a by-product of polysaccharide fermentation, can regulate host immunity and goblet cell activity and are important for host-microbe homeostasis. Mucin polysaccharides may also act as microbial binding sites, influencing intestinal colonization and translocation through the mucus gel barrier (Fekete & Buret, 2023). One mechanism by which mucins may facilitate microbial coexistence is providing complex nutritive substrates to enable niche partitioning and cooperative metabolism (C. M. Wu et al., 2023).

Also, mucin-type O-glycans are a critical resource utilized by this commensal to enable it to thrive when diet-derived polysaccharides are compromised as well as to persist in mammalian populations. In turn, *B. thetaiotaomicron* can affect host responses in beneficial ways, such as stimulating angiogenesis to increase absorptive capacity of the intestine, providing energy in the form of short-chain fatty acids (e.g., butyrate, propionate and acetate) elaborated as end-products of polysaccharide fermentation and promoting mucosal homeostasis by both limiting inflammatory tone of the epithelium and stimulating production of epithelial

antimicrobials to potentially reduce overall bacterial load at mucosal surfaces (Bergstrom & Xia, 2013). Thus, mucin-type O-glycans contribute both directly or indirectly to robust colonization of the gut by *B. fragilis* and production of commensal-derived symbiotic molecules such as PSA (Bergstrom & Xia, 2013).

## 1.2. The gut microbiota

### 1.2.1. Structure and function

The human gut microbiota is a complex, dynamic, and spatially heterogeneous microbial ecosystem including bacteria, fungi, archaea, and viruses. The microbiota colonises the GI tract across life, from the infant to the elderly although its composition differs during the different stages of life (Ling et al., 2022; Rodríguez et al., 2015).

The infant gut microbiota is influenced by the way of delivery. Indeed, vaginally delivered babies harbour a microbiota similar to the mother vaginal microbiota, highly composed of *Lactobacilli* bacteria (Avershina et al., 2014; Chong et al., 2018). In contrast, caesarean section delivered babies display an altered microbiota, constituted mostly of facultative anaerobes such as *Clostridium* species (Jakobsson et al., 2014; Shao et al., 2019). It is believed that vaginal delivery and breast feeding reduce the risks of developing health issues such as allergies or infection (Sitarik et al., 2018). Breast feeding promotes colonisation by *Bifidobacterium* spp. whereas their proportion is lower in formula fed infants (Ford et al., 2019; Henrick et al., 2021; Z. T. Yu et al., 2013). Once the child completes its transition to solid food, the gut microbiota transitions to an “adult-like” microbiota that can metabolise more complex substrates (Bäckhed et al., 2015; Lawson et al., 2020). The most predominant bacterial phyla in an established microbiota in adults are *Firmicutes*, *Bacteroidetes*, *Actinobacteria*, *Proteobacteria*, *Fusobacteria*, and *Verrucomicrobia*, with the two phyla *Firmicutes* and *Bacteroidetes* representing 90% of gut microbiota (Rinninella et al., 2019). The gut microbiota varies in composition and in abundance along the longitudinal axis and across

the transversal axis of the GI tract (Fig. 4). The colon harbours the highest density of microbial cells (Martinez-Guryn et al., 2019), with bacteria being mainly represented by *Firmicutes* and the *Bacteroides* (Vaga et al., 2020) while the small intestine is characterised by the presence of bacteria species from the *Streptococcus* genus and *Firmicutes* and *Proteobacteria* phyla (Miller et al., 2021). The gut microbiota composition also differs along the luminal-mucosa axis with *Bacteroides* being more represented in the lumen than in the mucosa, where *Firmicutes* are mostly present (Juge, 2022).

Dominant gut phyla:

Bacteroidetes, Firmicutes, Actinobacteria, Proteobacteria, Verrucomicrobia

Predominant families in the:

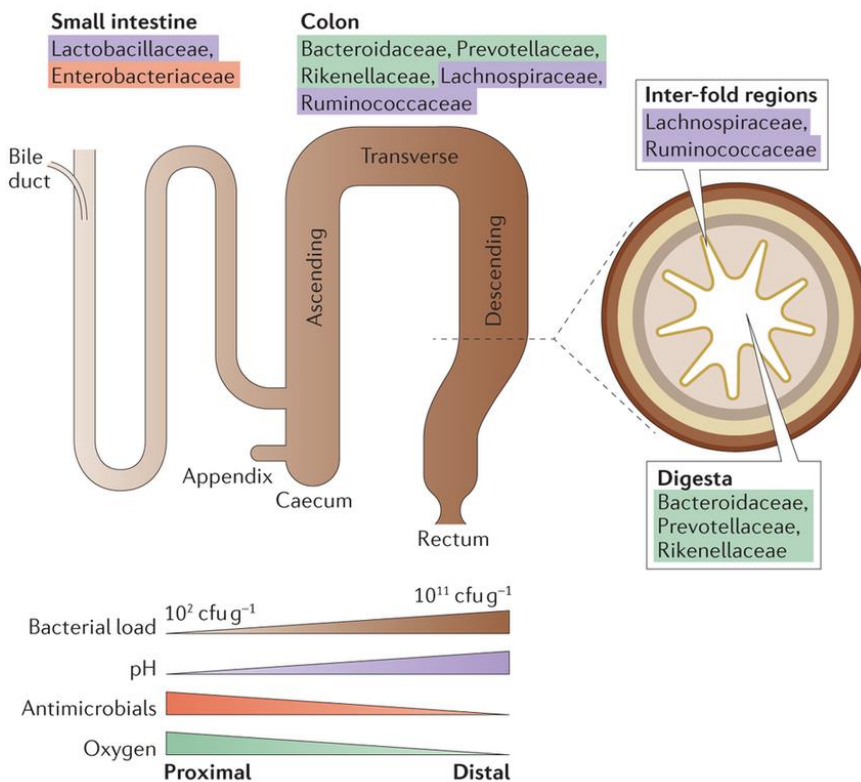


**Figure 4: Microbiota bacterial distribution through the GI tract.**

Description of the different physicochemical and gradient from the proximal to the distal region of the lower GI tract along with the description of the dominant bacterial phyla and families in the different region of the gut which is dependent on the gradient of oxygen, antimicrobial peptides presence and the pH. Redrawn from (Donaldson et al., 2016).

These differences in the composition of the microbial communities along the GI tract can be due to several gut physiological factors enlisted next (for a recent review, see Chikina & Matic Vignjevic (2021)). There is a gradient of O<sub>2</sub> from the small intestine to the large intestine, preventing the proliferation of strictly anaerobic microbes in the upper parts of the GI tract (Albenberg et al., 2014; Friedman et al., 2018; Kint et al., 2020). The microbial composition can also differ due to the presence of specific antimicrobial components or in response to the pH gradient (Donaldson et al., 2016; Zimmermann & Curtis, 2019). Also, the genetic of the host will determine the polysaccharide composition of the mucin glycosylation, which will have a direct impact on the microbiota composition as the different species will grow preferentially on different oligosaccharides (Thursby & Juge, 2017; Van Herreweghen et al., 2021).

Several environmental factors can affect the composition of the gut microbiota in adults, such as lifestyle, the use of antibiotics or changes in diet (Klingbeil & de La Serre, 2018; Ramirez et al., 2020). A change in the host diet can bring a turn in the gut microbial composition with the nature as the microbiota will grow preferentially on different accessible carbohydrates, promoting the growth of specific microbial species. For example, *Bacteroides* possess a vast array of polysaccharide degrading enzymes which enable them to degrade a wide range of complex carbohydrates such as chondroitin sulfate, hyaluronic acid, heparin, hyaluronan or polygalacturonate (Hansson, 2020; La Rosa et al., 2022; Martens et al., 2014; Porter et al., 2017; Rawat et al., 2022). The disruption of the microbial composition can be caused by a misuse of antibiotics or unbalanced diet (Petersen & Round, 2014).

### 1.2.2. Role in health and disease

The gut microbiota plays an important role in the host health through digesting food, maintaining the integrity of the gut barrier, training the host immune system, fighting against pathogens, and producing numerous molecules and metabolites, comprising short chain fatty acid (SCFA), niacin or indole, that influence the host. Notably, the microbiota synthesise,

modulate and degrade a large array of metabolites that plays a major role in the establishment of the host immunity, providing a functional complementation to the metabolic capacities (Levy et al., 2017). Those metabolites were shown to contribute to intestinal homeostasis through the modulation of inflammasome signaling in epithelial cells.

One of the major functions of the gut microbiota is to help digest the complex dietary polysaccharides that cannot be degraded by the host through their carbohydrate active enzymes (CAZymes) (Kaoutari et al., 2013; Koropatkin et al., 2012; La Rosa et al., 2022; Ndeh & Gilbert, 2018). The fermentation of dietary fibers by the gut microbiota gives rise to the production of SCFAs e.g., acetate, propionate and butyrate, which help maintain the integrity of the intestinal barrier as well as protect from inflammation (Conlon & Bird, 2014; Silva et al., 2020).

The gut microbiota is implicated in the development of the host immunity, enhancing the host defences against potential pathogens (Erttmann et al., 2022; Estorninos et al., 2021; Y. J. Kim et al., 2022; T. Y. Ma et al., 2004). The gut microbiota interacts with immune cells through the interaction between MAMPs such as the LPS or capsular polysaccharide (CPS) on bacteria and PRRs expressed on immune cells (D. Zheng et al., 2020). This interaction allows the modulation of immunity through the regulation of the cytokines, chemokines but also IgAs produced by the host. Germ-free mice have decreased levels of secretory IgA and less IELs (intraepithelial lymphocytes) which play a vital role in defence during inflammation (Round & Mazmanian, 2009). These immunity-associated molecules are important in the maintaining of gut microbiota homeostasis (Pabst et al., 2016).

Furthermore, the gut microbiota is involved in the biosynthesis of several vitamin K and B group vitamins such as cobalamin, biotin or folates amongst others (Rowland et al., 2018) and in the production of neurotransmitters such as dopamine, serotonin or  $\gamma$ -aminobutyric acid regulating gut endocrine function and neurological signalling (Strandwitz, 2018; Strandwitz et al., 2019).

As a result of this mutualistic relationship with the host, an alteration in the microbiota structure and function or so called 'dysbiosis' can lead to different disorders such as infection and inflammation including IBD, represented by Crohn's disease and the ulcerative colitis, (Maukonen et al., 2015). The alteration in the microbiota community in the gut has also been associated to immunity-related issues like allergies, asthma, type I diabetes, celiac disease and metabolic diseases such as obesity, type II diabetes or cardiovascular disease (Decker et al., 2010; Håkansson & Källén, 2003). Changes in the gut microbiota composition have also been associated with colorectal cancer, which is characterised by an increased abundance of *Fusobacterium nucleatum*, *B. fragilis* or *E. coli* species (Mo et al., 2020; Wirbel et al., 2019).

### 1.2.3. The cell surface of gut microbes

The interaction between gut microbes and the host plays a key role in the host health and potential diseases. These interactions are largely mediated by the composition of the polysaccharides composing the cell surface as described in more details in section 1.3. below and the presence of proteins such as adhesins, pili, fimbriae (Etienne-Mesmin et al., 2019; Juge, 2012). In addition, S-layer proteins can be found outermost constituent of many bacterial cells involved in several processes, such as protecting against environmental stresses, mediating bacterial adhesion to host cells, and modulating gut immune response (Mazzeo et al., 2022).

Gram-positive bacteria harbour a cytoplasmic membrane covered by a thick layer of peptidoglycan (PG) forming the cell wall (Fig. 5A). These PGs serve multiple purposes, they play a role in mobility, adherence and secretion (Zerbib, 2016). As they are anionic, the PGs are implicated in cation homeostasis (Silhavy et al., 2010). Furthermore, they are crucial in the integrity of the bacterial cell membrane in, for example, a low osmolarity medium; and the PG biosynthesis gene mutation often leads to cell lysis (Zerbib, 2016). It has also been observed that the administration of PGs to germ-free mice promoted the thickening of the mucus layer in the gut (Pettersson et al., 2011). PG also plays an important role in gut brain

axis, which is the set of biochemical signaling happening between the GI tract and the central nervous system, inducing host behavioural changes (Arentsen et al., 2017; Petersson et al., 2011; Wheeler et al., 2023; Zerbib, 2017; Arentsen et al., 2017; Petersson et al., 2011; Wheeler et al., 2023; Zerbib, 2016). PG is composed of carbohydrates units alternating *N*-acetylglucosamine (GlcNAc) and *N*-acetylmuramic acid (MurNAc), with the MurNAc residues cross-linked to peptides. The PG strands are cross-linked by pentapeptide containing L- or D-amino acids (Pazos & Peters, 2019). The PG layer is anchored to the cytoplasmic membrane through teichoic acids which are involved in the interaction of the bacteria with the host (Schade & Weidenmaier, 2016; Zerbib, 2016).

The cell wall of Gram-negative bacteria is composed of a thin layer of PG, an outer membrane and a layer of LPS, it plays a major role in the interaction with host components by maintaining homeostasis and preventing inflammation (Fig. 5B) (Di Lorenzo et al., 2019; Zerbib, 2016). LPS is composed of 3 regions: lipid A, the core oligosaccharide region and the O-antigen polysaccharide (Fig. 5B). The lipid A domain from pathogen-derived LPS binds to TLR4 receptors, resulting in a pro-inflammatory host response (Cabral et al., 2015). The gut commensal strain *Akkermansia muciniphila* ATCC BAA-835 produces LPS of which the acetylation of *N*-acetylmuramic acid (MurNAc) can be removed by dedicated enzymes expressed by the bacteria, allowing the bacteria to avoid recognition by host immune cells through LPS receptors NOD1 and NOD2 (Garcia-Vello et al., 2022).

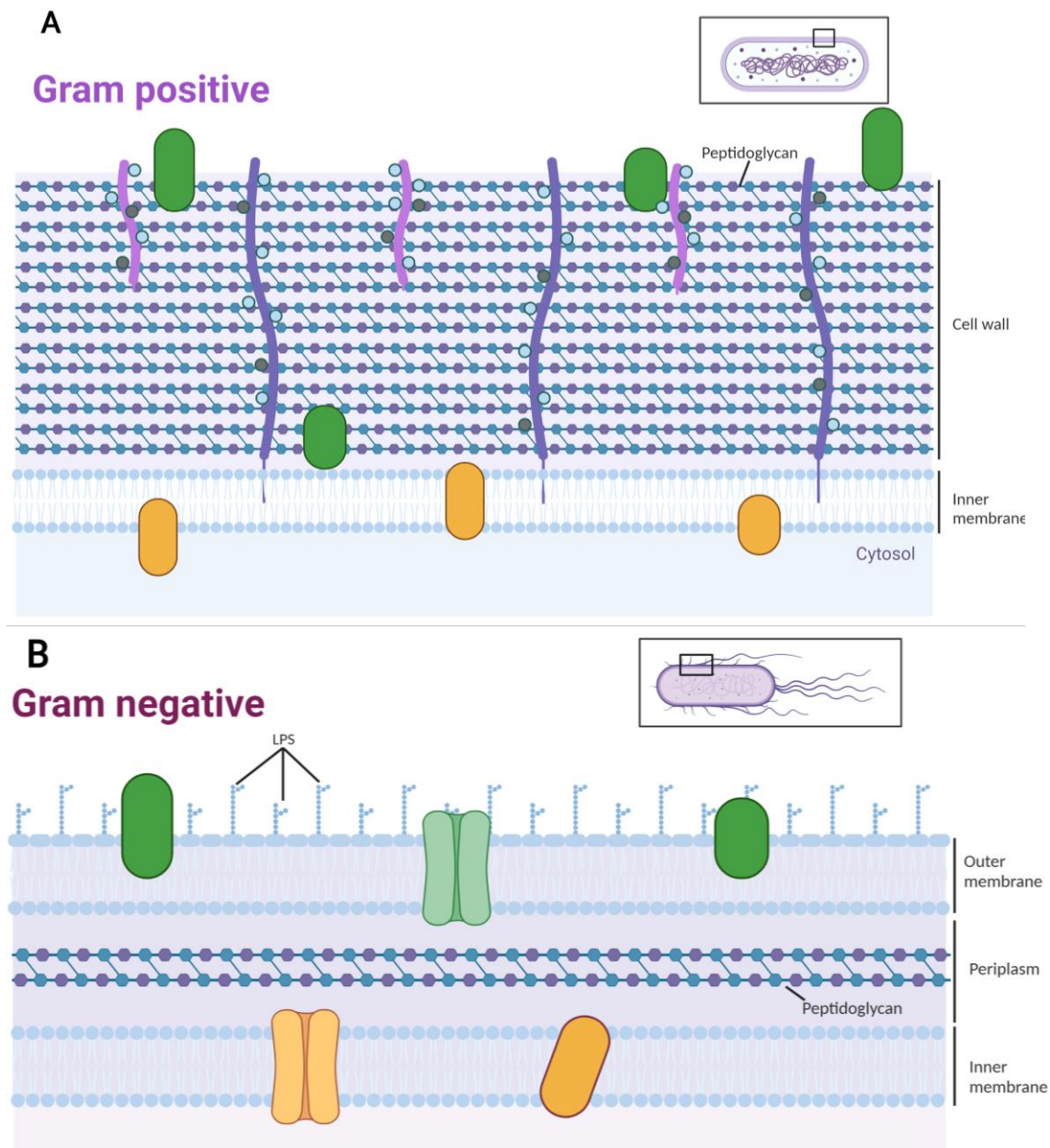


**Figure 5: General representation of Gram-positive and Gram-negative cell wall composition.**

(A) Gram-positive, (B) Gram-negative bacteria. Phospholipids are depicted in blue. Carbohydrate basic units from the peptidoglycan are in blue (*N*-acetylmuramic acid) and purple (*N*-acetylglucosamine). Wall teichoic acids are in pink with the embranchments by carbohydrates in pale blue and by alanine in black. Lipoteichoic acids are in purple and their modifications are symbolised as for wall teichoic acids. Covalently attached or non-covalently attached proteins are depicted in green. LPS core and O-antigen are both represented in blue. The transmembrane porins and the lipoproteins of outer membrane are in green. The periplasmic proteins and proteins of the inner membrane are in orange.

The cell surface of Gram-positive and Gram-negative bacteria can be surrounded by extracellular polysaccharides (EPS) or CPS as further described in section 1.3.

### 1.3. The mucosal interface

#### 1.3.1. The intestinal epithelium

Along the GI tract, the epithelium is organised by a single layer of cells of different types maintained by the presence of tight junction proteins (see Fig. 5). This intestinal barrier has two functions: first, it acts as a barrier to prevent the passage of harmful intraluminal entities including foreign antigens, microorganisms and their toxins; secondly, the intestinal barrier act as a selective filter allowing the translocation of essential dietary nutrients, electrolytes and water from the intestinal lumen into the circulation. The small intestine is characterised by finger-like projections known as villi, which extend into the lumen and increase the surface area of nutrients absorption. By contrast, villi are absent from the large intestine, where the surface is flat. The surface epithelium is continuously renewed by immature cells arising from invaginations known as the crypts of Lieberkühn, where multipotent stem cells will migrate and differentiate, first into transit amplifying cells, and then into specialised cells that will be displayed on the villi (Leedham et al., 2005).

To maintain adjacent epithelial cells bound together, the tight junction proteins play an important role as they are involved in the cell-to-cell adhesion and in the maintenance of intestinal mucosal barrier function (Chiba et al., 2008; X. Liu & Zhu, 2022). These proteins also regulate the transport of molecules based on the size and charge through the intercellular space (Ghosh et al., 2021). The main tight junction proteins in the intestinal epithelium include zonula occludens (ZO), claudin and occludin (Chelakkot et al., 2018; Kuo et al., 2022; B. Lee et al., 2018; Monaco et al., 2021). As shown in Fig. 5, tight junctions between cells are organised in a complex architecture where ZO are proteins bound to the cell membrane present in paracellular spaces, linking the cytoskeleton to the rest of the tight junction complex; while

occludins, claudins and junctional adhesion molecules (JAMs) are present in the intercellular space and are implicated in the binding between the different cells through the connection with ZO proteins (Neunlist et al., 2013).

The ZO proteins, which include ZO-1, ZO-2, and ZO-3, were the first tight junction proteins to be discovered (Traweger et al., 2013). As shown in Fig. 5, ZO connects proteins such as occludin and claudin to the actin cytoskeleton, and these protein interactions maintain tight junction formation and function (Kuo et al., 2022). ZO-1 is an intracellular scaffold protein, which plays a more important role than ZO-2 and ZO-3 in linking cytoskeleton and membrane proteins between different cells (Ghosh et al., 2021; X. Liu & Zhu, 2022). The claudin family is composed of 23 integral membrane protein (Heinemann & Schuetz, 2019). Claudin-1 (CLN-1) is a tetraspan transmembrane protein that plays a key role in the intestine to maintain epithelial barrier function and gut microbiota homeostasis (Pope et al., 2014). Occludin is highly expressed at cell-cell contact sites and is important in the assembly and maintenance of tight junctions between gut epithelial cells. It is a tetraspan transmembrane protein playing a key role in the physical separation between the lumen and the lamina propria and interacts with ZO-1 proteins to strengthen the tight junction (Feldman et al., 2005). A defective intestinal tight junction barrier has been implicated in inflammatory diseases of the gut including inflammatory bowel disease (IBD). Previous study have shown that pro-inflammatory cytokines, which are produced during intestinal inflammation, including interleukin-1 $\beta$  (IL-1 $\beta$ ), tumor necrosis factor- $\alpha$  (TNF- $\alpha$ ), and interferon- $\gamma$ , can regulate intestinal tight junction barrier (Kaminsky et al., 2021).

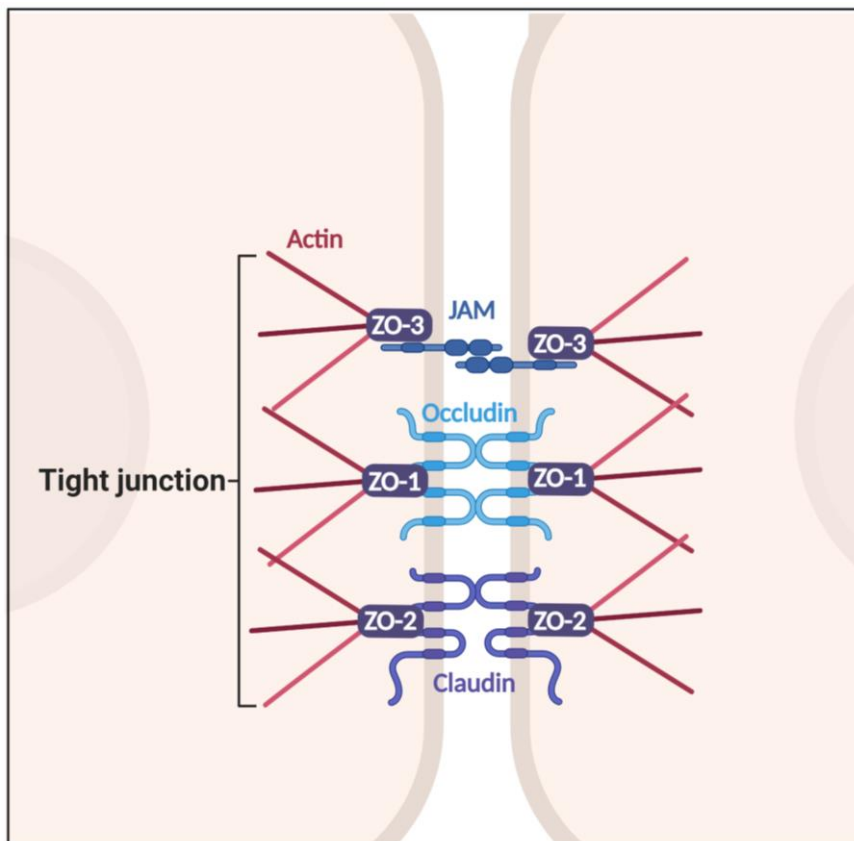


**Figure 6: Intestinal tight junction proteins.**

Schematic representation of intestinal tight junction proteins present on the apical end of the epithelial cells, all are connected to the cytoskeleton via scaffolding proteins. ZO: zonula occludens, JAM: junctional adhesion molecules.

The majority of cells present on the intestinal epithelium surface are enterocytes, which have the function of absorbing nutrients with microvilli increasing their absorptive capacity (Fig. 3). The digestion of the food bolus into nutrients in the gut lumen is facilitated by the secretion of hydrolytic enzymes, contributing to the absorption of salts, carbohydrates, lipids, proteins but also water. In addition to the mucins that form the mucus layer, enterocytes also produce glycoproteins which form the glycocalyx, formed by heavily glycosylated mucin, acidic mucopolysaccharides and other glycoproteins covering the surface of the enterocyte apical portion of microvilli. In addition, pattern recognition receptors (PRRs) like toll-like receptors (TLR) and nucleotide-binding and oligomerization domain (NOD)-like receptors (NLR), found on immune cells throughout the host body and, among others, on the epithelium layer. Those

PRRs are involved in the recognition of external signals like the pathogen-associated molecular pattern (PAMPs) (Snoeck et al., 2005; Kawai & Akira, 2010; Wells et al., 2011). PRRs allow the production of cytokines that regulate inflammation like IFN-I, IL-1, IL-6, TNF- $\alpha$  and other proinflammatory substances (Wicherska-pawłowska et al., 2021), this will result in the activation of immunity and in the recruitment of immune cells on the infection site (further discussed in section 1.1.4.). The recognition of PAMPs by PRRs can also result in the process of tolerance towards gut microbiota species through the activation of anti-inflammatory cytokines. PRRs can be found on the cell surface of, or inside, different immune cells like macrophages/monocytes, dendritic cells, natural killer (NK) cells, mast cells, neutrophils, and eosinophils but also of non-specialised cells, like epithelial cells, endothelial cells, or fibroblasts (Akira et al., 2006; Takeuchi & Akira, 2010).

Paneth cells are found mainly in the small intestine and more precisely, in the crypt base (Bevins & Salzman, 2011). They are involved in the secretion of immune related molecules as  $\alpha$ -defensins and lysozyme, these secretions are stimulated by the presence of PAMPs (Bevins & Salzman, 2011).

Goblet cells are specialised secretory cells which main function is to produce mucin, which is a major component of the mucus layer, along with water, electrolytes, lipids and various proteins. Therefore, goblet cells are involved in the protection of the gut epithelium against microbes and in the intestinal transit, as described above (section 1.1.2.). In addition, goblet cells are involved in the innate immunity by secreting anti-microbial proteins, chemokines and cytokines (Knoop et al., 2015) and have also the ability to form goblet cell associated passages, allowing the delivery of luminal substances to the lamina propria antigen-presenting cells (APCs) (Knoop & Newberry, 2018).

The enteroendocrine cells are involved in the secretion of hormones in response to different stimuli that have an impact on food digestion and absorption, appetite regulation and insulin secretion. They have key roles in the coordination of food digestion and absorption and in the peripheral assimilation of absorbed nutrients (Gribble & Reimann, 2019).

Enterocytes and Paneth cells also secrete antimicrobial proteins in the lumen of the small intestine, which flow through the lumen to reach the large intestine where they shape the gut microbiota profile (Dupont et al., 2015). Those antimicrobial proteins, like  $\beta$ -defensins, cryptdin or lysozyme, generate a gradient within the mucus layer from the bottom of the crypt (where the Paneth cells are located) to the villus tip. The antimicrobial proteins possess a broad spectrum of activities against most pathogenic but also commensal bacteria and will kill the bacteria via several activities like the inhibition of cell wall synthesis, alteration of the cytoplasmic membrane, activation of autolysin, inhibition of DNA, RNA, and protein synthesis, and inhibition of certain enzymes (Dupont et al., 2015).

Other cell types that can be found in the intestinal epithelium are the microfold (M) cells, which are involved in the defence of the body through the phagocytosis of pathogens but also commensal microbes and by presenting the produced antigens to immune cells present in the lamina propria (McGuckin et al., 2011). Tuft cells, present throughout the GI tract, are chemoreceptive cells that can sense chemical signals from the lumen, they also have been hypothesised to be associated to immune defence against pathogens like helminth (Gerbe et al., 2016). In addition, as represented in Fig. 2, intraepithelial lymphocytes (IELs) such as  $\gamma\delta$  IELs can be found interspersed between the epithelial cells as they play a crucial role in protecting the gut integrity. Indeed,  $\gamma\delta$  IELs are involved in the interaction of the commensal gut microbiota and its homeostasis, they are also involved in the suppression of pathogenic infections and cytotoxic threats through the recognition of associated pathogen patterns (Rampoldi & Prinz, 2022).

As represented in Fig. 2, the cells composing the epithelial layer varies along the longitudinal axis of the GI tract. For example, goblet cells are found mainly in the large intestine where they are ten times more abundant than in the small intestine (Mowat & Agace, 2014), in line with the increased mucus thickness in the colon (see section 1.1.2.) while M cells are found in the Peyer's patch in the small intestine (Mowat & Agace, 2014).

### 1.3.2. Tolerogenic signalling pathway

In addition to induce pro-inflammatory response when presented to pathogens in the gut, the gut immunity also has the responsibility to develop tolerance to inhabiting commensal bacteria. To do so, the host immune system act in two ways: it avoids to bring threat to commensal species, but also promotes their residence in the gut (Swiatczak & Cohen, 2015).

Because commensal bacteria are displaying on their cell surface and secreting components recognised by the host immunity as foreign, the host immune system must be tolerant of these bacterial molecules. Thus, host receptors like TLRs, NLRs or CLR which normally react to microbial-derived molecules (structural patterns and metabolites) to activate signaling pathways that control the expression of genes coding for a variety of immune mediators, another mechanism exist permitting the non-reaction to commensal species antigens. Therefore, PRRs in the submucosal tissues play seemingly conflicting functions. On the one hand, they promote destructive responses, as indicated by the observation that bone marrow chimeras, the hematopoietic cells of which are deficient in MyD88, fail to develop systemic inflammation in response to *Helicobacter hepaticus* (Asquith et al., 2010). On the other hand, they promote tolerance, as indicated by the fact that deletion of a critical component of the TLR signaling pathway, such as TNF receptor-associated factor in DCs, leads to a decrease in the number of FoxP3+ Tregs and provokes spontaneous inflammation in the small intestine that is driven by otherwise commensal bacteria (Han et al., 2013).

Safety signals can also help to prevent danger signals from activating proinflammatory cascades by inducing release of antagonists to proinflammatory receptors as illustrated by TLR5 on IECs, which prevents activation of the IL-1-mediated pathway by inducing release of secretory IL-1 receptor antagonist (Carvalho et al., 2011).

Taken altogether, stimulation of PRRs in the absence of infection or tissue damage promotes tolerance by limiting the ability of exogenous and endogenous danger signals to activate pro-inflammatory pathways in the gut and homeostasis signals promote long-term gut colonization.

### 1.3.3. The intestinal mucosal immune system

#### 1.3.3.1. *Immune niches and cellular immunity along the GI tract*

As in the rest of the body, the immune system of the GI tract works as two parts: the innate immune system which is the broadest specificity and the adaptative immune system, which is the most specialised in terms of pathogen recognition. Together with the epithelium, the lamina propria contains B cells, T cells and numerous innate immune cell populations — including dendritic cells (DCs), macrophages, eosinophils and mast cells (Kogut et al., 2020). DCs are subdivided in different functional types, depending on the cluster of differentiation (CD) they express; the CD103<sup>+</sup> DCs are migratory DCs found in the epithelial layers of the body and are involved in the activation of cytotoxic T cells (Ng et al., 2018). The T cell populations found in the GI tract are mainly represented by CD4<sup>+</sup> T cells (also called T helper cells or Th cells) but also in smaller proportion CD8<sup>+</sup> T cells (also called T cytotoxic cells or T<sub>C</sub> cells) (Sathaliyawala et al., 2013). The activation of T cells is mediated by the APCs of the lamina propria which will lead to the differentiation of T cells into different subtypes like Th1, Th2, Th17 or Tfh2 (T follicular helper 2) (Fig. 7). In the gut, the main enhanced subtypes are the regulatory T cells that will enable the tolerance upon commensal microbiota population (Harrison & Powrie, 2013).

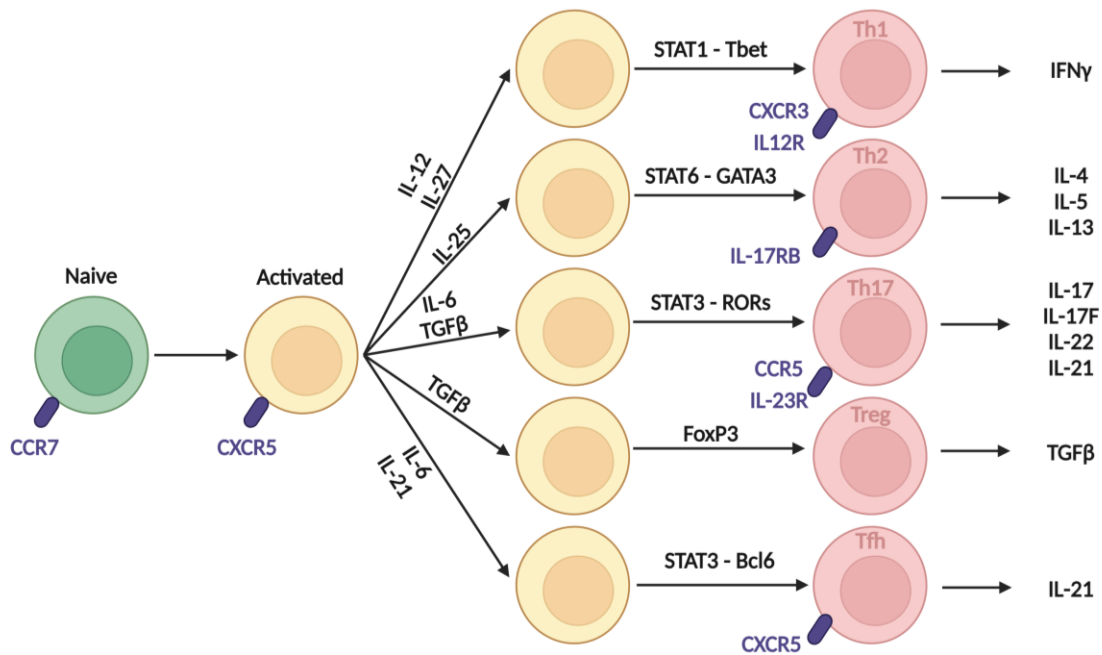


**Figure 7: Schematic of potential differentiation repertoire in T helper cells (Th cells).**

Naïve CD4<sup>+</sup> ( $\alpha\beta$ ) T cells can differentiate into different effector subsets after being presented an antigen by an APC: Th1, Th2, Th17, Treg or Tfh, which will produce a distinct set of cytokine and chemokine to induce a specific immune response. Bcl6, B-cell lymphoma 6; CCR, CC chemokine receptor; CXCR, CXC receptor; Foxp3, Forkhead box p3; IFN, interferon; ROR, retinoic acid-related orphan receptor; TGF, transforming growth factor; Treg, regulatory T.

Another important type of immune cells in the GI tract are the adaptive immunity-associated B cells, and more precisely plasma cells, which reside along the small intestine, provide a defence against pathogens via the production of IgA (immunoglobulin A) (James et al., 2020; Reboldi & Cyster, 2016). IgA are dimeric antibodies that will relocate into the lumen to directly address pathogens by neutralisation and agglutination, helping the following process of phagocytosis (Mantis et al., 2011). IgAs origins from different sources in the GI tract, mainly from the Peyer’s patch, but also B cells within mesenteric lymph nodes, spleen and intestinal isolated lymphoid follicles (Reboldi & Cyster, 2016).

In addition to being present in the epithelium (Fig. 2), a second layer of intestinal  $\gamma\delta$  T cells is found among lamina propria lymphocytes (LPLs). The  $\gamma\delta$  T cells are lymphocytes evolved in the innate immunity found in high abundance in the gut mucosa, they compose the major

population of IEL. These  $\gamma\delta$  LPLs can produce IL-17 and likely have functional overlap with local Th17 cells and innate lymphoid cells. In addition, a third population of  $\gamma\delta$  T cells resides within the Peyer's patches (see below), where it is probably involved in antigen presentation and supports the mucosal humoral immunity (Rampoldi & Prinz, 2022).

Most immune cells associated with the GI tract are present in the Peyer's patches, which are a cluster of cells present in the lamina propria constituted of macrophages, involved in the phagocytosis of pathogen-derived components and presentation to adaptive immunity cells, and CD103<sup>+</sup> DCs, also involved in the presenting of antigen to adaptive immune cells (Agace & McCoy, 2017).

The uptake of pathogenic/external antigens is monitored by the M cells and the DCs will then internalise these antigens and present them on the major histocompatibility complex II (MHCII). The macrophages present in the Peyer's patches display on their cell surface the CX3CR1 cell surface marker (Cerovic et al., 2014), and are mainly phagocytic and not migratory, suggesting that these macrophages act as activators of regulatory T (Treg) cells in the intestine rather than antigen presenting to T cells (Cerovic et al., 2014).

#### *1.3.3.2. Toll-like receptors (TLRs)*

Among the host immune receptors involved in the recognition of commensal and pathogenic microbes, TLRs play a major role in mediating a relevant immune response, notably as they are involved in making the connection between the innate and adaptive immunity. TLRs are involved especially in the recognition of pathogens and commensal microbes through the recognition of a large range of microbial associated molecular patterns (MAMPs) (Sameer & Nissar, 2021). In addition to their expression by intestinal epithelium cells (see section 1.1.3.), TLRs are expressed by APCs, which are implicated in the recruitment of other immune cells and will shape the immune response against specific types of pathogens (Sameer & Nissar, 2021).

TLRs are organised in dimers, which can be homodimers like for TLR4 and TLR5 or heterodimers, like TLR2/6 or TLR1/2. They can be found on the cell surface, in the endoplasmic reticulum or even secreted (ten Oever et al., 2014). As summarised in Fig. 8, TLRs recognise diverse pathogen-derived ligands, which can be extracellular or intracellular, and of different nature like proteins, nucleic acids, lipids or carbohydrates.

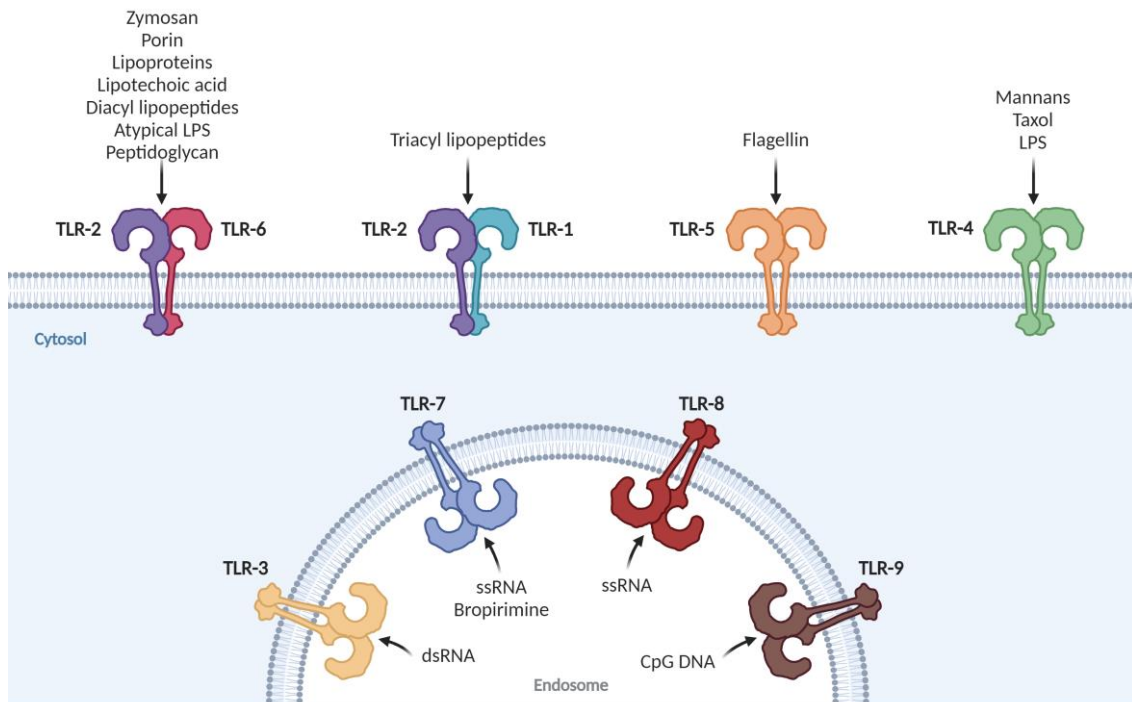


**Figure 8: TLRs in human immunity.**

Diagram showing TLR dimerisation and localisation in the cell and the PAMPs (pathogen-associated molecular pattern) they bind to. These signals culminating in the activation of transcription factors such as nuclear factor- $\kappa$ B (NF- $\kappa$ B) and interferon-regulatory factors (IRFs), which induce, respectively, the production of inflammatory cytokines and type 1 interferon (IFNs). Activation of endosomal TLRs (TLR7 and TLR9) via MyD88 activates NF- $\kappa$ B and also IRF7 leading, respectively, to the production of inflammatory cytokines and type-1 IFNs, while the adaptor protein TRIF is recruited by the endosome-localized receptors TLR3 and toll-like receptor-4 (TLR4). TLR3 can interact directly with TRIF, while the TLR4–TRIF interaction requires the bridging to adaptor molecule TRAM and both activate IRF3 that induce the production of type I IFNs.

Among them, TLR2, that forms heterodimers with TLR1 or TLR6, is implicated in the recognition of a broad range of Gram-positive and Gram-negative bacteria, parasites like *Trypanosoma cruzi* and *Plasmodium falciparum*, fungi, and viruses (Behzadi & Behzadi, 2016; Kawai & Akira, 2010; Qiu et al., 2013). The recognition of TLR1/2 occurs through interaction with pathogen-derived triacylated lipopeptides while the dimer TLR2/6 binds to diacylated lipopeptides (McLeod et al., 2020).

TLR4 forms a homodimer that together with the myeloid differentiation factor 2 (MD-2) is key in recognition of lipopolysaccharide (LPS) and activation of proinflammatory pathways. TLR4 has been shown to recognise monophosphoryl lipid A (MPLA) from *E. coli* F583 LPS (Cabral et al., 2015) but also glycoconjugates like aggregates of amyloid- $\beta$  peptides or  $\alpha$ -synuclein (Cabral et al., 2015; Leitner et al., 2019). The activation of TLR4 through its binding with previously mentioned PAMPs results in the induction of pro-inflammatory cytokines and chemokines like TNF- $\alpha$ , IL-1 $\beta$ , IL-6, IL-8, and MCP-1 that will lead to the recruitment of immune cells to the site of infection (Leitner et al., 2019).

The homodimer TLR5 recognises protein subunits of the bacterial flagella called flagellins (Clasen et al., 2022; Sameer & Nissar, 2021). Its activation leads to the secretion of IL-1 $\beta$  and IL-6 (Sameer & Nissar, 2021).

Finally, TLR3, TLR7, TLR8 and TLR9, which all form homodimers, are located in the endoplasmic reticulum and are involved in the recognition of intracellular pathogen-derived components. TLR3 recognises double stranded pathogens RNA, TLR7 and TLR8 recognise single stranded pathogens RNA while TLR9 binds to cytosine and guanine-abundant DNA (Sameer & Nissar, 2021).

TLRs are implicated in the recognition and control of pathogens proliferation but also in the interaction with commensal bacteria (Kaur & Ali, 2022). For example, the TLR1/2 heterodimer is implicated in the recognition of commensal bacteria *Bacteroides fragilis* through the binding with its polysaccharide A (PSA), leading to the modulation of Treg (Erturk-Hasdemir

et al., 2019; Round et al., 2011) while commensal staphylococcal bacteria have been shown to interact with TLR2 (Lai et al., 2009). In addition, computational and experimental analyses revealed that LPS-derived from the human gut microbiome could silence TLR4 signaling pathway to facilitate host tolerance of gut microbes (d’Hennezel et al., 2017).

#### *1. 3.3.3. C-type lectin receptors (CLRs)*

One of the mechanisms by which microbes in the gut may influence the host immune response is through their interactions with PRRs such as previously mentioned TLRs, NLRs but also C-type lectin receptors (CLRs) expressed on immune cells (Fig. 9).

CLRs bind polysaccharides including a broad range of carbohydrate ligands found on pathogens or commensal bacteria in a Ca<sup>2+</sup>-dependent manner (Tang et al., 2018). CLRs are classified into 17 different subgroups based on their domain types and phylogeny (Brown et al., 2018; Zelensky & Gready, 2005). CLR binding to carbohydrate ligands occurs through the carbohydrate recognition domains (CRDs) (Mayer et al., 2017; Zelensky & Gready, 2005; L. Zhang et al., 2018). A number of carbohydrate ligands have been identified to bind to CLRs with mannan and glucan residues being mostly represented as shown in Fig. 8. In CRDs, amino acid motifs EPN (glutamic acid, proline and asparagine) and QPD (glutamine, proline and aspartic acid) recognise mannose and galactose structures, respectively (Weis et al., 1998; Zelensky & Gready, 2005). However, CLRs can also recognise non-carbohydrate ligands including lipids, inorganic molecules and proteins (Drickamer & Fadden, 2002; Sano et al., 1998; Zelensky & Gready, 2005). CLRs exist as secreted and transmembrane-bound proteins; the latter are particularly important in many biological and cellular processes including immune responses. CLRs such as Dectin-1 (dendritic-cell-associated C-type lectin-1), DC-SIGN (DC-specific intercellular adhesion molecule-3-grabbing non-integrin), SIGN-R1 (specific intercellular adhesion molecule-3-grabbing nonintegrin-related 1) (mouse homologue of human DC-SIGN) and Dectin-2 are found on innate and adaptive immune cells and are

important for the recognition of pathogenic, opportunistic or commensal microorganisms (see for example Mayer et al., 2017).

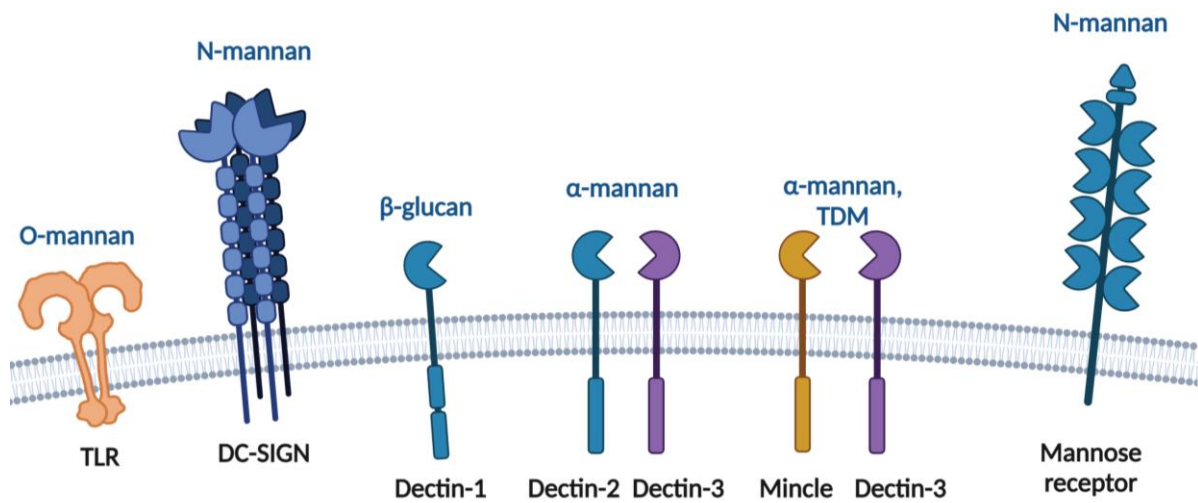


**Figure 9: Examples of PRRs on immune cells.**

PRRs found in human immune cells and their corresponding PAMPs. The human immune cells PRR repertoire present on the cell surface include TLRs and CLRs (which are comprised of DC-SIGN, Dectin-1, Dectin-2/Dectin-3 dimers, Mincle and Dectin-3 dimers and mannose receptors).

#### 1. 3.3.3.1. Dectin-1

Dectin-1 can be found on the cell surface of macrophages or specific subtypes of T-cells (Kalia et al., 2021). This CLR is involved in the recognition of  $\beta$ -(1,3) glucans and  $\beta$ -(1,6) glucans, present on fungal cell surfaces from *Saccharomyces cerevisiae*, *Pneumocystis carinii*, *Candida albicans*, *Candida tropicalis* or *Aspergillus fumigatus* (Iliev et al., 2012; Taylor et al., 2007). Dectin-1 has been associated with immune response and inflammation through cell signalling leading to the induction of cytokine secretion and macrophages recruitment. This signalling is mediated by the immune receptor tyrosine-based activation motif (ITAM)-recognition motif in Dectin-1 intracellular region which is involved in the activation nuclear factor of activated T-cells (NFAT) pathway, leading to the expression of immunity related genes (Kalia et al., 2021). Dectin-1 has been implicated in the defence against fungal pathogens, but also play important roles in immune responses to other pathogens such as bacteria, viruses and nematodes.

#### 1. 3.3.3.2. Dectin-2

Dectin-2 is found on the cell surface of macrophages and DCs (McGreal et al., 2006). It shows specificity for mannose-composed polysaccharides like  $\alpha$ -mannan (polysaccharides composed mainly of  $\alpha$ -mannose residues) (Porter & Martens, 2017) or mannose-capped lipoarabinomannan (Yonekawa et al., 2014) and has been implicated in the recognition of several commensal fungi like *S. cerevisiae* or *Kazachstania unispora* (Lamprinaki et al., 2017). This CLR interacts with mannose residues present on bacterial pathogens like *Streptococcus pneumoniae*, *Hafnia alvei*, *Salmonella enterica*, but also fungi such as *C. albicans*, *A. fumigatus*, *Mycobacterium tuberculosis*, *Microsporium audounii*, *Trichophyton rubrum*, *Paracoccoides brasiliensis*, *Histoplasma capsulatum* and capsule-deficient *Cryptococcus neoformans* (Akahori et al., 2016; Graham & Brown, 2009; Ifrim et al., 2016; McGreal et al., 2006; Robinson et al., 2009; Sato et al., 2006; Sun et al., 2014; Wittmann et al., 2016).

To induce a signalling pathway, Dectin-2 does not display an ITAM domain (Robinson et al., 2009), instead, Dectin-2 binds to an Fc receptor  $\gamma$  chain working as an adapter molecule to activate the signalling pathway leading to the host immune response (Sato et al., 2006). The action of Dectin-1 and Dectin-2 are crucial for the establishment of homeostasis in the gut as it has been shown that the deletion of both Dectin-1 and Dectin-2 in mice triggers a shift in microbial gut environment and bacterial population, further protecting the host against colitis (Y. Wang et al., 2022).

#### 1. 3.3.3.3. DC-SIGN/SIGN-R1

DC-SIGN recognises polysaccharides characterised by high content of mannose or fucose residues as well as Lewis antigens (Jarvis et al., 2019). This CLR is expressed on the cell surface of intestinal DCs and macrophages, but also on tissues like the placenta or the lung (Geijtenbeek et al., 2000). DC-SIGN has been involved in the recognition of commensal bacteria such as *Lactobacillus rhamnosus* or *Lactobacillus acidophilus* strains (Konieczna et al., 2015). SIGN-R1, the murine homologue of human DC-SIGN, recognises dextrans (Geijtenbeek

et al., 2002) and has been implicated in the host defence against *C. albicans* or *Yersinia pestis* strain 1418 (Takahara et al., 2012; Yang et al., 2019; Y. Zhang et al., 2020) as well as in the recognition of strains of the gut commensal bacteria *Limosilactobacillus* (formally *Lactobacillus* (Nakamura et al., 2023)) *reuteri* (Bene et al., 2017) and *Propionibacterium* strain UF1 (Colliou et al.(Colliou et al., 2017)).

## 1.4. Bacterial cell surface polysaccharides

### 1.4.1. Structure and biosynthesis

In addition to the cell wall polysaccharides described in section 1.2.3, Gram-positive and Gram-negative bacteria produce additional species-specific polysaccharides that can be tightly linked to the cell surface forming a capsular polysaccharide (CPS), loosely attached to the extracellular surface, or secreted to the environment as exopolysaccharides (EPS) (Tytgat & Lebeer, 2014; DiLorenzo, 2022). These polysaccharides are implicated in the interaction with the environment of the bacteria and can affect host-bacteria interactions and associated immune responses (Messner et al., 2013). Although they have mainly studied in pathogens due to their role in pathogenesis (Poole et al., 2018), these polysaccharides also play important roles in the interaction between gut commensal bacteria and the host. For example, *B. fragilis* and *Bacteroides thetaiotaomicron* produce CPSs [composed of 2-acetamido-4-amino-2,4,6-trideoxygalactose, Gal and GalNAc for *B. fragilis* (Baumann et al., 1992) and GlcNAc, Glc, Man and galacturonic acid (GalA) for *B. thetaiotaomicron* (Porter et al., 2017)] that interact and influence the host immunity (S. Hsieh et al., 2020; Sittipo et al., 2018) (see section 1.3.2.). Strains of *Lactobacillus* and *Bifidobacterium*, many of them with probiotic properties, produce EPS acting as a protective surface layer against antimicrobial peptides or physiological threats found in the GI tract such as low pH in the stomach and bile salts in combination with pancreatic enzymes in the duodenum. EPS also permit interacting with the surrounding environment (for a review, see Castro-Bravo et al. (2018)). And immune modulation (Hidalgo-Cantabrana et al., 2012). In the human gut, EPS produced by

bifidobacterial taxa such as *Bifidobacterium breve* and *Bifidobacterium longum* subsp. *Longum* is mainly composed of glucose, galactose, and rhamnose (Fanning, Hall, Cronin, et al., 2012; Inturri et al., 2017). The anti-inflammatory bacterium *Faecalibacterium prausnitzii*, member of the Firmicutes phylum and one of the most abundant species in healthy human colon, underrepresented in the microbiota of IBD patients, produces a cell surface polysaccharide (of which composition and structure are yet unknown) shown to modulate intestinal immunity (Rossi et al., 2015). Cell surface polysaccharides also play an important role in nutrition of the bacteria as they provide storage for nutrient acquisition, but also by allowing the cross feeding of gut microbiota species. For example, the digestion of inulin by a GH secreted by *Bifidobacterium ovatus* is dispensable for its own usage of the fiber yet allows *Bacteroides vulgatus* to feed on the produced saccharides (like arabinogalactan, inulin, pectin, xanthan gum or xylitol) (Rakoff-Nahoum et al., 2016).

These structures are often containing different type of monosaccharides and assembled in a linear or branched fashion to form polysaccharides of various sizes (from  $10^3$  to  $10^5$  Da in order of magnitude) (Sali et al., 2019; X. Wang et al., 2022), as shown in Table 1).

**Table 1: Examples of cell surface polysaccharide structures found on commensal bacteria.**

Description of the bacterial species source, its Gram coloration, the cell surface glycosylation type and its structure: blue round: Glc, yellow round: Gal, green triangle: Rha, blue square: GlcNAc, yellow square: GalNAc.

| Species/strain                        | Gram     | Polysaccharide class | Structure   | Reference                |
|---------------------------------------|----------|----------------------|---|--------------------------|
| <i>Lactobacillus johnsonii</i> FI9785 | Positive | EPS                  |   | (Dertli et al., 2013)    |
| <i>Lactobacillus brevis</i> E25       | Positive | EPS                  |   | (Dertli et al., 2018)    |
| <i>Lactobacillus helveticus</i> SNA12 | Positive | EPS                  |   | (X. Wang et al., 2022)   |
| <i>Bifidobacterium bifidum</i> PRI1   | Positive | CPS                  | $\beta$ -(1 $\rightarrow$ 6)-glucan, $\beta$ -(1 $\rightarrow$ 4)-galactan, $\beta$ -(1 $\rightarrow$ 6)-galactan, $\beta$ -galactofuranan and starch | (Speciale et al., 2019)  |
| <i>B. breve</i> YIT 4007              | Positive | EPS                  |   | (Habu et al., 1987)      |
| <i>B. longum</i> BIM B-476-D          | Positive | EPS                  |   | (Valueva et al., 2013)   |
| <i>B. thetaiotaomicron</i> VPI-5482   | Negative | CPS                  | 22% GlcNAc, 33% Glc, 9% Man, 36% GalA   | (Porter et al., 2017)    |
| <i>Bacteroides vulgatus</i> IMCJ 1204 | Negative | CPS                  |   | (Hashimoto et al., 2001) |

There are two types of EPS, homopolysaccharides (HoPS) and heteropolysaccharides (HePS), synthesised by *Bifidobacterium* and *Lactobacillus*. The *eps*-clusters harbour genes coding for glycosyltransferases, involved in the biosynthesis of the repeating units, proteins related to polymerisation and export of these units, as well as other genes with unknown functions including mobile elements. In addition, genes involved in the regulation of HePS synthesis are detected in lactobacilli but not in bifidobacterial *eps* clusters (Hidalgo-Cantabrana, Nikolic, et al. (Hidalgo-Cantabrana, Nikolic, et al., 2014). The *Bifidobacterium* genus contains 9 *eps* gene clusters conserved among different bifidobacterial species and a further 44 unique *eps* loci, together representing a large proportion of the inter(sub)species variability identified among bifidobacterial genomes (Ferrario et al., 2016; Hidalgo-Cantabrana, Sánchez, et al., 2014).

EPS are important actors in the health of the gut microbiota as it plays an important role in its homeostasis. For example, *L. johnsonii* strain FI9785 produces two EPS types with different structures involved in colonisation of the gut and competitive exclusion of pathogen *Clostridium perfringens* (Dertli et al., 2013). EPS isolated from *L. rhamnosus* strain ZFM231 when administrated to dextran sulfate solution (DSS)-induced IBD mice, was able to re-establish a healthy gut microbiota diversity and composition at the phylum and genus level (C. Wan et al., 2022).

*Bifidobacterium* is one of the most studied genus of the gut microbiota and comprises several species and strains inhabiting the GI tract (Azad et al., 2018). A large panel of EPS originating from this genus have been characterised (examples presented in Table 1) and shown to be associated with gut homeostasis and host immunity. These EPSs protect the bifidobacterial species against pathogens that can be found in the GI tract, therefore helping their persistence in the gut (Hidalgo-Cantabrana, Nikolic, et al., 2014). Bifidobacterial EPS has also been implicated in the modulation of the gut microbiota, helped through the cross feeding of several species, maintaining the gut population into homeostasis (Sabater et al., 2020). Indeed, the administration of *Bifidobacterium animalis* subsp. *Lactis* strains (DMS10140 and S89L) induced an increased abundance of the *Firmicutes* phylum and the *Alloprevotella* genus in healthy mice gut. Nonetheless, differences were also seen at the strain level: *B. animalis*

strain DMS10140 induced an increase of *Intestinomonas* genus while *B. animalis* strain S89L induced an increase of the *Faecalibaculum* genus and the *Erysipelotrichaceae* and *Lactobacillaceae* families (Sabater et al., 2020). In contrast, *B. breve* strain IPLA20004 EPS inhibited the growth of the commensal bacteria *B. thetaiotaomicron* strain DSM-2079 *in vitro* (Rios-Covian et al., 2013).

Finally, EPSs from Bifidobacteria species play a crucial role in the protection of the bacteria against the host immunity. For example, *B. breve* strain UCC2003 EPS promoted the reduction in immune reactivity from the host through the reduction of B cell response, while it was also implicated in the reduction of gut pathogen *Citrobacter rodentium* colonisation in mice (Fanning, Hall, & van Sinderen, 2012). Also, *B. longum* strain BCRC 1464 EPS induced the secretion of anti-inflammatory IL-10 and reduced LPS-induced pro-inflammatory TNF- $\alpha$  production in J774A.1 macrophages cells (M. H. Wu et al., 2010). In addition, *Bifidobacterium* EPSs have the ability to counteract the cytotoxic effect of some pathogen toxins (like from *Bacillus cereus* and *Streptococcus pyogenes*) on epithelial Caco2 cells and rabbit erythrocytes *in vitro* (Ruas-Madiedo et al., 2010).

CPSs from *Bacteroidetes* are encoded by diverse *cps* biosynthetic loci as shown in *B. thetaiotaomicron* (Porter et al., 2017), *B. fragilis* (Coyne & Comstock, 2008; Patrick et al., 2010), and human gut microbiome (Donia et al., 2014), underscoring the importance of CPS diversity to the fitness of bacteria that inhabit the gut. Indeed, the diversity of CPS harboured by microbiota species enables the modulation of immune responses to dominant antigens as they can be co-expressed on the bacterial cell surface (S. Hsieh et al., 2020; S. A. Hsieh et al., 2020; S. A. Hsieh et al., 2021). This diversity in CPS expression is therefore a demonstration of the long establishment of gut microbiota species adaptation to evade host immunity.

#### 1.4.2. Effect on gut homeostasis and immunity

Although cell surface polysaccharides have mainly been studied in the context of pathogen-host interaction, more recent work highlighted them as important factors of the symbiotic interaction between the gut microbiota and the host, they are involved in several mechanisms like the tolerogenesis or the resistance to antimicrobial peptides (see S. A. Hsieh & Allen (2020) for a review).

In the gut, CPS protects bacteria from host and environmental factors and these CPS can be phase variable. For example, the gut symbiont *B. thetaiotaomicron* VPI-5482 expresses eight different CPS to help adapt to various niches such as immune, bacteriophage, and antibiotic perturbations (S. Hsieh et al., 2020; S. A. Hsieh et al., 2021; Porter et al., 2017). The ability of *B. thetaiotaomicron* VPI-5482 to switch between multiple capsules confers increased fitness in the mouse gut (Porter et al., 2017). *B. thetaiotaomicron* CPS can be either pro-stimulatory or anti-stimulatory, resulting in inhibiting antigen (Ag) delivery to the immune system or activating Ag-specific T cell response (S. Hsieh et al., 2020; Sittipo et al., 2018). *B. fragilis* strain NCTC 9343 produces a PSA, a capsular polysaccharide which has, on host immunity, an anti-inflammatory effect through the induction of IL-10 by CD4<sup>+</sup> T cells (Blandford et al., 2019; S. Hsieh et al., 2020).

Altogether, these data support the importance of cell surface polysaccharides as major players of the interaction between the bacteria and the host in the gut microbiota.

### 1.5. *Ruminococcus gnavus*

#### 1.5.1. Role in health and disease

*Ruminococcus gnavus* is a Gram-positive, strictly anaerobic, non-spore forming bacterium, from the *Firmicutes* phylum, *Clostridia* class, *Clostridiales* order and *Lachnospiraceae* family. *R. gnavus* is present from the early life of infants where it has been found in the gut of 90% of 1 month to 2 years old infants (Lagkouvardos et al., 2023; Nilsen et al., 2020; Sagheddu et

al., 2016). *R. gnavus* persists across the lifetime as a component of the adult gut microbiota where it has been found in 90% of human faecal samples from healthy adults and represent on average 0.3% of the whole gut microbiota (Candeliere et al., 2022; Kraal et al., 2014; Qin et al., 2010).

Although *R. gnavus* is part of the healthy human gut microbiota, it shows disproportionate representation in gut and non-gut related diseases such as IBD (Hall et al., 2017), but also autism (Chua et al., 2018), hyperactivity (L. Wan et al., 2020), anxiety (Jiang et al., 2018), chronic heart failure (Cui et al., 2018), obesity and metabolic syndromes (Grahne et al., 2022), type 2 diabetes (Ruuskanen et al., 2022), malnutrition (Subramanian et al., 2014), cystic fibrosis (Debyser et al., 2016), allergy (de Filippis et al., 2021), depression (Chahwan et al., 2019), lupus (Azzouz et al., 2019; J. W. Kim et al., 2019) and irritable bowel syndrome (IBS) (Baumgartner et al., 2021; Čipčić Paljetak et al., 2022). These associations have been identified through metagenomic studies but in most cases, causality remains to be demonstrated.

An increased number of mouse studies have been performed to better understand the role of *R. gnavus* in health and disease. For example, in gnotobiotic mice, the addition of *R. gnavus* was shown to ameliorate growth and metabolic abnormalities in animals receiving faecal transplantation from undernourished infants aged 6–18 months (Blanton et al., 2016). *R. gnavus* mediated the catabolism of dietary phenylalanine and tryptophan to phenethylamine and tryptamine, respectively, that stimulated serotonin biosynthesis leading to elevated GI transit and colonic secretion which are characteristics to IBS symptoms (Zhai et al., 2023). Indeed, *R. gnavus* strains have been shown to produce tryptophan decarboxylase, an enzyme responsible for decarboxylation of tryptophan to tryptamine, a compound affecting GI motility through the transport of food but also commensal cells along the gut (Williams et al., 2014). The administration of *R. gnavus* ATCC 29149 induced in BALB/C mice the reduction of ovalbumin-induced atopic dermatitis symptoms through the enhancement of Treg cells (Ahn et al., 2022). *R. gnavus* has also been shown to influence brain regulation of spatial working memory behaviour in mice (Coletto et al., 2022).

Despite the positive association of *R. gnavus* with IBD, mouse studies showed that *R. gnavus* ATCC 29149 supplementation led to enhanced regenerating islet-derived protein 3 $\gamma$  (Reg3 $\gamma$ ) expression, an important antimicrobial peptide produced in gut epithelial Paneth cells, that helps maintain spatial segregation between the epithelium and the microbiota and promotes gut homeostasis (Surana & Kasper, 2017; Vaishnava et al., 2011). As a result, *R. gnavus* reduced colitis in gnotobiotic mice due to its interaction with immune and gut epithelial cells (Surana & Kasper, 2017). A further study supported these findings by showing that *R. gnavus* ATCC 29149 led to a decrease in the severity of inflammation in mouse models of colitis (Grabinger et al., 2019). On the other hand, germ-free mice colonised with *R. gnavus* lacking CPS (ATCC 35913) showed increased gut inflammation compared to those colonised with an encapsulated *R. gnavus* strain ATCC 29149 (Alrafas et al., 2019; Henke et al., 2021; S. Yu et al., 2020) (see section 1.4.3.).

Taken together, these studies underscore the importance of *R. gnavus* strain-specificity in driving an inflammatory response in gnotobiotic mice.

#### 1.5.2. *R. gnavus* factors of colonisation

The ability of *R. gnavus* to utilise mucin polysaccharides is strain dependent: unlike *R. gnavus* ATCC 29149 or ATCC 35913 strains which have the capacity to metabolise mucin polysaccharides and grow on mucin as sole carbon source (Crost et al., 2013, 2016), *R. gnavus* E1 is unable to grow on mucin as sole carbon source. *R. gnavus* strains have been shown to interact with the intestinal mucus layer through different mechanisms, one of this is the use of glycoside hydrolases (GHs), which are enzyme involved in the cleavage of saccharide, therefore allowing the bacteria to uptake saccharides from the mucin polysaccharides to use those as nutrient carbon sources. These strains differ in the repertoire of responsible for the cleavage of specific glycosidic bonds. The ability of *R. gnavus* strains to grow on mucins is mostly based on their capacity to metabolise mucin polysaccharide epitopes such as fucose, sialic acid or blood group antigens (Bell et al., 2019; Crost et al., 2013, 2016; H. Wu, Crost, et

al., 2021; H. Wu, Rebello, et al., 2021). *R. gnavus* ATCC 29149 and ATCC 35913 strains harbour in their genome an operon of genes called the *nan* cluster dedicated to the transport and metabolism of sialic acid (Crost et al., 2013; 2016). This cluster also contains a gene encoding an intramolecular *trans*-sialidase belonging to the GH33 family which cleaves off Neu5Ac (sialic acid) from mucin to release 2,7-anhydro-Neu5Ac instead of Neu5Ac, which will be bound to a target acceptor unindentified for now (Tailford et al., 2015). This *trans*-glycosylation product is then transported into the cell via a 2,7-anhydro-Neu5Ac specific transporter and metabolised inside the cell, conferring *R. gnavus* strains with a competitive nutritional advantage in the mucus niche (Bell et al., 2019; 2020).

Although *R. gnavus* E1 strain does not have such mucin polysaccharide metabolic pathways this strain has developed alternative mechanisms to interact with mucus. *R. gnavus* E1 has been shown to enhance Muc2 mucin expression by goblet cells, modulate mucin polysaccharide composition in mice (Graziani et al., 2016), and produce an adhesin called RadA which was shown to preferentially bind human immunoglobulins (IgA and IgG), and Gal and GalNAc residues in mucin polysaccharide chains *in vitro* (Maresca et al., 2021). In addition, *R. gnavus* E1 produces antimicrobial molecules such as Ruminococcin C, a peptide with anti-*Clostridium perfringens* activity (Balty et al., 2019; Chiumento et al., 2019; Roblin et al., 2021), which may contribute to *R. gnavus* fitness in the gut and maintain the homeostasis of the microbiota (Roblin et al., 2021).

### 1.5.3. Cell surface carbohydrate composition

*R. gnavus* strain ATCC 29149 has been shown to produce a glucorhamnan on the cell surface with pro-inflammatory properties *in vitro* using murine bone marrow-derived DCs (mBMDCs) (Henke et al., 2019). The rhamnose backbone of this glucorhamnan is made from (1,2)- and (1,3)-linked rhamnose units, and the sidechain has a terminal glucose linked to a (1,6)-glucose (Fig. 10A). The pentasaccharide repeat of glucorhamnan was sufficient to induce an immune

response and a release of inflammatory cytokines like TNF- $\alpha$  and IL-6 from mBMDCs through TLR4 recognition (Haynie et al., 2021).

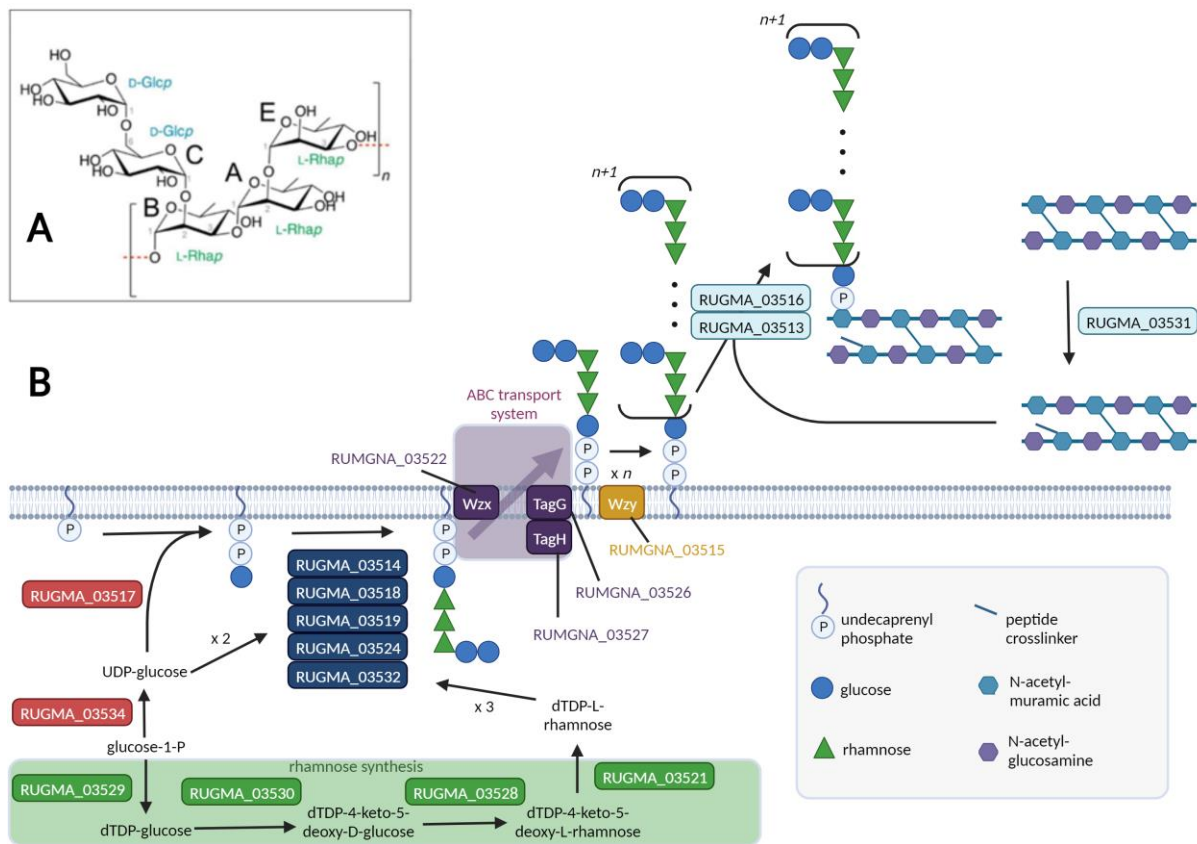


**Figure 10: *R. gnavus* ATCC 29149 cell surface glucorhamnan.**

(A) Polysaccharide structure composed of a rhamnose backbone and a glucose side chain. (B) Biosynthetic pathway allowing the production and translocalisation of the glucorhamnan present on ATCC 29149 cell surface: monosaccharide precursors are synthesized, assembled into the repeating unit, transported across the membrane, where they are polymerized to form the full-length glucorhamnan, which is then covalently attached to the peptidoglycan. Redrawn from Henke et al. (2019).

The biosynthetic pathway of glucorhamnan has been identified in *R. gnavus* ATCC 29149 strain (Henke et al., 2019). Fig. 10B provides a model of how monosaccharide precursors are produced, assembled into repeating units and then transported across the membrane before being polymerised into full length glucorhamnan which is then covalently bound to the PG layer (Henke et al., 2019).

In a follow up study, it was shown, that in addition to glucorhamnan, some strains of *R. gnavus*, such as ATCC 29149, display on their cell surface a CPS with a molecular weight of more than 100 kDa. Monosaccharide analysis revealed the capsule to be composed of glucose, *N*-acetylquinovosamine, and *N*-acetylgalactosamine in roughly a 6:2:1 stoichiometry, which is in accordance with the *cps* gene cluster, which contains nine glycosyltransferases—one for each of the monosaccharides in the repeating unit (see Fig. 11)Click or tap here to enter text. (Henke et al., 2019). This CPS has been shown to mute the immune response as *R. gnavus* strains displaying it (such as ATCC 29149) induce little to no cytokine production by innate immune cells *in vitro* and *in vivo*, unlike *R. gnavus* strains not displaying this CPS on their cell surface (such as ATCC 35913) which induce a pro-inflammatory immune response (Henke et al., 2021). In this study, germ-free mice were colonised with *R. gnavus* strain RJX1120 displaying the CPS on its cell surface had higher percentage of FOXP3<sup>+</sup>-Treg cells accumulating in the lamina propria, while a higher percentage of CD62L<sup>+</sup>-T cells were induced in the lamina propria of mice colonised with the CPS-free strain RJX1120 (Henke et al., 2021). Another question remaining uninvestigated is the potentiality of the growth condition influence on the bacterial cell surface glycosylation: indeed, *R. gnavus* strains evolving in different niche of the GI tract, it is therefore possible that the bacteria adapt the cell surface polysaccharide composition it displays on its cell surface.

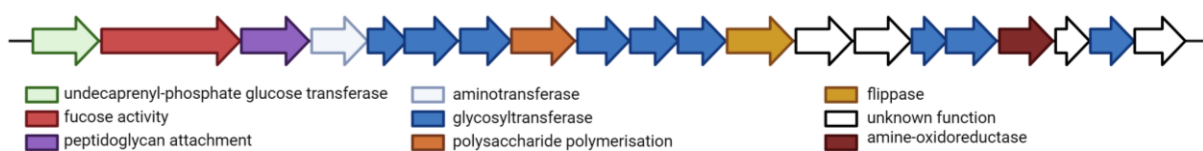


**Figure 11: *R. gnavus* ATCC 29149 *cps* biosynthesis cluster.**

Genes present in the ATCC 29149 *cps* cluster with their annotation name (shortened of ATCC 29149 locus convention from RUMGNA\_02411 on the far left to RUMGNA\_02392 on the far right). Each gene is colour based on associated activity of encoded proteins displayed underneath the gene cluster.

Together, these studies show the importance of *R. gnavus* in health and disease and highlight the importance of defining the immunomodulatory properties of *R. gnavus* at a strain level. This study will focus on *R. gnavus* ATCC 29149 which is the type strain of this species and

strains E1 and ATCC 35913, previously mentioned, each having shown their importance in the relation with the host.

## 1.6. Aim and Objectives

In this work, we hypothesised that *R. gnavus* cell surface glycosylation is strain/niche-dependent, contributing to differential health and disease outcome of *R. gnavus* strains in humans.

Specific aims include:

### 1. To characterise *R. gnavus* cell surface polysaccharide composition

- To screen cell surface polysaccharide epitopes of *R. gnavus* strains (E1, ATCC 29149, ATCC 35193) grown on different carbohydrate source using a flow cytometry lectin binding assay.
- To use bioinformatics tools to identify the genes involved in the glucorhamnan and *cps* biosynthetic pathway across *R. gnavus* strains
- To decipher the structural composition of *R. gnavus* cell surface polysaccharides by NMR and MS approaches

### 2. To study the effect of *R. gnavus* strain-specific cell surface glycosylation on host immune response *in vitro*

- To determine the effect of *R. gnavus* strains and associated glucorhamnan on gut barrier function using intestinal epithelial cell models
- To investigate the effect of *R. gnavus* strains and associated glucorhamnan on host immune response using reporter cells and immune cells

Understanding the relationship between *R. gnavus* strains and the host at a molecular level will help us to design microbiota-targeted strategies to promote host health.

## Chapter 2: Material and Methods

## 2.1. Bacterial growth assays

### 2.1.1. Bacterial strains and growth conditions

*R. gnavus* ATCC 29149 was isolated by Moore & Holdeman, (1974) Moore & Holdeman, (1974) and characterised by Moore, W E C; Johnson & Holdeman, Moore, W E C; Johnson & Holdeman, (1976), *R. gnavus* E1 was isolated by Ramare et al., (1993) and *R. gnavus* ATCC 35913 was isolated from healthy human faeces (Hoskins et al., 1985). Several growth media were used in this study. BHI-YH [brain heart infusion broth (Oxoid LTD, UK) supplemented with 5 g/l of Bacto™ yeast extract (Becton, Dickinson and Company, Sparks, MD) and 5 mg/l of haemin (Sigma-Aldrich, USA)] was used as rich medium. LAB medium (Tramontano et al., 2018) was used as minimum medium (composition described in Supplementary data 1). When specified, LAB was supplemented with 27.7 mM of mono- or oligosaccharides as sole carbon source. Glycerol stocks of the three *R. gnavus* strains (E1, ATCC 29149 and ATCC 35913), containing 50% of an overnight culture in BHI-YH and 40% glycerol, were prepared and stored at -80°C. For growth assays, *R. gnavus* E1, ATCC 29149 and ATCC 35913 were grown at 37°C in an anaerobic cabinet (85% N<sub>2</sub>, 10% H<sub>2</sub>, 5% CO<sub>2</sub>) (Don Whitley, Shipley, UK). First, starter cultures were prepared by inoculating BHI-YH medium at 4% (v/v) from glycerol stocks and grown for 24 h. Then for cultures in BHI-YH, the medium was inoculated at 2 % (v/v) with the starter culture. For cultures in LAB-based media, an aliquot of the starter culture was centrifuged and the cell pellet resuspended in the same volume of LAB. The LAB-based medium was then inoculated at 2 % (v/v) with this cell suspension. The growth was monitored by measurement of the optical density at 600nm (OD<sub>600nm</sub>) or by qPCR (see section 2.1.3.).

To determine the correlation between OD<sub>600nm</sub> and the concentration of cells, *R. gnavus* strains were cultured in BHI-YH for 24 h and the OD<sub>600nm</sub> was monitored throughout the 24h-growth. Cells from 1 ml of culture were collected at 8 h and 24 h, and the bacterial gDNA was extracted. The number of copies of 16S rRNA gene per mL of culture was quantified by qPCR for each timepoint (see section 2.1.3.). Since the number of copies of 16S rRNA gene per genome is known, it is then possible to determine the number of bacterial cells per mL of culture. The ratio between OD<sub>600nm</sub> and the concentration of cells can then be determined.

### 2.1.2. Transmission electronic microscopy (TEM)

For electronic microscopy, 1 ml of *R. gnavus* ATCC 29149 and ATCC 35913 grown for 18 h in BHI-YH were centrifuged for 5 min at 10'000 x g. The pellet was resuspended in 1 ml PBS and submitted for TEM analysis by negative staining. TEM grids (carbon-coated, copper grids, product number AGS160-4H, Agar Scientific, UK) were prepared by glow discharging using a Leica ACE200 (Leica Microsystems, UK) immediately before use. The samples were then prepared (in duplicate) by pipetting 10 µl of sample onto each grid, leaving for 1 minute, then wicking the excess liquid off using filter paper. Then 10 µl of 2% uranyl acetate (aqueous) was pipetted onto the grids, left for 1 minute then wicked off and allowed to thoroughly dry. The grids were imaged in an FEI Talos F200C TEM (Thermo Scientific, UK) at 200kV, using a Gatan OneView camera (Gatan, UK).

### 2.1.3. Quality control of *R. gnavus* glycerol stocks

PCR was used on *R. gnavus* strains to check culture integrity. First, 15 µl of cell culture were centrifuged at 17,000 x g for 3 min, then the supernatant was discarded and the cells were resuspended in 50 µl of sterile water. PCR mix was made with 2.5 µl of cell suspension, with 200 µM of each primer (listed in Table 2) and 5 µl of HotStarTaq Plus MasterMix (HotStarTaq DNA Polymerase, PCR buffer with 3 mM MgCl<sub>2</sub>, and 400 µM of each dNTP) (Qiagen, Hilden, Germany). Positive controls were prepared for each primer pair using purified genomic DNA of the appropriate strain (Table 2). The PCR program was as suggested by the supplier (starting step: 95°C for 5 min; 40 cycles: 94°C for 30 s, 60°C for 30 s and 72°C for 1 min; final extension: 72°C for 10 min). The PCR products (5 µl of the samples mixed with 1 µl of Midori Green Dye) were analysed by electrophoresis on agarose gel (2.5%) using TAE buffer (40 mM Tris (pH 7.6), 20 mM acetic acid, 1 mM EDTA). The gels were also loaded with HyperLadder IV (Bioline) (5 µl) or of Gibco/Invitrogen 100 bp ladder (5 µl), mixed with Midori Green dye (0.5 µl). The migration was set on 130 V for 45 min and the gel imaged under UV light using an Alphaimager.

**Table 2: List of primers used for quality control of *R. gnavus* glycerol stocks.**

| Primers             | Gene target (source)  | Source of the gDNA used as positive control | Amplicon size |
|---------------------|---|---|---------------|
| UniF/R              | 16S rRNA gene (all bacteria)  | <i>R. gnavus</i> E1                         | 147 nt        |
| 16SRg5F/R           | 16S rRNA gene ( <i>R. gnavus</i> )  | <i>R. gnavus</i> E1                         | 57 nt         |
| ATCC-02694-F/R      | RUMGNA_02694 ( <i>R. gnavus</i> ATCC 29149); RGNV35913_01292 ( <i>R. gnavus</i> ATCC 35913) | <i>R. gnavus</i> ATCC 29149                 | 61 nt         |
| 29149-02237-F3/R3   | RUMGNA_02237 ( <i>R. gnavus</i> ATCC 29149)   | <i>R. gnavus</i> ATCC 29149                 | 79 nt         |
| 29149-03003-F2/R2   | RUMGNA_03003( <i>R. gnavus</i> ATCC 29149)  | <i>R. gnavus</i> ATCC 29149                 | 64 nt         |
| ATCC 35913-C-F/R    | RGNV35913_03482( <i>R. gnavus</i> ATCC 35913)   | <i>R. gnavus</i> ATCC 35913                 | 83 nt         |
| E1-60291-F3/R3      | RUGNEv3_60291( <i>R. gnavus</i> E1)   | <i>R. gnavus</i> E1                         | 76 nt         |
| E1-60040-F3/R3      | RUGNEv3_60040( <i>R. gnavus</i> E1)   | <i>R. gnavus</i> E1                         | 114 nt        |
| RF1br730F/Clep866mR | 16S rRNA gene ( <i>Ruminococcus</i> spp.)   | <i>R. bromii</i> L2-63                      | 157 nt        |
| BifF/g-Bifid-       | 16S rRNA gene ( <i>Bifidobacterium</i> spp.)  | <i>B. adolescentis</i> L2-32                | 128 nt        |

#### 2.1.4. Bacteria quantification by qPCR

For bacteria quantification by qPCR, the bacteria were pelleted by centrifugation for 5 min at 10,000 x g and kept at -20°C until extraction. The DNA was extracted from the cell pellets using the GeneJET Genomic DNA Purification Kit (Thermo Fisher, USA) according to the manufacturer's instructions for Gram-positive bacteria. The extracted DNA was stored at -20°C until use. DNA was quantified using Qubit 2.0 Fluorometer (Thermo Fisher, USA). For

the qPCR, primers targeting 16S rRNA gene of all bacteria (UniF/R) and of *R. gnavus* (16SRg5F/R) were used (Table 2). The full-length 16S rRNA gene of *R. gnavus* ATCC 29149 previously amplified by PCR (Crosthair et al., 2018) was used to produce a standard curve with Ct values ranging from  $10^2$  to  $10^7$  copies per well. This was then used to calculate the 16S amount present in each sample from their Ct value. Briefly, 2  $\mu$ l of DNA at 1 ng/ $\mu$ l or a standard, 200  $\mu$ M of each primer (listed in Table 2) and 5  $\mu$ l QuantiFast SYBR Green PCR Master Mix (Qiagen, Hilden, Germany) were added to each well of a 96-well plate. The qPCR was run on a ABI7500 Real-Time PCR System (Thermo Fisher, USA). The device program was set at 95°C for 5 min followed by 40 cycles at 95°C for 10 s and 60°C for 35 s then 72°C for 1 min, followed by a dissociation stage comprising a step of temperature gradual decrease between 95°C and 60°C for 1 min, repeated twice. A linear standard curve was produced by plotting the Ct values obtained with the standards in the Y-axis against the log of 16S rRNA gene copies in the X-axis. This standard curve was used to determine the 16S copy number in the samples.

## 2.2. *R. gnavus* gene transcription analysis

### 2.2.1. RNA extraction and cDNA production

The strains ATCC 29149 and ATCC 35913 were grown in BHI-YH and ATCC 35913 was also grown in LAB supplemented with 27.7 mM melibiose (chosen following results obtained in section 3.2.1.). Two ml of culture were collected after 6 and 24 h of growth and 400  $\mu$ l of phenol-ethanol solution [phenol pH 4.3-ethanol (1:9)] was added to the collected culture which were then kept on ice for 30 min following addition of phenol-ethanol solution. The cells were harvested by centrifugation at 10,000 x g for 5 min at 4°C and then kept at -80°C until RNA extraction. This method was used in order to avoid the use of manufactured nucleic acid extraction kits do not allow to extract *R. gnavus* strain E1 DNA efficiently.

For RNA extraction, cells were resuspended in 500  $\mu$ l of TES buffer (50 mM Tris, 5 mM EDTA, 50 mM NaCl, pH 7.5) and lysed with the FastPrep-24™ Classic beadbeater (MP Biomedicals, US) following addition of 1 ml (ratio 2:1 bead volume/TES buffer) of 100  $\mu$ m beads using 3

cycles of 40 s each with 5-min rest on ice in between. Following centrifugation at 10,000 x g at 4°C for 10 min, the supernatant was collected and mixed with 600 µl of phenol and 100 µl of chloroform, the suspension was then centrifuged at 17,000 x g at 4°C for 5 min. The supernatant was collected and 600 µl of chloroform added to the supernatant. Following centrifugation at 17,000 x g at 4°C for 5 min, the supernatant was collected and 20 µl of sodium acetate (3 M, pH 5; final concentration: 78 mM) and 550 µl of ice cold 95% ethanol were added to 200 µl of the supernatant. Following 20 min incubation at -80°C, the samples were then centrifuged at 17,000 x g at 4°C for 20 min. The pellet was washed with 70% ethanol and centrifuged at 17,000 x g at 4°C for 5 min. The samples were air-dried and resuspended in 200 µl RNase free water (Qiagen, Hilden, Germany). The purified RNA quality was assessed using Qubit 2.0 Fluorometer (Thermo Fisher, USA) and used to generate the cDNA using the QuantiTect Reverse Transcription Kit (Qiagen, Hilden, Germany) following the manufacturer's instructions. Briefly, 1 µg of RNA in 12 µl was added to 2 µl of gDNA Wipeout Buffer 7X (Qiagen, Hilden, Germany), and incubated for 2 min at 42°C. Quantiscript Reverse Transcriptase (1 µl) (Qiagen, Hilden, Germany), Quantiscript RT Buffer 5X (4 µl) (Qiagen, Hilden, Germany) and RT Primer Mix (1 µl) (Qiagen, Hilden, Germany) were added and the samples were incubated for 15 min at 42°C and for 3 min at 95°C. The samples were then stored at -20°C until qPCR analysis.

#### 2.2.2. Quantitative PCR analysis (qPCR)

Quantitative PCR was performed using 5 ng of cDNA in 1 µl with QuantiNova® SYBR Green PCR kit (Qiagen, Hilden, Germany) on a StepOnePlus™ PCR System (Applied Biosystem, USA) following the manufacturer's instructions. Briefly, 1 µl of cDNA produced in section 2.2.1. (concentration: 5 ng/µl) and 1 µl of each primer pair (at a concentration of 0.5 µM for forward primer and reverse primer) were added into 5 µl of QuantiNova SYBR Green RT-PCR Master Mix, 0.5 µl QN ROX Reference Dye, QN SYBR Green RT-Mix and 2.4 µl of RNase-Free Water (final volume of 10 µl) and subjected to 40 cycles of 5 s at 95°C and by 10 s at 60°C followed by a dissociation step set between 60°C and 95°C with +0.3°C/s temperature increase. The

primers used in this assay are summarised in Table 3. 16S rRNA was used as reference gene. The fold change in gene transcription after 6 h bacterial growth compared to 24 h growth was calculated with the  $2^{-\Delta\Delta Ct}$  method.

**Table 3: List of primers used for *R. gnavus* gene qPCR analysis.**

| Primers         | Forward Primer<br>(5'→3') | Reverse Primer<br>(5'→3') |
|-----------------|---------------------------|---------------------------|
| RGNV35913_02506 | CACCGGAATTTGACCTGGC       | CTTCACCAGACGCATCCCTT      |
| RGNV35913_02510 | GAACAGACTTGCCGGGATTT      | TGCGTGACGTATCCCTTCAT      |
| RGNV35913_02516 | GCGTTACATTTGCCAAGGGT      | TTGCTCCTACGATTCCCACA      |
| RGNV35913_02524 | CTACATTCAGGGGCAGAGC       | TCCGTTCTCATCACCCTGA       |
| RGNV35913_02493 | ACGTGTCACCAGATATGGGA      | TTGTCACACGATCGTCCTGA      |
| RUMGNA_03514    | ATGATTCAGGCGGGATGGAA      | CGGATGATCTGCCTGTGAGA      |
| RUMGNA_03518    | ACAACCGTGGATTCTCGCTA      | TAGAGATCTCCTGCGCTGTC      |
| RUMGNA_03532    | CGAGGTTATTGCCGGAGATG      | ATGACCGGATCTTTGGCTCT      |
| RUMGNA_02407    | ATTCGGAGGAGATGATGGCG      | TGATATGCGCCAATCCGTTC      |
| 16SRg5F/R       | TGGCGGCGTGCTTAACA         | TCCGAAGAAATCCGTCAAGGT     |

### 2.3. Lectin binding screening by flow cytometry

The fluorescein-labelled lectins SNA (*Sambucus nigra* lectin), UEA1 (*Ulex europaeus* agglutinin I), GSLI (*Griffonia simplicifolia* lectin I isolectin B4), LTL (*Lotus tetragonolobus* lectin), ConA (Concanavalin A), GNL (*Galanthus nivalis* lectin), RCAI (*Ricinus communis* agglutinin I) and LCA (*Lens culinaris* agglutinin) were purchased from Vector Laboratories (Maravai LifeSciences, USA). The properties of the lectins used in this work are summarised in Table 4. The bacteria were grown anaerobically as described in the section 2.1.1. The culture was stopped when the OD<sub>600nm</sub> reached 0.65 and 100 µl of culture (containing 10<sup>7</sup> cells) was centrifuged at 10,000 x g for 5 min and the pellet washed with 800 µl PBS (137 mM NaCl, 2.7 mM KCl, 10 mM Na<sub>2</sub>HPO<sub>4</sub>, 1.8 mM KH<sub>2</sub>PO<sub>4</sub>, pH 7.4) and centrifuged at 10,000 x g for 5 min. The cells were then incubated with 20 ng/µl lectin in PBS (100 µl) for 1 h at 37°C or room temperature (following the manufacturer's instruction). For each condition, a no-lectin control was prepared with

PBS. After incubation, the cells were washed with 800 µl of PBS and centrifuged at 10,000 x g for 5 min. The pellets were then resuspended in 100 µl PBS for analysis by flow cytometry using BD LSRFortessa™ (BD Biosciences, USA). The data collection was set on a log scale and the threshold of FSC (forward scatter) and SSC (side scatter) parameter was set to 200 mV.

The flow cytometry events were first sorted using FSC and SSC and then analysed following relative fluorescence emitted by the lectin bound to the cells at 512 nm. The data were analysed using FlowJo software (Tree Star, Ashland, USA). The mean fluorescence intensity (MFI) is referred to the geometric mean fluorescence intensity value.

**Table 4: Lectins used this study.**

| Lectin   | Abbreviation | Cognate sugar    |
|--|--------------|------------------|
| Concanavalin A                                       | ConA         | Mannose, Glucose |
| <i>Galanthus nivalis</i> lectin                      | GNL          | Mannose          |
| <i>Griffonia simplicifolia</i> lectin I isolectin B4 | GSLI         | Galactose        |
| <i>Lens culinaris</i> agglutinin                     | LCA          | Mannose, Glucose |
| <i>Lotus tetragonolobus</i> lectin                   | LTL          | Fucose           |
| <i>Sambucus nigra</i> lectin                         | SNA          | Neu5Ac(α2,6)     |
| <i>Ulex europaeus</i> agglutinin I                   | UEAI         | Fucose           |
| <i>Ricinus communis</i> agglutinin I                 | RCAI         | Galactose        |

## 2.4. Structural analysis of *R. gnavus* cell surface polysaccharide

### 2.4.1. Cell preparation

For large-scale production, the bacteria were grown in 4 or 6 l of BHI-YH (rich medium) or 6 l of LAB medium supplemented with melibiose at 27.7 mM until OD<sub>630nm</sub> reached 0.65. The bacteria were then pelleted through successive centrifugation rounds (40 min at 4,000 x g at 4°C, then 1 h at 5,000 x g at 4°C, and finally 30 min at 7,000 x g at 4°C) to maximise the harvesting of cells. The cell pellet was then freeze-dried and kept at -20°C until further analysis.

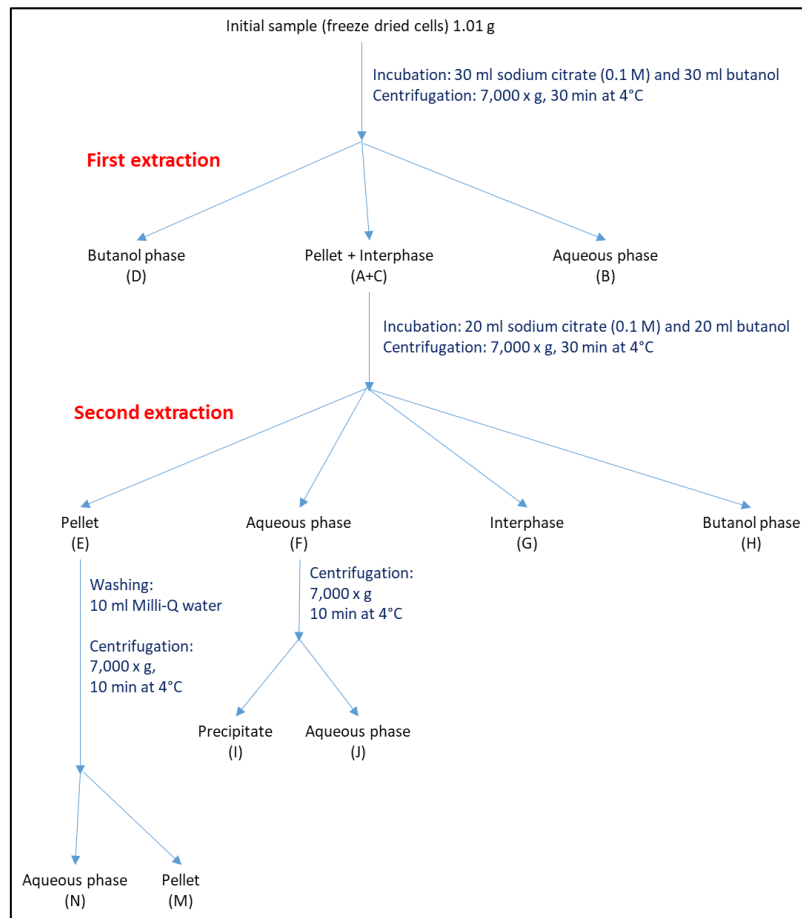
#### 2.4.2. Polysaccharide extraction

Following attempt to extract *R. gnavus* strains cell surface polysaccharide using diverse methods, including enzymatic extraction or ultrasonic-assisted extraction, we opted for a rougher method of extraction, comprising the use of hydrofluoric acid to detach polysaccharides from the cell surface of the bacteria. The bacterial cells were treated as described below following the procedure summarised in Fig. 12. Briefly, the freeze-dried cells were treated with 30 ml of citric acid (0.1 M) and 30 ml of absolute butanol, vortexed and centrifuged (7,000 x g, 30 min at 4°C). Four phases were then isolated: the pellet (called sample **A**), the aqueous phase (called sample **B**), the interphase (called sample **C**) and the butanol phase (called sample **D**) according to the extraction procedure described in Fig. 12. After this first extraction, samples **A** and **C** were pooled and the combined sample was treated with 30 ml of citric acid (0.1 M) and 30 ml of absolute butanol, vortexed and centrifuged (7,000 x g, 30 min at 4°C). This led to the subsequent extraction of four phases: the pellet (called sample **E**) which was washed with 10 ml of milliQ water and centrifuged at 7,000 x g for 30 min at 4°C to obtain sample **M** (pellet) and sample **N** (supernatant); the aqueous phase (called sample **F**), which was further centrifuged at 7,000 x g during 10 min at 4°C and separated into the pellet (called sample **I**) and the supernatant (called sample **J**), the interphase (called sample **G**) and the butanol phase (called sample **H**).

The resulting phases were then pooled as follows: samples **B**, **J** and **N** as the “aqueous phase” called sample **O**; samples **M**, **I** and **R** as the “pellet” called sample **Q** and samples **H** and **D** as the “butanol phase” called sample **P**. The aqueous phase, named sample **O**, was subjected to dialysis (3.5 kDa cut-off membrane) and centrifuged, the supernatant was collected, freeze-dried and stored at -20°C until further analysis. The sample **Q** (representing the pellet) was freeze-dried and treated to extract the polysaccharide using hydrofluoric acid (50%, allowing the efficient detachment of polysaccharides from the bacterial cell surface) for 48 h at 4°C. Following addition of 50 g ammonium acetate and 50 g ammonia to rise the pH to 7.0 the suspension was centrifuged at 7,000 x g for 30 min at 4°C and the resulting supernatant was dialysed against milliQ water with a 1 kDa cut-off membrane and the resulting fraction called

sample **S**. The butanol phase sample **P** was dried using a rotavapor (sample heated at 40°C and vacuum at 25 mbar), dissolved in water and freeze-dried. The interphase sample called sample **G** was freeze-dried.

A



B

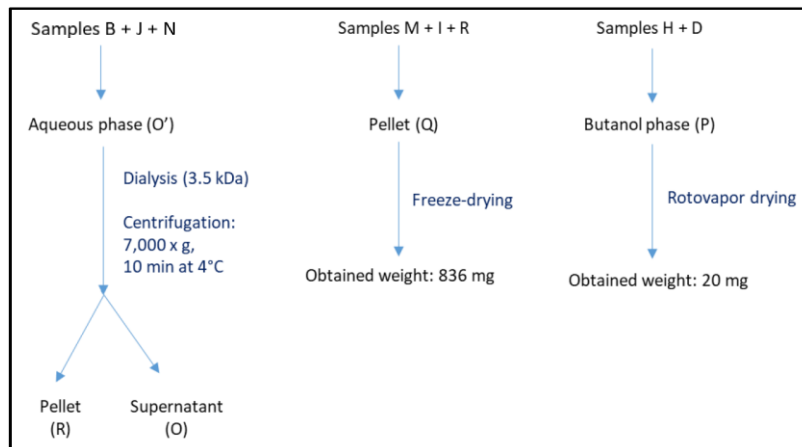


**Figure 12: Polysaccharide extraction of *R. gnavus* ATCC 35913 strain.**

(A) citric acid/butanol extraction scheme of *R. gnavus* ATCC 35913 dried cells. (B) pooling and use of the different samples obtained from the citric acid/butanol extraction.

#### 2.4.3. Monosaccharide structure and configuration analysis

To generate acetylated methyl glycosides (AMG), the samples **S** and **O** (described in section 2.4.2, 0.5 mg each) were first treated with 1 ml methanol with hydrogen chloride (1 M) overnight at 80°C, this step will permit the cleavage of the different glycosidic bounds, which will be result in the methylation of the hydroxyl groups previously involved in those glycosidic bonds. The suspension was then dried with a stream of air and treated with 100 µl absolute acetic anhydride and 200 µl of dry pyridine for 1 h at room temperature, resulting in the acetylation of the remaining hydroxyl groups (not previously involved in a glycosidic bond). The suspension was dried with a stream of air once again and resuspended in 500 µl of acetone prior GC-MS analysis.

The absolute configuration of the monosaccharides was determined using the acetylated octyl glycosides (AOG) method. The AMG sample **S** was dissolved in (R)-(-)-2-octanol (200 µl) and absolute acetyl chloride (15 µl) and incubated at 60°C overnight in order to attach octanol to the anomeric carbon of the monosaccharide. The suspension was then dried with a stream of air and treated with 100 µl absolute acetic anhydride and 200 µl of dry pyridine for 1 h at room temperature, in order to acetylate hydroxyl groups of the monosaccharides. The suspension was dried with a stream of air once again and resuspended in 500 µl of acetone prior GC-MS analysis.

The identification of the branching points in the oligosaccharides was determined using the partially methylated acetylated alditols (PMAA) method. Here, sample **S** was resuspended in dimethyl sulfoxide (DMSO) (1 ml) and NaOH (100 mg) was added to the solution. The suspension was then frozen in an ice bath, 200 µl of pure methyl-iodide was then added and incubated under agitation overnight, this step permit to add methyl groups on hydroxyl groups not involved in glycosidic bonds. Deionised water (15 ml) and chloroform (2 ml) were then added and stirred for 1 min at room temperature. The sample was then centrifuged at 550 x g for 3 min. The chloroform phase, containing the polysaccharide, was extracted following incubation with 200 µl of trifluoroacetic acid (2 M) at 120°C for 2 h to allow the cleavage of the polysaccharide. The sample was then dried with a stream of air, resuspended

with 50  $\mu\text{l}$  of isopropanol and 5 mg of *N*-acetyl(3,4-dihydroxybutyl) cysteine and dried with a stream of air again. Then, 50  $\mu\text{l}$  of acetic acid and of methanol are added to the sample for 1 h at room temperature to form the alditols. The suspension was then dried with a stream of air and treated with 100  $\mu\text{l}$  absolute acetic anhydride and 200  $\mu\text{l}$  of dry pyridine for 1 h at room temperature, resulting in the acetylation of the remaining hydroxyl groups (not previously involved in a glycosidic bond). The suspension was dried with a stream of air once again and resuspended in 500  $\mu\text{l}$  of acetone prior GC-MS analysis.

#### 2.4.4. Gas chromatography-Mass spectrometry (GC-MS)

For the GC-MS analysis, 0.5 mg dry matter from sample **S** and sample **O** treated with AMG, AOG and PPMA methods (as described in section 2.4.3.) were dissolved in 500  $\mu\text{l}$  acetone and analysed by GC-MS on a Hewlett–Packard 5890 instrument with a SPB-5 capillary column (0.25 mm  $\times$  30 m, Supelco) with a flow rate of 0.8 ml/min using helium as gas carrier as previously described (Speciale et al., 2019). The temperature program was as follows: 150°C for 3 min followed by 3°C/min up to 280°C, and finally 280°C for 10 min. Electron impact mass spectra were recorded with ionization energy of 70 eV and an ionizing current of 0.2 mA.

#### 2.4.5. Nuclear Magnetic Resonance (NMR) analysis

For the structural assignment of the cell surface polysaccharide, the sample **S** (13 mg) was resuspended in  $\text{D}_2\text{O}$  and analysed using a Bruker 600 MHz spectrometer equipped with a reverse cryo-probe with gradients along the z-axis. The NMR sequences used were (1H-1H homonuclear), DQ-COSY (double quantum COSY spectrum, hereafter referred as COSY), TOCSY, and NOESY, (1H-13C heteronuclear) HSQC, HMBC and HSQC-TOCSY, as previously described (Speciale et al., 2019). All the spectra were calibrated with acetone as internal standard (1H 2.225 ppm; 13C 31.45 ppm). The results were acquired with Topspin 2.0 and analysed using the Topspin 4.1 software (Bruker).

#### 2.4.6. High-Performance Liquid Chromatography (HPLC) analysis

The sample S (10 mg) was resuspended in 50 mM ammonium bicarbonate ( $\text{NH}_5\text{CO}_3$ ) and 10  $\mu\text{l}$  of the solution were injected into an Agilent 1100 HPLC system with either a TSK G-5000, a TSK G-3000 or a TSKgel G-Oligo-PW HPLC size exclusion column (30 cm  $\times$  7.8 mm). Briefly, the column was equilibrated with 50 mM  $\text{NH}_5\text{CO}_3$ , the sample was loaded onto the column, elution was also done with 50 mM  $\text{NH}_5\text{CO}_3$  at 0.5 ml/min flow rate, the eluate was monitored with a refractive index detector and the spectra analysed using the CHEM32 software. The column was calibrated by injecting dextran standards (Sigma-Aldrich, USA) (50  $\mu\text{l}$  of a 1 mg/ml solution) of known molecular weight (12, 50, 150, and 670 kDa).

### 2.5. Reporter cell assays

#### 2.5.1. C-type lectin reporter cells

The BWZ.36 cells expressing murine C-lectin receptors (CLR) mDectin-1, mDectin-2 and SIGN-R1 and QPD (Glutamine-Proline-Aspartic acid) mutants were used as described previously (Bene et al., 2017; Wittmann et al., 2016). The reporter cells were previously generated by Wittmann et al. (2016) by transducing the BWZ.36 cells with the pMXs-IRES-EGFP-Ly49A-CD3 $\zeta$  vector expressing the extracellular domain of mDectin-1 (Ser74 through Leu244), mDectin-2 (Gln49 through Leu209) or SIGN-R1 (Ser76 through Gly324) (Akatsuka et al., 2010). For the mDectin-2 and SIGN-R1 QPD reporter cells, two missense mutations in the carbohydrate recognition domain were introduced, resulting in amino acid substitutions E168Q and N170D for mDectin-2 and E285Q and D287N for SIGN-R1. The mock BWZ cells harbour the empty pMXs-IRES-EGFP-Ly49A-CD3 $\zeta$  vector. The reporter cells were grown in RPMI 1640 medium supplemented with 10% heat-inactivated FCS (Invitrogen), 2 mM glutamine (Sigma-Aldrich), 50  $\mu\text{M}$  2-mercaptoethanol, 100 U/ml of penicillin and 100  $\mu\text{g}/\text{ml}$  of streptomycin as previously reported (Bene et al., 2017; Wittmann et al., 2016), for 72 h in an incubator at 37°C atmosphere containing 5%  $\text{CO}_2$ . Fig. 13 describes the functioning of the CLR reporter cells used here.

For the assays, reporter cells ( $5 \times 10^5$  cells per well) were incubated with bacteria (MOI: 50:1) or 200  $\mu\text{g}/\text{ml}$  of purified glucorhamnan overnight at  $37^\circ\text{C}$  in 96-well microplates (Nunc). Scleroglucan (10  $\mu\text{g}/\text{ml}$ ) (ELICITYL, France) was used as a control as a specific ligand for mDectin-1, furfurman (10  $\mu\text{g}/\text{ml}$ ) (ELICITYL, France) was used as a control as a specific ligand for mDectin-2 and LPS from *Hafnia alvei* (10  $\mu\text{g}/\text{ml}$ ) (ELICITYL, France) was used as a control as a specific ligand for SIGN-R1. Following incubation, the microwell plates were centrifuged at  $510 \times g$  for 3 min and the supernatant was discarded. The  $\beta$ -galactosidase activity (encoded by the lacZ reporter gene) was determined by the addition of 100  $\mu\text{l}$  of 150 mM chlorophenol red- $\beta$ -D-galactopyrasonide (CPRG; Roche) diluted in a CPRG assay reaction buffer (PBS supplemented with 0.125% Triton X-100 and 100 mM 2-mercaptoethanol, Lonza) to each well. Following 30 min incubation at  $37^\circ\text{C}$ , the colour development was monitored at  $\text{OD}_{595\text{nm}}$  using an Omega FluoStar (BMG Labtech, UK) microtiter plate reader.

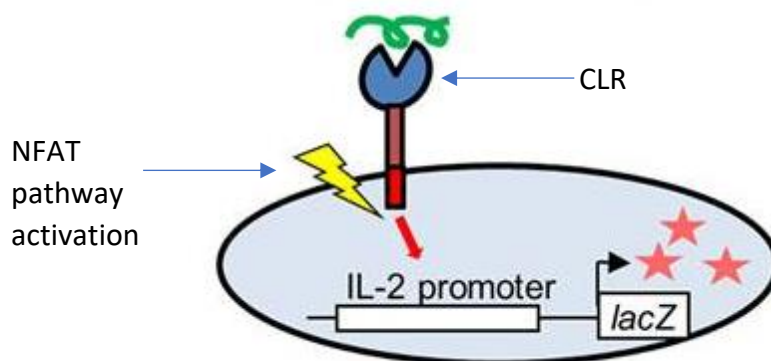


**Figure 13: Schematic representation of Lac operon activation via recognition of the ligand by C-type lectin receptor (CLR) through the carbohydrate recognition domain (CRD).**

Here, ligand (in green) binding stimulates IL-2 promoter and LACZ gene to produce  $\beta$ -galactosidase which can hydrolyse red- $\beta$ -D-galactopyrasonide, producing a colour change. NFAT stands for nuclear factor of activated T cells, CLR for C-type lectin receptors and IL-2 for interleukin-2.

### 2.5.2. NF- $\kappa$ B reporter cells

The THP-1 blue NF- $\kappa$ B (Nuclear Factor  $\kappa$ B) reporter cells (InvivoGen, USA) are derived from engineered human THP-1 monocyte cell line encoding an NF- $\kappa$ B-inducible SEAP (secreted embryonic alkaline phosphatase) reporter construct. THP-1 blue NF- $\kappa$ B reporter cells allow the monitoring of NF- $\kappa$ B activation by determining the activity of SEAP using QUANTI-Blue™ Solution, a SEAP detection reagent. The reporter cells were grown in RPMI 1640 medium supplemented with 10% heat-inactivated FCS (Invitrogen), 2 mM glutamine (Sigma-Aldrich), 25 mM HEPES (Lonza), in an incubator at 37°C atmosphere containing 5% CO<sub>2</sub>.

THP1 blue NF- $\kappa$ B reporter cells (10<sup>5</sup> cells per well) were incubated with bacteria (MOI: 50:1) or 200 µg/ml of glucorhamnan overnight at 37°C in 96-well microplates (Nunc). HKLM (heat killed *Listeria monocytogenes*) (2 x 10<sup>7</sup> cells per well) (InvivoGen, San Diego, USA) was used as a control for TLR (Toll-like receptor) activity. Following incubation, the microwell plates were centrifuged at 510 x g for 3 min and the supernatant was discarded. The SEAP activity was determined by the addition of 100 µl of QUANTI-Blue™ Solution (InvivoGen, USA) to 20 µl of the cell suspension from each well. Following 1 h incubation at 37°C, the colour development was monitored at OD<sub>630nm</sub> using an Omega FluoStar (BMG Labtech, UK) microtiter plate reader.

## 2.6. Mammalian cell assays

### 2.6.1. Culture of intestinal epithelial cell models

T84 and LS174T cell lines were obtained from the European Collection of Authenticated Cell Cultures (ECACC).

T84 human colon carcinoma cells (ECACC 88021101) were seeded in T75 flasks at a density of 1.0 x 10<sup>5</sup> cells/ml in Dulbecco's Modified Eagle's Medium/Nutrient F-12 Ham 1:1 (DMEM/F12) medium (Sigma-Aldrich) supplemented with 10% heat inactivated foetal bovine serum (FBS) (Sigma-Aldrich), 2 mM glutamine (Sigma-Aldrich), 100 U/ml penicillin and 100 µg/ml

streptomycin, as previously reported (Bene et al., 2017; McGrath et al., 2022; Wittmann et al., 2016) in an incubator at 37°C atmosphere containing 5% CO<sub>2</sub>.

Mucin-producing LS174T human colon carcinoma cells (ECACC 87060401) were seeded in T75 flasks at a density of  $1.0 \times 10^5$  cells/ml in DMEM (Sigma-Aldrich) supplemented with 10% heat inactivated FBS, 2 mM glutamine, 100 U/ml of penicillin and 100 µg/ml streptomycin, as previously reported (Bene et al., 2017; McGrath et al., 2022; Wittmann et al., 2016) in an incubator at 37°C atmosphere containing 5% CO<sub>2</sub>. Cell culture media for both cell lines were refreshed three times weekly and expanded before reaching 70-80% confluence by passaging them with a dilution of 1/10. T84 cells were used at passage 59 and LS174T cells at passage 18 in the subsequent experiments. When T84 and LS174T cells were used in co-culture (with a ratio of 1:10, respectively), the media consisted of 1:1 DMEM/F12 medium supplemented with 10% heat inactivated FBS, 2 mM glutamine, 100 U/ml of penicillin and 100 µg/ml of streptomycin and DEMEM supplemented with 10% heat inactivated FBS, 2 mM glutamine, 100 U/ml penicillin and 100 µg/ml streptomycin.

For the culture on transwells, either  $1.6 \times 10^5$  T84 cells or  $1.6 \times 10^5$  T84 cells with  $1.6 \times 10^4$  LS174T cells (in 100 µl) were seeded on either 6 mm or 12 mm large transwell with 0.4 µm pore polyester membrane insert (Corning) pre-coated with 10 µg/cm<sup>2</sup> of type I rat tail collagen. TEER (transepithelial electrical resistance) was measured regularly to check the integrity of the T84 and T84/LS174T epithelium monolayer on transwells using EndOhm chamber and EVOM resistance meter (World precision instruments). Resistance value above 1000 Ω×cm<sup>2</sup> for T84 or 90 Ω×cm<sup>2</sup> for T84/LS174T indicated the establishment of a tight monolayer (typically 8 to 13 days following seeding on transwells).

#### 2.6.2. Generation and culture of mBMDCs

All experimental procedures and protocols used in this study were reviewed and approved by the Animal Welfare and Ethical Review Body (AWERB) at the University of East Anglia and were conducted within the provisions of the Animals (Scientific Procedures) Act 1986 (ASPA)

and the LASA Guiding Principles for Preparing for and Undertaking Aseptic Surgery (2010). Care of the animals for the duration of the study was in accordance with the UK Home Office guidelines. C57BL/6 mice were bred and maintained at a conventional animal unit at the University of East Anglia (Norwich, UK). All animals were specific pathogen-free and had access to a standard mouse diet and water ad libitum. C57BL/6 were killed by cervical dislocation and disinfected in 75% ethanol for 5 min. The tibiae and femurs were removed under sterile conditions, then soaked in RPMI-1640 medium (Lonza) supplemented with 1% FBS. Both ends of the bone were cut off with scissors, and the needle of a 1 ml syringe was inserted into the bone cavity to rinse the bone marrow out of the cavity into a sterile culture dish with RPMI-1640 medium. The cell suspension in the dish was collected and centrifuged at 150 x g for 5 min, and the supernatant was discarded. The cell pellet was resuspended with Tris-NH<sub>4</sub>Cl red blood cell (RBC) lysis buffer (Lonza) to lyse the RBCs. Following a second centrifugation step at 150 x g for 5 min, the supernatant was discarded, and the pelleted cells were washed with PBS and collected.

The resulting mBMDCs were cultured in cell culture dishes at a density of  $5.0 \times 10^5$  cells/ml in Mercedes medium [RPMI 1640 (Lonza) supplemented with 25 mM HEPES, 2 mM L-glutamine, 100 U/ml penicillin/streptomycin, 10% FBS, 1mM sodium pyruvate solution, 1 mM non-essential amino acids and 55  $\mu$ M mercaptoethanol] supplemented with 80 ng/ml granulocyte monocyte stimulating factor (GM-CSF) (Gentaur Molecular Products, Brussels, Belgium) in an incubator at 37°C atmosphere containing 5% CO<sub>2</sub>.

### 2.6.3. Stimulation of mammalian cells with *R. gnavus* strains or glucorhamnan

In another experiment, the purified glucorhamnan was also used to assess their immuncity on murine BMDC. For that, the purified glucorhamnan from the three strains were used at different concentration (from 0.1 to 100  $\mu$ g/ml), and the production of TNF- $\alpha$  was measured. The results obtained, displayed in Fig. 14, show that the glucorhamnan from E1 enhances strong immune response when used at high concentrations. The glucorhamnan from the two other strains didn't permit a significant production of TNF- $\alpha$  even when used at high

concentrations. The concentration of purified glucorhamnan used for the future experiments was then increased to 200 ng/ml to optimise the immune response obtained from the different cell lines used.

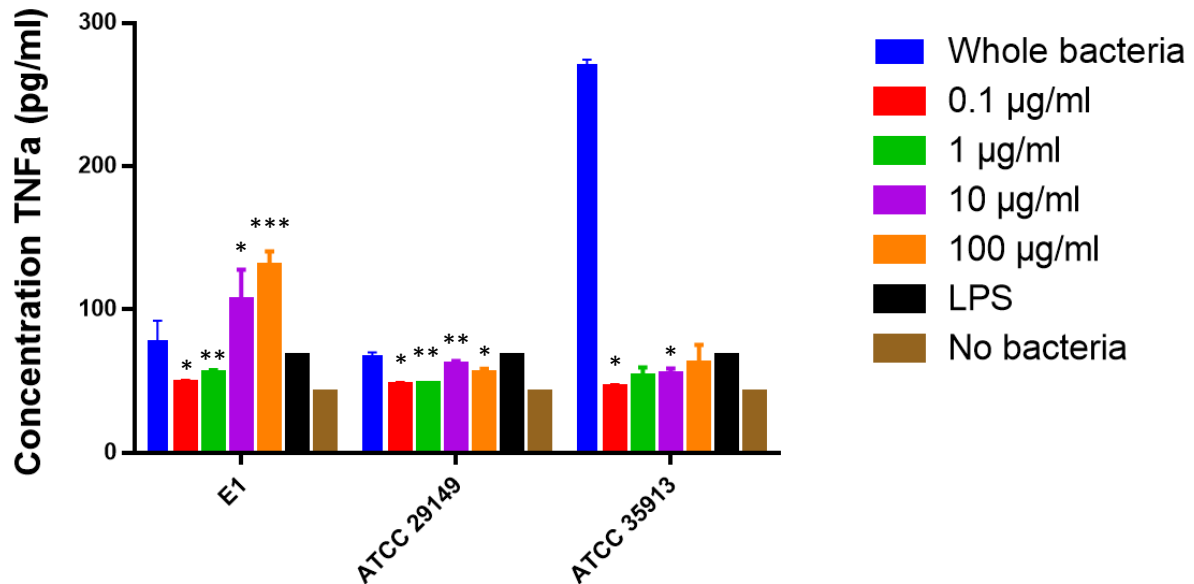


**Figure 14: Effect of *R. gnavus* strains and glucorhamnan on cytokine production by BMDCs.**

The assays were carried out in 3 replicates using glucorhamnan at 0.1, 1, 10 and 100 µg/ml concentrations, and whole bacteria at MOI of 50:1. The secretion of TNF-α was determined by ELISA. LPS at 100 µg/ml was used as a positive control. T-test was used for comparison with the negative control (\* for p<0.05, \*\* for p<0.01, \*\*\* for p<0.001).

To test the interaction with gut epithelial cell models, bacteria at MOI 20:1 or 200 µg/ml of purified glucorhamnan in DMEM/F12 medium were added to the apical part of the transwells. Untreated cells in DMEM/F12 medium were used as negative control. The cells were incubated at 37°C with 5% CO<sub>2</sub> for 18 h. The medium from both apical and basolateral compartments were then collected for cytokine analysis (see section 2.8.3.).

mBMDCs (5 x 10<sup>5</sup> cells per well) were incubated with the bacteria (MOI: 50:1) or purified glucorhamnan (200 µg/ml) for 18 h at 37°C in 96-well microplates (Nunc). LPS from *E. coli* O111:B4 (100 µg/ml) (InvivoGen, San Diego, USA) was used as a positive control. Growth

medium was used as negative control. Following incubation, the microwell plates were centrifuged at  $510 \times g$  for 3 min and the supernatant was collected and stored at  $-80^{\circ}\text{C}$  until further analysis.

In another experiment, the purified glucorhamnan was also used to assess their immuncity on murine BMDC. For that, the purified glucorhamnan from the three strains were used at different concentration (from 0.1 to 100  $\mu\text{g}/\text{ml}$ ), and the production of TNF-  $\alpha$  was measured. The results obtained, displayed in Fig. 14, show that the glucorhamnan from E1 enhances strong immune resposne when used at high concentrations. The glucorhamnan from the two other strains didn't permit a significant production of TNF- $\alpha$  even when used at high concentrations. After the incubation with bacteria/glucorhamnan, the apical and basolateral media were harvested, the cells were washed three times in  $\text{Ca}^{2+}$  and  $\text{Mg}^{2+}$  free PBS and TEER was then measured. The cells were lysed using TRIzol (Invitrogen, see section 2.7), snap frozen and kept at  $-80^{\circ}\text{C}$  until RNA or protein extraction.

## 2.7. Gene expression analysis

The RNA extraction was carried out using TRIzol following the manufacturer's instructions. Briefly, chloroform (160  $\mu\text{l}$ ) was added to the TRIzol lysates (800  $\mu\text{l}$ ) and centrifuged at 12,000  $\times g$  at  $4^{\circ}\text{C}$  for 15 min, resulting in two phases: a lower red phenol-chloroform phase which contains the protein fraction and a colourless upper aqueous phase which contains RNA.

The RNA fraction (87.5  $\mu\text{l}$ ) was first treated with DNase I (Qiagen, Hilden, Germany) to remove any potential DNA contamination in the sample. Briefly, 2.5  $\mu\text{l}$  of DNase I (corresponding to 7 Kunitz units) and 10  $\mu\text{l}$  of RDD buffer were added to the RNA fraction and then purified using the RNeasy MinElute kit (Qiagen, Hilden, Germany) following manufacturer's instructions. The purified RNA quality was determined using Nanodrop (Thermo Fisher Scientific). The cDNA was produced from the purified RNA using QuantiTect Reverse Transcription Kit (Qiagen, Hilden, Germany) following the manufacturer's instructions. Briefly, 1  $\mu\text{g}$  of RNA in 12  $\mu\text{l}$  was added to 2  $\mu\text{l}$  of gDNA Wipeout Buffer 7X (Qiagen, Hilden, Germany), and incubated

for 2 min at 42°C. Quantiscript Reverse Transcriptase (1 µl) (Qiagen, Hilden, Germany), Quantiscript RT Buffer 5X (4 µl) (Qiagen, Hilden, Germany) and RT Primer Mix (1 µl) (Qiagen, Hilden, Germany) were added and the samples were incubated for 15 min at 42°C and for 3 min at 95°C. The samples were then stored at -20°C until qPCR analysis. The qPCR was run using 20 ng of cDNA in QuantiTect SYBR Green PCR kit (Qiagen, Hilden, Germany) on a StepOnePlus™ PCR System (Applied Biosystem, USA). The primers used in this assay are summarised in Table 5. β-actin was used as house-keeping reference genes. The fold change in gene transcription when the cells were incubated with the bacteria or the glucorhamnan compared to the non-treated cells was calculated with the  $2^{-\Delta\Delta Ct}$  method. A fold change greater than 2 indicated an upregulation when comparing treatment to its control sample while a fold change lower than 0.5 indicated a downregulation. No effect on gene expression was considered for values between 2.0 and 0.5.

**Table 5: List of primers used for epithelium cells gene expression analysis.**

| Primers  | Forward Primer<br>(5'→3')  | Reverse Primer<br>(5'→3') |
|----------|--|---------------------------|
| GAPDH    | AGGTCGGAGTCAACGGATTT   | TGGAAGATGGTGATGGGATTT     |
| RPS13    | CGAAAGCATCTTGAGAGGAACA   | TCGAGCCAAACGGTGAATC       |
| Actin    | TGACGTGGACATCCGCAAAG   | CTGGAAGGTGGACAGCGAGG      |
| ZO-1     | AAGTCACACTGGTCAAATCC   | CTCTTGCTGCCAAACTATCT      |
| CLN-1    | GCAGATCCAGTGCAAAGTCT   | CATACACTTCATGCCAACGG      |
| Occludin | Commercially available primers Hs_OCLN_1_SG QuantiTect Primer Assay (Qiagen) |                           |
| TLR4     | Commercially available primers Hs_TLR4_2_SG QuantiTect Primer Assay (Qiagen) |                           |
| IL-1β    | Commercially available primers Hs_IL1B_1_SG QuantiTect Primer Assay (Qiagen) |                           |
| IL-6     | Commercially available primers Hs_IL6_1_SG QuantiTect Primer Assay (Qiagen)  |                           |
| IL-10    | Commercially available primers Hs_IL10_1_SG QuantiTect Primer Assay (Qiagen) |                           |

|               |   |
|---------------|---|
| IL-29         | Commercially available primers Hs_IFNL1_2_SG QuantiTect Primer Assay (Qiagen) |
| TNF- $\alpha$ | Commercially available primers Hs_TNF_1_SG QuantiTect Primer Assay (Qiagen)   |
| IFN- $\gamma$ | Commercially available primers Hs_IFNG_1_SG QuantiTect Primer Assay (Qiagen)  |
| CXCL5         | Commercially available primers Hs_CXCL5_1_SG QuantiTect Primer Assay (Qiagen) |
| CXCL8         | Commercially available primers Hs_CXCL8_1_SG QuantiTect Primer Assay (Qiagen) |

## 2.8. Protein analysis

### 2.8.1. Protein extraction

Proteins were extracted using the TRIzol protocol (Invitrogen) following the manufacturer's instructions (see section 2.7). Following the TRIzol extraction, 300  $\mu$ l of absolute ethanol was added to 1 ml of protein fraction, and the suspension was centrifuged at 2,000 x g at 4°C for 5 min. The supernatant was collected, and isopropanol (1.5 ml) was added to the supernatant (1 ml). The samples were then centrifuged at 12,000 x g at 4°C for 10 min and the supernatant was discarded. The pellet was then washed using a solution of 0.3 M guanidine hydrochloride in 95% ethanol and centrifuged at 7,500 x g at 4°C for 5 min, this step was repeated three times. To remove all washing solution from the tubes, absolute ethanol (2 ml) was then added, the samples were centrifuged at 7,500 x g at 4°C for 5 min, the supernatant was discarded and the tubes were then air dried. The samples were then resuspended in a PBS solution containing 1% SDS and stored at -20°C until further analysis.

### 2.8.2. Western blot analysis

Protein samples were loaded (6.5  $\mu$ g) with 10 mM of DTT (Dithiothreitol) and 1X NuPage LDS (lithium dodecyl sulfate) sample buffer (Invitrogen) on NuPage 4-12% Bis Tris gel (Invitrogen). Electrophoresis was carried out at 200 V, 300 mA and 50 W for 35 min in MES (2-morpholin-4-ylethanesulfonic acid) buffer. The transfer of the proteins from the gel to a 0.2  $\mu$ m pores

polyvinylidene fluoride membrane (Merck, Darmstadt, Germany) was carried out at 30 V, 300 mA and 50 W using a Novex NuPage transfer buffer (Invitrogen) for 90 min. After transfer, blocking of the membrane was done using Pierce's protein free blocking buffer (Thermo Fisher, USA). The membrane was then incubated with primary antibody diluted in PBS containing Tween 0.1% overnight under gentle shaking, followed by incubation with secondary fluorescent antibody for 1 h under shaking. The properties and concentration of antibodies used in this work are described in Table 6. Washes with PBS/Tween 0.1% were conducted between each step. Protein bands were detected with ChemiDoc MP imager (Biorad, USA).

**Table 6: List of antibodies used for western blot analysis.**

| Antibody       | Origin                             | Concentration in PBS+Tween 0.1% | Secondary antibody                             | Secondary antibody concentration in PBS+Tween 0.1% |
|----------------|------------------------------------|---------------------------------|--|--|
| $\beta$ -actin | Mouse monoclonal (Santa Cruz, USA) | 0.2 $\mu$ g/ml                  | Alexa Fluor™ 647 goat anti mouse (Invitrogen)  | 2 $\mu$ g/ml                                       |
| ZO-1           | Rabbit monoclonal (Invitrogen)     | 5 $\mu$ g/ml                    | Alexa Fluor™ 488 goat anti rabbit (Invitrogen) | 2 $\mu$ g/ml                                       |
| occludin       | Mouse monoclonal (Invitrogen)      | 10 $\mu$ g/ml                   | Alexa Fluor™ 647 goat anti mouse (Invitrogen)  | 2 $\mu$ g/ml                                       |

### 2.8.3. Enzyme-linked immunosorbent assay (ELISA)

Quantification of TNF- $\alpha$  and IL-10 secretion from mBMDCs was determined by ELISA using the protocols from Biolegend (San Diego, USA) for mouse TNF- $\alpha$  ELISA MAX Standard and mouse IL-10 ELISA MAX Standard assays. Briefly, wells of a 96-well microplate (Nunc) were coated with capture antibody (diluted 200 times in coating buffer: 8.4 g/l NaHCO<sub>3</sub>, 3.56 g/l Na<sub>2</sub>CO<sub>3</sub>,

pH 9.5), the supernatant (100 µl) from T84 cells or T84/LS174T cells incubated with *R. gnavus* strains, purified glucorhamnans or with medium only was added into wells and incubated for 2 h at room temperature, then 100 µl of the detection antibody (200 times diluted in PBS with 1% BSA) was added and incubated for 1 h at room temperature, streptavidin-HRP (100 µl, 250 times diluted in PBS with 1% Tween-20 and 10% BSA) was then added to the wells and incubated for 30 min at room temperature. After each step, the cells were washed with PBS containing 0.05% Tween-20. Following incubation with 3,3',5,5'-Tetramethylbenzidine (TMB) substrate for 15 min, the colour development was stopped using 2N H<sub>2</sub>SO acid solution and was then monitored using a Bio-Rad Benchmark Plus microtiter plate reader at OD<sub>570/450nm</sub>.

Quantification of IL-29, IL-6 and IL-10 secretion from epithelial cells was carried using human IL-29 (IFNλ1) ELISA, IL-6 ELISA and IL-10 ELISA (Invitrogen). Briefly, wells of a 96-well microplate (Nunc) were coated with capture antibody (diluted 250 times in PBS), the supernatant (100 µl) from T84 cells or T84/LS174T cells incubated with *R. gnavus* strains, purified glucorhamnans or with medium only was added into wells and then incubated with 50 µl of the detection antibody (250 times diluted in PBS with 1% BSA) for 2 h at room temperature, and then streptavidin-HRP (100 µl, 250 times diluted in PBS with 1% BSA). After each step, the cells were washed with PBS containing 0.05% Tween-20. Following incubation with 3,3',5,5'-Tetramethylbenzidine (TMB) substrate for 15 min, the colour development was stopped using 2N H<sub>2</sub>SO acid solution and was then monitored using a Bio-Rad Benchmark Plus microtiter plate reader at OD<sub>570/450nm</sub>.

**Table 7: Antibodies used for human or mouse cytokines in ELISA or U-PLEX assays in this study.**

|       | Human |        | Mouse |        |
|-------|-------|--------|-------|--------|
|       | ELISA | U-PLEX | ELISA | U-PLEX |
| MIF   | ×     | ✓      | ×     | ×      |
| CXCL5 | ×     | ✓      | ×     | ×      |
| IL-1β | ×     | ✓      | ×     | ✓      |
| IL-8  | ×     | ✓      | ×     | ×      |

|               |   |   |   |   |
|---------------|---|---|---|---|
| IL-6          | × | ✓ | × | ✓ |
| IL-17         | × | ✓ | × | × |
| IL-33         | × | ✓ | × | × |
| IL-4          | × | ✓ | × | ✓ |
| IL-29         | ✓ | ✓ | × | × |
| TNF- $\alpha$ | × | ✓ | × | ✓ |
| IFN- $\gamma$ | × | × | × | ✓ |
| IL-10         | × | × | ✓ | ✓ |
| IL-12p40      | × | × | × | ✓ |
| IL-13         | × | × | × | ✓ |
| CCL2          | × | × | × | ✓ |
| CXCL1         | × | × | × | ✓ |

U-PLEX Assays (Meso Scale Discovery, USA) were used to analyse secretion of MIF, CXCL5, IL-1 $\beta$ , IL-8, IL-6, IL-17, IL-33, IL-4, IL-29 and TNF- $\alpha$  from human epithelial cells and TNF- $\alpha$ , IFN- $\gamma$ , IL-1 $\beta$ , IL-4, IL-6, IL-10, IL-12p40, IL-13, CCL2 and CXCL1 from mBMDCs following the manufacturer's instructions. Briefly, each capture antibody was incubated for 30 min at room temperature with an associated U-PLEX linker (provided by the manufacturer, which enables the linkage between the biotinylated capture antibody and the spot on the U-PLEX plate) and the wells of a 96-well U-PLEX plate were coated with capture antibody/associated linker complex. The supernatant (50  $\mu$ l) from T84 cells or T84/LS174T cells incubated with *R. gnavus* strains, purified glucorhamnans or with medium only were added to the wells and were then incubated for 1 h at room temperature with the detection antibodies conjugated with SULFO-TAG (50  $\mu$ l, 100 times diluted in Diluent 3 provided by the manufacturer). After each step, the cells were washed with PBS containing 0.05% Tween-20. The read buffer (provided by the manufacturer, used to catalyse the electrochemiluminescent reaction associated with the SULFO-TAG present on the detection antibody) was then added and analysis of the plate was

then monitored using MESO™ QuickPlex SQ 120 MSD plate reader to quantify electrochemiluminescence as a readout.

#### 2.10. *In silico* analysis

BLASTP ([blast.ncbi.nlm.nih.gov/Blast.cgi](http://blast.ncbi.nlm.nih.gov/Blast.cgi)) was used for comparative alignments of genes between *R. gnavus* strains. Information on the genome of *R. gnavus* strains was obtained from the NCBI data bank ([www.ncbi.nlm.nih.gov](http://www.ncbi.nlm.nih.gov)) for ATCC 29149, the Genoscope website ([www.genoscope.cns.fr/agc/microscope](http://www.genoscope.cns.fr/agc/microscope)) for the E1 strain and the Earlham Institute (formerly the genome analysis center, TGAC) (Norwich, UK) for ATCC 35913.

#### 2.11. Statistics

Statistics were run using one-way or two-way ANOVA followed by Tukey's test for multiple comparison on Prism software (GraphPad). A p-value beneath 0.05 was considered as statistically significant, p values are represented on graphs as following: \*p<0.05; \*\*p<0.01; \*\*\*p<0.001.

Chapter 3: Investigation of *R. gnavus* cell surface glycosylation

### 3.1. Introduction

Microbes display cell surface components called MAMPs (microbial-associated molecular patterns) such as flagella, pili, surface layer proteins (SLPs), capsular polysaccharide (CPS), lipoteichoic acid, and lipopolysaccharide (LPS) among others (Q. Liu et al. (Q. Liu et al., 2020). Bacterial polysaccharides are the main actors of interaction with the external environment, and in the gut, these play key roles in bacterial adaptation to the intestinal microenvironment, gut barrier function and mucus production (Artis, 2008; Patel & Dupont, 2015; Porter & Martens, 2017; Rook et al., (Artis, 2008; Patel & Dupont, 2015; Porter & Martens, 2017; Rook et al., 2017). For example, *B. thetaiotaomicron* CPS enhances its competitiveness and colonisation in the murine gut and the tolerance of the bacterium to antibiotic stress (Porter et al., 2017). In addition, these cell surface polysaccharides have immunoregulatory properties in the gut through their interaction with the host PRRs, as shown for example with EPS from *Bifidobacteria* and *Lactobacillus* species (Hidalgo-Cantabrana et al., 2012; Udayan et al., 2021).

*R. gnavus* ATCC 29149 displays on its cell surface a glucorhamnan polysaccharide composed of repeating units based on a backbone of three rhamnoses and a sidechain of two glucoses (as shown in Fig. 10A). While this glucorhamnan can induce a pro-inflammatory response in mBMDCs *in vitro* (Henke et al., 2019), it has been shown that *R. gnavus* ATCC 29149 also presents a CPS on its cell surface which induces a tolerance from the host immunity to this strain (Henke et al., 2021). *R. gnavus* CPS has been reported to contain repeating units made of six glucose, two *N*-acetylquinovosamine and one *N*-acetylgalactosamine, although the exact structure remains to be determined (Henke et al., 2021). The biosynthetic clusters of glucorhamnan and CPS have been identified in *R. gnavus* ATCC 29149 genome (Henke et al., 2019, 2021).

Here, we investigated the cell surface glycosylation of *R. gnavus* E1 and ATCC 35913 strains in comparison to *R. gnavus* ATCC 29149 using a combination of *in silico* and biophysical approaches and tested the influence of carbohydrate source and growth phase on their

composition. To do so, a lectin-binding screening approach have been used in order to probe the cell surface glycosylation among the three *R. gnavus* strains. The lectin used for this screening were selected to offer a broad range of detection, enabling the bound to sialic acid, glucose, mannose, galactose and fucose, which are the main monosaccharides suspected to be present on *R. gnavus* strains cell surface. This way, we will assess the potential difference between *R. gnavus* strains and the influence of environment on the cell surface glycosylation production.

In addition, as *R. gnavus* different strains evolve in different niches in the host gut, we aimed to decipher the influence of the carbon source availability in the environment on *R. gnavus* strains cell surface glycosylation. As the *R. gnavus* strains studied here were observed to have differential influence on the host health outcomes, as mentioned in section 1.4.1, it is therefore suspectable that they display on their cell surface different factors of immunomodularity, which are potentially the cell surface glycosylation. To investigate this, bacteria will be grown in minimal medium supplemented with different carbohydrate sources during the experiment to visualise potential influence on the lectin binding profile of the conditions tested. This method will allow to overview a large number of conditions, including strains tested, growth conditions used and lectin assessed for binding with the available cell surface polysaccharide of *R. gnavus* strains.

## 3.2. Results

### 3.2.1. *In vitro* screening by flow cytometry

A flow cytometry lectin-based screening assay was developed to investigate the polysaccharide epitopes present on the cell surface of *R. gnavus* ATCC 29149, ATCC 35913 and E1 strains using a range of fluorescently-labelled lectins displaying different specificities for sugars (ConA, GNL, GSLI, LCA, LTL, SNA, UEAI and RCAI) (see Table 4). To determine the potential influence of the carbohydrate source on the cell surface glycosylation, *R. gnavus* strains were grown in rich medium (BHI-YH) or defined medium supplemented with a single

carbon source including glucose (Glc), fucose (Fuc), galactose (Gal), *N*-acetylglucosamine (GlcNAc), 3'-fucosyllactose (3'FL), lactose (Lac), 2'-fucosyllactose (2'FL), sucrose (Suc) or 3'-sialyllactose (3'SL), difucosyllactose (DFL), melibiose (Mel) or raffinose (Raf). Flow cytometry was used to monitor and quantify the binding of fluorescently-labelled lectins to the bacterial cell surface (as described in methods section 2.3.). Bacteria were collected at 0.6 OD<sub>600nm</sub>, corresponding to 1x10<sup>8</sup> CFU for each strain.

Using this approach, we first observed that the lectin-binding profiles differed between *R. gnavus* strains grown on the same medium. ConA showed a higher binding to *R. gnavus* ATCC 29149 compared to that observed for E1 and ATCC 35913 when the strains were grown on Glc, Fuc, 3'FL and Mel (Fig. 15). In addition, when grown in 2'FL and Raf, *R. gnavus* ATCC 29149 showed highest binding to RCAI among the different strains grown on the same carbohydrate sources (Fig. 16). When the bacteria were grown in Fuc, 3'FL, GlcNAc and Mel, ConA showed higher binding to *R. gnavus* E1 in comparison to ATCC 35913 (Fig. 15), while when the bacteria were grown in Glc, Fuc, 2'FL and 3'FL, *R. gnavus* ATCC 29149 showed highest binding to GSLI among the strains grown in the same media (Fig. 17). Finally, when the cells were grown in Glc, Lac, Raf, 2'FL or BHI-YH, RCAI showed higher binding to *R. gnavus* ATCC 35913 in comparison to the E1 strain grown in the same conditions (Fig 16).

Since Glc is a major component of glucorhamnan (see Fig. 10A), the observed difference between *R. gnavus* E1 and ATCC 35913 in comparison with ATCC 29149 strain with regards to ConA binding, suggests potential differences in the composition of this polysaccharide between the strains.

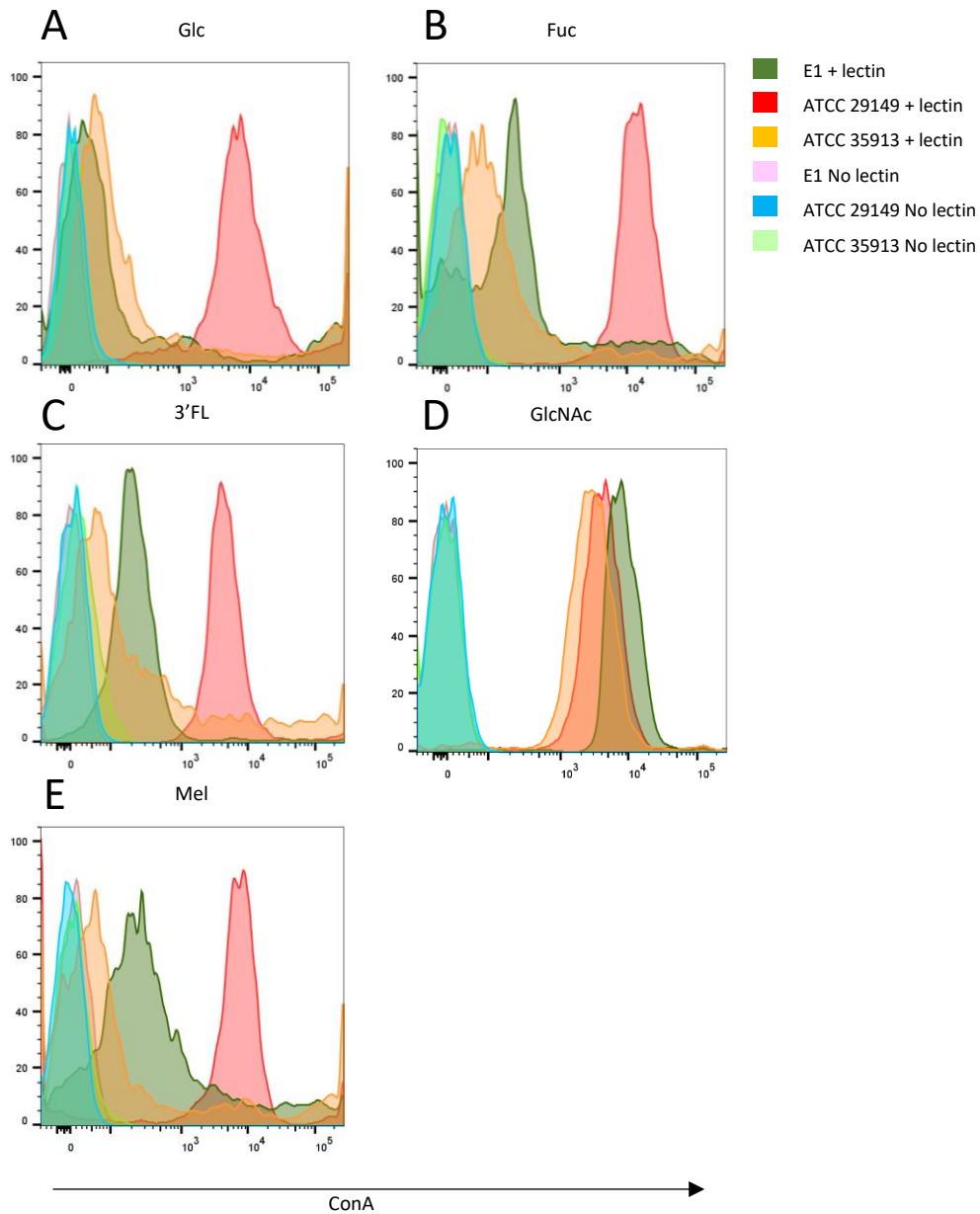


**Figure 15: *R. gnavus* strains grown with Glc, Fuc, 3'FL and GlcNAc lectin binding with ConA.**

*R. gnavus* E1 (dark green), ATCC 29149 (red) and ATCC 35913 (orange) were incubated with ConA after being grown with Glc (A), Fuc (B), 3'FL (C), GlcNAc (D) or Mel (E). Controls used were bacteria with no fluorescent lectin (pink for E1, blue for ATCC 29149 and green for ATCC 35913).

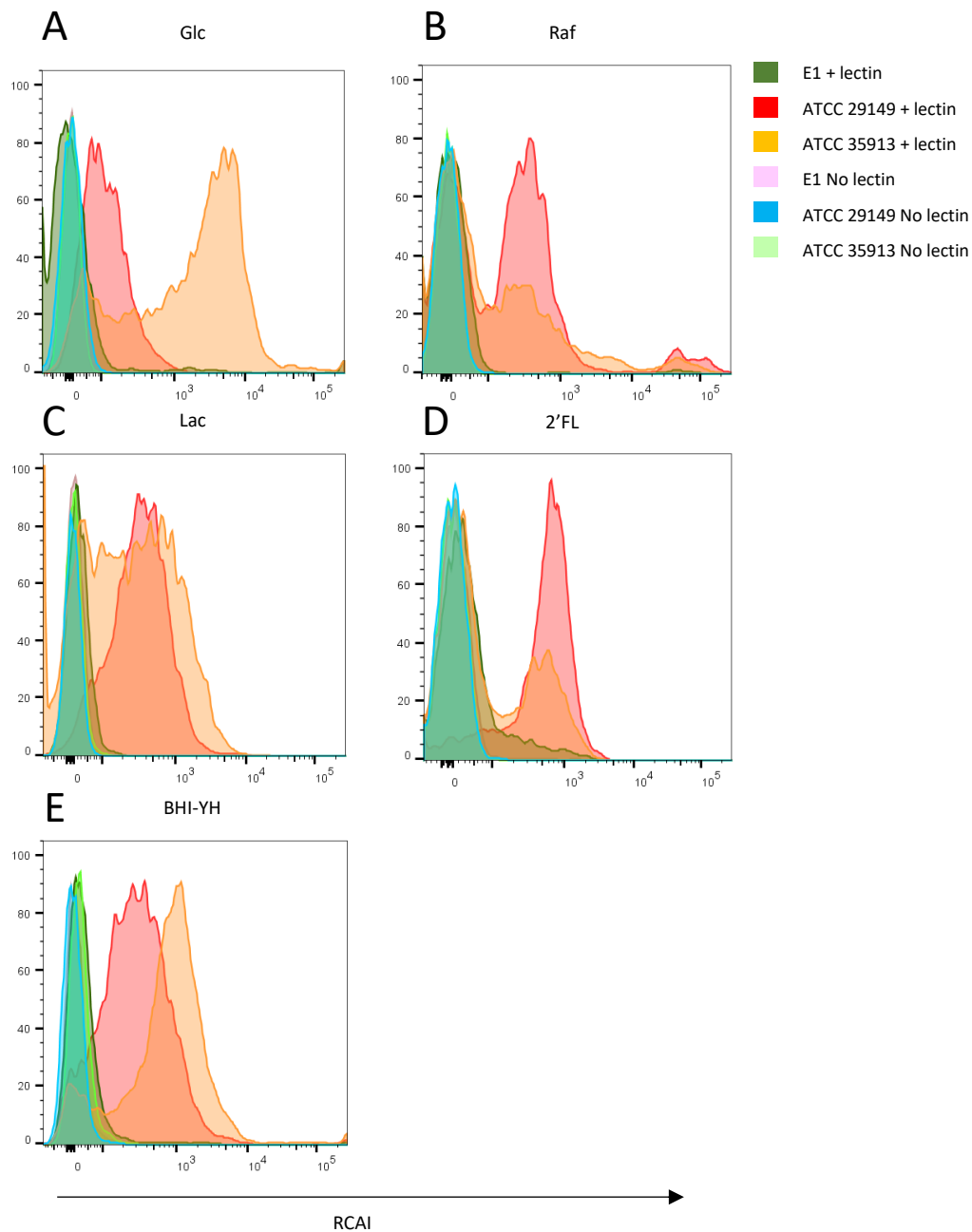


**Figure 16: *R. gnavus* strains grown with Glc, Raf, Lac, 2'FL and BHI-YH lectin binding with RCAI.**

*R. gnavus* E1 (dark green), ATCC 29149 (red) and ATCC 35913 (orange) were incubated with RCAI after being grown with Glc (A), Raf (B), Lac (C), 2'FL (D) or BHI-YH (E). Controls used were bacteria with no fluorescent lectin (pink for E1, blue for ATCC 29149 and green for ATCC 35913).

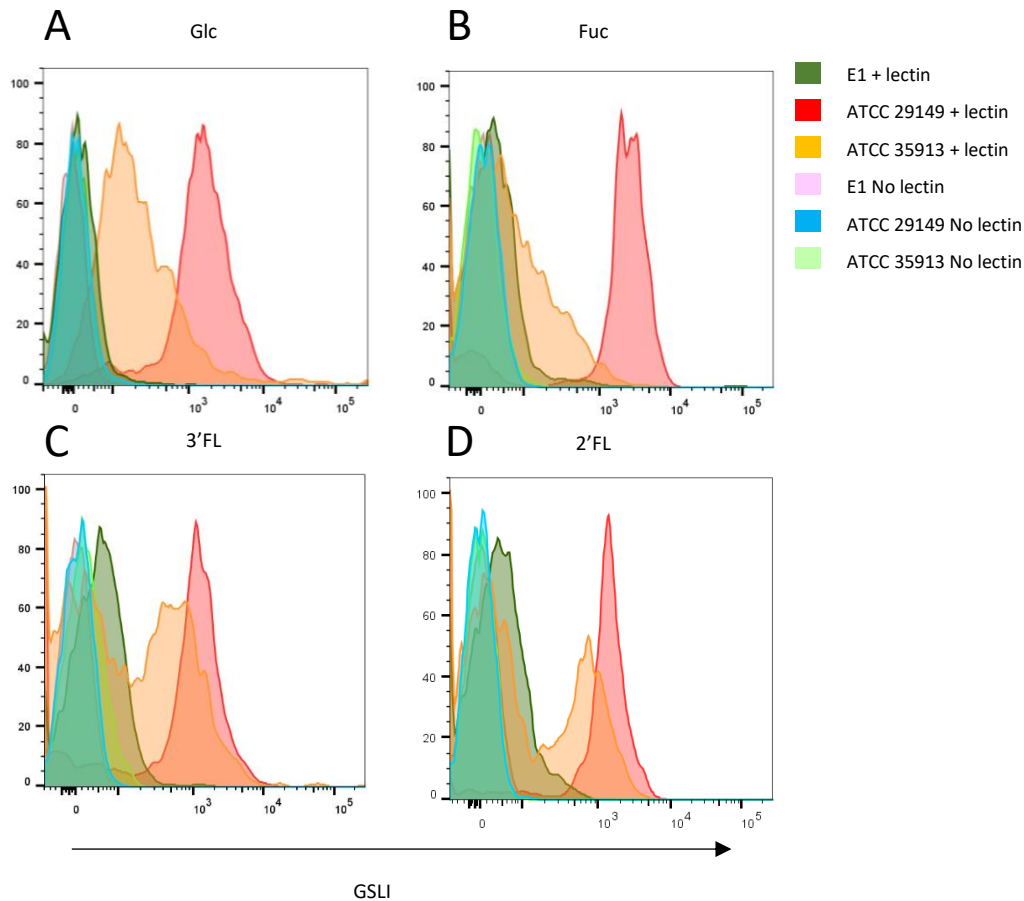


**Figure 17: *R. gnavus* strains grown with Glc, Fuc, 3'FL and 2'FL lectin binding with GSLI.**

*R. gnavus* E1 (dark green), ATCC 29149 (red) and ATCC 35913 (orange) were incubated with GSLI after being grown with Glc (A), Fuc (B), 3'FL (C) or 2'FL (D). Controls used were bacteria with no fluorescent lectin (pink for E1, blue for ATCC 29149 and green for ATCC 35913).

The lectin-binding fluorescence profile was also influenced by the carbohydrate source available to the bacteria. For example, ConA showed higher binding to *R. gnavus* E1 grown on GlcNAc or Suc as sole carbon source than to this strain grown on other carbon sources (Fig. 18A). When *R. gnavus* E1 was grown in Lac, this strain showed stronger binding to SNA than when it was grown with 2'FL, GlcNAc and Suc (Fig. 18B). *R. gnavus* ATCC 29149 grown with 2'FL showed highest binding to RCAI whereas when grown with 3'SL, RCAI showed higher

binding compared to the same strain grown on melibiose (Fig. 18D). For *R. gnavus* ATCC 35913, the bacteria grown in 2'FL showed highest binding to LCA as compared to growth in 3'SL and Mel (Fig. 18E), and to SNA, GSLI and RCAI when the bacteria were grown in 3'SL compared to growth in 2'FL or Mel (Fig. 18F, 18G and 18H).

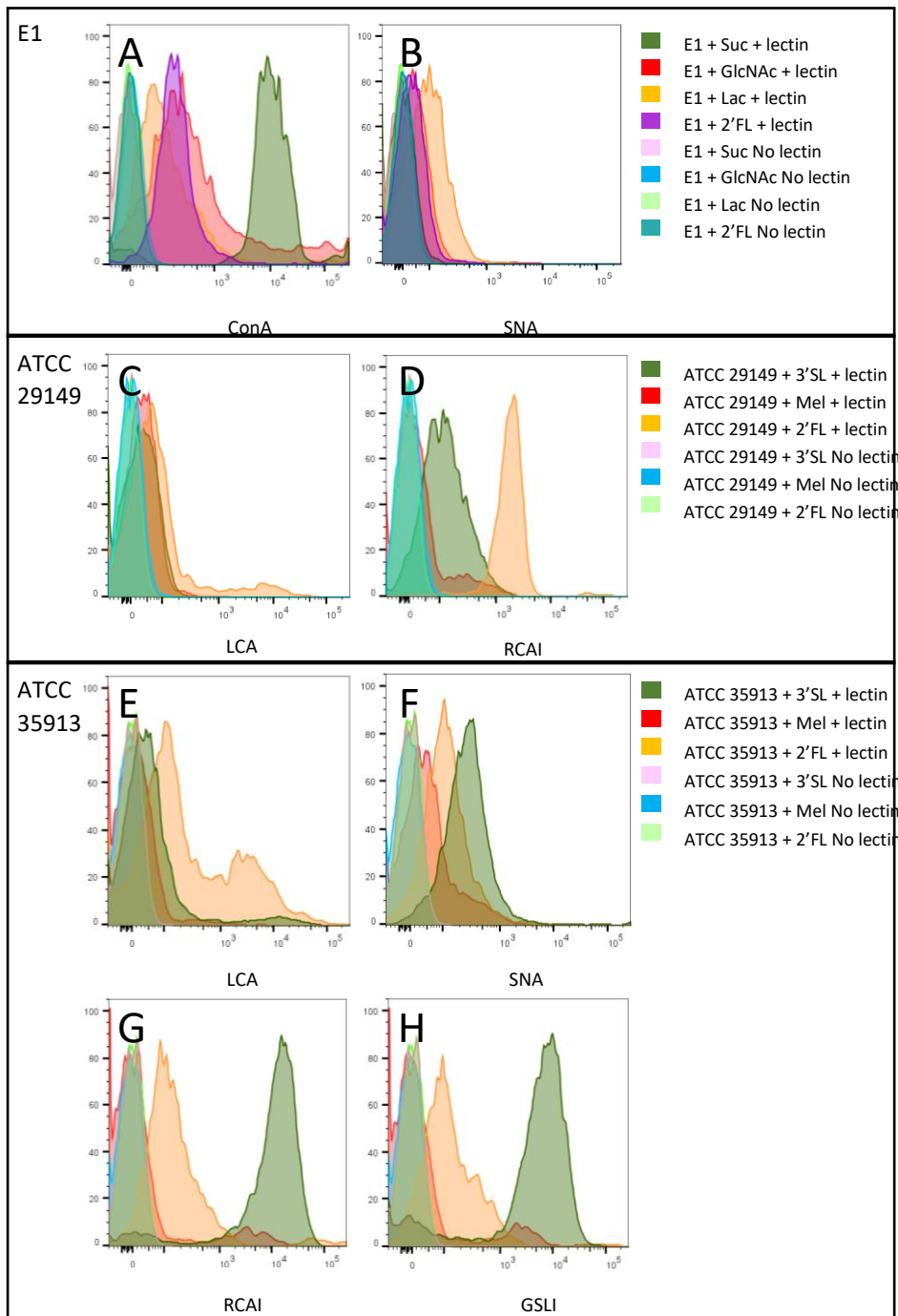


**Figure 18: Effect of carbohydrate source used to grow *R. gnavus* strains on binding with different lectins.**

*R. gnavus* E1 was incubated with ConA (A) or SNA (B) after being grown with Suc (dark green), GlcNAc (red), Lac (orange) or 2'FL (purple). Controls used were bacteria with no fluorescent lectin (pink for E1 grown with Suc, blue for E1 grown with GlcNAc, green for E1 grown with Lac and teal for E1 grown with 2'FL). *R. gnavus* ATCC 29149 was incubated with LCA (C) or RCAI (D) after being grown with 3'SL (dark green), Mel (red) or 2'FL (orange).

Controls used were bacteria with no fluorescent lectin (pink for ATCC 29149 grown with 3'SL, blue for ATCC 29149 grown with Mel and green for ATCC 29149 grown with 2'FL). *R. gnavus* ATCC 35913 was incubated with LCA (E), SNA (F), RCAI (G) or GSLI (H) after being grown with 3'SL (dark green), Mel (red) or 2'FL (orange). Controls used were bacteria with no fluorescent lectin (pink for ATCC 35913 grown with 3'SL, blue for ATCC 35913 grown with Mel and green for ATCC 35913 grown with 2'FL).

The data corresponding to the geometric mean fluorescence intensity (MFI) from each condition tested, calculated using the Flow Jo software are summarised in Fig. 19. In these results, we can see differences in the fluorescence profile of each strain depending on the carbohydrate source used to grow the bacteria: for example, in Fig. 19, we can see that MFI with ConA is stronger for E1 grown with Suc, Mel, Raf and DFL than with other carbohydrates. Also, there is a difference of MFI between strains grown in the same conditions: for example, in Fig. 19, between E1 and ATCC 29149 grown in BHI-YH resulting in a higher MFI with ConA. These data suggest differences in cell surface polysaccharide composition between strains and depending on the carbohydrate source.

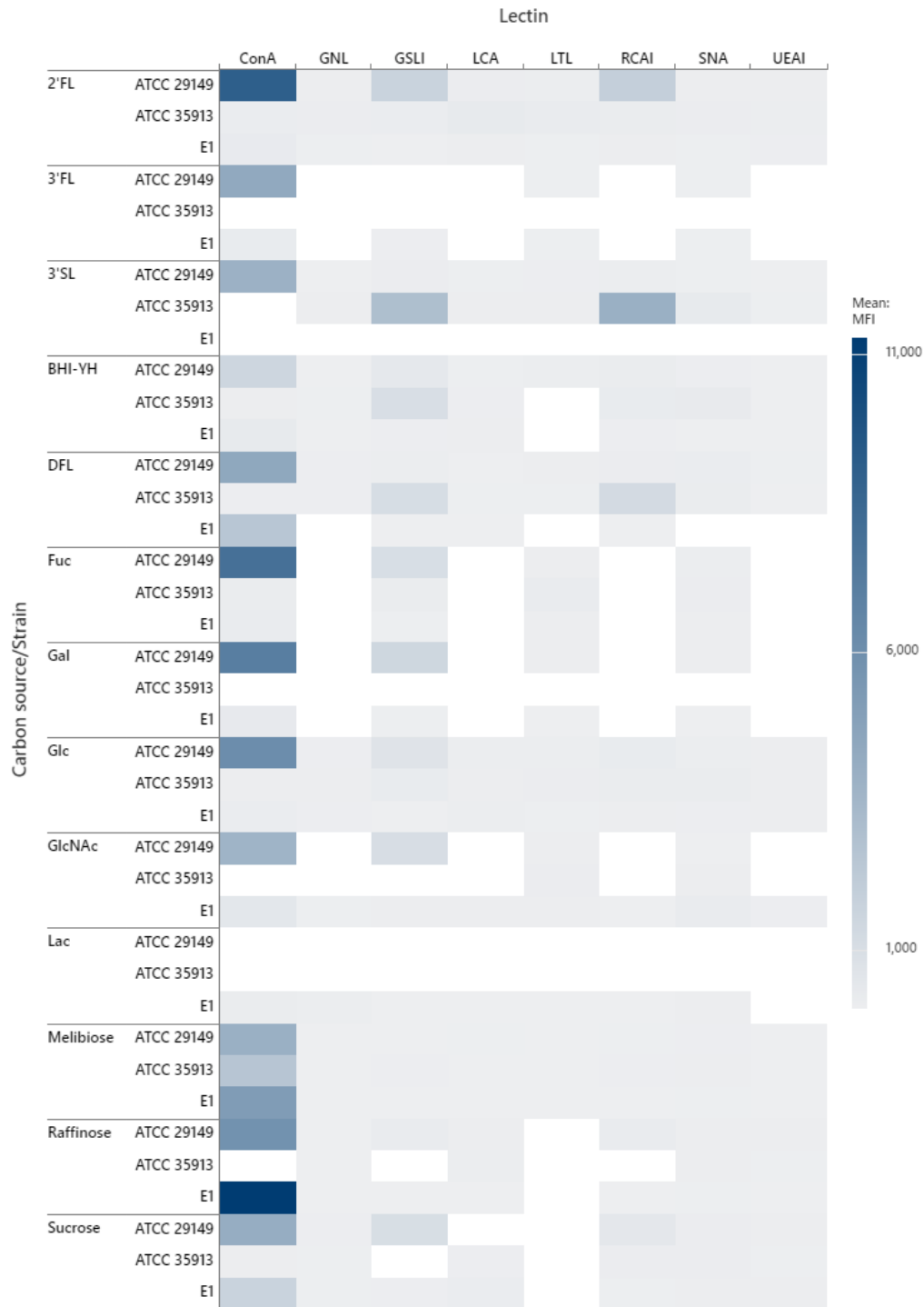


**Figure 19: Summary of *R. gnavus* lectin binding screening by flow cytometry.**

Relative fluorescence level of lectin binding profile of *R. gnavus* strains grown on different carbohydrates as sole carbon-source.

### 3.2.2. Bioinformatics analysis

Following the results from the lectin screening assay, bioinformatic analyses of the glucorhamnan and *cps* biosynthetic clusters in *R. gnavus* strains were carried out to gain further insights into potential differences in cell surface glycosylation. *R. gnavus* strain ATCC 29149 synthesises glucorhamnan with a rhamnose backbone and glucose sidechains (Henke *et al.*, 2019). The rhamnose backbone is made from  $\alpha$ -(1,2)- and  $\alpha$ -(1,3)-linked rhamnose units, and the sidechain has a terminal glucose linked to a  $\alpha$ -(1,6)-glucose (Fig. 20). The biosynthetic cluster for this molecule is made of 23 genes encompassing four biosynthetic genes (RUMGNA\_03521, RUMGNA\_03528, RUMGNA\_03529 and RUMGNA\_03530) needed to convert glucose to rhamnose and five glycosyltransferases (GTs) (RUMGNA\_03514, RUMGNA\_03518, RUMGNA\_03519, RUMGNA\_03524 and RUMGNA\_03532) needed to build the repeating pentasaccharide unit of the glucorhamnan (Fig. 20).

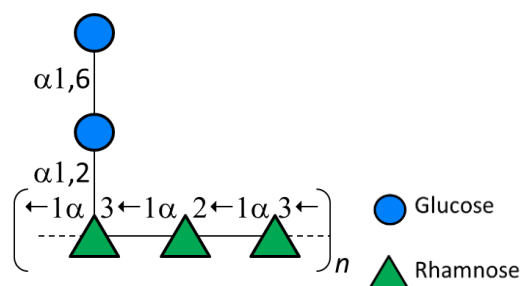


**Figure 20: *R. gnavus* ATCC 29149 cell surface glucorhamnan**

Polysaccharide structure composed of a rhamnose backbone and a glucose side chain.

Using BLASTP, we identified genes in *R. gnavus* E1 and ATCC 35913 with homology to those encoded by *R. gnavus* ATCC 29149 glucorhamnan biosynthetic cluster, suggesting an overall conservation of the cluster in these strains (Fig. 21). However, some strain-specific differences within the cluster were found: out of the 23 genes in the *R. gnavus* ATCC 29149 cluster, 19 genes were shared with E1, 4 genes were absent in E1 with 4 additional genes present in this strain. Nineteen genes from *R. gnavus* ATCC 29149 strain were shared with ATCC 35913, 4 genes were absent in ATCC 35913 with 3 additional genes present in this strain (Fig. 21).

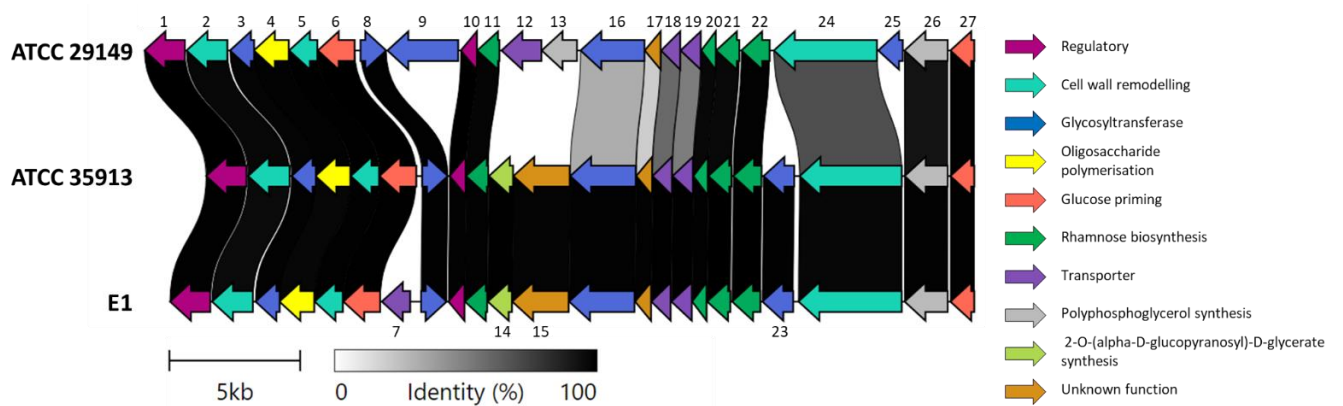


**Figure 21: Bioinformatic analysis of glucorhamnan clusters.**

Comparison of glucorhamnan-like biosynthesis cluster in *R. gnavus* strains. Gene family functions are grouped by colour. Each gene homologues are labelled from 1 to 27 and associated label numbers are integrated in Supplementary data 2. Drawn using Clinker (Galaxy, USA).

Further information on the predicted function of each protein encoded by the genes present in the glucorhamnan cluster of the three strains was obtained by searching for homologous proteins in the NCBI data bank (summarised in Supplementary data 2). Although the function of some of these genes could not be predicted, this analysis showed that the 4 genes (locus tags 11, 20, 21 and 22) predicted to encode rhamnose biosynthesis proteins in *R. gnavus* ATCC 29149 were also present in both E1 and ATCC 35913, suggesting that the rhamnose polysaccharide is identical between the different strains. The three genes predicted to encode cell wall remodelling proteins were also conserved across the three strains, namely polyisoprenyl-teichoic acid-peptidoglycan teichoic acid transferase TagV (locus tag 2), LCP family protein (locus tag 5) and *N*-acetylmuramoyl-L-alanine amidase (locus tag 24), which suggests that the final steps leading to the transfer of the glucorhamnan from the lipid-linked precursor to the cell wall peptidoglycan are the same between the different strains. In addition, the two genes predicted to encode glucose priming proteins in *R. gnavus* ATCC 29149 (locus tags 6 and 27) were present in both E1 and ATCC 35913 strains. Out of the two genes predicted to encode polyphosphoglycerol synthesis proteins in *R. gnavus* ATCC 29149 (locus tags 13 and 26), only RUMGNA\_03533 (locus tag 13) was present in both E1 and ATCC

35913 while RUMGNA\_03523 (locus tag 26) was absent in these strains; and the gene RUMGNA\_03515 (locus tag 4) predicted to encode oligosaccharide polymerisation protein in *R. gnavus* ATCC 29149 was also present in the two other strains. Also, *R. gnavus* E1 displays an additional transporter gene (locus tag 7), not present in the two other strains. Apart from this gene, *R. gnavus* ATCC 35913 gene cluster is identical to that of E1.

Differences in the number and type of GTs (Summarised in Table 8) were observed between *R. gnavus* ATCC 29149 and the other two strains. As shown in Fig. 21, *R. gnavus* ATCC 29149 cluster contained five genes encoding GTs, four belonging to GT2 family (locus tags 3, 8, 16 and 25) and one belonging to GT4 family (locus tag 9), while *R. gnavus* E1 and ATCC 35913 strains encode four GTs belonging to the GT2 family (locus tags 3, 8, 16 and 23) (Fig. 21). The three GT2 genes shared between *R. gnavus* ATCC 29149, E1 and ATCC 35913 strains are predicted to encode a rhamnosyltransferase (locus tag 3), a *N*-acetylglucosaminyl-diphosphodecaprenol L-rhamnosyltransferase (locus tag 8) and a hyaluronan synthase (locus tag 16), therefore all implicated in the addition of rhamnose in the repeating unit of the cell surface polysaccharide. The GT4 (locus tag 9) and the GT2 (locus tag 25) genes unique to *R. gnavus* ATCC 29149 are predicted to encode a polysaccharide pyruvyl transferase family protein and a bactoprenol glucosyl transferase, respectively. The GT2 gene (locus tag 23) unique *R. gnavus* E1 and ATCC 35913 strains is predicted to encode a *N*-acetylgalactosaminyl-diphosphoundecaprenol glucuronosyltransferase. Polyspecificity (enzymes with different donor and/or acceptor found in the same family) is common among GT families, which makes precise functional predictions difficult. However, while the GT2 family encompasses glucosyltransferases and rhamnosyltransferases, no rhamnosyltransferase has been reported in the GT4 family, suggesting that, in *R. gnavus* ATCC 29149 glucorhamnan biosynthetic cluster, this enzyme (predicted to encode for a polysaccharide pyruvyl transferase; absent in *R. gnavus* E1 and ATCC 35913) can hypothetically be responsible for the addition of glucose. Previous results obtained in the lectin binding screening showed that the strain ATCC 29149 showed higher binding to ConA (which as affinity for glucose) than E1 and ATCC 35913 strains when grown in BHI-YH. Put together, those information prompt us to think that ATCC 29149

display on its cell surface one or several polysaccharides, comprising the glucorhamnan, containing glucose in their structure.

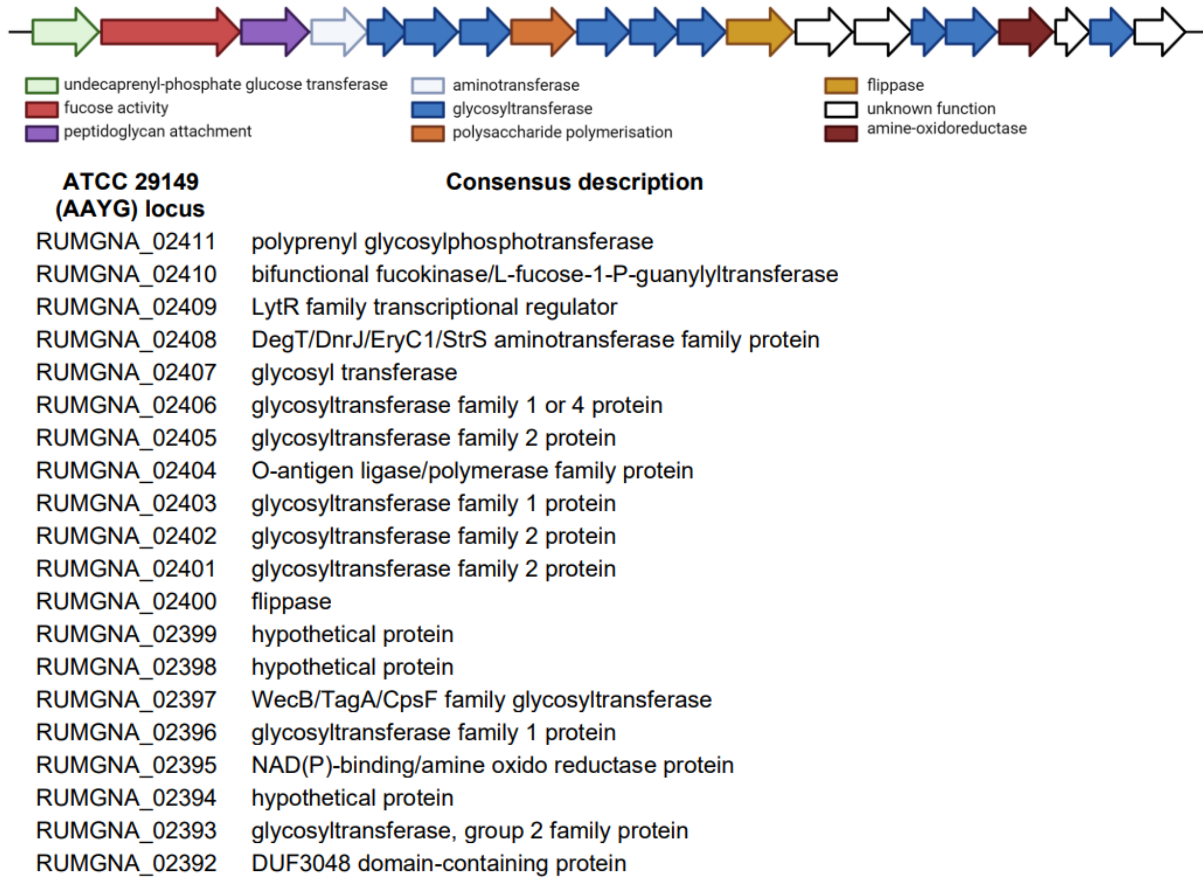
**Table 8: Summary of GTs present in the glucorhamnan cluster of *R. gnavus* strains.**

Homologous genes are represented on the same rows of the table. Blue corresponds to GT2 family, red to GT4 family.

| Locus tag | ATCC 29149   | E1            | ATCC 35913                          | GT family |
|-----------|--------------|---------------|-------------------------------------|-----------|
| 3         | RGMGNA_03514 | RUGNEv3_61017 | RGNV35913_02506                     | GT2       |
| 8         | RGMGNA_03518 | RUGNEv3_61022 | RGNV35913_02510                     | GT2       |
| 9         | RGMGNA_03519 | Not present   | Not present                         | GT4       |
| 16        | RGMGNA_03524 | RUGNEv3_61027 | RGNV35913_02516;<br>RGNV35913_02517 | GT2       |
| 23        | Not present  | RUGNEv3_61034 | RGNV35913_02524                     | GT2       |
| 25        | RGMGNA_03532 | Not present   | Not present                         | GT2       |

In addition to the glucorhamnan cluster, *R. gnavus* ATCC 29149 harbours an additional *cps* cluster (see Fig. 22), which is also present in ATCC 35913 but reported to have nonsense mutations in several genes likely leading to a non-functional cluster Henke *et al.* (2021). Using BLASTN, taking as reference ATCC 29149 *cps* cluster genes, we showed that this cluster was absent in *R. gnavus* E1 strain.

**A**



**B**

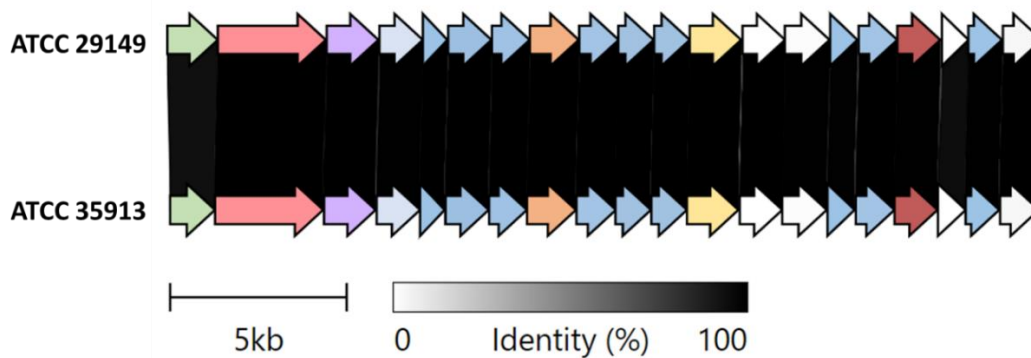


**Figure 22: *R. gnavus* ATCC 29149 *cps* biosynthetic gene cluster.**

(A) Biosynthetic cluster of the CPS in ATCC 29149. Gene family functions are grouped by colour. RUMGNA\_02411 correspond to the gene present on the far left. (B) Comparison of *cps* biosynthesis cluster between ATCC 29149 and ATCC 35913.

Using transmission electronic microscopy (TEM), we observed that *R. gnavus* ATCC 29149 displayed a thick and dense capsular layer on its cell surface, in agreement with the presence of the *cps* biosynthetic cluster while *R. gnavus* ATCC 35913 strain only displayed a thin layer, also in accordance with the *cps* biosynthetic cluster being non-functional in this strain (Fig. 23). The strain E1 couldn't have been observed in TEM here but as it have been observed earlier, *R. gnavus* strain E1 display a thick capsule layer as for ATCC 29149, we would then expect E1 bacteria to form a thick and dense capsular layer on its cell surface as well.

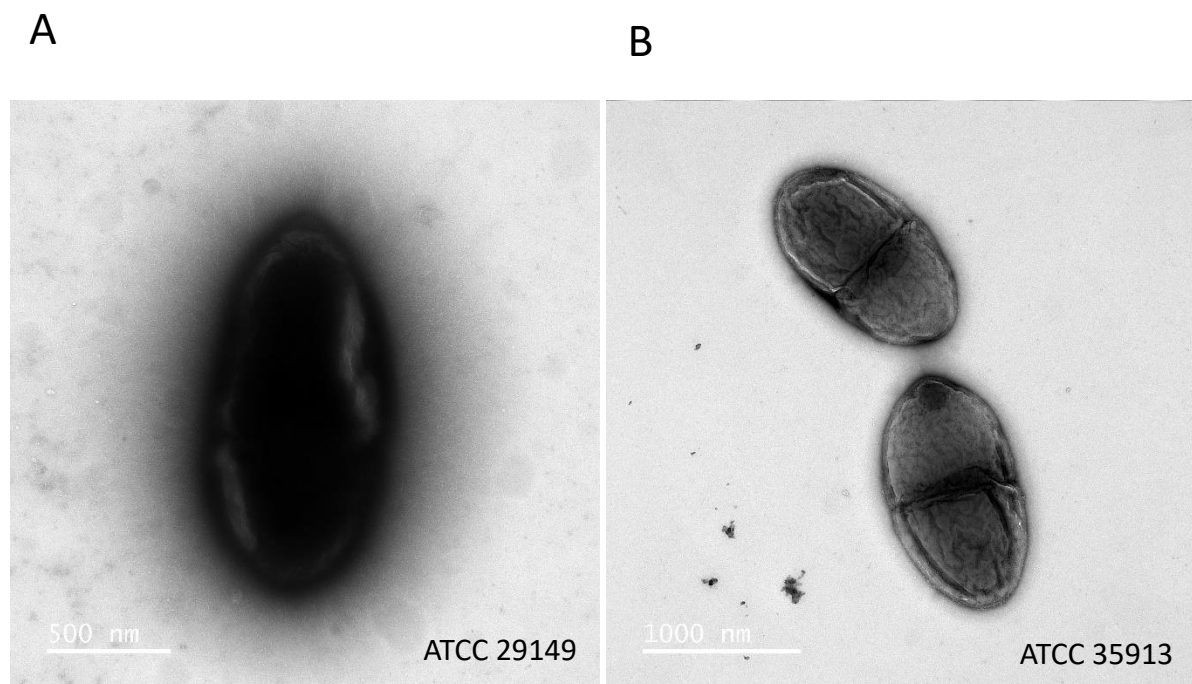


**Figure 23: Transmission electronic microscopy (TEM) of *R. gnavus* strains.**

*R. gnavus* strain ATCC 29149 (A) and ATCC 35913 (B) grown in BHI-YH were negatively-stained with uranyl acetate and imaged by TEM. Images courtesy of Kathryn Gotts.

### 3.2.3. Structural characterisation of *R. gnavus* cell surface polysaccharide

Having shown strain-specific differences in the lectin binding profile of *R. gnavus* strains, supported by differences in their polysaccharide biosynthetic clusters, we next structurally

characterised the cell surface polysaccharides of *R. gnavus* ATCC 35913 grown in BHI-YH by GC-MS and proton NMR.

As described in section 2.4.1 and 2.4.2 and in Supplementary data 6, the freeze-dried bacteria were treated with citric acid and butanol, resulting in the generation of a pellet (sample **S**), aqueous phase (sample **O**), interphase (sample **G**) and butanol phase (sample **P**), corresponding to different component of the bacterial cells. To extract the cell surface polysaccharide, sample **S** was further treated with hydrofluoric acid. The pellet (sample **S**) and aqueous samples were converted to AMG (acetylated methyl glycosides) and analysed by GC-MS along with oligosaccharide standards. The GC-MS chromatograms indicated the presence of glucose and rhamnose in the pellet (Fig. 24A) while glucose, rhamnose, mannose and ribose in the aqueous phase (Fig. 24B).

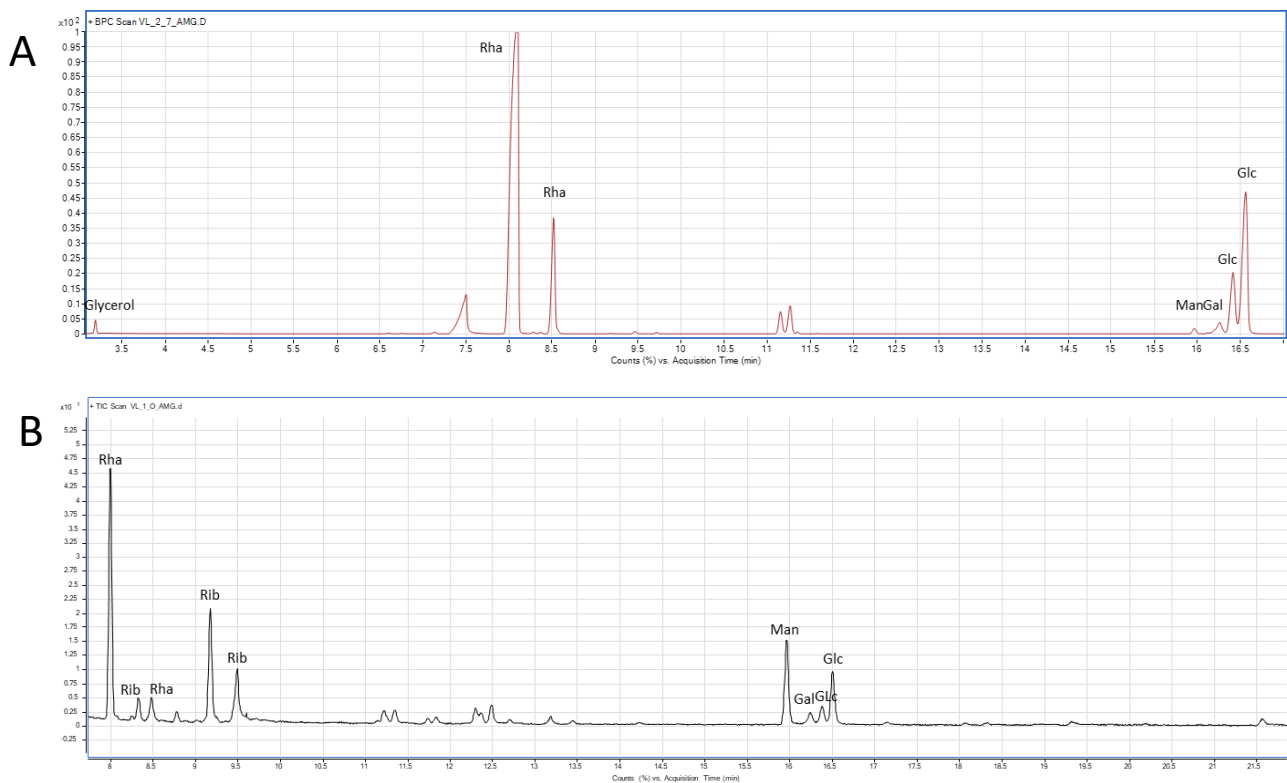


**Figure 24: GC-MS analysis of the pellet fraction and the aqueous phase of *R. gnavus* ATCC 35913 cell surface polysaccharide.**

GC-MS analysis of (A) the sample **S** corresponding to the pellet fraction from the citric acid/butanol extraction and (B) the sample **O** corresponding to the aqueous phase with the AMG method. Rha for rhamnose, Man for mannose, Glc for glucose, Rib for ribose and Gal for galactose.

Next, in order to determine the absolute configuration of glucose and rhamnose present in sample **S**, (R)-(-)-2-octanol was used to generate AOG (acetylated octyl glycosides) which were analysed using GC-MS. By comparing with standards, the monosaccharides present in the sample **S** were identified as L-rhamnose (Fig. 25) and D-glucose (Fig. 26).

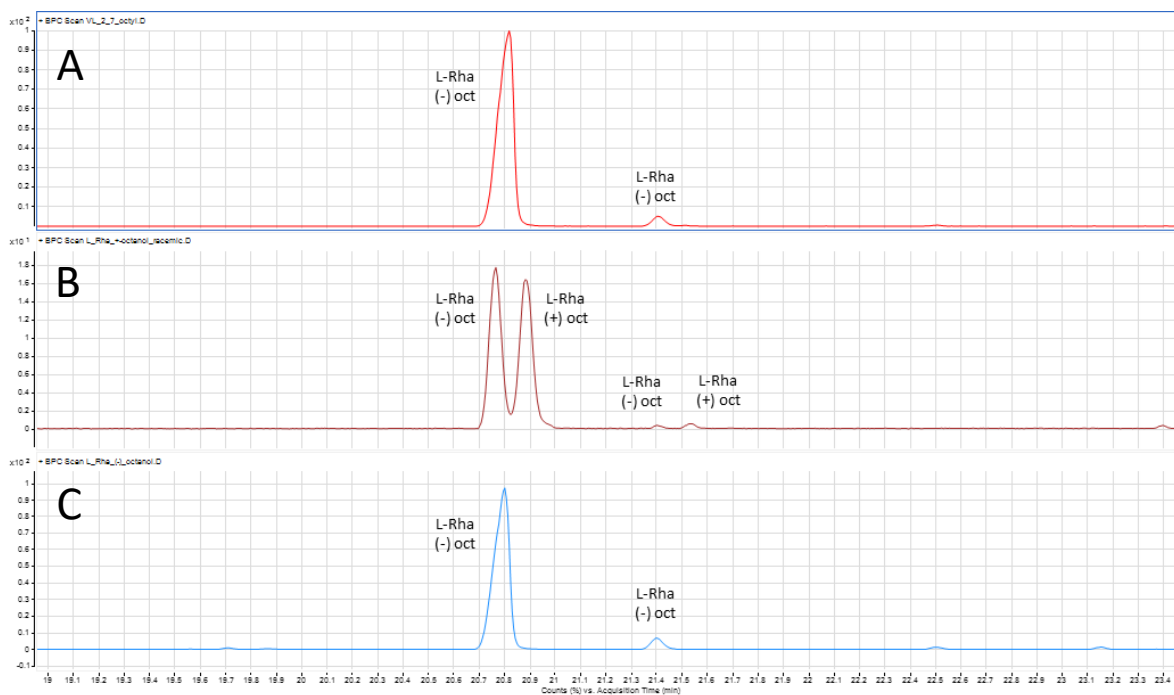


**Figure 25: Absolute configuration analysis of rhamnose by GC-MS of *R. gnavus* ATCC 35913 pellet fraction.**

(A) The sample **S** corresponding to the pellet fraction from the citrate/butanol extraction described in section 2.4.2, treated with (R)-(-)-2-octanol; (B) Rhamnose sample treated with racemic 2-octanol; (C) Rhamnose sample treated with (R)-(-)-2-octanol. L-Rha(-)oct stands for L-rhamnose-(-)-2-octanol and L-Rha(+ )oct stands for L-rhamnose-(+)-2-octanol.

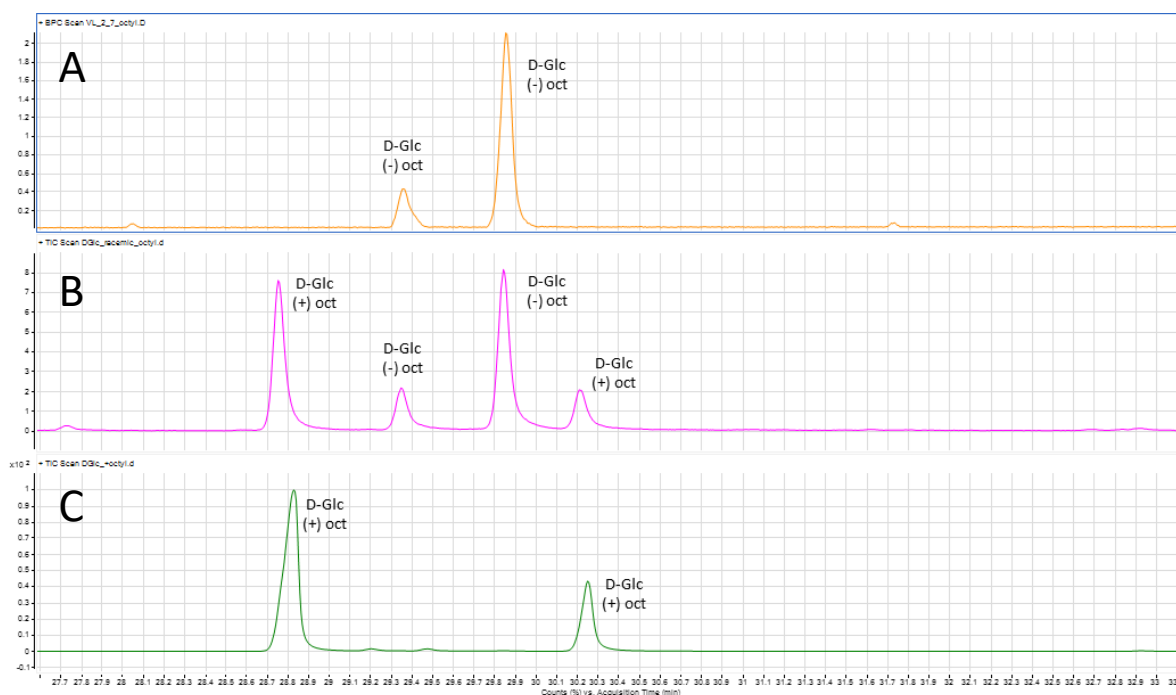


**Figure 26: Absolute configuration analysis of glucose by GC-MS of *R. gnavus* ATCC 35913 pellet fraction.**

(A) The sample **S** corresponding to the pellet fraction from the citrate/butanol extraction described in section 2.4.2, treated with (R)-(-)-2-octanol; (B) Glucose sample treated with racemic 2-octanol; (C) Glucose sample treated with (R)-(-)-2-octanol. D-Glc(-)oct stands for D-glucose-(-)-2-octanol and D-Glc(+/-)oct stands for D-glucose -(-)-2-octanol.

Finally, the linkage between the different monosaccharides was determined using the PMAA (partially methylated acetylated alditols) method. This reaction results in the methylation of the free hydroxide groups in the carbohydrate cycle, while the hydroxide groups generated after the separation of the different monosaccharides composing the polysaccharide are acetylated. The analysis of the PMAA compounds by GC-MS allows to identify which hydroxide group was involved in a linkage with another carbohydrate. The mass spectra associated with the GC showed the presence of 2-6-deoxy-hexose, 3-6-deoxy-hexose, 2,3-6-deoxy-hexose, 3,4-6-deoxy-hexose, 2,4-6-deoxy-hexose, t-hexose, 3-hexose, 3-hexose, 4-hexose, 6-hexose and 3,4-hexose (Fig. 27). This analysis indicates that the cell surface polysaccharide is composed of a terminal hexose and 6-deoxy-hexoses linked by either their carbon 2, 3 or both.

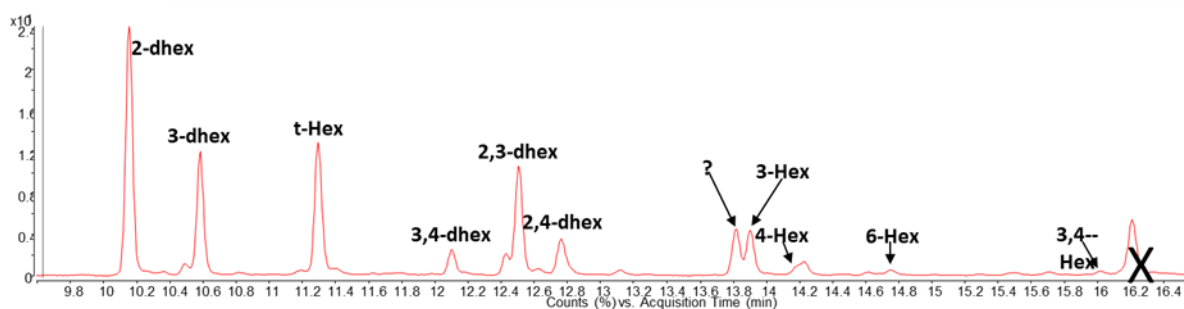


**Figure 27: GC-MS analysis of the pellet fraction from ATCC 35913 glucorhamnan purification with the PMAA method.**

“hex” stands for hexose and “dhex” stands for 6-deoxy-hexose.

Next, we used 2D NMR to determine the presence and configuration of polysaccharides present in the pellet. The analysis of the spectra indicates that the polysaccharide is composed of four  $\alpha$ -6-deoxy hexose and  $\beta$ -1-hexose (Fig. 28). Together with the GC-MS results, these data indicate that the polysaccharide is composed of four  $\alpha$ -L-rhamnoses and one  $\beta$ -D-glucose. Furthermore, based on the analysis of the 2D NMR spectra, we propose that the *R. gnavus* ATCC 35913 cell surface polysaccharide is a glucorhamnan with a backbone composed of four  $\alpha$ -(1,2) and  $\alpha$ -(1,3) linked rhamnose and sidechains composed of one  $\beta$ -(1,3) linked glucose, therefore different from that of ATCC 29149 (Fig. 10A).

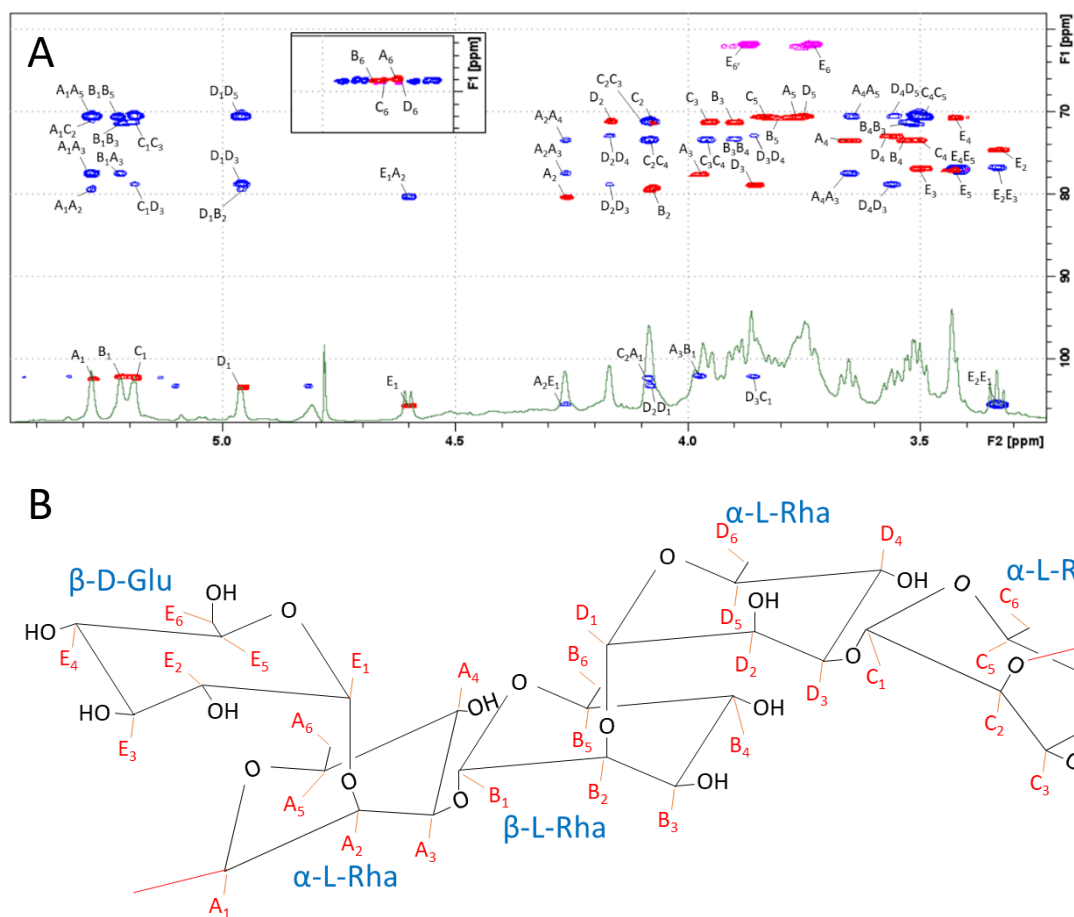


**Figure 28: 2D NMR spectrum of *R. gnavus* ATCC 35913 glucorhamnan.**

(A) Superposed 2D NMR spectra of ATCC 35913 purified cell surface polysaccharide with HSQC (in red and pink) and HMBC (in blue). In the HSQC spectrum, red dots correspond to carbon bound to two hydrogens while pink dots correspond to carbon bound to one or three hydrogens. (B) Representation of the glucorhamnan structure established from 2D NMR with associated dot denomination.

Large-scale culture of *R. gnavus* E1 grown in BHI-YH was provided to our collaborator in Naples. GC-MS and NMR showed the same structural composition as *R. gnavus* ATCC 35913 purified cell surface polysaccharide (Cristina de Castro, personal communication).

Then, to investigate the influence of the carbohydrate source on *R. gnavus* glucorhamnan composition, and based on the lectin-binding screening results, large-scale culture of *R. gnavus* ATCC 35913 strain grown with melibiose (D-Gal- $\alpha$ (1 $\rightarrow$ 6)-D-Glc) as sole carbon source was provided to our collaborator for structural characterisation. 1D NMR (shown in

Supplementary data 3) analysis revealed differences in the rhamnose/glucose ratio of *R. gnavus* ATCC 35913 glucorhamnan when the bacteria were grown with melibiose which was 6.6 as compared to 5.1 when grown in BHI-YH while the rhamnose/glucose ratio of *R. gnavus* grown on BHI-YH was 3.2 (Table 9). The expected rhamnose/glucose ratio is theoretically 4 as each repeating unit is composed of 4 rhamnoses and 1 glucose. These data indicate that the glucorhamnan structure of *R. gnavus* ATCC 35913 and E1 strains, although displaying the same repeating unit structure and a similar biosynthetic gene cluster, can be influenced by growth conditions. This indicates a potential reshaping of the glucorhamnan structure which would be done after the initial synthesis, resulting in a different final composition of rhamnose/glucose in the glucorhamnan depending on the strain and the nutritional niche of the bacteria.

**Table 9: Relative quantification of monosaccharides of *R. gnavus* strains E1 and ATCC 35913 glucorhamnans.**

The cell surface polysaccharides of *R. gnavus* E1 grown in BHI-YH and ATCC 35913 grown in BHI-YH or LAB+melibiose were determined by 1D NMR and area under the curve was measured for each anomeric region peak of the spectra from Supplementary data 3. The values are normalised to the glucose anomeric region area conditions. Calculated rhamnose/glucose ratio displayed in the last row. Data from E1 grown in BHI-YH and ATCC 35913 provided by our collaborators from Cristina De Castro's team in the University of Naples, Italy.

| Conditions                 | E1 grown in BHI-YH | ATCC 35913 grown in BHI-YH | ATCC 35913 grown with melibiose |
|----------------------------|--------------------|----------------------------|---------------------------------|
| Area Rha A                 | 0.763158           | 1.016129                   | 1.111111                        |
| Area Rha B+C               | 15.52632           | 2.532258                   | 3.148148                        |
| Area Rha D                 | 0.842105           | 1.596774                   | 2.296296                        |
| Area Glc                   | 1                  | 1                          | 1                               |
| <b>A<sub>Rha/Glc</sub></b> | <b>3.2</b>         | <b>5.1</b>                 | <b>6.6</b>                      |

### 3.2.4. *R. gnavus* gene transcription analysis of GTs from glucorhamnan and *cps* clusters

To gain a better understanding of the factors underpinning the differences in the glucose/rhamnose ratio of the glucorhamnan between *R. gnavus* ATCC 29149 and ATCC 35913 strains (section 3.2.3), we investigated the influence of the culture medium and growth phase on the gene expression level of GTs present in the glucorhamnan cluster of these strains. The bacteria were grown in BHI-YH (both strains) or minimal medium supplemented with melibiose (ATCC 35913 only) at exponential and stationary phase.

Quantitative PCR was first used to determine the expression level of RUMGNA\_03514, RUMGNA\_03518, RUMGNA\_03532 GT genes (encoding, respectively, predicted rhamnosyltransferase, *N*-acetylglucosaminyl-diphospho-decaprenol L-rhamnosyltransferase and bactoprenol glucosyl transferase homolog from prophage CPS-53) in *R. gnavus* ATCC 29149 and RGNV35913\_02506, RGNV35913\_02510, RGNV35913\_02516, RGNV35913\_02524 GT genes (encoding, respectively, predicted rhamnosyltransferase, *N*-acetylglucosaminyl-diphospho-decaprenol L-rhamnosyltransferase, hyaluronan synthase and *N*-acetylgalactosaminyl- diphosphoundecaprenol glucuronosyltransferase) in *R. gnavus* ATCC 35913.

As shown in Fig. 29A, in *R. gnavus* ATCC 29149 grown in BHI-YH, the three genes (RUMGNA\_03514, RUMGNA\_03518 and RUMGNA\_03532) displayed similar levels of expression after 6 h of growth. Also, the expression of each GT gene tested was higher after 6 h culture compared to the expression level after 24 h culture. These data are in accordance with previous results showing that the expression of several genes in the glucorhamnan cluster of *R. gnavus* ATCC 29149 (RUMGNA\_03521, RUMGNA\_03528, RUMGNA\_03519, RUMGNA\_03514 and RUMGNA\_03524) decreased after 24 h of growth (Henke *et al.*, 2019). Though, as these data were acquired using only one assay, this experiment would need repeating to confirm the results obtained.

In *R. gnavus* ATCC 35913, the expression level varied among the selected GT genes from the glucorhamnan cluster. When *R. gnavus* ATCC 35913 was grown in BHI-YH, RGNV35913\_02516

gene showed the highest expression level, followed by RGNV35913\_02506, which showed a higher expression level than RGNV35913\_02510 and RGNV35913\_02524 after either 6 h or 24 h culture; also, RGNV35913\_02506 and RGNV35913\_02516 showed higher expression level after 24 h than 6 h of growth while RGNV35913\_02510 and RGNV35913\_02524 showed higher expression level after 6 h than 24 h of growth. When *R. gnavus* ATCC 35913 was grown on melibiose, RGNV35913\_02506 showed the highest level of expression after 6 h of growth, followed by RGNV35913\_02516, which showed higher level of expression than RGNV35913\_02516 and RGNV35913\_02524; while RGNV35913\_02516 showed the highest level of expression after 24 h of growth, followed by RGNV35913\_02506, RGNV35913\_02516 and RGNV35913\_02524.

These results showed that differences in gene expression levels are dependent on the strain and growth medium. If we consider that each GT gene in the glucorhamnan cluster is responsible for the addition of one monosaccharide in the repeating unit composition of the glucorhamnan, as suggested by Henke *et al.* (2019), then the level of expression for each GT in this cluster may directly influence the composition of rhamnose and glucose in the glucorhamnan, consistent with the differences observed in the ratio of rhamnose to glucose in showed in Table 9. Together these data indicate that *R. gnavus* E1 and ATCC 35913 strains may display subtle differences in glucorhamnan composition although they possess the same repeating unit structure.

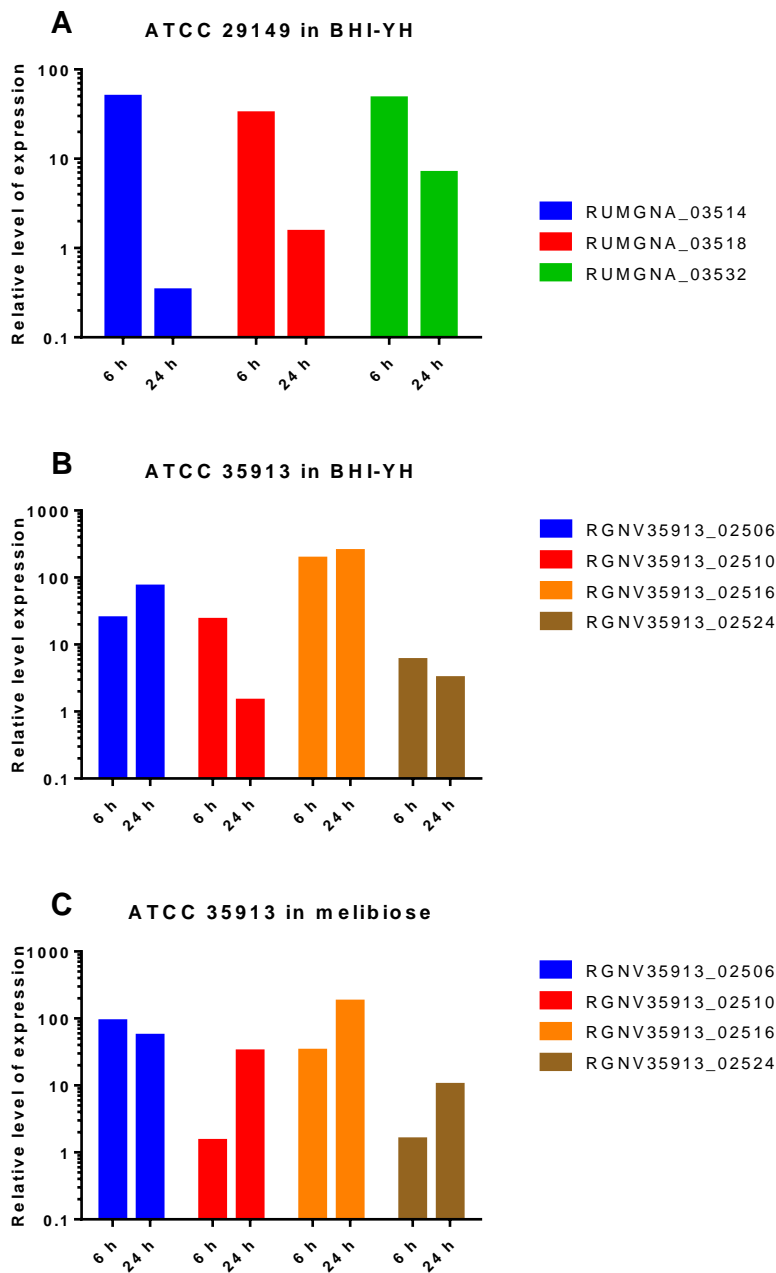


**Figure 29: *R. gnavus* glucorhamnan cluster GT gene expression.**

Expression of RUMGNA\_03514, RUMGNA\_03518 and RUMGNA\_03532 GTs in *R. gnavus* ATCC 29149 grown in BHI-YH (A) and RGNV35913\_02506, RGNV35913\_02510, RGNV35913\_02516 RGNV35913\_02524 GTs in *R. gnavus* ATCC 35913 grown in BHI-YH (B) or melibiose (C). Analysis was carried out after 6 h or 24 h of culture. The 16SRg5 expression was used as reference to normalise the data. The experiment was done using one assay.

The qPCR approach was also used to determine the gene expression of one of the GT gene RUMGNA\_02407 in *R. gnavus* ATCC 29149 *cps* biosynthetic cluster. The results confirmed the expression of the GT when the bacteria were grown in BHI-YH with 3.5-fold more expression during the exponential phase (6 h) than during the stationary phase (24 h) (Fig. 30). A similar pattern of expression was obtained for several GT genes of the *R. gnavus* ATCC 29149 glucorhamnan cluster, indicating that both the glucorhamnan and CPS follow a similar synthesis pattern throughout the different stages of bacterial growth.

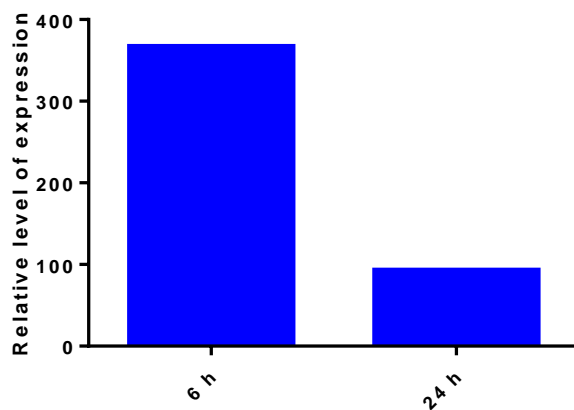


**Figure 30: *R. gnavus cps* cluster GT gene expression.**

Relative expression of the *cps* biosynthetic cluster gene RUMGNA\_02407 in *R. gnavus* ATCC 29149 after 6 h or 24 h of growth. The 16SRg5 expression was used as reference to normalise the data. The experiment was done using one biological and technical replicate.

### 3.3. Discussion

The results from the lectin binding screening and bioinformatics analyses suggest strain-specific differences in the cell surface glycosylation of *R. gnavus*. As the lectin binding is assessing the presence of different monosaccharides available on cell surface of the bacteria, this experiment limited the polysaccharide residue detection to the monosaccharide available at the apex of the capsule, as it is *in vivo*, where host immune cells only detects superficial residues while other saccharides hidden underneath the capsule would be undetected by the

host immunity, but other methods could have been used, like histochemistry or lectin microarrays, to investigate further *R. gnavus* strains cell surface whole cell surface glycosylation. PBS was used even though it does not contain  $\text{Ca}^{2+}$ , needed for the binding of some lectins, therefore not allowing the experiment to be conclusive, TBS should be used here instead as it contains the necessary  $\text{Ca}^{2+}$  mentioned. Nonetheless, the strain-specific cell surface glycosylation was confirmed by structural analyses of *R. gnavus* ATCC 35913 using a combination of NMR and GC-MS approaches. We showed that although glucorhamnan was present in the three *R. gnavus* strains tested, its structural composition was different in *R. gnavus* ATCC 35913 and E1 strains as compared to the previously characterised ATCC 29149 strain (Henke *et al.*, 2019). The glucorhamnan of *R. gnavus* ATCC 35913 and E1 strains revealed a backbone composed of four  $\alpha$ -(1,2) and  $\alpha$ -(1,3)-linked rhamnoses and sidechains composed of one  $\beta$ -(1,3)-linked glucose (Fig. 31A).

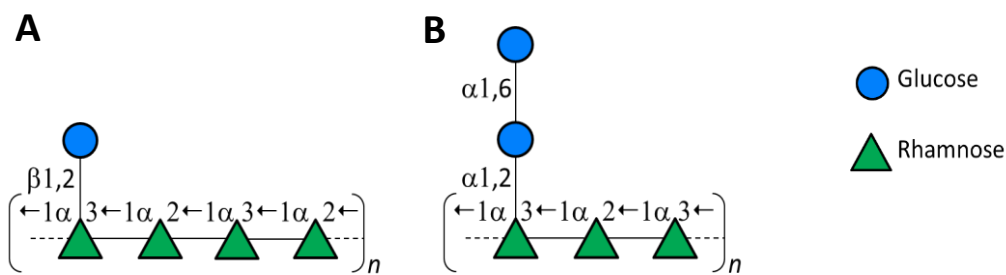


**Figure 31: Structure of *R. gnavus* glucorhamnan.**

(A) ATCC 35913 (this work) and E1 (unpublished). (B) ATCC 29149 (Henke *et al.* 2019).

A similar structure has been identified in *Streptococcus uberis* strain 233, and *Streptococcus mutans* serotype c, both pathogens in bovine and human, respectively, but no associated function has been elucidated yet (Czabańska *et al.*, 2013; King *et al.*, 2021) (Fig. 32A). Other polysaccharides with similar structure were found in *Shigella flexneri* strain 2a (Hlozek *et al.*, 2020) described in Fig. 32B, this polysaccharide has been shown to induce a pro-inflammatory immune response in mouse (Tian *et al.*, 2021).

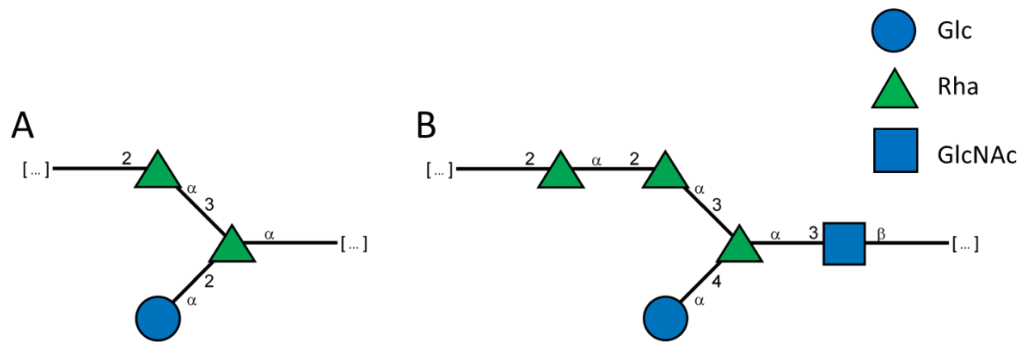


**Figure 32: Polysaccharides sharing similar structures with *R. gnavus* glucorhamnan.**

Polysaccharides present on the cell surface of (A) *Streptococcus uberis* strain 233 (Czabańska et al., 2013) and (B) *Shigella flexneri* strain 2a (Hlozek et al., 2020).

The strain-specific differences in the glucorhamnan structure between *R. gnavus* E1, ATCC 35913 and ATCC 29149 is consistent with the differences in the GT profile observed in the glucorhamnan biosynthesis gene cluster of these three strains. However, the structural composition of *R. gnavus* CPS remains elusive since it was not possible to identify it using NMR and GC-MS methods in *R. gnavus* ATCC 29149 (Cristina deCastro, personal communication). Strain-specific differences in cell surface glycosylation have been reported for pathogens such as *Streptococcus suis*, a pathogen in pigs that can cause severe systemic infection in humans, where four strains showed differences in the structure of their CPS due to one single nucleotide polymorphism (SNP) present in the gene encoding a GT (Roy et al., 2017). Differences were also reported from diverse strains of *Neisseria* (both *N. meningitidis* and *N. gonorrhoeae*) with lipooligosaccharide (LOS) structure and CPS greatly influencing the virulence of the organism and the host innate immune responses (Pridmore et al., 2003). The lipid A structure of both *N. meningitidis* and *N. gonorrhoeae* consists of  $\alpha$   $\beta$ -d-glucosaminyl-(1'→6)-d-glucosamine disaccharide backbone with variable patterns of phosphorylation and fatty acid acylation (Kulshin et al., 1992; Takayama et al., 1986). These differences in cell surface polysaccharide composition could be a competitive advantage as it would give *R. gnavus* strains a broader diversity of microbial patterns recognised by the host, leading to a more likely tolerance and evading against the host immunity in comparison with other gut bacterial species.

In addition, the lectin binding screening suggests that *R. gnavus* cell surface glycosylation may be influenced by the carbon source accessible to the bacteria. This is particularly relevant to gut bacteria which depending on their biogeography along and across the GI tract live in different nutritional niches. This relates to *R. gnavus*, as previous work showed that some of *R. gnavus* strains are mucin polysaccharide foraging (such as *R. gnavus* ATCC 29149 or ATCC 35913) whereas others such as E1 are non-mucin polysaccharide foraging strains (Croft et al., 2013, 2016), suggesting differences in spatial colonisation of the gut (Bell et al., 2019). The influence of carbohydrate availability on cell surface glycosylation has been reported for *E. coli* strains K4 and K5, where the composition of the bacterial CPS and its secretion level differed following the carbohydrate used to grow the bacteria (Francesca Restaino et al., 2017). However, less is known about strain-differences and the influence of the carbohydrate source on CPS in commensal bacteria. Furthermore, the data from GC-MS and NMR analysis showed differences in the rhamnose/glucose ratio displayed by E1 and ATCC 35913, and that following the condition of culture in which the bacteria were grown in. As the biosynthesis clusters in the two strains show no difference in GT profile, we can hypothesise that the differences observed could be due to the action of GTs and GH reshaping the glucorhamnan structure. To test that, the activity of GTs and GHs can be assessed using RT-qPCR with *R. gnavus* strains grown in different medium to quantify associated RNA level and correlate it with the rhamnose/glucose ratio.

It is therefore possible that the cell surface glycosylation of *R. gnavus* strains inhabiting the mucus niche differ from *R. gnavus* luminal strains and as a result differentially impact host health. In the next chapters, we will investigate the effect of *R. gnavus* strains and their associated glucorhamnans on the host immune and epithelial cell responses.

Chapter 4: Effect of *R. gnavus* strain-specific cell surface glycosylation on gut barrier function

#### 4.1. Introduction

Interactions occurring at the mucosal interface between the gut microbiota and the host are critical to the development and maintenance of gut barrier function. This is particularly relevant to gut bacteria living in proximity to the host epithelium. As the mucus layer serves as a physical barrier between the gut microbiota and the intestinal monolayer, the bacteria inhabiting the gut secrete extracellular polysaccharides, extracellular proteins, indole, extracellular vesicles, short-chain fatty acids, but also bacteriocins which can interact with receptors on intestinal cells, enhancing the expression of tight junction genes, or in goblet cells, promoting the production of mucus (Kumar et al., 2020).

Cell surface polysaccharides such as CPS, LPS or EPS expressed by members of the gut microbiota can influence gut barrier function through the modulation of the expression or distribution of tight junction proteins in the intestinal epithelium. For example, EPS from *Lactobacillus plantarum* strain HY7714 has been reported to upregulate ZO-1 and occludin in Caco-2 cells (K. Lee et al., 2021). In contrast, LPS from *E. coli* strain O111:B4 has been shown to disrupt gut barrier function in intestinal cells by down regulating the expression of tight junction genes like ZO-1, claudin-1 or occludin (Bian et al., 2021; J. Wu et al., 2020).

Although less studied than in pathogens, the polysaccharides decorating the surface of gut commensal bacteria have also been shown to influence the production of cytokines by intestinal enterocytes. For example, the CPS from the probiotic strain *E. coli* Nissle 1917 (EcN), has been shown to induce the secretion of IL-10 or IL-12 by Caco-2 cells, leading to alleviation of intestinal inflammation (Q. Liu et al., 2020; Schlee et al., 2007). The interaction between the gut microbiota cell surface polysaccharides and the host immunity is permitted by the PRRs, which upon microbial polysaccharides exposure, will activate NF- $\kappa$ B and MAPK signalling cascades, directly enabling the expression of cytokines, chemokines and antimicrobial peptides encoding genes (Q. Liu et al., 2020).

Since, in homeostatic conditions, *R. gnavus* strains are confined in the mucus layer in close proximity to the host epithelium, we next investigated the role of *R. gnavus* strains and

associated glucorhamnans characterised in Chapter 1 on intestinal epithelium cells focusing on cytokines and tight junction proteins. To that end, cytokine production was determined to assess the induction of immune response from intestinal cells. Also, gene expression analysis and assessment of cytokines and tight junction proteins production were run to investigate the effect of *R. gnavus* strains and derived glucorhamnan on gut barrier function.

## 4.2. Results

### 4.2.2. Effect of *R. gnavus* strains and glucorhamnans on gut barrier integrity

Then, to investigate further the influence of *R. gnavus* on gut barrier function, the capacity of *R. gnavus* strains and purified glucorhamnan was first assessed using T84 cocultured with LS174T cells grown on transwells as a simplified model of the intestinal epithelium. LS174T are goblet-like cells able to produce mucus (van Klinken et al., 1996). T84 and LS174T cells were co-cultured on transwells (6.5 mm, coated with type I collagen) at a ratio 10:1 to form an epithelial monolayer (Fig. 33). Fluorescence-based immunohistochemical analysis of the T84/LS174T cells after fixation with 4% PFA confirmed the formation of a tight layer (with staining of tight-junction protein occludin) and the production of mucus by the goblet cells (by staining of MUC2) (Fig. 33). As the cytokine secretion is polarised *in vivo*, sample medium from apical and basolateral compartments will be extracted in the following experiments in order to assess the cytokine secretion in both the lumen and the lamina propria side, respectively.

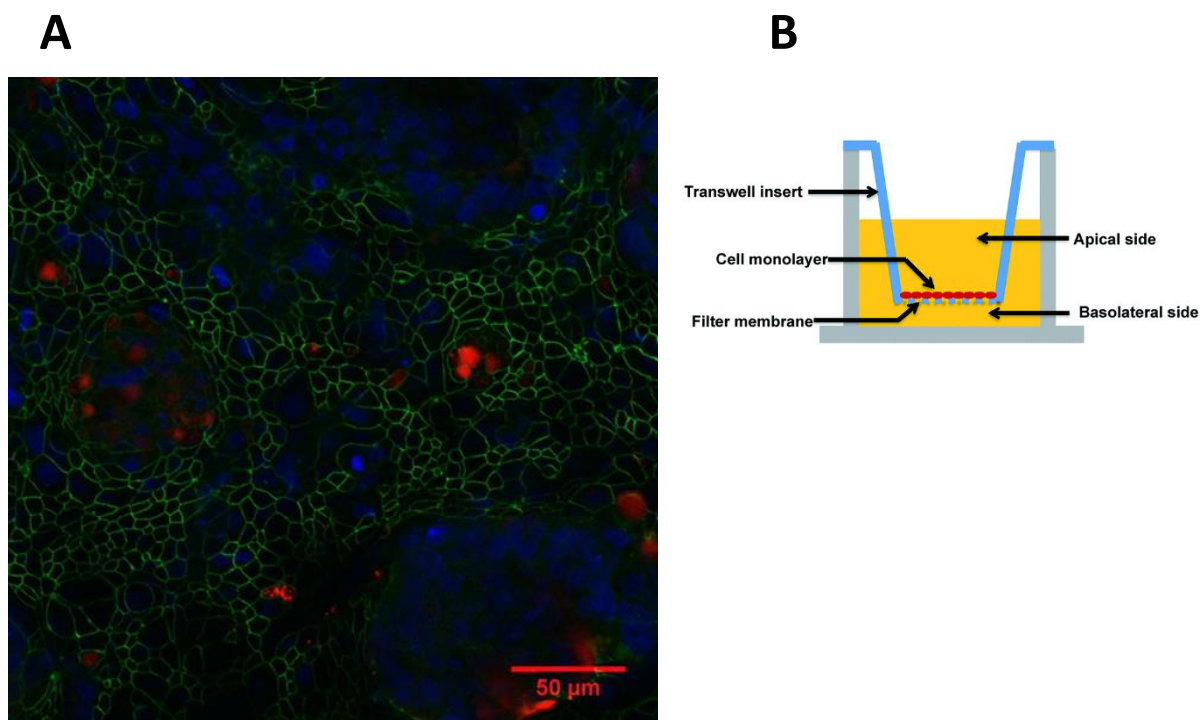


**Figure 33: Immunohistochemical fluorescence microscopy of T84 monolayer grown with LS174T on transwell.** T84 and LS174T cells were grown on transwell at a ratio 10:1 respectively. The cells were fixed with 4% paraformaldehyde. **(A)** Antibodies used were rabbit anti-MUC2 antibody (with secondary antibody goat anti-rabbit Alexa594 (red)) and mouse anti-occludin antibody conjugated to Alexa488 (green). Cell nuclei were counterstained with DAPI (blue). Image was acquired with Zeiss LSM880 confocal microscope and processed with ImageJ software (courtesy of Tanja Šuligoj). **(B)** Diagram of transwell setup for T84/LS174T cells epithelial monolayer growth.

To investigate the effect of *R. gnavus* strains and associated glucorhamnans on gut barrier function, the effect of the treatments on expression of tight junction proteins in T84 cells on transwells was analysed at the protein level by western blotting and at the gene level by qPCR using RPS13 as house-keeping gene. T84 are human intestinal epithelial cell lines derived from colorectal adenocarcinoma. There was no significant change in gene expression level for ZO-1, claudin-1 (CLN-1) and occludin, although a small decrease was observed with the glucorhamnan from ATCC 29149 grown in BHI-YH (Fig. 34).

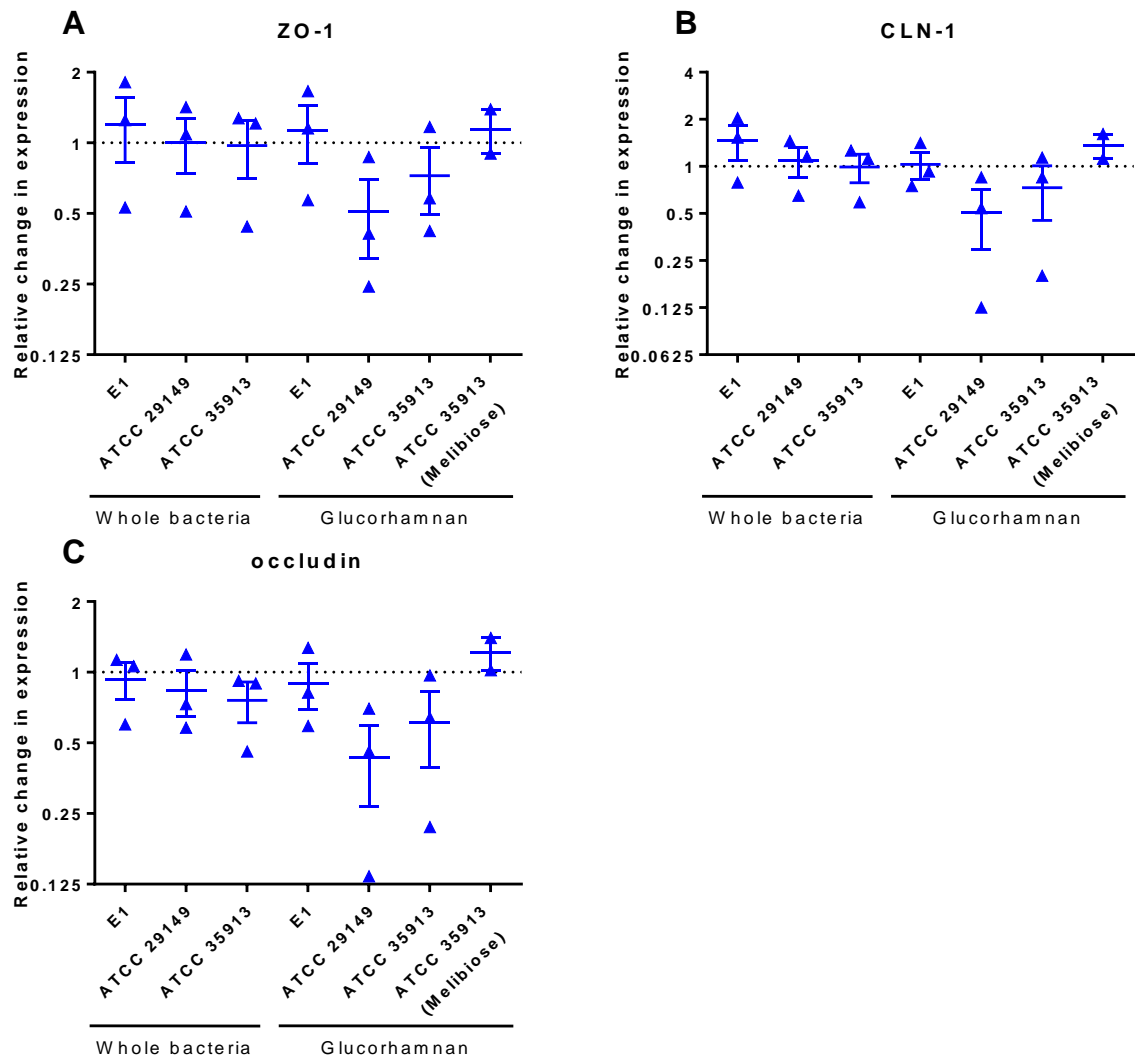


**Figure 34: Effect of *R. gnavus* strains and purified glucorhamnan on tight junction gene expression.**

T84 cells were grown on transwells and treated with *R. gnavus* E1, ATCC 29149 or ATCC 35913 or with associated glucorhamnans. The gene expression level of ZO-1, CLN-1 and occludin was determined by qPCR. RPS13 was used as house-keeping gene to normalise the data. The relative changes were calculated using 3 biological replicates. The dotted line indicates the level of expression in the 'T84 cells only' cells. Statistics were determined using the  $\Delta C_t$  values.

To complete this experiment, western blotting was used to complete qPCR. As shown in Fig. 35, ZO-1 and occludin were quantified using  $\alpha$ -actin as a house-keeping reference gene, and the quantification results were put together in Fig. 36. As shown in Fig. 36, the influence of

bacteria and glucorhamnan treatments on protein production by T84 cells was not statistically significant although the mean relative quantity of ZO-1 and occludin seems to be down-regulated by *R. gnavus* ATCC 35913 strain by 3.9-fold for ZO-1 and 2.4-fold for occludin.

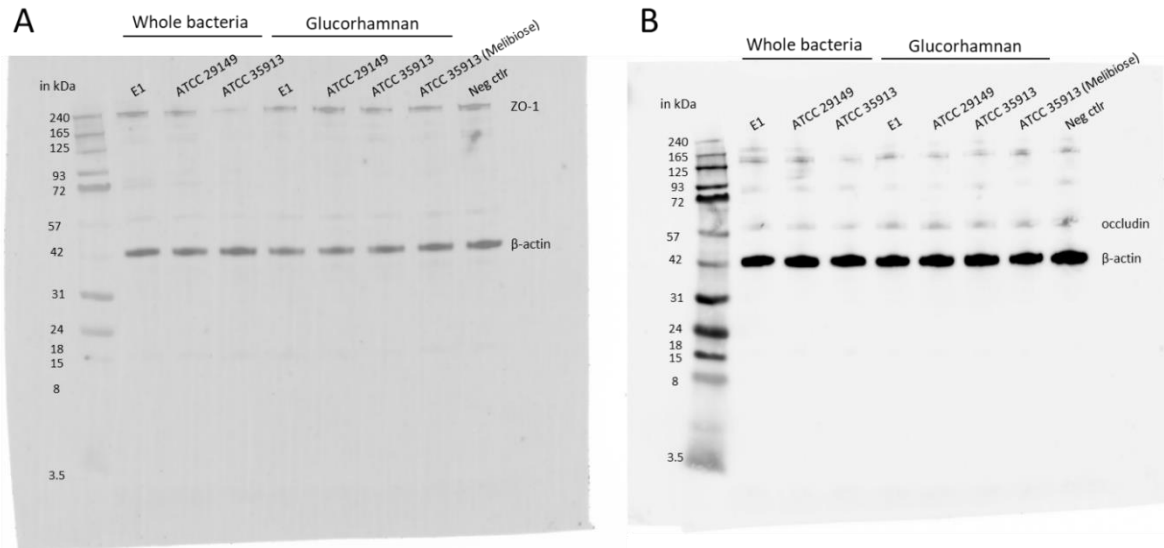


**Figure 35: Effect of *R. gnavus* strains and purified glucorhamnan on tight junction proteins in the T84 model.**

T84 cells were grown on transwells and treated with *R. gnavus* E1, ATCC 29149 or ATCC 35913 (MOI: 20:1) or with associated glucorhamnans (200  $\mu$ g/ml). The level of ZO-1 (A) and occludin (B) in the total protein fraction was determined using western blotting with  $\beta$ -actin as reference and in comparison with the 'T84 cells only' negative control. The extra broad molecular weight marker (5 - 245 kDa) is shown on the side of the membranes.

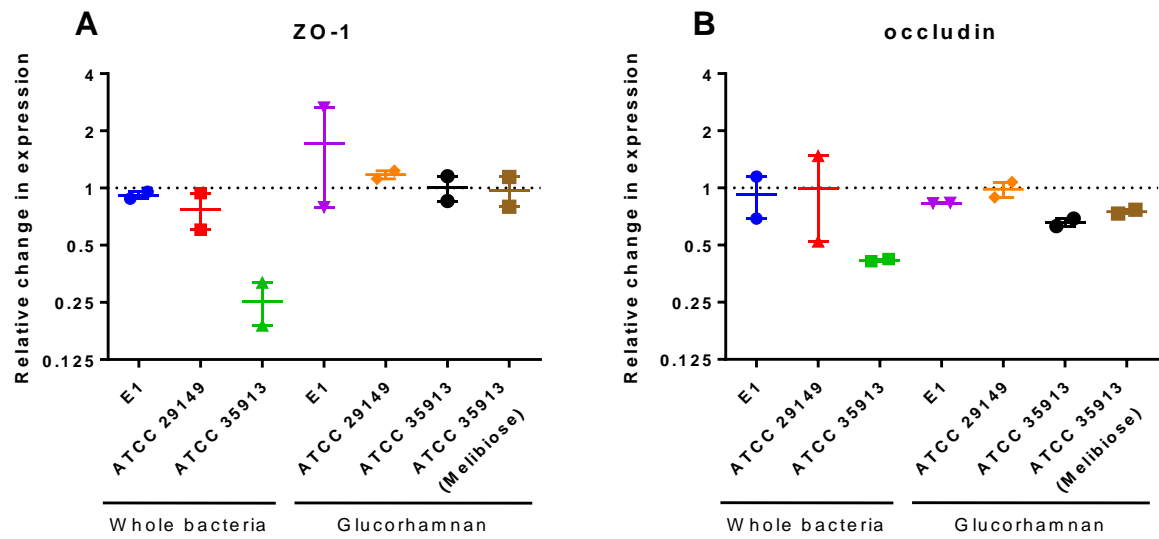


**Figure 36: Effect of *R. gnavus* strains and purified glucorhamnan on tight junction proteins expression.**

T84 cells were grown on transwells and treated with *R. gnavus* E1, ATCC 29149 or ATCC 35913 or with associated glucorhamnans. The presence of ZO-1 (A) and occludin (B) in total protein fraction was assessed using western blotting (described in section 2.8.2.). The relative quantification of ZO-1 and occludin was done by ImageJ (NIH, USA) using  $\beta$ -actin as reference and in comparison with the 'T84 cells only' negative control (Original gels images represented in Supplementary data 6). The experiment was reproduced in 2 technical replicates. The dotted line indicates the level of expression in the 'T84 cells only' control. Statistics were determined using the  $\Delta$ Ct values.

The integrity of the monolayer barrier function was further assessed using transepithelial electrical resistance (TEER) prior and after treatment (Fig. 37). The results obtained showed no significant effect of *R. gnavus* strains and their purified glucorhamnan on gut barrier integrity of T84 monolayer as the TEER stayed above the minimal value for good epithelium monolayer barrier function under the experimental conditions tested.

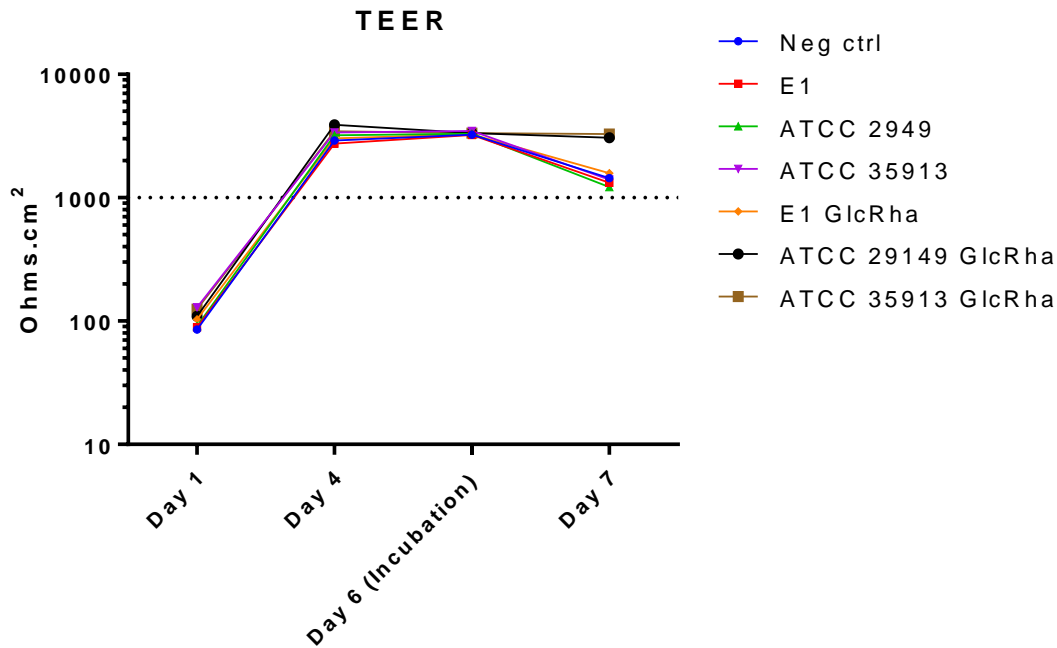


**Figure 37: Transepithelial electrical resistance (TEER) of T84 cells grown on transwells and effect of *R. gnavus* strains and associated purified glucorhamnans.**

Measurements were done after 1, 4 6 and 7 days following seeding of the transwells with T84 cells. At day 6, the cells were treated with *R. gnavus* strains (ATCC 29149, ATCC 35913 and E1) and associated glucorhamnans and TEER measured after 18 h treatment. Data are presented as mean resistance of four independent replicates. The dotted lines represent the minimum considered value for good barrier function of the epithelium monolayer.

#### 4.2.1. Effect of *R. gnavus* strains and glucorhamnans on cytokine secretion

Using the T84/LS174T cells, the effect of *R. gnavus* ATCC 29149, ATCC 35913 and E1 strains and their purified glucorhamnan was first screened using a panel of cytokines previously shown to be produced by T84 cells in presence of *R. gnavus* strains or other gut commensal bacteria (Gaisawat et al., 2022; Liévin-Le Moal & Servin, 2013; McGrath et al., 2022; Nikolić et al., 2017). Those cytokines include MIF, CXCL5, IL-1 $\beta$ , IL-8, IL-6, IL-17, IL-33, IL-4 and TNF- $\alpha$ . Briefly, the T84/LS174T monolayer was treated with *R. gnavus* ATCC 29149, ATCC 35913 or E1 strains (at MOI 20:1) or with glucorhamnans (at 200  $\mu$ g/ml) purified from these strains for

18 h; the medium from the apical and the basolateral compartments was collected and the production of the cytokines was measured using U-PLEX Assay (Meso Scale Discovery). The quantification from obtained results were produced with AssayFit (assayfit.com). The results for the production of IL-1 $\beta$  and the chemokines CXCL5 and CXCL8 in the apical or basolateral sides are shown in Fig. 38 and Fig. 39, respectively.

These results showed that *R. gnavus* ATCC 35913 was the only strain significantly enhancing the production of IL-1 $\beta$ , CXCL5 and CXCL8 (by 2.4-fold, 5.0-fold and 3.4-fold, respectively; p-value<0.001) in the apical compartment and CXCL8 (by 2.5-fold, p-value<0.001) in the basolateral compartment, while *R. gnavus* E1 and ATCC 29149 led to a significant decreased production of IL-1 $\beta$  (E1: by 38%, p-value<0.01; ATCC 29149: by 34%, p-value<0.05) and CXCL8 (E1: by 41%, p-value<0.01; ATCC 29149: by 35%, p-value<0.05) in the apical compartment. In addition, *R. gnavus* E1 and ATCC 29149 associated glucorhamnans induced a decreased production of IL-1 $\beta$  (E1: by 38%, p-value<0.01; ATCC 29149: by 50%, p-value<0.001) in the basolateral compartment. It is interesting to observe that the presence of LS174T cells change the profile of cytokine produced in this experiment. From that information, we can hypothesis that LS174T cells either produce themselves these cytokines, or, that the presence of mucus on the epithelial monolayer induce the production of these cytokines by the T84 cells. To investigate further this point, LS174T cells could be grown on their own on transwells in this experiment to assess the cytokine production profile by these cells.

No increase in cytokine production could be observed with *R. gnavus* E1, ATCC 29149 and ATCC 35913 derived glucorhamnans. Additionally, no significant production of MIF, IL-6 and IL-29 was observed with any of the *R. gnavus* strains tested or their purified glucorhamnans in the T84/LS174T model (Supplementary data 4); and no detectable amount of cytokine IL-4, IL-33, IL-17 and TNF- $\alpha$  cytokines production was observed in this model (data not shown, values being bellow LLOD).

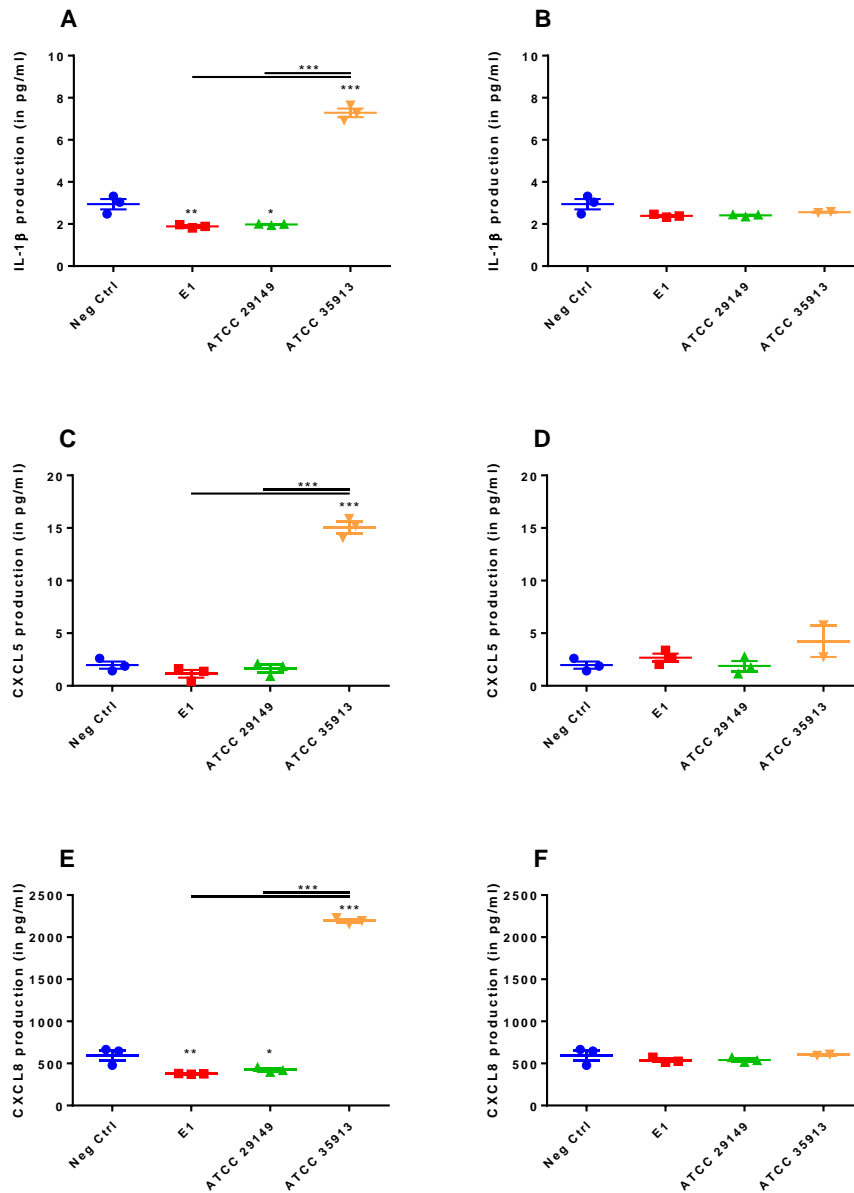


**Figure 38: Effect of *R. gnavus* strains and purified glucorhamnans on cytokine production by intestinal cells in apical side of the T84/LS174T model.**

*R. gnavus* ATCC 29149, ATCC 35913 and E1 a MOI of 20:1 (A, C and E) and purified glucorhamnan (200  $\mu$ g/ml) from these strains (B, D and F) were incubated with T84/LS174T cells for 18 h. Neg ctrl refers to T84/LS174T cells cultured without bacteria or glucorhamnan. The panels provide the relative cytokine production in the apical side of the transwell of IL-1 $\beta$  (A and B), CXCL5 (C and D) and CXCL8 (E and F) by T84/LS174T cells as determined with the U-plex kit (MSD). The experiment was reproduced in 3 biological replicates. One way ANOVA was used for comparison with the negative control (\* for  $p < 0.05$ , \*\* for  $p < 0.01$ , \*\*\* for  $p < 0.001$ ).

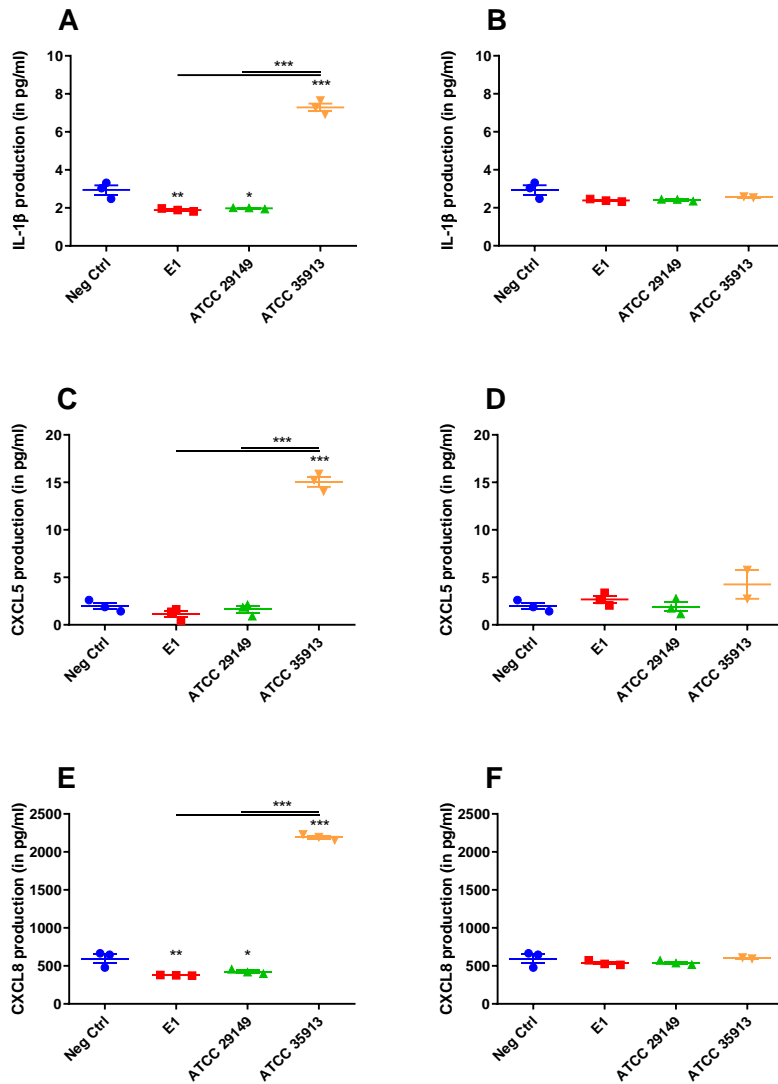


**Figure 39: Effect of *R. gnavus* strains and purified glucorhamnans on cytokine production by intestinal cells in basolateral side of the T84/LS174T model.**

*R. gnavus* ATCC 29149, ATCC 35913 and E1 a MOI of 20:1 (A and C) and purified glucorhamnans (200  $\mu$ g/ml) from these strains (B and D) were incubated with T84/LS174T cells for 18 h. Neg ctrl refers to T84/LS174T cells cultured without bacteria or glucorhamnan. The panels provide the relative cytokine production in the basolateral side of the transwell of IL-1 $\beta$  (A and B), CXCL5 (C and D) and CXCL8 (E and F) by T84/LS174T cells as determined with the U-plex kit (MSD). The dotted line corresponds to the LLOD (lower limit of detection) and any value beneath that limit cannot be considered. *The experiment was reproduced in 3 biological replicates.* One way ANOVA was used for comparison with the negative control (\* for p<0.05, \*\* for p<0.01, \*\*\* for p<0.001).

As previously presented by McGrath et al., (2022), *R. gnavus* strain ATCC 35913 is supposed to induce the production of IL-29 in T84/LS174T cells, which goes against the results obtained here (Supplementary data 4). In order to address this difference, we next tested the effect of *R. gnavus* ATCC 29149, ATCC 35913 and E1 strains and their purified glucorhamnan on the production of IL-29 using ELISA. IL-29 is a pro-inflammatory cytokine belonging to the type 3 interferon family which has been associated with antiviral, anti-proliferative, and immunomodulatory activities (De Weerd et al., 2007; Plataniias, 2005). We showed that the three strains of *R. gnavus* tested were able to significantly induce the production of IL-29 (E1: by 114.3-fold, p-value<0.001; ATCC 29149: by 68.8-fold p-value<0.01; ATCC 35913: by 100.2-fold p-value<0.001) by epithelium cells as shown in Fig. 40. Especially, *R. gnavus* E1 was the strain inducing the highest production of IL-29. In contrast, no IL-29 production was observed with the glucorhamnans purified from the three strains (Fig. 40B).

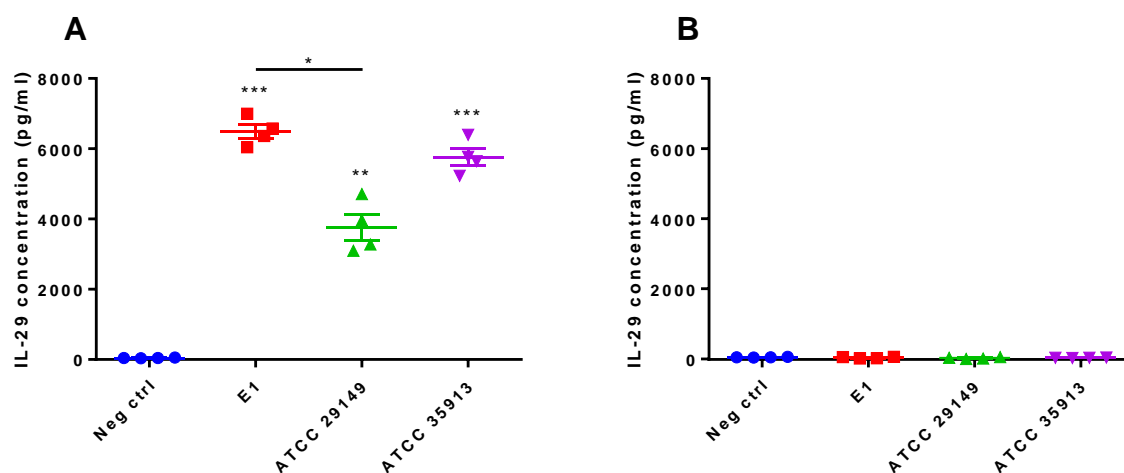


**Figure 40: Effect of *R. gnavus* strains and glucorhamnan on IL-29 production by T84/LS174T cells.**

T84/LS174T cells were treated with *R. gnavus* E1, ATCC 29149 or ATCC 35913 at MOI of 50:1 (A) or associated glucorhamnans at 200 µg/ml (B). Neg ctrl refers to cells grown without bacteria nor glucorhamnan. The secretion of IL-29 was determined by ELISA. The experiment was reproduced in 3 biological replicates. One-way ANOVA was used for comparison with the negative control (\* for p<0.05, \*\* for p<0.01, \*\*\* for p<0.001).

To determine the influence of mucus on the capacity of *R. gnavus* strains to modulate host response described above, these experiments were repeated using T84 cells grown on transwells in the absence of mucin-producing cells. In this model, the cells formed a polarised monolayer with an apical and basolateral compartment after 8 to 13 days as determined by TEER measurements (Fig. 37). As shown in Fig. 41, *R. gnavus* ATCC 35913 significantly induced the highest production of IL-29 (p-value<0.001), followed by ATCC 29149 (p-value<0.01), and E1. As shown for the T84/LS174T cell model, none of the purified glucorhamnans induced production of IL-29 when compared to the negative control (Fig. 41).

However, no effect was observed on MIF, IL-6, IL-1 $\beta$ , CXCL5, CXCL8 and IL-29 production and no detection of IL-4, IL-33, IL-17 and TNF- $\alpha$  was observed in this experiment.

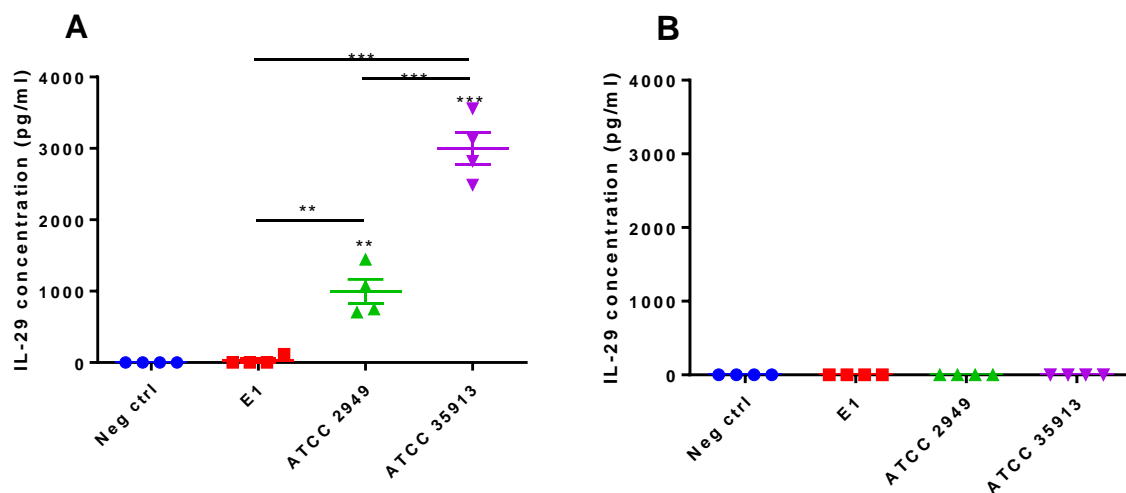


**Figure 41: Effect of *R. gnavus* strains and glucorhamnan on IL-29 production by T84 cells.**

T84 cells were treated with *R. gnavus* E1, ATCC 29149 or ATCC 35913 at MOI (A) of 50:1 or with associated glucorhamnans at 200  $\mu$ g/ml (B). Neg ctrl refers to cells grown without bacteria nor glucorhamnan. The secretion of IL-29 was determined by ELISA. The experiment was reproduced in 3 biological replicates. One-way ANOVA was used for comparison with the negative control (\* for p<0.05, \*\* for p<0.01, \*\*\* for p<0.001).

We next investigated the expression of a panel of cytokine genes, IL-29, IL-1 $\beta$ , IL-6, IL-10, TNF- $\alpha$ , IFN- $\gamma$  and CXCL5 and CXCL8 chemokines in response to the treatment of T84 cells grown on transwells with *R. gnavus* strains and associated glucorhamnans. The level of expression

of the previously mentioned cytokines was determined by qPCR using GAPDH, actin and RPS13 as reference genes. RPS13 showed consistent expression across all technical and biological replicates and was therefore chosen as reference house-keeping gene for subsequent gene expression analyses. The results obtained using GAPDH and actin as reference genes are presented in Supplementary data 5. To determine the effect of *R. gnavus* strains and associated glucorhamnan on the different assessed gene expression, the  $\Delta\Delta Ct$  method was used: briefly, the difference of Ct value for each test condition with reference gene expression from the same condition was calculated and this  $\Delta Ct$  was then compared to the negative control to determine the  $\Delta\Delta Ct$ , the fold change between the treatment and the 'T84 cells only' control was then determined from this values. In contrast to the ELISA results, there was no significant changes in gene expression across all conditions tested and a major variation can be observed (Fig. 42) using either the whole bacteria or the purified glucorhamnans, which may be due a transient enhanced gene expression and degradation, which, unlike the effect on proteins, cannot be detected after 18 h treatment.

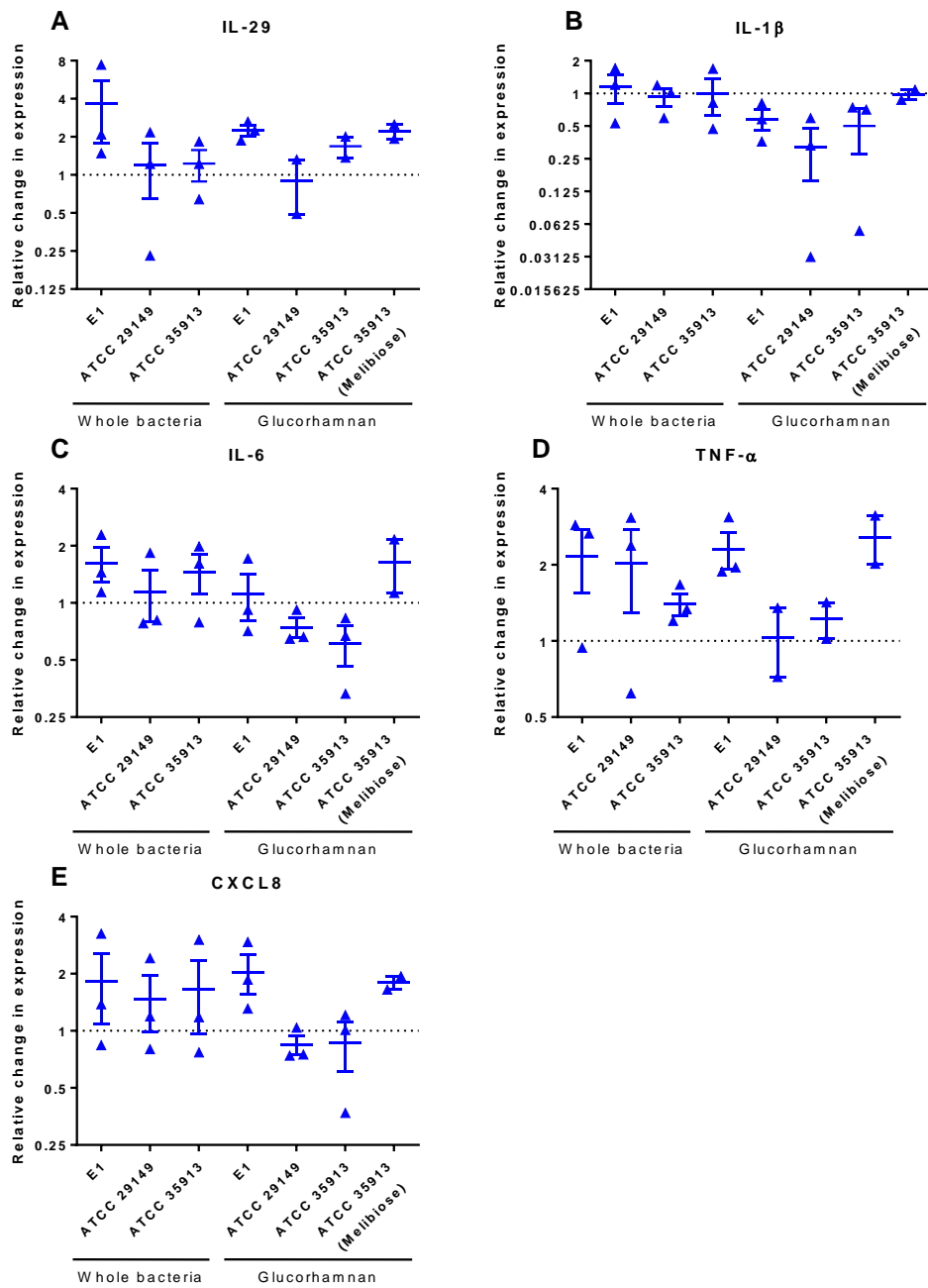


**Figure 42: Effect of *R. gnavus* strains and associated glucorhamnan on cytokines gene expression.**

T84 cells were grown on transwells and treated with *R. gnavus* E1, ATCC 29149 or ATCC 35913 or with associated glucorhamnans. The gene expression level of IL-29, IL-1 $\beta$ , IL-6, TNF- $\alpha$  and CXCL8 was assessed using qPCR. RPS13 was used as house-keeping gene to normalise the data. The relative changes were calculated using 3 biological replicates. The dotted line indicates the level of expression in the 'T84 cells only' cells. Statistics were determined using the  $\Delta$ Ct values. Statistics were determined using the  $\Delta$ Ct values.

Similarly, no significant change in expression of TLR4 gene could be detected across the different treatments.

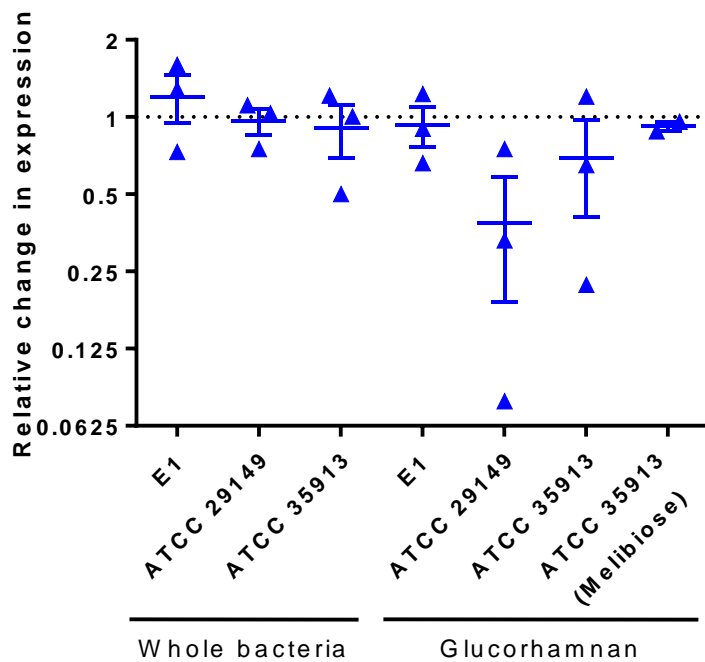


**Figure 43: Effect of *R. gnavus* strains and purified glucorhamnan on TLR4 gene expression.**

T84 cells were grown on transwells and treated with *R. gnavus* E1, ATCC 29149 or ATCC 35913 or with associated glucorhamnans. The gene expression level of TLR4 was determined using qPCR. RPS13 was used as the house-keeping gene to normalise the data. The relative changes were calculated using 3 biological replicates. The dotted line indicates the level of expression in the 'T84 cells only' cells. Statistics were determined using the  $\Delta Ct$  values.

### 4.3. Discussion

Using two epithelium cell models, we showed that the capacity of *R. gnavus* to modulate intestinal epithelium response *in vitro* was strain dependent. *R. gnavus* ATCC 35913 was the strain showing the highest induction of cytokines in the multiplex and the ELISA experiments (IL-1 $\beta$ , CXCL5, CXCL8 in T84/LS174T model and IL-29 in T84 model); these cytokines are involved in pro-inflammatory mechanisms. Since this was not observed with the purified glucorhamnan, it is likely that other components of *R. gnavus* ATCC 35913 cell surface are

involved in the epithelium response. These results also underline the importance of the presence of goblet cells (and therefore mucus), in the interaction between *R. gnavus* strains and epithelial cells and show the importance of analysing the production of cytokines in both apical and the basolateral compartments. Also, in these experiments, no positive control was used as epithelial cells are producing little to no amount of certain cytokines unlike immune cells, which produce high quantity of cytokines when activated.

*R. gnavus* ATCC 29149 glucorhamnan showed significant induction of CXCL8 production by epithelial cells which was not observed with the whole bacteria. This may be due to the presence of *R. gnavus* CPS masking the effect of glucorhamnan, as previously suggested for *R. gnavus* RJX1120 strain with immune cells (Henke *et al.*, 2021).

It is also interesting to note that *R. gnavus* ATCC 29149 glucorhamnan, which possesses a different structure than E1 and ATCC 35913 glucorhamnans induced the highest decrease in the production of IL-1 $\beta$  in the T84/LS174T model, therefore showing that differences in glucorhamnan structure, and cell surface glycosylation in general, can impact the cytokine response by epithelial cells. Though, the level of IL-1 $\beta$  obtained in this experiment was low and close to the LLOD values, limiting the possible interpretation of the experiment. Also, the results have to be put in the context that *R. gnavus* cell surface harbour more cell surface polysaccharides than the glucorhamnan, such as the CPS previously mentioned in section 1.4.3, which mute the immune response in the host.

Most pro-inflammatory cytokines including IFN- $\gamma$ , TNF- $\alpha$ , IL-12 and IL-1 $\beta$  have been shown to cause an increase in tight junction permeability, while some anti-inflammatory cytokines such as IL-10 and TGF- $\beta$  protect against the disruption of intestinal tight junction barrier and development of intestinal inflammation (Al-Sadi, 2009; Onyiah & Colgan,(Al-Sadi, 2009; Onyiah & Colgan, 2016). However, despite the pro-inflammatory response observed in response to treatment with some *R. gnavus* strains or glucorhamnans, the gut barrier integrity remained intact, as shown by TEER measurement and analysis of tight-junction proteins.

Additionally, the mucus production have not been assessed here but we could hypothesise that there is an effect of *R. gnavus* strains on the either the production by epithelium cells or through its digestion, as it has been previously mentioned in other gut bacteria in section 1.2.3.

Collectively these data suggest that, unlike infection with pathogens such as enteropathogenic *Escherichia coli* (EPEC) which often lead to disrupted barrier (Singh & Aijaz, 2016; Van Nhieu & Romero, 2016), the host can maintain epithelium integrity even when in direct contact with *R. gnavus* strains *in vitro*. This is particularly important in pathophysiological conditions, where disruption of the mucus layer may lead to enhanced contact of commensal bacteria inhabiting the mucus niche with the intestinal epithelium. However, this is likely to be context- and strain-dependent, as shown *in vivo* where while *R. gnavus* ATCC 29149 (isolated from a healthy donor) had little or no effects on intestinal permeability in mice (in line with our *in vitro* work), while lupus-derived *R. gnavus* strains induced functional alterations associated with leaky gut (including *R. gnavus* translocation to mesenteric lymph nodes, increased serum levels of zonulin and serum IgG anti-*R. gnavus* cell-wall lipoglycan) and features of autoimmunity (Silverman et al., 2022).

Chapter 5: Effect of *R. gnavus* strain-specific cell surface glycosylation on host immune response

## 5.1. Introduction

Bacterial cell surface polysaccharides are part of microbial-associated molecular patterns (MAMPs). MAMPs are recognised by toll-like receptors (TLRs) and other pattern recognition receptors (PRRs) which will respond by activating signalling cascades involving adaptor proteins which activate regulator protein complex like NF- $\kappa$ B or NFAT (Nuclear factor of activated T-cells), leading to the induction of a broad range of immunity and defense associated genes encoding cytokines, chemokines or antimicrobial peptides (Claes et al., 2012; Q. Liu et al., 2020). For example, the polysaccharide A (PSA) from *B. fragilis* induces the production of IL-10 production in Foxp3<sup>+</sup> Tregs through the interaction with TLR2 (Mazmanian et al., 2005). EPS isolated from *L. reuteri* strain DSM 17938 and L26 Biocenol<sup>TM</sup> exerts up-regulation of the mRNA level of IL-1 $\beta$ , NF- $\kappa$ B, TNF- $\alpha$ , and IL-6 in IPEC-1 cells (Kšonžeková et al. (Kšonžeková et al., 2016). The  $\beta$ -glucan produced by *B. bifidum* has been shown to modulate the host immune response by inducing T<sub>reg</sub> (regulatory T cells) activation, preventing intestinal inflammation (Verma et al., 2018). The anti-inflammatory effects of *F. prausnitzii* HTF-F cell surface polysaccharide have been shown to be mediated through TLR2-dependent modulation of IL-12 and IL-10 cytokine production in antigen presenting cells (Rossi et al., 2015).

In addition to TLRs, C-type lectin receptors (CLRs) are another example of PRRs expressed by immune cells which are involved in the regulation of the host innate immunity through recognition of microbial polysaccharides (see section 1.1.4.3). Their interaction with commensal bacteria or pathogens contributes to homeostasis or inflammation, respectively (M. Li et al., 2022; T.-H. Li et al., 2019). CLRs recognise a range of carbohydrate structures on the surface of microbes via their carbohydrate through their carbohydrate recognition domain (CRD) in a Ca<sup>2+</sup>-dependent manner. While CLRs have mainly been studied for their interaction with pathogens, some studies have reported their recognition by gut commensal bacteria such as *L. rhamnosus*, *L. acidophilus* or *L. reuteri*, leading to pro- and anti-stimulation in lymphocytes and monocytes (Bene et al., 2017; Konieczna et al., 2015).

Having shown that *R. gnavus* strains harbour differences in cell surface glycan structure and since *R. gnavus* ATCC 29149 has been shown to influence host immune response in a TLR-4-dependent manner resulting in the production of pro-inflammatory TNF- $\alpha$  in BMDCs (Haynie et al., 2021; Henke et al., 2019) while CPS-containing strains were shown to be tolerogenic (inducing an immune tolerance, here in mBMDCs) (Henke et al., 2021). In this study, *R. gnavus* RJX1120 strain harbouring CPS inhibited the activation of T cells, and the production of IL-1 $\beta$  and TNF- $\alpha$  *in vivo*, while it enhanced the production of Treg cells as compared to *R. gnavus* RJX1125 strain which does not produce CPS (Henke et al., 2021). We therefore hypothesised that these differences in strain-specific glycosylation may influence host immune response through interactions with C-type lectins in order to understand the mechanisms implicated in the recognition and interaction process of the host immunity in the context of health and inflammation *in vivo*.

To investigate this, the effects of *R. gnavus* ATCC 29149, E1 and ATCC 35913 strains and their purified glucorhamnans on cytokine production were determined in mBMDCs while mDectin-2, mDectin-1 and SIGN-R1 reporter cells and THP1-Blue™ NF- $\kappa$ B reporter cells were used to further investigate the receptors of the interaction and signalling pathway involved in the host immune response.

## 5.2. Results

### 5.2.1. Effect of *R. gnavus* and glucorhamnan on cytokine production in mBMDCs

The immunomodulatory properties of *R. gnavus* E1, ATCC 29149 and ATCC 35913 strains and their respective purified glucorhamnans were assessed *in vitro* by monitoring cytokine production in mBMDCs. Here, the production of 10 cytokines (TNF- $\alpha$ , IFN- $\gamma$ , IL-1 $\beta$ , IL-4, IL-6, IL-10, IL-12p40, IL-13, CCL2 and CXCL1) was quantified using an MSD multiplex method as described in section 2.8.3 and the results are shown in Fig. 44. In addition, IL-10, an anti-inflammatory cytokine, was quantified by ELISA as described in section 2.8.3. The results are presented in Fig. 45.

As shown in Fig. 44 and 45, *R. gnavus* ATCC 35913 enhanced significantly more production of several cytokines at  $p$ -value $<0.001$  in mBMDCs than the two other strains tested, including IL-6 (43% more than E1,  $p$ -value $<0.001$ ; and 34% more than ATCC 29149,  $p$ -value $<0.01$ ), CXCL1 (29% more than E1,  $p$ -value $<0.001$ ; and 25% more than ATCC 29149,  $p$ -value $<0.001$ ), CCL2 (29% more than E1,  $p$ -value $<0.001$ ; and 13% more than ATCC 29149,  $p$ -value $<0.001$ ) and IL-10 (40% more than E1,  $p$ -value $<0.001$ ; 47% more than ATCC 29149,  $p$ -value $<0.001$ ). *R. gnavus* ATCC 29149 showed higher induction of CCL2 than E1 (by 12%,  $p$ -value $<0.001$ ) while a decreased expression of CXCL1, was observed with E1 and ATCC 29149 in comparison with the negative control (by 13% and 14% respectively,  $p$ -value $<0.01$ ). These data indicate that *R. gnavus* ATCC 35913 is the most immunogenic *R. gnavus* strain under the conditions tested.

The purified glucorhamnans also showed an effect on cytokine production in mBMDCs, in contrast to the lack of effect on intestinal epithelium cells (section 4.2.1.). The glucorhamnan isolated from *R. gnavus* ATCC 35913 grown with melibiose induced significantly more production of CXCL1 and CCL2 than the glucorhamnans from E1 (by 16% and 18% respectively,  $p$ -value $<0.05$ ) and ATCC 35913 grown in BHI-YH (by 22% and 24% respectively,  $p$ -value $<0.01$ ) while the glucorhamnan from *R. gnavus* ATCC 29149 grown in BHI-YH induced more production of IL-6 (by 54%,  $p$ -value $<0.001$ ) and IL-12p40 (by 60%,  $p$ -value $<0.01$ ) than the glucorhamnan from ATCC 35913 grown in BHI-YH. Interestingly, the glucorhamnan from *R. gnavus* ATCC 35913 showed different cytokine responses depending on the medium used for its growth where the glucorhamnan isolated from *R. gnavus* ATCC 35913 grown with melibiose induced significantly more production of IL-6, CXCL1 and CCL2 (by 28%, 22% and 24% respectively,  $p$ -value $<0.01$ ) than the glucorhamnan from *R. gnavus* ATCC 35913 grown in BHI-YH. This suggests that difference in cell surface glycosylation induced by the influence of the carbon source in the growth media can influence immunogenicity of *R. gnavus* strains.

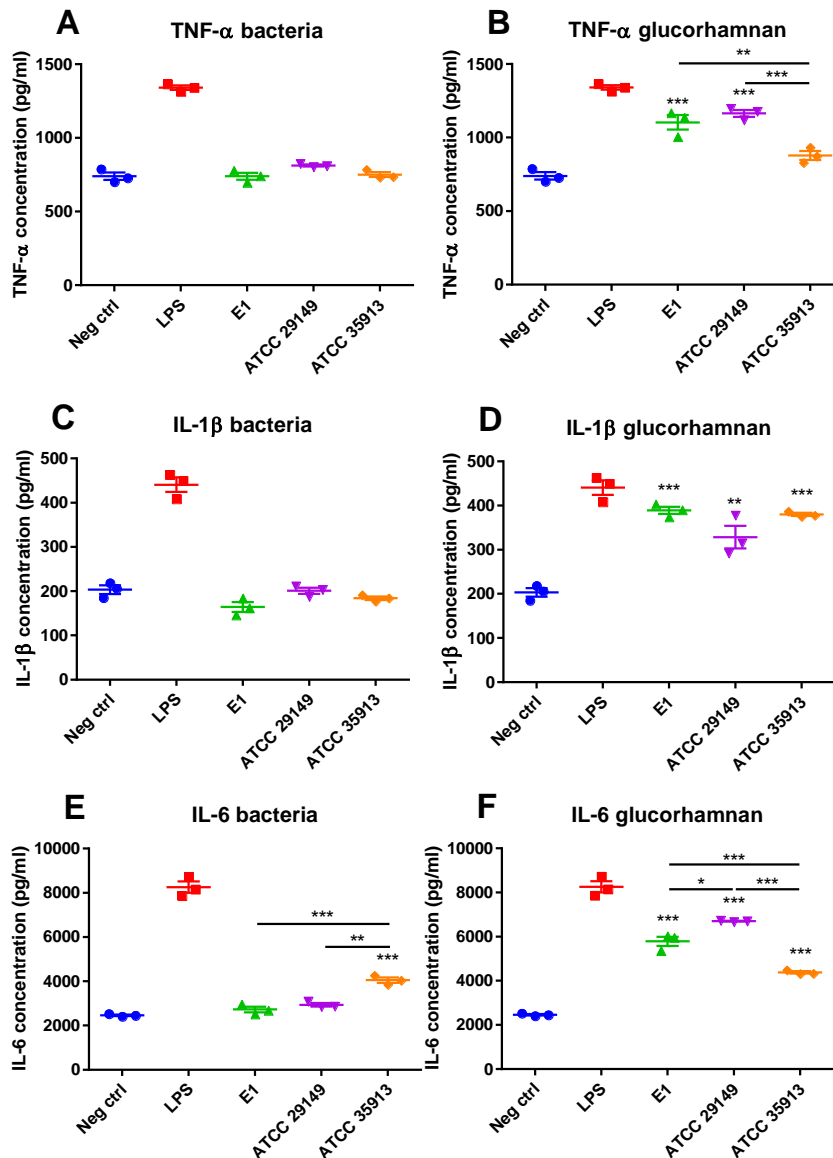


**Figure 44: Effect of *R. gnavus* strains and purified glucorhamnans on cytokine production by mBMDCs.**

mBMDCs were incubated with *R. gnavus* ATCC 29149, ATCC 35913 or E1 strains at a MOI of 50:1 or with purified glucorhamnan (200 µg/ml) from these strains for 18 h. Neg ctrl refers to mBMDCs cultured without bacteria or glucorhamnan. The panels provide the relative cytokine production by mBMDCs of TNF-α following treatment with whole bacteria (A) or glucorhamnans (B), IL-1β following treatment with whole bacteria (C) or glucorhamnans (D), IL-6 following treatment with whole bacteria (E) or glucorhamnans (F) using the U-plex kit (MSD). LPS from *E. coli* O111:B4 at 100 µg/ml was used as a positive control. The experiment was reproduced in 3 biological replicates. One way ANOVA was used for comparison with the negative control (\* for p<0.05, \*\* for p<0.01, \*\*\* for p<0.001).

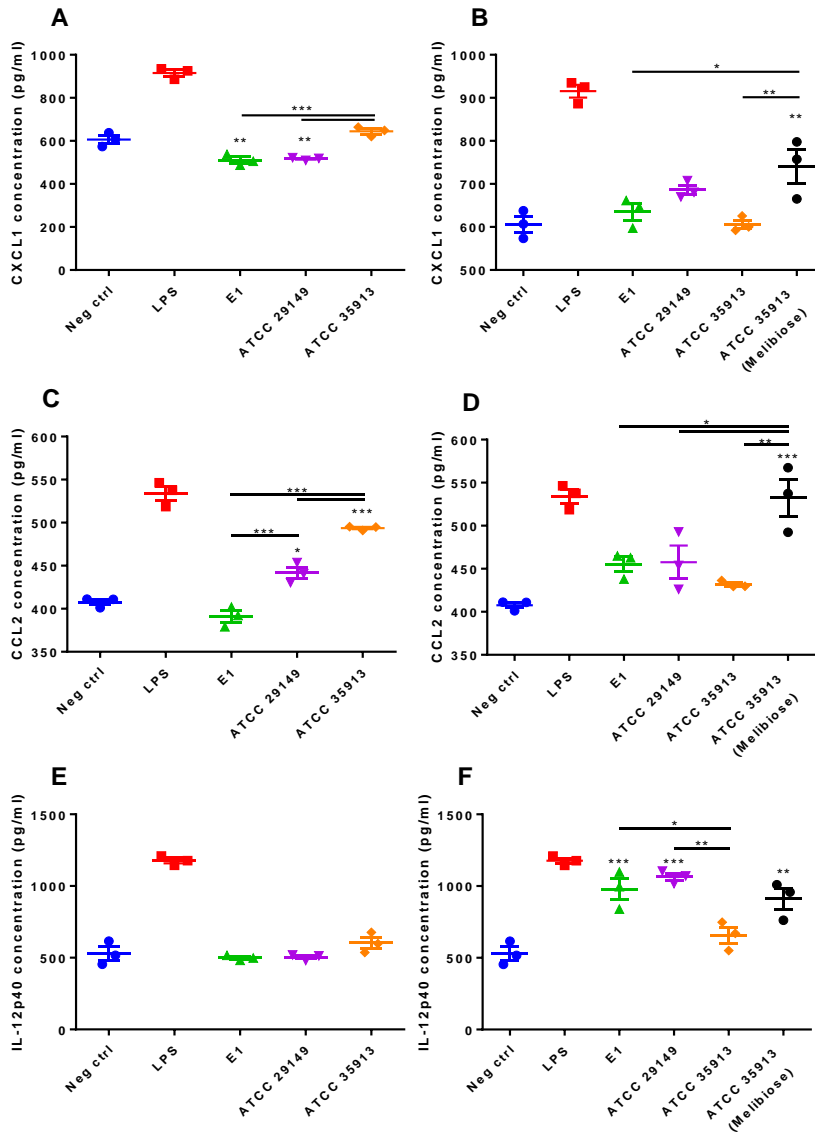


**Figure 45: Effect of *R. gnavus* strains and purified glucorhamnans on cytokine production by mBMDCs.**

mBMDCs were incubated with *R. gnavus* ATCC 29149, ATCC 35913 or E1 strains at a MOI of 50:1 or with purified glucorhamnan (200 µg/ml) from these strains for 18 h. Neg ctrl refers to mBMDCs cultured without bacteria or glucorhamnan. The panels provide the relative cytokine production by mBMDCs of CXCL1 following treatment with whole bacteria (A) or glucorhamnans (B), CCL2 following treatment with whole bacteria (C) or glucorhamnans (D) and IL-12p40 following treatment with (whole bacteria (E) or glucorhamnans (F)) using the U-plex kit (MSD). LPS from *E. coli* O111:B4 at 100 µg/ml was used as a positive control. The experiment was reproduced in 3 biological replicates. One way ANOVA was used for comparison with the negative control (\* for  $p < 0.05$ , \*\* for  $p < 0.01$ , \*\*\* for  $p < 0.001$ ).

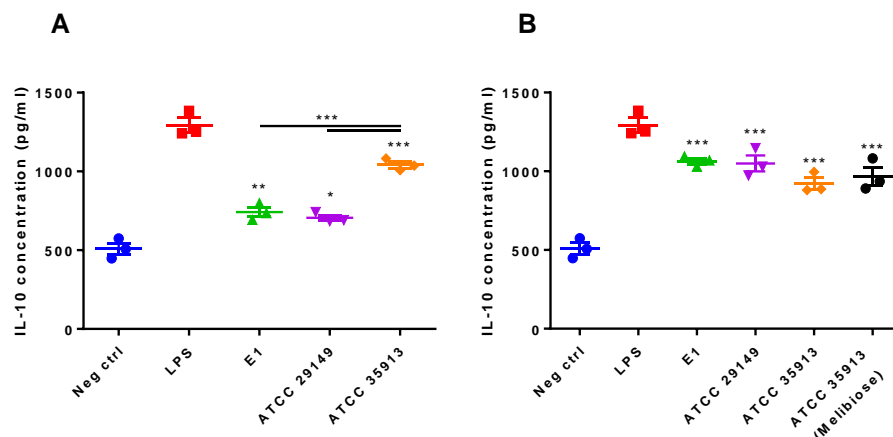


**Figure 46: Effect of *R. gnavus* strains and purified glucorhamnan on IL-10 production by mBMDCs.**

mBMDCs were incubated with *R. gnavus* ATCC 29149, ATCC 35913 or E1 strains (at MOI of 50:1) (A) or with purified glucorhamnan (200 µg/ml) from these strains (B) for 18 h. The panels refer to the relative cytokine production of IL-10 as determined by ELISA. LPS from *E. coli* O111:B4 at 100 µg/ml was used as a positive control. The experiment was reproduced in 3 biological replicates. One way ANOVA was used for comparison with the negative control (\* for p<0.05, \*\* for p<0.01, \*\*\* for p<0.001).

### 5.2.2. Role of NF-κB activation pathway in the interaction between *R. gnavus* and immune cells

Here, human THP1-Blue™ NF-κB cells were used to determine the effect of *R. gnavus* strains and associated glucorhamnans on the NF-κB signal transduction pathway. This cell line is derived from the human THP-1 monocyte cell line by stable integration of an NF-κB-inducible SEAP (secreted embryonic alkaline phosphatase) reporter construct. As a result, THP1-Blue™ NF-κB cells allow the monitoring of NF-κB activation by determining the activity of SEAP in the cell culture supernatant which can be monitored by spectrophotometry at 610 nm using QUANTI-Blue™, a SEAP detection reagent. This cell line is highly responsive to PRR agonists that trigger the NF-κB pathway comprising TLR4. More precisely, these reporter cells are particularly responsive to TLR2, TLR1/2 and TLR2/6 interactions with cognate ligands followed by TLR4, TLR5, TLR8 while responses to TLR3, TLR7 and TLR9 are hardly detectable. THP1-Blue™ NF-κB cells also respond to NOD1 and NOD2 agonists (Zuliani-Alvarez et al., 2017). As

shown by Henke et al. (2019), the induction of pro-inflammatory cytokines in immune cells, more precisely, the production of TNF- $\alpha$  in mBMDCs is independent to TLR4. Here, we want to assess further this by using THP1-Blue™ NF- $\kappa$ B cells in order to validate this hypothesis.

The results showed that *R. gnavus* ATCC 35913 strain induced the highest response in THP1-Blue™ NF- $\kappa$ B cells among the three *R. gnavus* strains tested (p-value<0.001) (Fig. 47). In addition, the purified glucorhamnans from all three strains were shown to activate the NF- $\kappa$ B pathway in a strain-dependent manner. The glucorhamnan derived from *R. gnavus* E1 and ATCC 35913, which share the same structure, showed the same extent of activation which was significantly higher (p-value<0.001) than the response generated with the glucorhamnan from ATCC 29149, which has a different structure (see section 3.3).

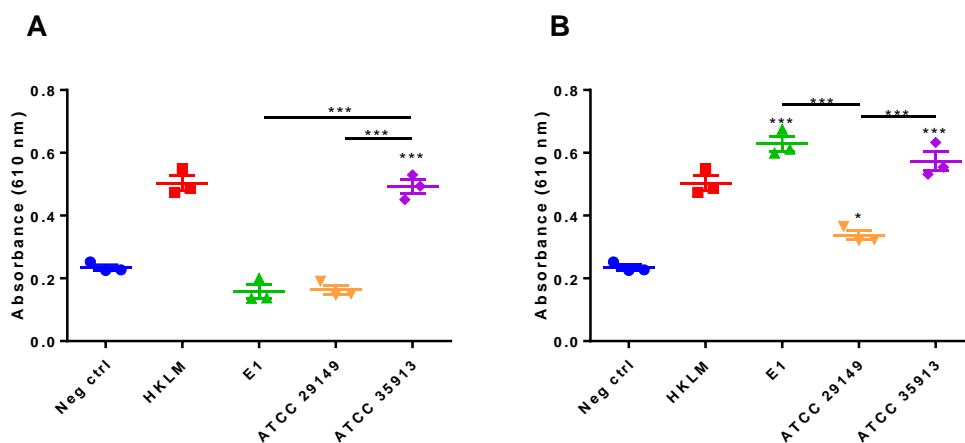


**Figure 47: Effect of *R. gnavus* strains and purified glucorhamnans on the NF- $\kappa$ B pathway.**

THP1-Blue™ NF- $\kappa$ B cells were incubated with *R. gnavus* ATCC 29149, ATCC 35913 or E1 strains at MOI of 50:1 (A) or with their associated glucorhamnans (100  $\mu$ g/ml) (B) for 18 h. NF- $\kappa$ B activation was measured by monitoring absorbance at 610 nm. at 100  $\mu$ g/ml. HKLM (heat killed *Listeria monocytogenes*) was used as a positive control. The experiment was reproduced in 3 biological replicates. One-way ANOVA was operated in comparison with negative control (\* for p<0.05, \*\* for p<0.01, \*\*\* for p<0.001).

These results showed that *R. gnavus* ATCC 35913 is the bacterial strain showing the most immunogenicity by inducing the production of IL-6, CXCL1, CCL2 and IL-10 cytokines.

### 5.2.3. Role of CLRs in the interaction between *R. gnavus* and immune cells

The interaction of *R. gnavus* ATCC 29149, E1 and ATCC 35913 strains with CLR was investigated using BWZ.36 reporter cells expressing mDectin-2, mDectin-1 and SIGN-R1, and compared to BWZ.36 mock cells. In the reporter cells, binding to C-type lectin leads to the activation of NFAT-LacZ construct which will allow the expression of  $\beta$ -galactosidase, resulting in changes in absorbance at 595 nm in the presence of chlorophenol-red  $\beta$ -d-galactopyranoside (CPRG), a substrate for galactosidase which turns red when cleaved by  $\beta$ -galactosidase. This will allow us to investigate the involvement of other PRR than TLR, studied in the previous section, and assess the role of CLR in the interaction of the host immunity with *R. gnavus* strains, and more specifically, the *R. gnavus* strains cell surface glycosylation, of which CLR are specific to.

*R. gnavus* ATCC 35913 consistently showed increased signal in the three reporter cell lines tested but this was also observed with mock cells (Fig. 48). In mDectin-2 reporter cells, the increase was comparable to that induced by fufurman used as positive control (Fig. 48A). However, a similar response was also observed using mock cells or mDectin-2 QPD inactive mutant carrying E168Q and N170D mutations in the carbohydrate recognition domain (Fig. 48A), suggesting that the response was not CRD mediated.

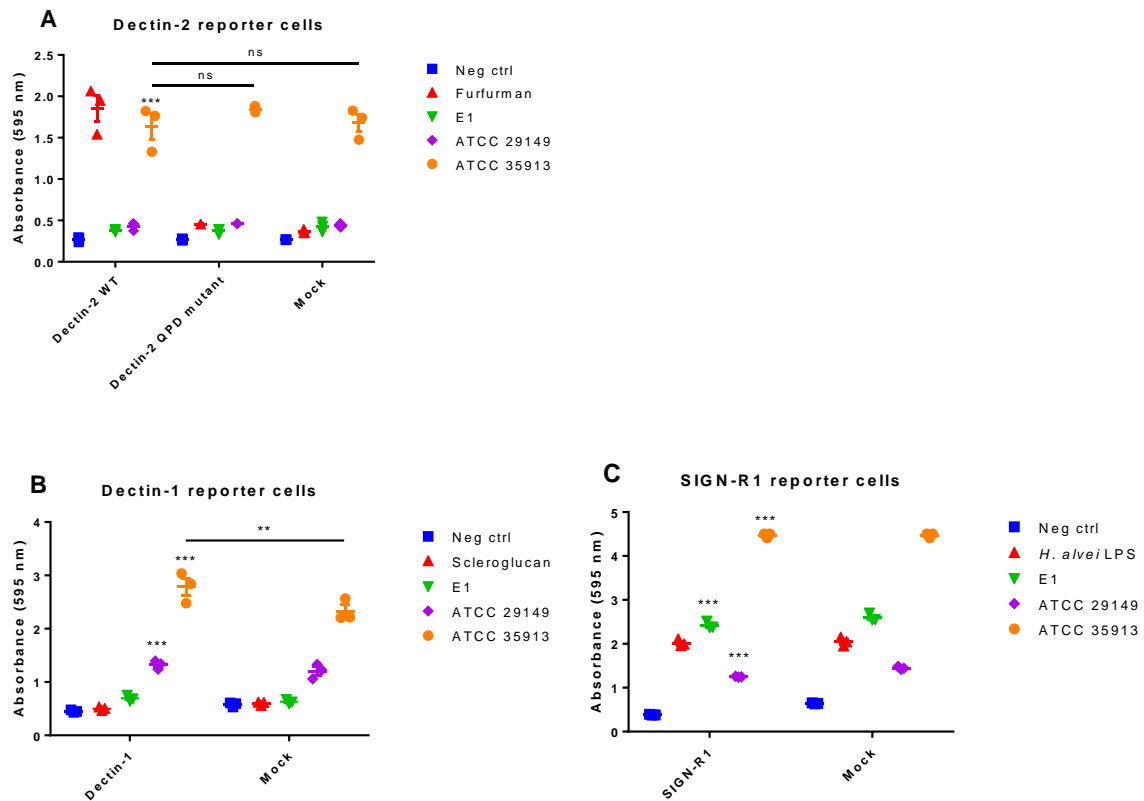


**Figure 48: Analysis of the interaction between *R. gnavus* strains and C-type lectin reporter cells.**

C-type lectin reporter cells and mock cells (Mock) were incubated with *R. gnavus* ATCC 29149, ATCC 35913 or E1 strains at a MOI of 50:1. (A) mDectin-2 wild type (mDectin-2 WT) or carbohydrate recognition domain mutant mDectin-2 (mDectin-2 QPD mutant), (B) mDectin-1 wild type (mDectin-1), and (C) SIGN-R1 wild type (SIGN-R1). The activation of the reporter gene was measured by spectrophotometry at 595 nm. Furfurman (10 µg/ml), scleroglucan (10 µg/ml) or *H. alvei* LPS (10 µg/ml) were used as positive control for mDectin-2, mDectin-1, and SIGN-R1 reporter cells, respectively. The experiment was reproduced in 3 biological replicates. Two-way ANOVA was operated in comparison with negative control or between same condition in mDectin-2, mDectin-1 or SIGN-R1 and Mock cell lines (\* for  $p < 0.05$ , \*\* for  $p < 0.01$ , \*\*\* for  $p < 0.001$ ).

Significant differences were also reported in mDectin-1 and SIGN-R1 cell reporter cells with the different *R. gnavus* strains tested (Fig. 48B and Fig. 48C). However, the positive controls, scleroglucan from *Sclerotium rolfsii* for mDectin-1 failed to trigger activation in these cell reporter cells in the conditions tested, which prevented conclusive interpretation of the results.

### 5.3. Discussion

Of the three *R. gnavus* strains tested for their immunological properties, *R. gnavus* ATCC 35913 showed the highest induction of cytokine production in mBMDCs including IL-6, CXCL1, CCL2 and IL-10. Also, for CCL2, *R. gnavus* ATCC 29149 induced more production than E1, indicating strain-dependent response of the following pattern ATCC 35913 > ATCC 29149 > E1 in the conditions tested. This pattern was also observed in epithelial cells (Chapter 4) where *R. gnavus* ATCC 35913 showed the highest induction of multiple cytokines in epithelium cell models, with highest TNF- $\alpha$  and IL-10 production. In these experiments, the concentration of glucorhamnan used was 200  $\mu\text{g}/\text{ml}$ , which is higher than usual polysaccharide concentration used in immunoassays. This choice was made because of the data obtained in an optimization process described in section 2.6.3. (Fig. 14) where lower values of glucorhamnan failed to activate mBMDCs cytokine production. The results should therefore be interpreted in the way that the glucorhamnan influence on immune cells is far from what could be seen *in vitro* and are rather indicative of the difference of cytokine production induction between the different strains of *R. gnavus* depending on the glucorhamnan structure.

This strain-specific immunomodulation has been reported in other gut commensal bacteria such as *B. longum* CCDM 372 which showed enhanced production of cytokines TNF- $\alpha$ , IL-10, IL-6 and IL-12p70 in mBMDCs compared to the strain CCM 7952 from the same species (Srutkova et al., 2015). These differences may be clade specific as shown for human associated *L. reuteri* strains which differed in their ability to modulate human cytokine production (TNF- $\alpha$ , MCP-1, IL-1 $\beta$ , IL-5, IL-7, IL-12, and IL-13) by myeloid cells (Spinler et al., 2014). Interestingly, a pangenome analysis of *R. gnavus* metagenomic sequencing data identified two distinct clades of *R. gnavus* strains, one of which is enriched in IBD patients (Hall et al., 2017). Although it is not known whether the increased abundance of *R. gnavus* in IBD is a cause or effect of inflammation, it is possible that the immunoregulatory properties of *R. gnavus* strains associated with IBD contribute to the exacerbated immune response to the gut microbiome.

In contrast to the results obtained with epithelial cells (Chapter 4), the glucorhamnans purified from *R. gnavus* E1, ATCC 29149 and ATCC 35913 induced the production of cytokines in mBMDCs (IL-1 $\beta$ , IL-6, IL-10, IL-12, TNF- $\alpha$ , CXCL1 and CXCL2), further expanding previous results reporting TNF- $\alpha$  and IL-6 production by *R. gnavus* ATCC 29149 glucorhamnan in mBMDCs (Henke *et al.*, 2019; Haynie *et al.*, 2021). *Shigella flexneri* strain 2a presents a similar glucorhamnan structure on its cell surface (Hlozek *et al.*, 2020) and this polysaccharide has been shown to induce a pro-inflammatory immune response enabling the immunisation against the bacteria in mouse (Tian *et al.*, 2021). As mentioned in section 3.3, *S. uberis* strain 233 and *S. mutans* serotype c strains also display a cell surface polysaccharide similar to that of ATCC 35913 and E1 strains but its inflammatory properties have not been investigated.

In addition, we showed that the role of glucorhamnan in modulating host immune response was dependent on the carbohydrate source used to grow the bacteria, as the glucorhamnan from *R. gnavus* ATCC 35913 grown with melibiose showed increased induction of IL-6, CXCL1, CCL2 and IL-12p40 in comparison with the glucorhamnan from the same strain grown in BHI-YH. This supports the notion that the carbon source has an influence on the glucorhamnan structure, which in turn, will influence the immunomodulatory properties of the strains and their impact on host immunity, even though the glucorhamnan must not be the only component influencing the immunomodulation of the bacteria, comprising the CPS harboured by ATCC 29149 (Henke *et al.*, 2021).

The use of NF- $\kappa$ B reporter cells demonstrated that *R. gnavus* ATCC 35913 strain and its associated glucorhamnan had the highest capacity to induce a NF- $\kappa$ B-associated immune response in monocytes, indicating, here again, that *R. gnavus* ATCC 35913 was the most immunogenic strain of the three strains tested. The glucorhamnan from *R. gnavus* E1 and ATCC 35913 (which share the same structure) induced a stronger response than the glucorhamnan from *R. gnavus* ATCC 29149 in these cells, suggesting that *R. gnavus* E1 and ATCC 35913 glucorhamnan (composed of repeating units of 4 rhamnoses and 1 glucose) is more immunogenic than the glucorhamnan from *R. gnavus* ATCC 29149 (composed of repeating units of 3 rhamnoses and 2 glucoses). The NF- $\kappa$ B signaling pathway in these reporter

cells is dependent on *R. gnavus* interaction with PRRs such as TLR2, TLR1/2, TLR2/6, TLR4, TLR5, TLR8, NOD1 and NOD2 which are all known to be expressed in this cell line. The cells used here were monocytes as those cells have been shown to harbour a larger panel of PRRs on their cell surface than other immune cell types like macrophages, making them good candidates for their use as reporter cells in this experiment. Our results are in agreement with previous work showing that *R. gnavus* ATCC 29149 glucorhamnan induction of TNF- $\alpha$  and IL-6 was TLR4 dependent as this response was abrogated using mBMDCs isolated from TLR4 knockout mice (Haynie et al., 2021; Henke et al., 2019). The results obtained here have to be considered with the potentiality that other components on the cell surface of the bacteria, coming from the bacterial growth medium or from the purification process, can interfere with the experiment results obtained while assessing the interaction between the bacteria and the immune cells. To address this issue, different methods can be used as fixation of bacteria before the incubation with the immune cells, using for example paraformaldehyde; another method that could be used is blocking assays, using lectin or antibodies specific to *R. gnavus* cell surface polysaccharides, this process will allow to observe the interaction between the bacteria and the immune cells without the influence of these polysaccharides.

Since the glucorhamnans of *R. gnavus* E1 and ATCC 29149 strains induced a NF- $\kappa$ B response but not the whole bacteria, it may be that other compounds on *R. gnavus* cell surface of these two strains may be masking or inhibiting the interaction of glucorhamnans and PRRs. This supports the notion that the glucorhamnan from *R. gnavus* ATCC 29149 activates a response in immune cells through the interaction with TLR4 but that this interaction may be prevented when using whole bacterial cells by the presence of non-immunogenic cell surface components, such as CPS, as previously proposed (Henke, *et al.*, 2021). Since *R. gnavus* cell surface glucorhamnan is composed of D-glucose and L-rhamnose and that rhamnose is a deoxy-mannose, we further hypothesised that the *R. gnavus* strains could interact with mDectin-2. Using mDectin-2, mDectin-1 and SIGN-R1 reporter cells, the results obtained were inconclusive due to technical aberrations like false positive values in mock cell and negative control conditions, showing that these preliminary results would need to be repeated. The

problem encountered here might be due to deficiency in the mDectin-1 gene expression, avoiding the recognition by the cells of Dectin-1-specific ligand scleroglucan. To address this issue, the cell line reporter gene could be investigated using PCR to detect its presence.

Our *in vitro* work supports that the sum of bacterial cell surface factors contributes to the development of different immune responses induced by *R. gnavus* strains leading to pro- and anti-inflammatory response. This is particularly relevant to the *in vivo* situation where disruption of the gut barrier function triggers excessive inflammation, as seen in the case of IBD or IBS which are both associated with increase in *R. gnavus* relative abundance (Croft et al., 2023). In a recent study, the cytokine profile (IL-1 $\beta$ , IL-2, IL-8, IL-10, IL-13, IL-17, TNF- $\alpha$  and IFN- $\gamma$ ) of colonic biopsies stimulated *ex vivo* with a range of commensal bacteria including *R. gnavus* showed differences in cytokine release between biopsies from post-Infectious IBS patients and healthy controls (Sundin et al., 2015), while it induced the production of IL-17A in mouse colitis models (Grabinger et al., 2019). Together, these findings show that the capacity of *R. gnavus* to influence the host immune response, by inducing the production of anti-inflammatory or pro-inflammatory cytokines, is dependent on the strain but also the experimental model and the conditions tested.

## Chapter 6: General discussion

The gut microbiota plays a major role in human health and an alteration in gut microbiota structure and function has been implicated in several diseases. In humans, some of the gut bacteria such as *R. gnavus* have evolved to inhabit the colonic mucus niche. *R. gnavus* is an important member of the 'normal' gut microbiota and over-represented in IBD. IBD encompassing Crohn's disease and ulcerative colitis, is characterised by a prolonged inflammation resulting in damages in the GI tract. In 2020, more than 6.8 million persons experienced IBD-related symptoms (Jairath & Feagan, 2020). There is therefore interest in deciphering the mechanisms implicated in the establishment of the disease, its associated symptoms and potential treatment.

The gut microbiota plays a major role in human health and an alteration in gut microbiota structure and function has been implicated in several diseases. In humans, some of the gut bacteria such as *R. gnavus*, have evolved to inhabit the colonic mucus niche. *R. gnavus* is an important member of the 'normal' gut microbiota and over-represented in inflammatory bowel disease.

The type-strain *R. gnavus* ATCC 29149 has been extensively studied and shown to be implicated in inducing a pro- or anti-inflammatory response depending on the gut environment. In addition, structural features have been associated with this strain such as the presence of cell surface polysaccharides of different size and composition, glucorhamnan (Henke *et al.*, 2019; Haynie *et al.*, 2021) and CPS (Henke *et al.*, 2021). However, accumulating evidence shows that *R. gnavus* strategy of adaptation to the gut, like the production of GH to degrade mucin polysaccharides or immunomodulatory factors are strain-specific, as recently reviewed (Crost *et al.*, 2023) and this may contribute to the capacity of some of *R. gnavus* strains to proliferate in IBD conditions.

Here, we tested the hypothesis that different strains of *R. gnavus* influence differently the host response and investigated the contribution of strain-specific cell surface glycosylation on gut barrier function and host immune response.

In this work, we focused on three *R. gnavus* strains, ATCC 29149, ATCC 35913 and E1, isolated from adult healthy donors. Using a combination of approaches including GC-MS and NMR, we showed that the three strains shared glucorhamnan as a cell surface polysaccharide but with differences in the repeating unit composition, as also reflected in the biosynthesis clusters of the strains. Furthermore, we could observe differences in the cell surface glycosylation linked with the carbon source used for the bacterial growth which may be relevant to the nutritional niche of *R. gnavus* strains *in vivo*. Furthermore, we could observe differences in the cell surface glycosylation through the use of lectin-binding assay which showed evidence that the carbon source used for the bacterial growth also had an effect on the cell surface glycosylation additionally to the difference observed between the strains. This was also demonstrated through the differences observed in the gene expression level between the different strains when using different carbon source for bacterial growth and at different growth stages. Taken together, this information shows that *R. gnavus* display on its cell surface glycosylations, comprising the glucorhamnan, influenced by environmental factors but also differ among the strains.

Polysaccharides with composition and structure similar to *R. gnavus* glucorhamnans have been described in pathogens such as *Shigella flexneri* strain 2a (Hlozek et al., 2020), *Streptococcus uberis* strain 233 (Czabańska et al., 2013), and *Streptococcus mutans* serotype c (King et al., 2021). Therefore, we next tested the effect of *R. gnavus* strains and their purified glucorhamnan structures on the gut epithelial barrier function and immune response.

We showed that *R. gnavus* ATCC 35913 was the most immunogenic strain when measuring cytokine response in both epithelium and immune cells as compared to the two other strains. However, none of the *R. gnavus* strains (nor their glucorhamnans) affected the integrity of the gut barrier. Then, the glucorhamnan from the different strains seemed to have no influence on the epithelial cell cytokine production either. Also, no effect of the different strains or purified glucorhamnans could be observed on gut barrier function of epithelial cells tested. These results shows that *R. gnavus* has no strong effect on epithelial cells, neither on

the immune response or the gut barrier function, to the exception of ATCC 35913, that was able to induce some cytokine production in those cells.

Finally, the interaction of *R. gnavus* strain but also their purified glucorhamnan with the host immunity was investigated through the use of dendritic cells (mBMDCs) and PRR reporter cells, comprising CLR reporter cells and TLR reporter cells. Using this, we were able to observe the following: first, as seen with the epithelial cells, ATCC 35913 seems to be the most immunogenic strain in all models tested, followed by ATCC 29149. Furthermore, the glucorhamnans seemed to have great impact on the mBMDCs cytokine production and reporter cells activation, which wasn't the case in epithelial cells, and allowed us to note several interesting points: in first place, the glucorhamnan from E1 and ATCC 35913 both grown in BHI-YH shared the most similarity of immunogenicity, while the ATCC 29149 glucorhamnan had the most outlying effect on immune response induced. After that, the glucorhamnan from ATCC 35913 grown in either BHI-YH or with melibiose as sole carbon source displayed significant differences in immunogenicity (the glucorhamnan from ATCC 35913 grown with melibiose being the most immunogenic among those two). This observation can be correlated with the fact that the glucorhamnan from those two conditions were shown to harbour different rhamnose/glucose ratio in their glucorhamnan structure, therefore potentially influencing the lectin-binding profile and immunogenicity outcome of the strain and associated glucorhamnan. The cytokines induced by *R. gnavus* ATCC 35913 strain in the assays reported in this work (IL-29, IL-1 $\beta$ , CXCL5 and CXCL8) are involved in pro-inflammatory mechanisms, suggesting an induction of immunity in the host.

In contrast, *R. gnavus* glucorhamnans affected cytokine production by mBMDCs and NF- $\kappa$ B reporter cells activation. Interestingly, the glucorhamnan isolated from *R. gnavus* E1 and ATCC 35913, which shared a common structure led to similar immunogenicity, while the glucorhamnan isolated from *R. gnavus* ATCC 29149 with a distinct repeating unit composition, led to a different host immune response. These differences were also observed when using *R. gnavus* ATCC 35913 glucorhamnans grown on different carbohydrate sources which also reflects differences in the rhamnose/glucose ratio of their glucorhamnan structure.

However, the purified glucorhamnans do not always recapitulate the response obtained with the whole bacteria. For example, we showed induction of CXCL8 production by epithelial cells with *R. gnavus* ATCC 29149 glucorhamnan but not with the whole bacteria. This may be due to the presence of CPS masking the effect of glucorhamnan, as previously suggested (Henke *et al.*, 2021) although this CPS remains to be fully characterised at the structural level. In addition, more work is needed to determine the function of the proteins encoded by the glucorhamnan and the CPS biosynthetic gene clusters in *R. gnavus* strains, in particular GTs. This information will allow us to explore genomic information of *R. gnavus* strain sequenced to date to better predict the type of cell surface polysaccharides encoded by *R. gnavus* strains, reducing the need for labour-intensive structural characterisation.

These results also showed that the TLRs are involved in *R. gnavus* strains recognition by immune cells as shown in section 5.2.2. Those cells, the THP1, which are human T cells, have their reporter gene expression triggered through the binding with TLR1/2, TLR2/6, TLR4, TLR5 and TLR8, following suppliers' information ([www.invivogen.com/thp1-blue-nfkb](http://www.invivogen.com/thp1-blue-nfkb)).

Results reported by Henke *et al.* (2019) shows that TLR2 was only slightly involved in the induction of TNF- $\alpha$  production by BMDCs by *R. gnavus* ATCC 29149 glucorhamnan. Taken together, those data indicate that the NF-KB induction in THP1 cells by *R. gnavus* strains was therefore mainly induced by TLR4 and TLR5.

As described in section 1.1.4.3., TLR4 is implicated in the recognition of bacterial-derived cell surface components like LPS, lipid A and mannans, while TLR5 is implicated in the recognition of flagellin, not present on *R. gnavus* cell surface. This mean *R. gnavus* strains interact with TLR4 through their cell surface glycosylation, playing therefore an important role in the interaction with host immunity.

Altogether, the data acquired in this project supports the idea that the carbon source present in *R. gnavus* strains environment influences the glycosylation present on their cell surface,

which will have in turn an influence on the gut epithelium and the host immunity, suggesting that *R. gnavus* indeed influence the host health outcome, and this in a strain-dependent way.

Similar results were observed with other bacteria like *Lactobacillus acidophilus* and *Lactobacillus plantarum* which were shown to stimulate TLR2 in Caco-2 cells, and induced the relocalisation of ZO-1 and occludin on the apical side of the epithelial layer (Rose et al., 2021). Other clusters for CPS and EPS biosynthesis have been identified in gut microbiota-associated bacteria as playing a major role in gut homeostasis. For example, *B. longum* strain 105-A harbours an EPS biosynthesis cluster composed of 24 putative genes, and the knockout of this cluster affects bacterial physical properties, including the loss of a thick capsule but also an enhanced fimbriae formation in comparison with the wild-type strain (Tahoun et al., 2017). Additionally, the mutant bacteria showed a higher rate of sedimentation in liquid culture (Tahoun et al., 2017), as also observed in our work for *R. gnavus* ATCC 35913, which does not produce the CPS as shown by electronic microscopy and sedimented the easiest out of the 3 strains tested. Unfortunately, despite promising results using the Clostron methodology (Bell et al., 2019), *R. gnavus* is not genetically tractable, hampering the generation of mutant CPS or glucorhamnan mutant strains.

The cytokines induced by *R. gnavus* ATCC 35913 strain in the assays reported in this work (IL-29, IL-1 $\beta$ , CXCL5 and CXCL8) are involved in pro-inflammatory responses, in line with the absence of tolerogenic CPS on *R. gnavus* ATCC 35913 cell surface. IL-1 $\beta$  is involved in the activation of several immune cell types like monocytes while CXCL5 and CXCL8 are chemokines produced by epithelial cells and are neutrophils chemoattractant, which may lead to the recruitment of immune cells involved in the phagocytosis of pathogens. Also, the results obtained here underlined the importance of the involvement of goblet cells and mucus-production in the interaction of *R. gnavus* strains with epithelial cell layer as the cytokine production in the two epithelium models used were differing significantly. This is relevant with the findings recently obtained by Asnicar et al. (2021), where they were able to find a negative correlation between *R. gnavus* present in the gut microbiota and the host

health, more specifically, *R. gnavus* was correlated with increased fasting and postprandial inflammation.

Our results also showed that TLRs are involved in *R. gnavus* strains recognition by THP1 immune cells, in line with previous work showing that TLR4 is implicated in the recognition of ATCC 29149 strain using mBMDCs derived from TLR4-K/O mice (Henke *et al.*, 2019). TLR4 has been shown to interact with bacterial-derived cell surface components like LPS, lipid A and mannans. In the future, it will be interesting to use TLR4-reporter cells to confirm direct interaction with glucorhamnan structures and identify the epitopes involved in the recognition.

*Lactobacillus acidophilus* and *Lactobacillus plantarum* have been shown to stimulate TLR2 in Caco-2 cells, and to induce the relocalisation of ZO-1 and occludin on the apical side of the epithelial layer (Rose *et al.*, 2021). Also, *E. coli* strain Nissle 1917 showed to alter both the expression and relocalisation of ZO-2 to cell boundaries in T84 cells (Zyrek *et al.*, 2007a) while *L. plantarum* induced the translocation of ZO-1 in tight junction regions in Caco-2 cells (Karczewski *et al.*, 2010a). Here, using two types of intestinal epithelium models (T84 and T84/LS174T cells), we did not observe any changes in tight junction expression or permeability following treatment with *R. gnavus* strains or their derived glucorhamnans. However, it would be interesting in future work to determine the effect on their spatial distribution. In addition, other molecular mediators, not tested in this work, may influence the ability of *R. gnavus* strains to affect gut barrier function. For example, butyrate produced by gut bacteria can promote the expression of tight junction genes *in vitro* (X. Ma *et al.*, 2012), repress paracellular permeability *in vivo* (L. S. Liu *et al.*, 2018), and inhibit permeability-promoted claudin-2 tight junction protein expression (L. Zheng *et al.*, 2017). Furthermore, *Bifidobacterium infantis* has been shown to secrete an extracellular protein that up-regulates the secretion of occludin and ZO-1 tight junction proteins, improving mucosal barrier in mouse (Ewaschuk *et al.*, 2008).

Another potential role of bacterial cell surface polysaccharides in the gut beyond their immunomodulatory properties and role in modulating gut barrier function is that they could be a source of nutrients for other gut bacteria, therefore playing a role in shaping the gut microbiota. For example, EPS from *B. longum* IPLA E44 and *B. animalis* subsp. lactis IPLA R1 were able to induce changes in the gut microbiota composition and metabolic activity of human faecal microbiota (Salazar et al., 2008, 2009). *B. breve* UCC2003 EPS has been found to be metabolised by the infant gut microbiota, leading to differential microbial metabolite by-products, which may contribute to differences in health outcome in these infants (Püngel et al., 2020). Several EPS synthesised by lactic acid bacteria are used as fermentable substrate by the intestinal microbiota (Salazar et al., 2016). Since gut bacteria can produce glycoside hydrolases such as glucosidases and rhamnosidases, the possible use of *R. gnavus* glucorhamnan as a nutrient source in the gut microbiota may be worth investigating in the future.

Also, the polysaccharide harboured by *B. thetaiotaomicron* has been shown to play an important role in the bacterial resistance against other bacteria in the gut, phages and the host immunity, and acapsular strains loses in competitive colonisation against strains harbouring a capsule (Hoces et al., 2023). A process of defence that have been put in place by microbial bacteria against phages was identified in *B. thetaiotaomicron* strain VPI-5482 and consists of the expression of non-permissive CPS variants which are selected under the phage predation (Porter et al., 2020). Interestingly, phages have been shown to co-exist with *R. gnavus* population in the gut of mice (Buttimer et al., 2023), while patients with IBD had an overrepresentation of *R. gnavus* virome (Buttimer et al., 2023). As phages only infect strains harbouring a specific capsule complex, they drive the loss of capsule for survival, therefore leading to a serotype switch *in vivo*, as shown for *Klebsiella pneumoniae* (de Sousa et al., 2020), a scenario that may be also relevant to *R. gnavus* strains in the gut. In the pathogen *K. pneumoniae* strain ST258, a high frequency of recombination and large-scale genomic rearrangements was associated with switching and variation of the CPS encoding locus, allowing the bacteria to evade bacteriophage predation (Venturini et al., 2020). In the future,

it would be interesting to assess the link between *R. gnavus* CPS loss (in some of the strains) and phages.

In our work we looked at tight junction genes expression and presence in the cells but not relocation on tight junction sites which may be interesting to do in the future as there has been example showing the influence of gut microbiota on the relocalisation of tight junction proteins like ZO-1 or ZO-2, this through the stimulation of TLR2 by gut bacteria (Blackwood et al., 2017; Karczewski et al., 2010b; Zyrek et al., 2007b). It would therefore be interesting to determine if *R. gnavus* strains has an influence on these tight junction proteins relocalisation on tight junction sites and therefore on the gut barrier function.

Another information that needs to be deciphered following information acquired about cell surface glycosylation difference between the different strains of *R. gnavus* would be to determine the precise function of each gene in the glucorhamnan and the CPS cluster in *R. gnavus* different strains, and more specifically the different GT function in those biosynthetic clusters. This would allow us to further understand the biosynthetic pathways leading to the production of the different cell surface polysaccharides on *R. gnavus* strains cell surface and understand better the genetic mechanism behind the differences between the different strains.

Also, the influence of the carbon source used to grown E1 and ATCC 35913 seemed to have an influence on the rhamnose/glucose ratio of the glucorhamnan in those strains influenced by the GT expression and activity, depending on the growth phase and the carbon source the bacteria dispose of. The influence of this rhamnose/glucose ratio on the immunogenicity of the resulting glucorhmnan should be investigated to understand better the dynamic of *R. gnavus* strains interaction with the host *in vivo*.

Altogether, our *in vitro* data support the notion that *R. gnavus* strains adapted to different nutritional niches in the gut may differentially influence host health outcome in a strain-dependent way implicating cell surface polysaccharides.

This work should contribute to advance in the development of diagnostic tools and potential treatment against IBD associated conditions in patients, by understanding better the role of *R. gnavus* strains in this disease, establishing specific biomarkers and make advances in therapeutic fields like faecal microbiota transplantation, where the relation between the gut microbiota and the host health outcome needs to be understand further to allow efficient application of such a treatment.

This work therefore underlines the importance of studying *R. gnavus* but also other microbial species at a strain level. Data generated by future work in this field should contribute to advance our understanding of the role of *R. gnavus* in health and diseases and inform the development of strain-specific biomarkers and potential treatment against *R. gnavus*-associated conditions in patients.

## References

- Agace, W. W., & McCoy, K. D. (2017). Regionalized Development and Maintenance of the Intestinal Adaptive Immune Landscape. In *Immunity* (Vol. 46, Issue 4, pp. 532–548). Cell Press. <https://doi.org/10.1016/j.immuni.2017.04.004>
- Ahn, J. R., Lee, S. H., Kim, B., Nam, M. H., Ahn, Y. K., Park, Y. M., Jeong, S. M., Park, M. J., Song, K. B., Lee, S. Y., & Hong, S. J. (2022). Ruminococcus gnavus ameliorates atopic dermatitis by enhancing Treg cell and metabolites in BALB/c mice. *Pediatric Allergy and Immunology*, 33(1). <https://doi.org/10.1111/pai.13678>
- Akahori, Y., Miyasaka, T., Toyama, M., Matsumoto, I., Miyahara, A., Zong, T., Ishii, K., Kinjo, Y., Miyazaki, Y., Saijo, S., Iwakura, Y., & Kawakami, K. (2016). Dectin-2-dependent host defense in mice infected with serotype 3 Streptococcus pneumoniae. *BMC Immunology*, 17(1). <https://doi.org/10.1186/s12865-015-0139-3>
- Akatsuka, A., Ito, M., Yamauchi, C., Ochiai, A., Yamamoto, K., & Matsumoto, N. (2010). Tumor cells of non-hematopoietic and hematopoietic origins express activation-induced C-type lectin, the ligand for killer cell lectin-like receptor F1. *International Immunology*, 22(9), 783–790. <https://doi.org/10.1093/intimm/dxq430>
- Akira, S., Uematsu, S., & Takeuchi, O. (2006). Pathogen recognition and innate immunity. In *Cell* (Vol. 124, Issue 4, pp. 783–801). <https://doi.org/10.1016/j.cell.2006.02.015>
- Albenberg, L., Esipova, T. V., Judge, C. P., Bittinger, K., Chen, J., Laughlin, A., Grunberg, S., Baldassano, R. N., Lewis, J. D., Li, H., Thom, S. R., Bushman, F. D., Vinogradov, S. A., & Wu, G. D. (2014). Correlation between intraluminal oxygen gradient and radial partitioning of intestinal microbiota. *Gastroenterology*, 147(5), 1055-1063.e8. <https://doi.org/10.1053/j.gastro.2014.07.020>
- Almeida, A., Mitchell, A. L., Boland, M., Forster, S. C., Gloor, G. B., Tarkowska, A., Lawley, T. D., & Finn, R. D. (2019). A new genomic blueprint of the human gut microbiota. *Nature*, 568(7753), 499–504. <https://doi.org/10.1038/s41586-019-0965-1>
- Alrafas, H. R., Busbee, P. B., Nagarkatti, M., & Nagarkatti, P. S. (2019). Resveratrol modulates the gut microbiota to prevent murine colitis development through induction of Tregs and suppression of Th17 cells. *Journal of Leukocyte Biology*, 106(2), 467–480. <https://doi.org/10.1002/JLB.3A1218-476RR>
- Al-Sadi, R. (2009). Mechanism of cytokine modulation of epithelial tight junction barrier. *Frontiers in Bioscience, Volume*(14), 2765. <https://doi.org/10.2741/3413>
- Arentsen, T., Qian, Y., Gkotzlis, S., Femenia, T., Wang, T., Udekwu, K., Forssberg, H., & Diaz Heijtz, R. (2017). The bacterial peptidoglycan-sensing molecule Pglyrp2 modulates

- brain development and behavior. *Molecular Psychiatry*, 22(2), 257–266.  
<https://doi.org/10.1038/mp.2016.182>
- Arike, L., Holmén-Larsson, J., & Hansson, G. C. (2017). Intestinal Muc2 mucin O-glycosylation is affected by microbiota and regulated by differential expression of glycosyltransferases. *Glycobiology*, 27(4), 318–328.  
<https://doi.org/10.1093/glycob/cww134>
- Artis, D. (2008). Epithelial-cell recognition of commensal bacteria and maintenance of immune homeostasis in the gut. In *Nature Reviews Immunology* (Vol. 8, Issue 6, pp. 411–420). <https://doi.org/10.1038/nri2316>
- Asnicar, F., Berry, S. E., Valdes, A. M., Nguyen, L. H., Piccinno, G., Drew, D. A., Leeming, E., Gibson, R., Le Roy, C., Khatib, H. Al, Francis, L., Mazidi, M., Mompeo, O., Valles-Colomer, M., Tett, A., Beghini, F., Dubois, L., Bazzani, D., Thomas, A. M., ... Segata, N. (2021). Microbiome connections with host metabolism and habitual diet from 1,098 deeply phenotyped individuals. *Nature Medicine*, 27(2), 321–332.  
<https://doi.org/10.1038/s41591-020-01183-8>
- Asquith, M. J., Boulard, O., Powrie, F., & Maloy, K. J. (2010). Pathogenic and Protective Roles of MyD88 in Leukocytes and Epithelial Cells in Mouse Models of Inflammatory Bowel Disease. *Gastroenterology*, 139(2), 519–529.e2.  
<https://doi.org/10.1053/j.gastro.2010.04.045>
- Atuma, C., Strugala, V., Allen, A., & Holm, L. (2001). The adherent gastrointestinal mucus gel layer: Thickness and physical state in vivo. *American Journal of Physiology - Gastrointestinal and Liver Physiology*, 280(5 43-5), 922–929.  
<https://doi.org/10.1152/ajpgi.2001.280.5.g922>
- Avershina, E., Storrø, O., Øien, T., Johnsen, R., Pope, P., & Rudi, K. (2014). Major faecal microbiota shifts in composition and diversity with age in a geographically restricted cohort of mothers and their children. *FEMS Microbiology Ecology*, 87(1), 280–290.  
<https://doi.org/10.1111/1574-6941.12223>
- Azad, M. A. K., Sarker, M., Li, T., & Yin, J. (2018). Probiotic Species in the Modulation of Gut Microbiota: An Overview. In *BioMed Research International* (Vol. 2018). Hindawi Limited. <https://doi.org/10.1155/2018/9478630>
- Azzouz, D., Omarbekova, A., Heguy, A., Schwudke, D., Gisch, N., Rovin, B. H., Caricchio, R., Buyon, J. P., Alekseyenko, A. V., & Silverman, G. J. (2019). Lupus nephritis is linked to disease-activity associated expansions and immunity to a gut commensal. *Annals of the Rheumatic Diseases*, 78(7), 947–956. <https://doi.org/10.1136/annrheumdis-2018-214856>

- Bäckhed, F., Roswall, J., Peng, Y., Feng, Q., Jia, H., Kovatcheva-Datchary, P., Li, Y., Xia, Y., Xie, H., Zhong, H., Khan, M. T., Zhang, J., Li, J., Xiao, L., Al-Aama, J., Zhang, D., Lee, Y. S., Kotowska, D., Colding, C., ... Wang, J. (2015). Dynamics and Stabilization of the Human Gut Microbiome during the First Year of Life. *Cell Host & Microbe*, *17*(5), 690–703. <https://doi.org/10.1016/j.chom.2015.04.004>
- Balty, C., Guillot, A., Fradale, L., Brewee, C., Boulay, M., Kubiak, X., Benjdia, A., & Berteau, O. (2019). Ruminococcin C, an anti-clostridial sactipeptide produced by a prominent member of the human microbiota *Ruminococcus gnavus*. *Journal of Biological Chemistry*, *294*(40), 14512–14525. <https://doi.org/10.1074/jbc.RA119.009416>
- Barker, N. (2014). Adult intestinal stem cells: Critical drivers of epithelial homeostasis and regeneration. In *Nature Reviews Molecular Cell Biology* (Vol. 15, Issue 1, pp. 19–33). <https://doi.org/10.1038/nrm3721>
- Baumann, H., Tzianabos, A. O., Brisson, J. R., Kasper, D. L., & Jennings, H. J. (1992). Structural elucidation of two capsular polysaccharides from one strain of *Bacteroides fragilis* using high-resolution NMR spectroscopy. *Biochemistry*, *31*(16), 4081–4089. <https://doi.org/10.1021/bi00131a026>
- Baumgartner, M., Lang, M., Holley, H., Crepez, D., Hausmann, B., Pjevac, P., Moser, D., Haller, F., Hof, F., Beer, A., Orgler, E., Frick, A., Khare, V., Evstatiev, R., Strohmaier, S., Primas, C., Dolak, W., Köcher, T., Klavins, K., ... Gasche, C. (2021). Mucosal Biofilms Are an Endoscopic Feature of Irritable Bowel Syndrome and Ulcerative Colitis. *Gastroenterology*, *161*(4), 1245-1256.e20. <https://doi.org/10.1053/j.gastro.2021.06.024>
- Behzadi, E., & Behzadi, P. (2016). The role of Toll-Like receptors (TLRs) in urinary tract infections (UTIs). In *Central European Journal of Urology* (Vol. 69, Issue 4, pp. 404–410). Polish Urological Association. <https://doi.org/10.5173/cej.2016.871>
- Bell, A., Brunt, J., Crost, E., Vaux, L., Nepravishta, R., Owen, C. D., Latousakis, D., Xiao, A., Li, W., Chen, X., Walsh, M. A., Claesen, J., Angulo, J., Thomas, G. H., & Juge, N. (2019). Elucidation of a sialic acid metabolism pathway in mucus-foraging *Ruminococcus gnavus* unravels mechanisms of bacterial adaptation to the gut. *Nature Microbiology*, *4*(12), 2393–2404. <https://doi.org/10.1038/s41564-019-0590-7>
- Bene, K. P., Kavanaugh, D. W., Leclaire, C., Gunning, A. P., MacKenzie, D. A., Wittmann, A., Young, I. D., Kawasaki, N., Rajnavolgyi, E., & Juge, N. (2017). *Lactobacillus reuteri* surface mucus adhesins upregulate inflammatory responses through interactions with innate C-Type lectin receptors. *Frontiers in Microbiology*, *8*(MAR). <https://doi.org/10.3389/fmicb.2017.00321>

- Bergstrom, K. S. B., & Xia, L. (2013). Mucin-type O-glycans and their roles in intestinal homeostasis. In *Glycobiology* (Vol. 23, Issue 9, pp. 1026–1037). <https://doi.org/10.1093/glycob/cwt045>
- Bevins, C. L., & Salzman, N. H. (2011). Paneth cells, antimicrobial peptides and maintenance of intestinal homeostasis. In *Nature Reviews Microbiology* (Vol. 9, Issue 5, pp. 356–368). <https://doi.org/10.1038/nrmicro2546>
- Bian, S., Zeng, W., Li, Q., Li, Y., Wong, N. K., Jiang, M., Zuo, L., Hu, Q., & Li, L. (2021). Genetic Structure, Function, and Evolution of Capsule Biosynthesis Loci in *Vibrio parahaemolyticus*. *Frontiers in Microbiology*, 11. <https://doi.org/10.3389/fmicb.2020.546150>
- Birchenough, G. M. H., Johansson, M. E. V., Gustafsson, J. K., Bergström, J. H., & Hansson, G. C. (2015). New developments in goblet cell mucus secretion and function. In *Mucosal Immunology* (Vol. 8, Issue 4, pp. 712–719). Nature Publishing Group. <https://doi.org/10.1038/mi.2015.32>
- Blackwood, B. P., Yuan, C. Y., Wood, D. R., Nicolas, J. D., Grothaus, J. S., & Hunter, C. J. (2017). Probiotic *Lactobacillus* Species Strengthen Intestinal Barrier Function and Tight Junction Integrity in Experimental Necrotizing Enterocolitis. *Journal of Probiotics & Health*, 05(01). <https://doi.org/10.4172/2329-8901.1000159>
- Blandford, L. E., Johnston, E. L., Sanderson, J. D., Wade, W. G., & Lax, A. J. (2019). Promoter orientation of the immunomodulatory *Bacteroides fragilis* capsular polysaccharide A (PSA) is off in individuals with inflammatory bowel disease (IBD). *Gut Microbes*, 10(5), 569–577. <https://doi.org/10.1080/19490976.2018.1560755>
- Blanton, L. V., Charbonneau, M. R., Salih, T., Barratt, M. J., Venkatesh, S., Ilkaveya, O., Subramanian, S., Manary, M. J., Trehan, I., Jorgensen, J. M., Fan, Y., Henrissat, B., Leyn, S. A., Rodionov, D. A., Osterman, A. L., Maleta, K. M., Newgard, C. B., Ashorn, P., Dewey, K. G., & Gordon, J. I. (2016). Gut bacteria that prevent growth impairments transmitted by microbiota from malnourished children. *Science*, 351(6275). <https://doi.org/10.1126/science.aad3311>
- Brown, G. D., Willment, J. A., & Whitehead, L. (2018). C-type lectins in immunity and homeostasis. *Nature Reviews Immunology*, 18(6), 374–389. <https://doi.org/10.1038/s41577-018-0004-8>
- Buttimer, C., Khokhlova, E. V., Stein, L., Hueston, C. M., Govi, B., Draper, L. A., Ross, R. P., Shkoporov, A. N., & Hill, C. (2023). Temperate bacteriophages infecting the mucin-degrading bacterium *Ruminococcus gnavus* from the human gut. *Gut Microbes*, 15(1), 2194794. <https://doi.org/10.1080/19490976.2023.2194794>

- Cabral, J. M., Grácio, D., Soares-da-Silva, P., & Magro, F. (2015). Short- and long-term regulation of intestinal Na<sup>+</sup>/H<sup>+</sup> exchange by Toll-like receptors TLR4 and TLR5. *American Journal of Physiology-Gastrointestinal and Liver Physiology*, 309(8), G703–G715. <https://doi.org/10.1152/ajpgi.00124.2015>
- Candeliere, F., Raimondi, S., Ranieri, R., Musmeci, E., Zambon, A., Amaretti, A., & Rossi, M. (2022). β-Glucuronidase Pattern Predicted From Gut Metagenomes Indicates Potentially Diversified Pharmacomicrobiomics. *Frontiers in Microbiology*, 13. <https://doi.org/10.3389/fmicb.2022.826994>
- Carvalho, F. A., Aitken, J. D., Gewirtz, A. T., & Vijay-Kumar, M. (2011). TLR5 activation induces secretory interleukin-1 receptor antagonist (sIL-1Ra) and reduces inflammasome-associated tissue damage. *Mucosal Immunology*, 4(1), 102–111. <https://doi.org/10.1038/mi.2010.57>
- Castro-Bravo, N., Wells, J. M., Margolles, A., & Ruas-Madiedo, P. (2018). Interactions of surface exopolysaccharides from bifidobacterium and lactobacillus within the intestinal environment. In *Frontiers in Microbiology* (Vol. 9, Issue OCT). Frontiers Media S.A. <https://doi.org/10.3389/fmicb.2018.02426>
- Cerovic, V., Bain, C. C., Mowat, A. M., & Milling, S. W. F. (2014). Intestinal macrophages and dendritic cells: What's the difference? In *Trends in Immunology* (Vol. 35, Issue 6, pp. 270–277). Elsevier Ltd. <https://doi.org/10.1016/j.it.2014.04.003>
- Chahwan, B., Kwan, S., Isik, A., van Hemert, S., Burke, C., & Roberts, L. (2019). Gut feelings: A randomised, triple-blind, placebo-controlled trial of probiotics for depressive symptoms. *Journal of Affective Disorders*, 253, 317–326. <https://doi.org/10.1016/j.jad.2019.04.097>
- Chelakkot, C., Ghim, J., & Ryu, S. H. (2018). Mechanisms regulating intestinal barrier integrity and its pathological implications. In *Experimental and Molecular Medicine* (Vol. 50, Issue 8). Nature Publishing Group. <https://doi.org/10.1038/s12276-018-0126-x>
- Chiba, H., Osanai, M., Murata, M., Kojima, T., & Sawada, N. (2008). Transmembrane proteins of tight junctions. In *Biochimica et Biophysica Acta - Biomembranes* (Vol. 1778, Issue 3, pp. 588–600). Elsevier. <https://doi.org/10.1016/j.bbamem.2007.08.017>
- Chikina, A., & Matic Vignjevic, D. (2021). At the right time in the right place: How do luminal gradients position the microbiota along the gut? In *Cells and Development* (Vol. 168). Elsevier B.V. <https://doi.org/10.1016/j.cdev.2021.203712>
- Chiumento, S., Roblin, C., Kieffer-Jaquinod, S., Tachon, S., Leprêtre, C., Basset, C., Adityarini, D., Olleik, H., Nicoletti, C., Bornet, O., Iranzo, O., Maresca, M., Hardré, R., Fons, M., Giardina, T., Devillard, E., Guerlesquin, F., Couté, Y., Atta, M., ... Duarte, V. (2019). M I C

R O B I O L O G Y Ruminococcin C, a promising antibiotic produced by a human gut symbiont. In *Sci. Adv* (Vol. 5).

- Chong, C. Y. L., Bloomfield, F. H., & O'Sullivan, J. M. (2018). Factors affecting gastrointestinal microbiome development in neonates. In *Nutrients* (Vol. 10, Issue 3). MDPI AG. <https://doi.org/10.3390/nu10030274>
- Chua, H. H., Chou, H. C., Tung, Y. L., Chiang, B. L., Liao, C. C., Liu, H. H., & Ni, Y. H. (2018). Intestinal Dysbiosis Featuring Abundance of Ruminococcus gnavus Associates With Allergic Diseases in Infants. *Gastroenterology*, *154*(1), 154–167. <https://doi.org/10.1053/j.gastro.2017.09.006>
- Čipčić Paljetak, H., Barešić, A., Panek, M., Perić, M., Matijašić, M., Lojkić, I., Barišić, A., Vranešić Bender, D., Ljubas Kelečić, D., Brinar, M., Kalauz, M., Miličević, M., Grgić, D., Turk, N., Karas, I., Čuković-Čavka, S., Krznarić, Ž., & Verbanac, D. (2022). Gut microbiota in mucosa and feces of newly diagnosed, treatment-naïve adult inflammatory bowel disease and irritable bowel syndrome patients. *Gut Microbes*, *14*(1). <https://doi.org/10.1080/19490976.2022.2083419>
- Claes, I. J., Segers, M. E., Verhoeven, T. La, Dusselier, M., Sels, B. F., De Keersmaecker, S. C., Vanderleyden, J., & Lebeer, S. (2012). *Lipoteichoic acid is an important microbe-associated molecular pattern of Lactobacillus rhamnosus GG*. <http://www.microbialcellfactories.com/content/11/1/161>
- Clasen, S. J., Bell, M. E. W., Borbón, A., Lee, D.-H., Henseler, Z. M., De La Cuesta-Zuluaga, J., Parys, K., Zou, J., Wang, Y., Altmannova, V., Youngblut, N. D., Weir, J. R., Gewirtz, A. T., Belkhadir, Y., & Ley, R. E. (2022). *INNATE IMMUNITY Silent recognition of flagellins from human gut commensal bacteria by Toll-like receptor 5*. <https://www.science.org>
- Coletto, E., Latousakis, D., Pontifex, M. G., Crost, E. H., Vaux, L., Perez Santamarina, E., Goldson, A., Brion, A., Hajihosseini, M. K., Vauzour, D., Savva, G. M., & Juge, N. (2022). The role of the mucin-glycan foraging Ruminococcus gnavus in the communication between the gut and the brain. *Gut Microbes*, *14*(1). <https://doi.org/10.1080/19490976.2022.2073784>
- Colliou, N., Ge, Y., Sahay, B., Gong, M., Zadeh, M., Owen, J. L., Neu, J., Farmerie, W. G., Alonzo, F., Liu, K., Jones, D. P., Li, S., & Mohamadzadeh, M. (2017). Commensal Propionibacterium strain UF1 mitigates intestinal inflammation via Th17 cell regulation. *Journal of Clinical Investigation*, *127*(11), 3970–3986. <https://doi.org/10.1172/JCI95376>
- Conlon, M., & Bird, A. (2014). The Impact of Diet and Lifestyle on Gut Microbiota and Human Health. *Nutrients*, *7*(1), 17–44. <https://doi.org/10.3390/nu7010017>

- Coyne, M. J., & Comstock, L. E. (2008). Niche-Specific Features of the Intestinal *Bacteroidales*. *Journal of Bacteriology*, *190*(2), 736–742.  
<https://doi.org/10.1128/JB.01559-07>
- Crost, E. H., Coletto, E., Bell, A., & Juge, N. (2023). Ruminococcus gnavus: friend or foe for human health. *FEMS Microbiology Reviews*, *47*(2).  
<https://doi.org/10.1093/femsre/fuad014>
- Crost, E. H., Le Gall, G., Laverde-Gomez, J. A., Mukhopadhyaya, I., Flint, H. J., & Juge, N. (2018). Mechanistic insights into the cross-feeding of Ruminococcus gnavus and Ruminococcus bromii on host and dietary carbohydrates. *Frontiers in Microbiology*, *9*(NOV).  
<https://doi.org/10.3389/fmicb.2018.02558>
- Crost, E. H., Tailford, L. E., Le Gall, G., Fons, M., Henrissat, B., & Juge, N. (2013). Utilisation of Mucin Glycans by the Human Gut Symbiont Ruminococcus gnavus Is Strain-Dependent. *PLoS ONE*, *8*(10). <https://doi.org/10.1371/journal.pone.0076341>
- Crost, E. H., Tailford, L. E., Monestier, M., Swarbreck, D., Henrissat, B., Crossman, L. C., & Juge, N. (2016). The mucin-degradation strategy of Ruminococcus gnavus: The importance of intramolecular trans-sialidases. *Gut Microbes*, *7*(4), 302–312.  
<https://doi.org/10.1080/19490976.2016.1186334>
- Cui, X., Ye, L., Li, J., Jin, L., Wang, W., Li, S., Bao, M., Wu, S., Li, L., Geng, B., Zhou, X., Zhang, J., & Cai, J. (2018). Metagenomic and metabolomic analyses unveil dysbiosis of gut microbiota in chronic heart failure patients. *Scientific Reports*, *8*(1).  
<https://doi.org/10.1038/s41598-017-18756-2>
- Czabańska, A., Holst, O., & Duda, K. A. (2013). Chemical structures of the secondary cell wall polymers (SCWPs) isolated from bovine mastitis *Streptococcus uberis*. *Carbohydrate Research*, *377*, 58–62. <https://doi.org/10.1016/j.carres.2013.05.015>
- Danese, E., Ruzzenente, A., Montagnana, M., & Lievens, P. M.-J. (2018). Current and future roles of mucins in cholangiocarcinoma—recent evidences for a possible interplay with bile acids. *Annals of Translational Medicine*, *6*(17), 333–333.  
<https://doi.org/10.21037/atm.2018.07.16>
- de Filippis, F., Paparo, L., Nocerino, R., della Gatta, G., Carucci, L., Russo, R., Pasolli, E., Ercolini, D., & Berni Canani, R. (2021). Specific gut microbiome signatures and the associated pro-inflammatory functions are linked to pediatric allergy and acquisition of immune tolerance. *Nature Communications*, *12*(1). <https://doi.org/10.1038/s41467-021-26266-z>
- de Sousa, J. A. M., Buffet, A., Haudiquet, M., Rocha, E. P. C., & Rendueles, O. (2020). Modular prophage interactions driven by capsule serotype select for capsule loss under

phage predation. *ISME Journal*, 14(12), 2980–2996. <https://doi.org/10.1038/s41396-020-0726-z>

- De Weerd, N. A., Samarajiwa, S. A., & Hertzog, P. J. (2007). Type I interferon receptors: Biochemistry and biological functions. In *Journal of Biological Chemistry* (Vol. 282, Issue 28, pp. 20053–20057). American Society for Biochemistry and Molecular Biology Inc. <https://doi.org/10.1074/jbc.R700006200>
- Debyser, G., Mesuere, B., Clement, L., van de Weygaert, J., van Hecke, P., Duytschaever, G., Aerts, M., Dawyndt, P., de Boeck, K., Vandamme, P., & Devreese, B. (2016). Faecal proteomics: A tool to investigate dysbiosis and inflammation in patients with cystic fibrosis. *Journal of Cystic Fibrosis*, 15(2), 242–250. <https://doi.org/10.1016/j.jcf.2015.08.003>
- Decker, E., Engelmann, G., Findeisen, A., Gerner, P., Laaß, M., Ney, D., Posovszky, C., Hoy, L., & Hornef, M. W. (2010). Cesarean delivery is associated with celiac disease but not inflammatory bowel disease in children. *Pediatrics*, 125(6). <https://doi.org/10.1542/peds.2009-2260>
- Dertli, E., Colquhoun, I. J., Côté, G. L., Le Gall, G., & Narbad, A. (2018). Structural analysis of the  $\alpha$ -D-glucan produced by the sourdough isolate *Lactobacillus brevis* E25. *Food Chemistry*, 242, 45–52. <https://doi.org/10.1016/j.foodchem.2017.09.017>
- Dertli, E., Colquhoun, I. J., Gunning, A. P., Bongaerts, R. J., Le Gall, G., Bonev, B. B., Mayer, M. J., & Narbad, A. (2013). Structure and biosynthesis of two exopolysaccharides produced by *Lactobacillus johnsonii* FI9785. *Journal of Biological Chemistry*, 288(44), 31938–31951. <https://doi.org/10.1074/jbc.M113.507418>
- d’Hennezel, E., Abubucker, S., Murphy, L. O., & Cullen, T. W. (2017). Total Lipopolysaccharide from the Human Gut Microbiome Silences Toll-Like Receptor Signaling. *MSystems*, 2(6). <https://doi.org/10.1128/msystems.00046-17>
- Di Lorenzo, F., De Castro, C., Silipo, A., & Molinaro, A. (2019). Lipopolysaccharide structures of Gram-negative populations in the gut microbiota and effects on host interactions. In *FEMS Microbiology Reviews* (Vol. 43, Issue 3). Oxford University Press. <https://doi.org/10.1093/femsre/fuz002>
- Donaldson, G. P., Lee, S. M., & Mazmanian, S. K. (2016). Gut biogeography of the bacterial microbiota. *Nature Reviews Microbiology*, 14(1), 20–32. <https://doi.org/10.1038/nrmicro3552>
- Donia, M. S., Cimermanic, P., Schulze, C. J., Wieland Brown, L. C., Martin, J., Mitreva, M., Clardy, J., Linington, R. G., & Fischbach, M. A. (2014). A Systematic Analysis of

- Biosynthetic Gene Clusters in the Human Microbiome Reveals a Common Family of Antibiotics. *Cell*, 158(6), 1402–1414. <https://doi.org/10.1016/j.cell.2014.08.032>
- Drickamer, K., & Fadden, A. J. (2002). Genomic analysis of C-type lectins. *Biochemical Society Symposia*, 69(69), 59–72. <https://doi.org/10.1042/bss0690059>
- Duangnumsawang, Y., Zentek, J., & Goodarzi Boroojeni, F. (2021). Development and Functional Properties of Intestinal Mucus Layer in Poultry. In *Frontiers in Immunology* (Vol. 12). Frontiers Media S.A. <https://doi.org/10.3389/fimmu.2021.745849>
- Dupont, A., Heinbockel, L., Brandenburg, K., & Hornef, M. W. (2015). Antimicrobial peptides and the enteric mucus layer act in concert to protect the intestinal mucosa. *Gut Microbes*, 5(6), 761–765. <https://doi.org/10.4161/19490976.2014.972238>
- Ermund, A., Schütte, A., Johansson, M. E. V., Gustafsson, J. K., & Hansson, G. C. (2013). Studies of mucus in mouse stomach, small intestine, and colon. I. Gastrointestinal mucus layers have different properties depending on location as well as over the Peyer's patches. *American Journal of Physiology-Gastrointestinal and Liver Physiology*, 305(5), G341–G347. <https://doi.org/10.1152/ajpgi.00046.2013>
- Erttmann, S. F., Swacha, P., Aung, K. M., Brindefalk, B., Jiang, H., Härtlova, A., Uhlin, B. E., Wai, S. N., & Gekara, N. O. (2022). The gut microbiota prime systemic antiviral immunity via the cGAS-STING-IFN-I axis. *Immunity*, 55(5), 847–861.e10. <https://doi.org/10.1016/j.immuni.2022.04.006>
- Erturk-Hasdemir, D., Oh, S. F., Okan, N. A., Stefanetti, G., Gazzaniga, F. S., Seeberger, P. H., Plevy, S. E., & Kasper, D. L. (2019). Symbionts exploit complex signaling to educate the immune system. *Proceedings of the National Academy of Sciences*, 116(52), 26157–26166. <https://doi.org/10.1073/pnas.1915978116>
- Estorninos, E., Lawenko, R. B., Palestroque, E., Lebumfacil, J., Marko, M., & Cercamondi, C. I. (2021). Infant formula containing bovine milk-derived oligosaccharides supports age-appropriate growth and improves stooling pattern. *Pediatric Research*. <https://doi.org/10.1038/s41390-021-01541-3>
- Etienne-Mesmin, L., Chassaing, B., Desvaux, M., de Paepe, K., Gresse, R., Sauvaitre, T., Forano, E., de Wiele, T. van, Schüller, S., Juge, N., & Blanquet-Diot, S. (2019). Experimental models to study intestinal microbes–mucus interactions in health and disease. *FEMS Microbiology Reviews*, 43(5), 457–489. <https://doi.org/10.1093/femsre/fuz013>
- Ewaschuk, J. B., Diaz, H., Meddings, L., Diederichs, B., Dmytrash, A., Backer, J., Langen, M. L. Van, & Madsen, K. L. (2008). Secreted bioactive factors from *Bifidobacterium infantis* enhance epithelial cell barrier function. *American Journal of Physiology* -

- Gastrointestinal and Liver Physiology*, 295(5).  
<https://doi.org/10.1152/ajpgi.90227.2008>
- Fang, J., Wang, H., Zhou, Y., Zhang, H., Zhou, H., & Zhang, X. (2021). Slimy partners: the mucus barrier and gut microbiome in ulcerative colitis. *Experimental & Molecular Medicine*, 53(5), 772–787. <https://doi.org/10.1038/s12276-021-00617-8>
- Fanning, S., Hall, L. J., Cronin, M., Zomer, A., MacSharry, J., Goulding, D., Motherway, M. O. C., Shanahan, F., Nally, K., Dougan, G., & Van Sinderen, D. (2012). Bifidobacterial surface-exopolysaccharide facilitates commensal-host interaction through immune modulation and pathogen protection. *Proceedings of the National Academy of Sciences of the United States of America*, 109(6), 2108–2113.  
<https://doi.org/10.1073/pnas.1115621109>
- Fanning, S., Hall, L. J., & van Sinderen, D. (2012). Bifidobacterium breve UCC2003 surface exopolysaccharide production is a beneficial trait mediating commensal-host interaction through immune modulation and pathogen protection. *Gut Microbes*, 3(5), 420–425. <https://doi.org/10.4161/gmic.20630>
- Fekete, E., & Buret, A. G. (2023). The role of mucin O-glycans in microbiota dysbiosis, intestinal homeostasis, and host-pathogen interactions. *American Journal of Physiology-Gastrointestinal and Liver Physiology*, 324(6), G452–G465.  
<https://doi.org/10.1152/ajpgi.00261.2022>
- Feldman, G. J., Mullin, J. M., & Ryan, M. P. (2005). Occludin: Structure, function and regulation. In *Advanced Drug Delivery Reviews* (Vol. 57, Issue 6, pp. 883–917). Elsevier.  
<https://doi.org/10.1016/j.addr.2005.01.009>
- Ferrario, C., Milani, C., Mancabelli, L., Lugli, G. A., Duranti, S., Mangifesta, M., Viappiani, A., Turrone, F., Margolles, A., Ruas-Madiedo, P., Sinderen, D. van, & Ventura, M. (2016). Modulation of the eps-ome transcription of bifidobacteria through simulation of human intestinal environment. *FEMS Microbiology Ecology*, 92(4), 1–12.  
<https://doi.org/10.1093/femsec/fiw056>
- Ford, S. L., Lohmann, P., Preidis, G. A., Gordon, P. S., O'Donnell, A., Hagan, J., Venkatachalam, A., Balderas, M., Luna, R. A., & Hair, A. B. (2019). Improved feeding tolerance and growth are linked to increased gut microbial community diversity in very-low-birth-weight infants fed mother's own milk compared with donor breast milk. *American Journal of Clinical Nutrition*, 109(4), 1088–1097.  
<https://doi.org/10.1093/ajcn/nqz006>
- Francesca Restaino, O., di Lauro, I., Di Nuzzo, R., De Rosa, M., & Schiraldi, C. (2017). New insight into chondroitin and heparosan-like capsular polysaccharide synthesis by

profiling of the nucleotide sugar precursors. *Bioscience Reports*.  
<https://doi.org/10.1042/BSR20160548>

- Friedman, E. S., Bittinger, K., Esipova, T. V., Hou, L., Chau, L., Jiang, J., Mesaros, C., Lund, P. J., Liang, X., FitzGerald, G. A., Goulian, M., Lee, D., Garcia, B. A., Blair, I. A., Vinogradov, S. A., & Wu, G. D. (2018). Microbes vs. chemistry in the origin of the anaerobic gut lumen. *Proceedings of the National Academy of Sciences of the United States of America*, *115*(16), 4170–4175. <https://doi.org/10.1073/pnas.1718635115>
- Fu, C., Zhao, H., Wang, Y., Cai, H., Xiao, Y., Zeng, Y., & Chen, H. (2016). Tumor-associated antigens: Tn antigen,  $\alpha$ -Tn antigen, and T antigen. *HLA*, *88*(6), 275–286. <https://doi.org/10.1111/tan.12900>
- Gaisawat, M. B., Lopez-Escalera, S., MacPherson, C. W., Iskandar, M. M., Tompkins, T. A., & Kubow, S. (2022). Probiotics Exhibit Strain-Specific Protective Effects in T84 Cells Challenged With *Clostridioides difficile*-Infected Fecal Water. *Frontiers in Microbiology*, *12*. <https://doi.org/10.3389/fmicb.2021.698638>
- Garcia-Vello, P., Di Lorenzo, F., Zucchetta, D., Zamyatina, A., De Castro, C., & Molinaro, A. (2022). Lipopolysaccharide lipid A: A promising molecule for new immunity-based therapies and antibiotics. In *Pharmacology and Therapeutics* (Vol. 230). Elsevier Inc. <https://doi.org/10.1016/j.pharmthera.2021.107970>
- Geijtenbeek, T. B. H., Groot, P. C., Nolte, M. A., Van Vliet, S. J., Gangaram-Panday, S. T., Van Duijnhoven, G. C. F., Kraal, G., Van Oosterhout, A. J. M., & Van Kooyk, Y. (2002). Marginal zone macrophages express a murine homologue of DC-SIGN that captures blood-borne antigens in vivo. *Blood*, *100*(8), 2908–2916. <https://doi.org/10.1182/blood-2002-04-1044>
- Geijtenbeek, T. B. H., Torensma, R., van Vliet, S. J., van Duijnhoven, G. C. F., Adema, G. J., van Kooyk, Y., & Figdor, C. G. (2000). Identification of DC-SIGN, a Novel Dendritic Cell-Specific ICAM-3 Receptor that Supports Primary Immune Responses efficient T cell activation (Hernandez-Caselles et al., 1993). Indeed, antibody engagement of ICAM-3 results in elevation of intracellular calcium levels and induction of tyrosine phosphorylation (Juan et al The 2 integrins LFA-1 (L2) and D2 have both. In *Cell* (Vol. 100).
- Gerbe, F., Sidot, E., Smyth, D. J., Ohmoto, M., Matsumoto, I., Dardalhon, V., Cesses, P., Garnier, L., Pouzolles, M., Brulin, B., Bruschi, M., Harcus, Y., Zimmermann, V. S., Taylor, N., Maizels, R. M., & Jay, P. (2016). Intestinal epithelial tuft cells initiate type 2 mucosal immunity to helminth parasites. *Nature*, *529*(7585), 226–230. <https://doi.org/10.1038/nature16527>

- Ghosh, S., Whitley, C. S., Haribabu, B., & Jala, V. R. (2021). Regulation of Intestinal Barrier Function by Microbial Metabolites. In *CMGH* (Vol. 11, Issue 5, pp. 1463–1482). Elsevier Inc. <https://doi.org/10.1016/j.jcmgh.2021.02.007>
- Grabinger, T., Garzon, J. F. G., Hausmann, M., Geirnaert, A., Lacroix, C., & Hennet, T. (2019). Alleviation of intestinal inflammation by oral supplementation with 2-fucosyllactose in mice. *Frontiers in Microbiology*, *10*(JUN), 1–14. <https://doi.org/10.3389/fmicb.2019.01385>
- Graham, L. M., & Brown, G. D. (2009). The Dectin-2 family of C-type lectins in immunity and homeostasis. In *Cytokine* (Vol. 48, Issues 1–2, pp. 148–155). <https://doi.org/10.1016/j.cyto.2009.07.010>
- Grahnmemo, L., Nethander, M., Coward, E., Gabrielsen, M. E., Sree, S., Billod, J.-M., Engstrand, L., Abrahamsson, S., Langhammer, A., Hveem, K., & Ohlsson, C. (2022). Cross-sectional associations between the gut microbe *Ruminococcus gnavus* and features of the metabolic syndrome: the HUNT study. *The Lancet Diabetes & Endocrinology*, *10*(7), 481–483. [https://doi.org/10.1016/S2213-8587\(22\)00113-9](https://doi.org/10.1016/S2213-8587(22)00113-9)
- Graziani, F., Pujol, A., Nicoletti, C., Dou, S., Maresca, M., Giardina, T., Fons, M., & Perrier, J. (2016). *Ruminococcus gnavus* E1 modulates mucin expression and intestinal glycosylation. *Journal of Applied Microbiology*, *120*(5), 1403–1417. <https://doi.org/10.1111/jam.13095>
- Gribble, F. M., & Reimann, F. (2019). Function and mechanisms of enteroendocrine cells and gut hormones in metabolism. In *Nature Reviews Endocrinology* (Vol. 15, Issue 4, pp. 226–237). Nature Publishing Group. <https://doi.org/10.1038/s41574-019-0168-8>
- Grondin, J. A., Kwon, Y. H., Far, P. M., Haq, S., & Khan, W. I. (2020). Mucins in Intestinal Mucosal Defense and Inflammation: Learning From Clinical and Experimental Studies. *Frontiers in Immunology*, *11*. <https://doi.org/10.3389/fimmu.2020.02054>
- Habu, Y., Nagaoka, M., Yokokura, T., & Azuma, I. (1987). Structural Studies of Cell Wall Polysaccharides from *Bifidobacterium breve* YIT 4010 and Related *Bifidobacterium* Species 1. In *J. Biochem* (Vol. 102, Issue 6).
- Håkansson, S., & Källén, K. (2003). Caesarean section increases the risk of hospital care in childhood for asthma and gastroenteritis. *Clinical and Experimental Allergy*, *33*(6), 757–764. <https://doi.org/10.1046/j.1365-2222.2003.01667.x>
- Hall, A. B., Yassour, M., Sauk, J., Garner, A., Jiang, X., Arthur, T., Lagoudas, G. K., Vatanen, T., Fornelos, N., Wilson, R., Bertha, M., Cohen, M., Garber, J., Khalili, H., Gevers, D., Ananthakrishnan, A. N., Kugathasan, S., Lander, E. S., Blainey, P., ... Huttenhower, C.

- (2017). A novel *Ruminococcus gnavus* clade enriched in inflammatory bowel disease patients. *Genome Medicine*, 9(1), 1–12. <https://doi.org/10.1186/s13073-017-0490-5>
- Han, D., Walsh, M. C., Cejas, P. J., Dang, N. N., Kim, Y. F., Kim, J., Charrier-Hisamuddin, L., Chau, L., Zhang, Q., Bittinger, K., Bushman, F. D., Turka, L. A., Shen, H., Reizis, B., DeFranco, A. L., Wu, G. D., & Choi, Y. (2013). Dendritic Cell Expression of the Signaling Molecule TRAF6 Is Critical for Gut Microbiota-Dependent Immune Tolerance. *Immunity*, 38(6), 1211–1222. <https://doi.org/10.1016/j.immuni.2013.05.012>
- Hansson, G. C. (2020). Mucins and the Microbiome. In *Annual Review of Biochemistry* (Vol. 89, pp. 769–793). Annual Reviews Inc. <https://doi.org/10.1146/annurev-biochem-011520-105053>
- Harrison, O. J., & Powrie, F. M. (2013). Regulatory T cells and immune tolerance in the intestine. *Cold Spring Harbor Perspectives in Biology*, 5(7). <https://doi.org/10.1101/cshperspect.a018341>
- Hashimoto, M., Kirikae, F., Dohi, T., Kusumoto, S., Suda, Y., & Kirikae, T. (2001). Structural elucidation of a capsular polysaccharide from a clinical isolate of *Bacteroides vulgatus* from a patient with Crohn's disease. *European Journal of Biochemistry*, 268(11), 3139–3144. <https://doi.org/10.1046/j.1432-1327.2001.02147.x>
- Haynie, T., Gubler, S., Drees, C., Heaton, T., Mitton, T., Gleave, Q., Bendelac, A., Deng, S., & Savage, P. B. (2021). Synthesis of the pentasaccharide repeating unit from: *Ruminococcus gnavus* and measurement of its inflammatory properties. *RSC Advances*, 11(24), 14357–14361. <https://doi.org/10.1039/d1ra01918j>
- Heinemann, U., & Schuetz, A. (2019). Structural features of tight-junction proteins. In *International Journal of Molecular Sciences* (Vol. 20, Issue 23). MDPI AG. <https://doi.org/10.3390/ijms20236020>
- Henke, M. T., Brown, E. M., Cassilly, C. D., Vlamakis, H., Xavier, R. J., & Clardy, J. (n.d.). *Capsular polysaccharide correlates with immune response to the human gut microbe Ruminococcus gnavus*. <https://doi.org/10.1073/pnas.2007595118/-/DCSupplemental>
- Henke, M. T., Brown, E. M., Cassilly, C. D., Vlamakis, H., Xavier, R. J., & Clardy, J. (2021). Capsular polysaccharide correlates with immune response to the human gut microbe *Ruminococcus gnavus*. *Proceedings of the National Academy of Sciences*, 118(20). <https://doi.org/10.1073/pnas.2007595118>
- Henke, M. T., Kenny, D. J., Cassilly, C. D., Vlamakis, H., Xavier, R. J., & Clardy, J. (2019). *Ruminococcus gnavus*, a member of the human gut microbiome associated with Crohn's disease, produces an inflammatory polysaccharide. *Proceedings of the National*

*Academy of Sciences of the United States of America*, 116(26), 12672–12677.

<https://doi.org/10.1073/pnas.1904099116>

Henrick, B. M., Rodriguez, L., Lakshmikanth, T., Pou, C., Henckel, E., Arzoomand, A., Olin, A., Wang, J., Mikes, J., Tan, Z., Chen, Y., Ehrlich, A. M., Bernhardsson, A. K., Mugabo, C. H., Ambrosiani, Y., Gustafsson, A., Chew, S., Brown, H. K., Pramps, J., ... Brodin, P. (2021). Bifidobacteria-mediated immune system imprinting early in life. *Cell*, 184(15), 3884-3898.e11. <https://doi.org/10.1016/j.cell.2021.05.030>

Hidalgo-Cantabrana, C., López, P., Gueimonde, M., de los Reyes-Gavilán, C. G., Suárez, A., Margolles, A., & Ruas-Madiedo, P. (2012). Immune Modulation Capability of Exopolysaccharides Synthesised by Lactic Acid Bacteria and Bifidobacteria. *Probiotics and Antimicrobial Proteins*, 4(4), 227–237. <https://doi.org/10.1007/s12602-012-9110-2>

Hidalgo-Cantabrana, C., Nikolic, M., López, P., Suárez, A., Miljkovic, M., Kojic, M., Margolles, A., Golic, N., & Ruas-Madiedo, P. (2014). Exopolysaccharide-producing Bifidobacterium animalis subsp. lactis strains and their polymers elicit different responses on immune cells from blood and gut associated lymphoid tissue. *Anaerobe*, 26, 24–30. <https://doi.org/10.1016/j.anaerobe.2014.01.003>

Hidalgo-Cantabrana, C., Sánchez, B., Milani, C., Ventura, M., Margolles, A., & Ruas-Madiedo, P. (2014). Genomic overview and biological functions of exopolysaccharide biosynthesis in bifidobacterium spp. *Applied and Environmental Microbiology*, 80(1), 9–18. <https://doi.org/10.1128/AEM.02977-13>

Hlozek, J., Ravenscroft, N., & Kuttel, M. M. (2020). Effects of Glucosylation and O-Acetylation on the Conformation of Shigella flexneri Serogroup 2 O-Antigen Vaccine Targets. *Journal of Physical Chemistry B*, 124(14), 2806–2814. <https://doi.org/10.1021/acs.jpccb.0c01595>

Hoces, D., Greter, G., Arnoldini, M., Stäubli, M. L., Moresi, C., Sintsova, A., Berent, S., Kolinko, I., Bansept, F., Woller, A., Häfliger, J., Martens, E., Hardt, W. D., Sunawaga, S., Loverdo, C., & Slack, E. (2023). Fitness advantage of Bacteroides thetaiotaomicron capsular polysaccharide in the mouse gut depends on the resident microbiota. *ELife*, 12. <https://doi.org/10.7554/eLife.81212>

Hoskins, L. C., Agustines, M., Mckee, W. B., Boulding, E. T., Krians, M., & Niedermeyer, G. (1985). Mucin Degradation in Human Colon Ecosystems Isolation and Properties of Fecal Strains that Degrade ABH Blood Group Antigens and Oligosaccharides from Mucin Glycoproteins. In *J. Clin. Invest* (Vol. 75).

Hsieh, S. A., & Allen, P. M. (2020). Immunomodulatory Roles of Polysaccharide Capsules in the Intestine. In *Frontiers in Immunology* (Vol. 11). Frontiers Media S.A. <https://doi.org/10.3389/fimmu.2020.00690>

- Hsieh, S. A., Donermeyer, D. L., Horvath, S. C., & Allen, P. M. (2021). Phase-variable bacteria simultaneously express multiple capsules. *Microbiology (United Kingdom)*, 167(7). <https://doi.org/10.1099/MIC.0.001066>
- Hsieh, S., Porter, N. T., Donermeyer, D. L., Horvath, S., Strout, G., Saunders, B. T., Zhang, N., Zinselmeyer, B., Martens, E. C., Stappenbeck, T. S., & Allen, P. M. (2020). Polysaccharide Capsules Equip the Human Symbiont *Bacteroides thetaiotaomicron* to Modulate Immune Responses to a Dominant Antigen in the Intestine. *The Journal of Immunology*, 204(4), 1035–1046. <https://doi.org/10.4049/jimmunol.1901206>
- Ifrim, D. C., Quintin, J., Courjol, F., Verschuere, I., van Krieken, J. H., Koentgen, F., Fradin, C., Gow, N. A. R., Joosten, L. A. B., van der Meer, J. W. M., van de Veerdonk, F., & Netea, M. G. (2016). The Role of Dectin-2 for Host Defense Against Disseminated Candidiasis. *Journal of Interferon and Cytokine Research*, 36(4), 267–276. <https://doi.org/10.1089/jir.2015.0040>
- Iliev, I. D., Funari, V. A., Taylor, K. D., Nguyen, Q., Reyes, C. N., Strom, S. P., Brown, J., Becker, C. A., Fleshner, P. R., Dubinsky, M., Rotter, J. I., Wang, H. L., McGovern, D. P. B., Brown, G. D., & Underhill, D. M. (2012). Interactions between commensal fungi and the C-type lectin receptor dectin-1 influence colitis. *Science*, 336(6086), 1314–1317. <https://doi.org/10.1126/science.1221789>
- Inturri, R., Molinaro, A., Di Lorenzo, F., Blandino, G., Tomasello, B., Hidalgo-Cantabrana, C., De Castro, C., & Ruas-Madiedo, P. (2017). Chemical and biological properties of the novel exopolysaccharide produced by a probiotic strain of *Bifidobacterium longum*. *Carbohydrate Polymers*, 174, 1172–1180. <https://doi.org/10.1016/j.carbpol.2017.07.039>
- Jairath, V., & Feagan, B. G. (2020). Global burden of inflammatory bowel disease. In *The Lancet Gastroenterology and Hepatology* (Vol. 5, Issue 1, pp. 2–3). Elsevier Ltd. [https://doi.org/10.1016/S2468-1253\(19\)30358-9](https://doi.org/10.1016/S2468-1253(19)30358-9)
- Jakobsson, H. E., Abrahamsson, T. R., Jenmalm, M. C., Harris, K., Quince, C., Jernberg, C., Björkstén, B., Engstrand, L., & Andersson, A. F. (2014). Decreased gut microbiota diversity, delayed *Bacteroidetes* colonisation and reduced Th1 responses in infants delivered by Caesarean section. *Gut*, 63(4), 559–566. <https://doi.org/10.1136/gutjnl-2012-303249>
- James, K. R., Gomes, T., Elmentaite, R., Kumar, N., Gulliver, E. L., King, H. W., Stares, M. D., Bareham, B. R., Ferdinand, J. R., Petrova, V. N., Polański, K., Forster, S. C., Jarvis, L. B., Suchanek, O., Howlett, S., James, L. K., Jones, J. L., Meyer, K. B., Clatworthy, M. R., ... Teichmann, S. A. (2020). Distinct microbial and immune niches of the human colon. *Nature Immunology*, 21(3), 343–353. <https://doi.org/10.1038/s41590-020-0602-z>

- Jarvis, C. M., Zwick, D. B., Grim, J. C., Alam, M. M., Prost, L. R., Gardiner, J. C., Park, S., Zimdars, L. L., Sherer, N. M., & Kiessling, L. L. (2019). Antigen structure affects cellular routing through DC-SIGN. *Proceedings of the National Academy of Sciences of the United States of America*, *116*(30), 14862–14867. <https://doi.org/10.1073/pnas.1820165116>
- Jiang, H. yin, Zhang, X., Yu, Z. he, Zhang, Z., Deng, M., Zhao, J. hua, & Ruan, B. (2018). Altered gut microbiota profile in patients with generalized anxiety disorder. *Journal of Psychiatric Research*, *104*, 130–136. <https://doi.org/10.1016/j.jpsychires.2018.07.007>
- Johansson, M. E. V., Jakobsson, H. E., Holmén-Larsson, J., Schütte, A., Ermund, A., Rodríguez-Piñeiro, A. M., Arike, L., Wising, C., Svensson, F., Bäckhed, F., & Hansson, G. C. (2015). Normalization of host intestinal mucus layers requires long-term microbial colonization. *Cell Host and Microbe*, *18*(5), 582–592. <https://doi.org/10.1016/j.chom.2015.10.007>
- Johansson, M. E. V., Phillipson, M., Petersson, J., Velcich, A., Holm, L., & Hansson, G. C. (2008). The inner of the two Muc2 mucin-dependent mucus layers in colon is devoid of bacteria. *Proceedings of the National Academy of Sciences of the United States of America*, *105*(39), 15064–15069. <https://doi.org/10.1073/pnas.0803124105>
- Juge, N. (2022). Relationship between mucosa-associated gut microbiota and human diseases. In *Biochemical Society Transactions* (Vol. 50, Issue 5, pp. 1225–1236). Portland Press Ltd. <https://doi.org/10.1042/BST20201201>
- Kalia, N., Singh, J., & Kaur, M. (2021). The role of dectin-1 in health and disease. In *Immunobiology* (Vol. 226, Issue 2). Elsevier GmbH. <https://doi.org/10.1016/j.imbio.2021.152071>
- Kaminsky, L. W., Al-Sadi, R., & Ma, T. Y. (2021). IL-1 $\beta$  and the Intestinal Epithelial Tight Junction Barrier. In *Frontiers in Immunology* (Vol. 12). Frontiers Media S.A. <https://doi.org/10.3389/fimmu.2021.767456>
- Kaoutari, A. el, Armougom, F., Gordon, J. I., Raoult, D., & Henrissat, B. (2013). The abundance and variety of carbohydrate-active enzymes in the human gut microbiota. *Nature Reviews Microbiology*, *11*(7), 497–504. <https://doi.org/10.1038/nrmicro3050>
- Karczewski, J., Troost, F. J., Konings, I., Dekker, J., Kleerebezem, M., Brummer, R.-J. M., & Wells, J. M. (2010a). Regulation of human epithelial tight junction proteins by *Lactobacillus plantarum* in vivo and protective effects on the epithelial barrier. *Am J Physiol Gastrointest Liver Physiol*, *298*, 851–859. <https://doi.org/10.1152/ajpgi.00327.2009>-Lactobacillus

- Karczewski, J., Troost, F. J., Konings, I., Dekker, J., Kleerebezem, M., Brummer, R.-J. M., & Wells, J. M. (2010b). Regulation of human epithelial tight junction proteins by *Lactobacillus plantarum* in vivo and protective effects on the epithelial barrier. *Am J Physiol Gastrointest Liver Physiol*, *298*, 851–859. <https://doi.org/10.1152/ajpgi.00327.2009.-Lactobacillus>
- Kaur, H., & Ali, S. A. (2022). Probiotics and gut microbiota: mechanistic insights into gut immune homeostasis through TLR pathway regulation. *Food & Function*, *13*(14), 7423–7447. <https://doi.org/10.1039/D2FO00911K>
- Kawai, T., & Akira, S. (2010). The role of pattern-recognition receptors in innate immunity: Update on toll-like receptors. In *Nature Immunology* (Vol. 11, Issue 5, pp. 373–384). <https://doi.org/10.1038/ni.1863>
- Kayama, H., Okumura, R., & Takeda, K. (2020). Interaction Between the Microbiota, Epithelia, and Immune Cells in the Intestine. *IY38CHO2\_Takeda ARjats.Cls April*, *5*. <https://doi.org/10.1146/annurev-immunol-070119>
- Kim, J. W., Kwok, S. K., Choe, J. Y., & Park, S. H. (2019). Recent advances in our understanding of the link between the intestinal microbiota and systemic lupus erythematosus. In *International Journal of Molecular Sciences* (Vol. 20, Issue 19). MDPI AG. <https://doi.org/10.3390/ijms20194871>
- Kim, Y. J., Lee, J. Y., Lee, J. J., Jeon, S. M., Silwal, P., Kim, I. S., Kim, H. J., Park, C. R., Chung, C., Han, J. E., Choi, J. W., Tak, E. J., Yoo, J. H., Jeong, S. W., Kim, D. Y., Ketphan, W., Kim, S. Y., Jhun, B. W., Whang, J., ... Jo, E. K. (2022). Arginine-mediated gut microbiome remodeling promotes host pulmonary immune defense against nontuberculous mycobacterial infection. *Gut Microbes*, *14*(1). <https://doi.org/10.1080/19490976.2022.2073132>
- King, H., Castro, S. A., Pohane, A. A., Scholte, C. M., Fischetti, V. A., Korotkova, N., Nelson, D. C., & Dorfmueller, H. C. (2021). Molecular basis for recognition of the Group A Carbohydrate backbone by the PlyC streptococcal bacteriophage endolysin. *Biochemical Journal*, *478*(12), 2385–2397. <https://doi.org/10.1042/BCJ20210158>
- Kint, N., Feliciano, C. A., Martins, M. C., Morvan, C., Fernandes, S. F., Folgosa, F., Dupuy, B., Texeira, M., & Martin-Verstraete, I. (2020). *How the Anaerobic Enteropathogen Clostridioides difficile Tolerates Low O<sub>2</sub> Tensions*. <https://doi.org/10.1128/mBio>
- Klingbeil, E., & de La Serre, C. B. (2018). Microbiota modulation by eating patterns and diet composition: impact on food intake. *American Journal of Physiology-Regulatory, Integrative and Comparative Physiology*, *315*(6), R1254–R1260. <https://doi.org/10.1152/ajpregu.00037.2018>

- Knoop, K. A., McDonald, K. G., McCrate, S., McDole, J. R., & Newberry, R. D. (2015). Microbial sensing by goblet cells controls immune surveillance of luminal antigens in the colon. *Mucosal Immunology*, 8(1), 198–210. <https://doi.org/10.1038/mi.2014.58>
- Knoop, K. A., & Newberry, R. D. (2018). Goblet cells: multifaceted players in immunity at mucosal surfaces. In *Mucosal Immunology* (Vol. 11, Issue 6, pp. 1551–1557). Nature Publishing Group. <https://doi.org/10.1038/s41385-018-0039-y>
- Kogut, M. H., Lee, A., & Santin, E. (2020). Microbiome and pathogen interaction with the immune system. *Poultry Science*, 99(4), 1906–1913. <https://doi.org/10.1016/j.psj.2019.12.011>
- Konieczna, P., Schiavi, E., Ziegler, M., Groeger, D., Healy, S., Grant, R., & O'Mahony, L. (2015). Human dendritic cell DC-SIGN and TLR-2 mediate complementary immune regulatory activities in response to *Lactobacillus rhamnosus* JB-1. *PLoS ONE*, 10(3). <https://doi.org/10.1371/journal.pone.0120261>
- Koropatkin, N. M., Cameron, E. A., & Martens, E. C. (2012). How glycan metabolism shapes the human gut microbiota. *Nature Reviews Microbiology*, 10(5), 323–335. <https://doi.org/10.1038/nrmicro2746>
- Kraal, L., Abubucker, S., Kota, K., Fischbach, M. A., & Mitreva, M. (2014). The prevalence of species and strains in the human microbiome: A resource for experimental efforts. *PLoS ONE*, 9(5). <https://doi.org/10.1371/journal.pone.0097279>
- Kšonžeková, P., Bystrický, P., Vlčková, S., Pätoprstý, V., Pulzová, L., Mudroňová, D., Kubašková, T., Csank, T., & Tkáčiková, L. (2016). Exopolysaccharides of *Lactobacillus reuteri*: Their influence on adherence of *E. coli* to epithelial cells and inflammatory response. *Carbohydrate Polymers*, 141, 10–19. <https://doi.org/10.1016/j.carbpol.2015.12.037>
- Kulshin, V. A., Zahringer, U., Lindner, B., Frasch, C. E., Tsai, C.-M., Dmitriev, B. A., & Rietschel, E. T. (1992). Structural Characterization of the Lipid A Component of Pathogenic *Neisseria meningitidis*. Downloaded from. In *JOURNAL OF BACTERIOLOGY* (Vol. 174, Issue 6). <http://jb.asm.org/>
- Kumar, A., Kumar Hinge, V., Venugopal, A., Kumar Nadimpalli, S., & Rao, P. (n.d.). *Lectins-glycoconjugates interactions: Experimental and computational docking studies of the binding and agglutination of eight different lectins in a comparative manner*. <https://doi.org/10.1101/2020.05.01.070102>
- Kuo, W. T., Odenwald, M. A., Turner, J. R., & Zuo, L. (2022). Tight junction proteins occludin and ZO-1 as regulators of epithelial proliferation and survival. *Annals of the New York Academy of Sciences*, 1514(1), 21–33. <https://doi.org/10.1111/nyas.14798>

- La Rosa, S. L., Ostrowski, M. P., Vera-Ponce de León, A., McKee, L. S., Larsbrink, J., Eijsink, V. G., Lowe, E. C., Martens, E. C., & Pope, P. B. (2022). Glycan processing in gut microbiomes. In *Current Opinion in Microbiology* (Vol. 67). Elsevier Ltd. <https://doi.org/10.1016/j.mib.2022.102143>
- Lagkouvardos, I., Intze, E., Schaubeck, M., Rooney, J. P., Hecht, C., Piloquet, H., & Clavel, T. (2023). Early life gut microbiota profiles linked to synbiotic formula effects: a randomized clinical trial in European infants. *The American Journal of Clinical Nutrition*, *117*(2), 326–339. <https://doi.org/10.1016/j.ajcnut.2022.11.012>
- Lai, Y., Di Nardo, A., Nakatsuji, T., Leichtle, A., Yang, Y., Cogen, A. L., Wu, Z. R., Hooper, L. V., Schmidt, R. R., Von Aulock, S., Radek, K. A., Huang, C. M., Ryan, A. F., & Gallo, R. L. (2009). Commensal bacteria regulate toll-like receptor 3-dependent inflammation after skin injury. *Nature Medicine*, *15*(12), 1377–1382. <https://doi.org/10.1038/nm.2062>
- Lamprinaki, D., Beasy, G., Zhekova, A., Wittmann, A., James, S., Dicks, J., Iwakura, Y., Saijo, S., Wang, X., Chow, C. W., Roberts, I., Korcsmaros, T., Mayer, U., Wileman, T., & Kawasaki, N. (2017). LC3-associated phagocytosis is required for dendritic cell inflammatory cytokine response to gut commensal yeast *Saccharomyces cerevisiae*. *Frontiers in Immunology*, *8*(OCT). <https://doi.org/10.3389/fimmu.2017.01397>
- Larsson, J. M. H., Karlsson, H., Sjövall, H., & Hansson, G. C. (2009). A complex, but uniform O-glycosylation of the human MUC2 mucin from colonic biopsies analyzed by nanoLC/MSn. *Glycobiology*, *19*(7), 756–766. <https://doi.org/10.1093/glycob/cwp048>
- Lawson, M. A. E., O'Neill, I. J., Kujawska, M., Gowrinadh Javvadi, S., Wijeyesekera, A., Flegg, Z., Chalklen, L., & Hall, L. J. (2020). Breast milk-derived human milk oligosaccharides promote *Bifidobacterium* interactions within a single ecosystem. *The ISME Journal*, *14*(2), 635–648. <https://doi.org/10.1038/s41396-019-0553-2>
- Leal, J., Smyth, H. D. C., & Ghosh, D. (2017). Physicochemical properties of mucus and their impact on transmucosal drug delivery. In *International Journal of Pharmaceutics* (Vol. 532, Issue 1, pp. 555–572). Elsevier B.V. <https://doi.org/10.1016/j.ijpharm.2017.09.018>
- Lee, B., Moon, K. M., & Kim, C. Y. (2018). Tight junction in the intestinal epithelium: Its association with diseases and regulation by phytochemicals. In *Journal of Immunology Research* (Vol. 2018). Hindawi Limited. <https://doi.org/10.1155/2018/2645465>
- Lee, K., Kim, H. J., Kim, S. A., Park, S. D., Shim, J. J., & Lee, J. L. (2021). Exopolysaccharide from *Lactobacillus plantarum* hy7714 protects against skin aging through skin–gut axis communication. *Molecules*, *26*(6). <https://doi.org/10.3390/molecules26061651>

- Leedham, S. J., Brittan, M., McDonald, S. A. C., & Wright, N. A. (2005). Intestinal stem cells. *Journal of Cellular and Molecular Medicine*, 9(1), 11–24. <https://doi.org/10.1111/j.1582-4934.2005.tb00333.x>
- Leitner, G. R., Wenzel, T. J., Marshall, N., Gates, E. J., & Klegeris, A. (2019). Targeting toll-like receptor 4 to modulate neuroinflammation in central nervous system disorders. In *Expert Opinion on Therapeutic Targets* (Vol. 23, Issue 10, pp. 865–882). Taylor and Francis Ltd. <https://doi.org/10.1080/14728222.2019.1676416>
- Levy, M., Blacher, E., & Elinav, E. (2017). Microbiome, metabolites and host immunity. *Current Opinion in Microbiology*, 35, 8–15. <https://doi.org/10.1016/j.mib.2016.10.003>
- Li, M., Zhang, R., Li, J., & Li, J. (2022). The Role of C-Type Lectin Receptor Signaling in the Intestinal Microbiota-Inflammation-Cancer Axis. In *Frontiers in Immunology* (Vol. 13). Frontiers Media S.A. <https://doi.org/10.3389/fimmu.2022.894445>
- Li, T.-H., Liu, L., Hou, Y.-Y., Shen, S.-N., & Wang, T.-T. (2019). C-type lectin receptor-mediated immune recognition and response of the microbiota in the gut. *Gastroenterology Report*, 7(5), 312–321. <https://doi.org/10.1093/gastro/goz028>
- Liao, D. H., Zhao, J. B., & Gregersen, H. (2009). Gastrointestinal tract modelling in health and disease. In *World Journal of Gastroenterology* (Vol. 15, Issue 2, pp. 169–176). Baishideng Publishing Group Co. <https://doi.org/10.3748/wjg.15.169>
- Liévin-Le Moal, V., & Servin, A. L. (2013). Pathogenesis of Human Enterovirulent Bacteria: Lessons from Cultured, Fully Differentiated Human Colon Cancer Cell Lines. *Microbiology and Molecular Biology Reviews*, 77(3), 380–439. <https://doi.org/10.1128/mnbr.00064-12>
- Ling, Z., Liu, X., Cheng, Y., Yan, X., & Wu, S. (2022). Gut microbiota and aging. In *Critical Reviews in Food Science and Nutrition* (Vol. 62, Issue 13, pp. 3509–3534). Taylor and Francis Ltd. <https://doi.org/10.1080/10408398.2020.1867054>
- Liu, L. S., Firman, J., Tanes, C., Bittinger, K., Thomas-Gahring, A., Wu, G. D., Van den Abbeele, P., & Tomasula, P. M. (2018). Establishing a mucosal gut microbial community in vitro using an artificial simulator. *PLoS ONE*, 13(7). <https://doi.org/10.1371/journal.pone.0197692>
- Liu, Q., Yu, Z., Tian, F., Zhao, J., Zhang, H., Zhai, Q., & Chen, W. (2020). Surface components and metabolites of probiotics for regulation of intestinal epithelial barrier. In *Microbial Cell Factories* (Vol. 19, Issue 1). BioMed Central Ltd. <https://doi.org/10.1186/s12934-020-1289-4>

- Liu, X., & Zhu, H. (2022). Curcumin Improved Intestinal Epithelial Barrier Integrity by Up-Regulating ZO-1/Occludin/Claudin-1 in Septic Rats. *Evidence-Based Complementary and Alternative Medicine*, 2022. <https://doi.org/10.1155/2022/2884522>
- Ma, T. Y., Iwamoto, G. K., Hoa, N. T., Akotia, V., Pedram, A., Boivin, M. A., & Said, H. M. (2004). *TNF-induced increase in intestinal epithelial tight junction permeability requires NF-B activation*. <https://doi.org/10.1152/ajpgi.00173.2003>.-Crohn
- Ma, X., X. Fan, P., Li, L. S., Qiao, S. Y., Zhang, G. L., & Li, D. F. (2012). Butyrate promotes the recovering of intestinal wound healing through its positive effect on the tight junctions1. *Journal of Animal Science*, 90(suppl\_4), 266–268. <https://doi.org/10.2527/jas.50965>
- Mantis, N. J., Rol, N., & Corthésy, B. (2011). Secretory IgA's complex roles in immunity and mucosal homeostasis in the gut. In *Mucosal Immunology* (Vol. 4, Issue 6, pp. 603–611). <https://doi.org/10.1038/mi.2011.41>
- Maresca, M., Alatou, R., Pujol, A., Nicoletti, C., Perrier, J., Giardina, T., Simon, G., Méjean, V., & Fons, M. (2021). Rada, a msccrmm adhesin of the dominant symbiote ruminococcus gnavus e1, binds human immunoglobulins and intestinal mucins. *Biomolecules*, 11(11). <https://doi.org/10.3390/biom11111613>
- Martens, E. C., Kelly, A. G., Tauzin, A. S., & Brumer, H. (2014). The devil lies in the details: How variations in polysaccharide fine-structure impact the physiology and evolution of gut microbes. In *Journal of Molecular Biology* (Vol. 426, Issue 23, pp. 3851–3865). Academic Press. <https://doi.org/10.1016/j.jmb.2014.06.022>
- Martinez-Guryn, K., Leone, V., & Chang, E. B. (2019). Regional Diversity of the Gastrointestinal Microbiome. In *Cell Host and Microbe* (Vol. 26, Issue 3, pp. 314–324). Cell Press. <https://doi.org/10.1016/j.chom.2019.08.011>
- Maukonen, J., Kolho, K. L., Paasela, M., Honkanen, J., Klemetti, P., Vaarala, O., & Saarela, M. (2015). Altered Fecal Microbiota in Paediatric Inflammatory Bowel Disease. *Journal of Crohn's & Colitis*, 9(12), 1088–1095. <https://doi.org/10.1093/ecco-jcc/jjv147>
- Mayer, S., Raulf, M. K., & Lepenies, B. (2017). C-type lectins: their network and roles in pathogen recognition and immunity. *Histochemistry and Cell Biology*, 147(2), 223–237. <https://doi.org/10.1007/s00418-016-1523-7>
- Mazmanian, S. K., Cui, H. L., Tzianabos, A. O., & Kasper, D. L. (2005). An immunomodulatory molecule of symbiotic bacteria directs maturation of the host immune system. *Cell*, 122(1), 107–118. <https://doi.org/10.1016/j.cell.2005.05.007>

- Mazzeo, M. F., Reale, A., Di Renzo, T., & Siciliano, R. A. (2022). Surface Layer Protein Pattern of *Levilactobacillus brevis* Strains Investigated by Proteomics. *Nutrients*, *14*(18). <https://doi.org/10.3390/nu14183679>
- McGrath, C. J., Laveckis, E., Bell, A., Crost, E., Juge, N., & Schuller, S. (2022). Development of a novel human intestinal model to elucidate the effect of anaerobic commensals on *Escherichia coli* infection. *DMM Disease Models and Mechanisms*, *15*(4). <https://doi.org/10.1242/dmm.049365>
- McGreal, E. P., Rosas, M., Brown, G. D., Zamze, S., Wong, S. Y. C., Gordon, S., Martinez-Pomares, L., & Taylor, P. R. (2006). The carbohydrate-recognition domain of Dectin-2 is a C-type lectin with specificity for high mannose. *Glycobiology*, *16*(5), 422–430. <https://doi.org/10.1093/glycob/cwj077>
- McGuckin, M. A., Lindén, S. K., Sutton, P., & Florin, T. H. (2011). Mucin dynamics and enteric pathogens. *Nature Reviews Microbiology*, *9*(4), 265–278. <https://doi.org/10.1038/nrmicro2538>
- McLeod, J., Park, C., Cunningham, A., O'Donnell, L., Brown, R. S., Kelly, F., & She, Z. (2020). Developing a toll-like receptor biosensor for Gram-positive bacterial detection and its storage strategies. *The Analyst*, *145*(18), 6024–6031. <https://doi.org/10.1039/D0AN01050B>
- Messner, P., Schäffer, C., & Kosma, P. (2013). Bacterial cell-envelope glycoconjugates. In *Advances in Carbohydrate Chemistry and Biochemistry* (Vol. 69, pp. 209–272). Academic Press Inc. <https://doi.org/10.1016/B978-0-12-408093-5.00006-X>
- Miller, B. M., Liou, M. J., Lee, J. Y., & Bäumler, A. J. (2021). The longitudinal and cross-sectional heterogeneity of the intestinal microbiota. In *Current Opinion in Microbiology* (Vol. 63, pp. 221–230). Elsevier Ltd. <https://doi.org/10.1016/j.mib.2021.08.004>
- Mo, Z., Huang, P., Yang, C., Xiao, S., Zhang, G., Ling, F., & Li, L. (2020). *Meta-analysis of 16S rRNA Microbial Data Identified Distinctive and Predictive Microbiota Dysbiosis in Colorectal Carcinoma Adjacent Tissue*. <https://doi.org/10.1128/mSystems>
- Monaco, A., Ovrzyn, B., Axis, J., & Amsler, K. (2021). The epithelial cell leak pathway. In *International Journal of Molecular Sciences* (Vol. 22, Issue 14). MDPI. <https://doi.org/10.3390/ijms22147677>
- Moore, W. E. C., & Holdeman, L. V. (1974). Human Fecal Flora: The Normal Flora of 20 Japanese-Hawaiians. In *APPLIED MICROBIOLOGY* (Vol. 27, Issue 5).
- Moore, W E C; Johnson, J. L., & Holdeman, L. V. (1976). Emendation of Bacteroidaceae and *Butyrvibrio* and Descriptions of *Desulfornonas* gen. nov. and Ten New Species in the

Genera *Desulfomonas*, *Butyrivibrio*, *Eubacterium*, *CZostridium*, and *Ruminococcus*. *International Journal of Systematic Bacteriology*, 26(2), 238–252.

- Mowat, A. M., & Agace, W. W. (2014). Regional specialization within the intestinal immune system. In *Nature Reviews Immunology* (Vol. 14, Issue 10, pp. 667–685). Nature Publishing Group. <https://doi.org/10.1038/nri3738>
- Nakamura, S., Kurata, R., Tonozuka, T., Funane, K., Park, E. Y., & Miyazaki, T. (2023). Bacteroidota polysaccharide utilization system for branched dextran exopolysaccharides from lactic acid bacteria. *Journal of Biological Chemistry*, 104885. <https://doi.org/10.1016/j.jbc.2023.104885>
- Ndeh, D., & Gilbert, H. J. (2018). Biochemistry of complex glycan depolymerisation by the human gut microbiota. In *FEMS Microbiology Reviews* (Vol. 42, Issue 2, pp. 146–164). Oxford University Press. <https://doi.org/10.1093/femsre/fuy002>
- Neunlist, M., Van Landeghem, L., Mahé, M. M., Derkinderen, P., Des Varannes, S. B., & Rolli-Derkinderen, M. (2013). The digestive neuronal-glia-epithelial unit: A new actor in gut health and disease. In *Nature Reviews Gastroenterology and Hepatology* (Vol. 10, Issue 2, pp. 90–100). <https://doi.org/10.1038/nrgastro.2012.221>
- Ng, S. L., Teo, Y. J., Setiagani, Y. A., Karjalainen, K., & Ruedl, C. (2018). Type 1 Conventional CD103+ Dendritic Cells Control Effector CD8+ T Cell Migration, Survival, and Memory Responses During Influenza Infection. *Frontiers in Immunology*, 9. <https://doi.org/10.3389/fimmu.2018.03043>
- Nikolić, J., Nešić, A., Čavić, M., Đorđević, N., Anđelković, U., Atanasković-Marković, M., Drakulić, B., & Gavrović-Jankulović, M. (2017). Effect of malondialdehyde on the ovalbumin structure and its interactions with T84 epithelial cells. *Biochimica et Biophysica Acta (BBA) - General Subjects*, 1861(2), 126–134. <https://doi.org/10.1016/j.bbagen.2016.11.021>
- Nilsen, M., Saunders, C. M., Angell, I. L., Arntzen, M., Lødrup Carlsen, K. C., Carlsen, K. H., Haugen, G., Hagen, L. H., Carlsen, M. H., Hedlin, G., Jonassen, C. M., Nordlund, B., Rehbinder, E. M., Skjerven, H. O., Snipen, L., Staff, A. C., Vettukattil, R., & Rudi, K. (2020). Butyrate levels in the transition from an infant-to an adult-like gut microbiota correlate with bacterial networks associated with *eubacterium rectale* and *ruminococcus gnavus*. *Genes*, 11(11), 1–15. <https://doi.org/10.3390/genes11111245>
- Onyiah, J. C., & Colgan, S. P. (2016). Cytokine responses and epithelial function in the intestinal mucosa. In *Cellular and Molecular Life Sciences* (Vol. 73, Issue 22, pp. 4203–4212). Birkhauser Verlag AG. <https://doi.org/10.1007/s00018-016-2289-8>

- Pabst, O., Cerovic, V., & Hornef, M. (2016). Secretory IgA in the Coordination of Establishment and Maintenance of the Microbiota. In *Trends in Immunology* (Vol. 37, Issue 5, pp. 287–296). Elsevier Ltd. <https://doi.org/10.1016/j.it.2016.03.002>
- Paone, P., & Cani, P. D. (2020). Mucus barrier, mucins and gut microbiota: The expected slimy partners? In *Gut* (Vol. 69, Issue 12, pp. 2232–2243). BMJ Publishing Group. <https://doi.org/10.1136/gutjnl-2020-322260>
- Patel, R., & Dupont, H. L. (2015). New approaches for bacteriotherapy: Prebiotics, new-generation probiotics, and synbiotics. *Clinical Infectious Diseases*, *60*, S108–S121. <https://doi.org/10.1093/cid/civ177>
- Patrick, S., Blakely, G. W., Houston, S., Moore, J., Abratt, V. R., Bertalan, M., Cerdeño-Tárraga, A. M., Quail, M. A., Corton, N., Corton, C., Bignell, A., Barron, A., Clark, L., Bentley, S. D., & Parkhill, J. (2010). Twenty-eight divergent polysaccharide loci specifying within- and amongst-strain capsule diversity in three strains of *Bacteroides fragilis*. *Microbiology*, *156*(11), 3255–3269. <https://doi.org/10.1099/mic.0.042978-0>
- Pazos, M., & Peters, K. (2019). *Peptidoglycan* (pp. 127–168). [https://doi.org/10.1007/978-3-030-18768-2\\_5](https://doi.org/10.1007/978-3-030-18768-2_5)
- Petersen, C., & Round, J. L. (2014). Defining dysbiosis and its influence on host immunity and disease. *Cellular Microbiology*, *16*(7), 1024–1033. <https://doi.org/10.1111/cmi.12308>
- Petersson, J., Schreiber, O., Hansson, G. C., Gendler, S. J., Velcich, A., Lundberg, J. O., Roos, S., Holm, L., & Phillipson, M. (2011). Importance and regulation of the colonic mucus barrier in a mouse model of colitis. *Am J Physiol Gastrointest Liver Physiol*, *300*, 327–333. <https://doi.org/10.1152/ajpgi.00422.2010.-The>
- Platanias, L. C. (2005). Mechanisms of type-I- and type-II-interferon-mediated signalling. In *Nature Reviews Immunology* (Vol. 5, Issue 5, pp. 375–386). <https://doi.org/10.1038/nri1604>
- Poole, J., Day, C. J., Von Itzstein, M., Paton, J. C., & Jennings, M. P. (2018). Glycointeractions in bacterial pathogenesis. In *Nature Reviews Microbiology* (Vol. 16, Issue 7, pp. 440–452). Nature Publishing Group. <https://doi.org/10.1038/s41579-018-0007-2>
- Pope, J. L., Bhat, A. A., Sharma, A., Ahmad, R., Krishnan, M., Washington, M. K., Beauchamp, R. D., Singh, A. B., & Dhawan, P. (2014). Claudin-1 regulates intestinal epithelial homeostasis through the modulation of Notch-signalling. *Gut*, *63*(4), 622–634. <https://doi.org/10.1136/gutjnl-2012-304241>
- Porter, N. T., Canales, P., Peterson, D. A., & Martens, E. C. (2017). A Subset of Polysaccharide Capsules in the Human Symbiont *Bacteroides thetaiotaomicron* Promote Increased

- Competitive Fitness in the Mouse Gut. *Cell Host and Microbe*, 22(4), 494-506.e8.  
<https://doi.org/10.1016/j.chom.2017.08.020>
- Porter, N. T., Hryckowian, A. J., Merrill, B. D., Fuentes, J. J., Gardner, J. O., Glowacki, R. W. P., Singh, S., Crawford, R. D., Snitkin, E. S., Sonnenburg, J. L., & Martens, E. C. (2020). Phase-variable capsular polysaccharides and lipoproteins modify bacteriophage susceptibility in *Bacteroides thetaiotaomicron*. *Nature Microbiology*, 5(9), 1170–1181.  
<https://doi.org/10.1038/s41564-020-0746-5>
- Porter, N. T., & Martens, E. C. (2017). The Critical Roles of Polysaccharides in Gut Microbial Ecology and Physiology. *Annual Review of Microbiology*, 71(1), 349–369.  
<https://doi.org/10.1146/annurev-micro-102215-095316>
- Pridmore, A. C., Jarvis, G. A., John, C. M., Jack, D. L., Dower, S. K., & Read, R. C. (2003). † Present address: MandalMed. *INFECTION AND IMMUNITY*, 71(7), 3901–3908.  
<https://doi.org/10.1128/IAI.71.7.3901-3908.2003>
- Pruss, K. M., Marcobal, A., Southwick, A. M., Dahan, D., Smits, S. A., Ferreyra, J. A., Higginbottom, S. K., Sonnenburg, E. D., Kashyap, P. C., Choudhury, B., Bode, L., & Sonnenburg, J. L. (2021). Mucin-derived O-glycans supplemented to diet mitigate diverse microbiota perturbations. *The ISME Journal*, 15(2), 577–591.  
<https://doi.org/10.1038/s41396-020-00798-6>
- Pucci, M., Malagolini, N., & Dall'Olio, F. (2021). Glycobiology of the epithelial to mesenchymal transition. In *Biomedicines* (Vol. 9, Issue 7). MDPI AG.  
<https://doi.org/10.3390/biomedicines9070770>
- Püngel, D., Treveil, A., Dalby, M. J., Caim, S., Colquhoun, I. J., Booth, C., Ketskemety, J., Korcsmaros, T., van Sinderen, D., Lawson, M. A. E., & Hall, L. J. (2020). *Bifidobacterium breve* UCC2003 exopolysaccharide modulates the early life microbiota by acting as a potential dietary substrate. *Nutrients*, 12(4). <https://doi.org/10.3390/nu12040948>
- Qin, J., Li, R., Raes, J., Arumugam, M., Burgdorf, K. S., Manichanh, C., Nielsen, T., Pons, N., Levenez, F., Yamada, T., Mende, D. R., Li, J., Xu, J., Li, S., Li, D., Cao, J., Wang, B., Liang, H., Zheng, H., ... Zoetendal, E. (2010). A human gut microbial gene catalogue established by metagenomic sequencing. *Nature*, 464(7285), 59–65.  
<https://doi.org/10.1038/nature08821>
- Qiu, Y., Ding, Y., Zou, L., Tan, Z., Liu, T., Fu, X., & Xu, W. (2013). Divergent Roles of Amino Acid Residues Inside and Outside the BB Loop Affect Human Toll-Like Receptor (TLR)2/2, TLR2/1 and TLR2/6 Responsiveness. *PLoS ONE*, 8(4).  
<https://doi.org/10.1371/journal.pone.0061508>

- Rakoff-Nahoum, S., Foster, K. R., & Comstock, L. E. (2016). The evolution of cooperation within the gut microbiota. *Nature*, *533*(7602), 255–259. <https://doi.org/10.1038/nature17626>
- Ramare, F., Nicoli, J., Dabard, J., Corring, T., Ladire, M., Gueugneau, A. M., & Raibaud, P. (1993). Trypsin-dependent production of an antibacterial substance by a human *Peptostreptococcus* strain in gnotobiotic rats and in vitro. *Applied and Environmental Microbiology*, *59*(9), 2876–2883. <https://doi.org/10.1128/aem.59.9.2876-2883.1993>
- Ramirez, J., Guarner, F., Bustos Fernandez, L., Maruy, A., Sdepanian, V. L., & Cohen, H. (2020). Antibiotics as Major Disruptors of Gut Microbiota. *Frontiers in Cellular and Infection Microbiology*, *10*. <https://doi.org/10.3389/fcimb.2020.572912>
- Rampoldi, F., & Prinz, I. (2022). Three Layers of Intestinal  $\gamma\delta$  T Cells Talk Different Languages With the Microbiota. In *Frontiers in Immunology* (Vol. 13). Frontiers Media S.A. <https://doi.org/10.3389/fimmu.2022.849954>
- Rawat, P. S., Seyed Hameed, A. S., Meng, X., & Liu, W. (2022). Utilization of glycosaminoglycans by the human gut microbiota: participating bacteria and their enzymatic machineries. In *Gut Microbes* (Vol. 14, Issue 1). Taylor and Francis Ltd. <https://doi.org/10.1080/19490976.2022.2068367>
- Reboldi, A., & Cyster, J. G. (2016). Peyer's patches: organizing B-cell responses at the intestinal frontier. *Immunological Reviews*, *271*(1), 230–245. <https://doi.org/10.1111/imr.12400>
- Rinninella, E., Raoul, P., Cintoni, M., Franceschi, F., Miggiano, G. A. D., Gasbarrini, A., & Mele, M. C. (2019). What is the healthy gut microbiota composition? A changing ecosystem across age, environment, diet, and diseases. *Microorganisms*, *7*(1). <https://doi.org/10.3390/microorganisms7010014>
- Rios-Covian, D., Arboleya, S., Hernandez-Barranco, A. M., Alvarez-Buylla, J. R., Ruas-Madiedo, P., Gueimonde, M., & De Los Reyes-Gavilan, C. G. (2013). Interactions between *Bifidobacterium* and *Bacteroides* species in cofermentations are affected by carbon sources, including exopolysaccharides produced by bifidobacteria. *Applied and Environmental Microbiology*, *79*(23), 7518–7524. <https://doi.org/10.1128/AEM.02545-13>
- Robbe, C., Capon, C., Coddeville, B., & Michalski, J.-C. (2004). Structural diversity and specific distribution of O-glycans in normal human mucins along the intestinal tract. In *Biochem. J* (Vol. 384).
- Robbe, C., Capon, C., Maes, E., Rousset, M., Zweibaum, A., Zanetta, J. P., & Michalski, J. C. (2003a). Evidence of regio-specific glycosylation in human intestinal mucins: Presence

of an acidic gradient along the intestinal tract. *Journal of Biological Chemistry*, 278(47), 46337–46348. <https://doi.org/10.1074/jbc.M302529200>

Robbe, C., Capon, C., Maes, E., Rousset, M., Zweibaum, A., Zanetta, J. P., & Michalski, J. C. (2003b). Evidence of regio-specific glycosylation in human intestinal mucins: Presence of an acidic gradient along the intestinal tract. *Journal of Biological Chemistry*, 278(47), 46337–46348. <https://doi.org/10.1074/jbc.M302529200>

Robinson, M. J., Osorio, F., Rosas, M., Freitas, R. P., Schweighoffer, E., Groß, O., Verbeek, J. S., Ruland, J., Tybulewicz, V., Brown, G. D., Moita, L. F., Taylor, P. R., & Reis E Sousa, C. (2009). Dectin-2 is a Syk-coupled pattern recognition receptor crucial for Th17 responses to fungal infection. *Journal of Experimental Medicine*, 206(9), 2037–2051. <https://doi.org/10.1084/jem.20082818>

Roblin, C., Chiumento, S., Jacqueline, C., Pinloche, E., Nicoletti, C., Olleik, H., Courvoisier-Dezord, E., Amouric, A., Basset, C., Dru, L., Ollivier, M., Bogey-Lambert, A., Vidal, N., Atta, M., Maresca, M., Devillard, E., Duarte, V., Perrier, J., & Lafond, M. (2021). The multifunctional sactipeptide ruminococcin c1 displays potent antibacterial activity in vivo as well as other beneficial properties for human health. *International Journal of Molecular Sciences*, 22(6). <https://doi.org/10.3390/ijms22063253>

Rodríguez, J. M., Murphy, K., Stanton, C., Ross, R. P., Kober, O. I., Juge, N., Avershina, E., Rudi, K., Narbad, A., Jenmalm, M. C., Marchesi, J. R., & Collado, M. C. (2015). The composition of the gut microbiota throughout life, with an emphasis on early life. *Microbial Ecology in Health & Disease*, 26(0), 1–17. <https://doi.org/10.3402/mehd.v26.26050>

Rook, G., Bäckhed, F., Levin, B. R., Mcfall-Ngai, M. J., & Mclean, A. R. (2017). Evolutionary public health 3 Evolution, human-microbe interactions, and life history plasticity. In *www.thelancet.com* (Vol. 390). [www.thelancet.com](http://www.thelancet.com)

Rose, E. C., Odle, J., Blikslager, A. T., & Ziegler, A. L. (2021). Probiotics, prebiotics and epithelial tight junctions: A promising approach to modulate intestinal barrier function. In *International Journal of Molecular Sciences* (Vol. 22, Issue 13). MDPI. <https://doi.org/10.3390/ijms22136729>

Rossi, O., Khan, M. T., Schwarzer, M., Hudcovic, T., Srutkova, D., Duncan, S. H., Stolte, E. H., Kozakova, H., Flint, H. J., Samsom, J. N., Harmsen, H. J. M., & Wells, J. M. (2015). Faecalibacterium prausnitzii strain HTF-F and its extracellular polymeric matrix attenuate clinical parameters in DSS-induced colitis. *PLoS ONE*, 10(4). <https://doi.org/10.1371/journal.pone.0123013>

- Round, J. L., Lee, S. M., Li, J., Tran, G., Jabri, B., Chatila, T. A., & Mazmanian, S. K. (2011). The toll-like receptor 2 pathway establishes colonization by a commensal of the human microbiota. *Science*, *332*(6032), 974–977. <https://doi.org/10.1126/science.1206095>
- Round, J. L., & Mazmanian, S. K. (2009). The gut microbiota shapes intestinal immune responses during health and disease. In *Nature Reviews Immunology* (Vol. 9, Issue 5, pp. 313–323). <https://doi.org/10.1038/nri2515>
- Rowland, I., Gibson, G., Heinken, A., Scott, K., Swann, J., Thiele, I., & Tuohy, K. (2018). Gut microbiota functions: metabolism of nutrients and other food components. In *European Journal of Nutrition* (Vol. 57, Issue 1). Dr. Dietrich Steinkopff Verlag GmbH and Co. KG. <https://doi.org/10.1007/s00394-017-1445-8>
- Roy, D., Athey, T. B. T., Auger, J. P., Goyette-Desjardins, G., Van Calsteren, M. R., Takamatsu, D., Okura, M., Teatero, S., Alcorlo, M., Hermoso, J. A., Segura, M., Gottschalk, M., & Fittipaldi, N. (2017). A single amino acid polymorphism in the glycosyltransferase CpsK defines four *Streptococcus suis* serotypes. *Scientific Reports*, *7*(1). <https://doi.org/10.1038/s41598-017-04403-3>
- Ruas-Madiedo, P., Medrano, M., Salazar, N., De Los Reyes-Gavilán, C. G., Pérez, P. F., & Abraham, A. G. (2010). Exopolysaccharides produced by *Lactobacillus* and *Bifidobacterium* strains abrogate in vitro the cytotoxic effect of bacterial toxins on eukaryotic cells. *Journal of Applied Microbiology*, *109*(6), 2079–2086. <https://doi.org/10.1111/j.1365-2672.2010.04839.x>
- Ruuskanen, M. O., Erawijantari, P. P., Havulinna, A. S., Liu, Y., Méric, G., Tuomilehto, J., Inouye, M., Jousilahti, P., Salomaa, V., Jain, M., Knight, R., Lahti, L., & Niiranen, T. J. (2022). Gut Microbiome Composition Is Predictive of Incident Type 2 Diabetes in a Population Cohort of 5,572 Finnish Adults. *Diabetes Care*, *45*(4), 811–818. <https://doi.org/10.2337/dc21-2358>
- Sabater, C., Molinero-García, N., Castro-Bravo, N., Diez-Echave, P., Hidalgo-García, L., Delgado, S., Sánchez, B., Gálvez, J., Margolles, A., & Ruas-Madiedo, P. (2020). Exopolysaccharide Producing *Bifidobacterium animalis* subsp. *lactis* Strains Modify the Intestinal Microbiota and the Plasmatic Cytokine Levels of BALB/c Mice According to the Type of Polymer Synthesized. *Frontiers in Microbiology*, *11*. <https://doi.org/10.3389/fmicb.2020.601233>
- Sagheddu, V., Patrone, V., Miragoli, F., Puglisi, E., & Morelli, L. (2016). Infant early gut colonization by Lachnospiraceae: High frequency of *Ruminococcus gnavus*. *Frontiers in Pediatrics*, *4*(JUN), 7–12. <https://doi.org/10.3389/fped.2016.00057>
- Salazar, N., Gueimonde, M., de los Reyes-Gavilán, C. G., & Ruas-Madiedo, P. (2016). Exopolysaccharides Produced by Lactic Acid Bacteria and Bifidobacteria as Fermentable

Substrates by the Intestinal Microbiota. In *Critical Reviews in Food Science and Nutrition* (Vol. 56, Issue 9, pp. 1440–1453). Taylor and Francis Inc.  
<https://doi.org/10.1080/10408398.2013.770728>

Salazar, N., Gueimonde, M., Hernández-Barranco, A. M., Ruas-Madiedo, P., & De Los Reyes-Gavilán, C. G. (2008). Exopolysaccharides produced by intestinal Bifidobacterium strains act as fermentable substrates for human intestinal bacteria. *Applied and Environmental Microbiology*, 74(15), 4737–4745. <https://doi.org/10.1128/AEM.00325-08>

Salazar, N., Ruas-Madiedo, P., Kolida, S., Collins, M., Rastall, R., Gibson, G., & de los Reyes-Gavilán, C. G. (2009). Exopolysaccharides produced by Bifidobacterium longum IPLA E44 and Bifidobacterium animalis subsp. lactis IPLA R1 modify the composition and metabolic activity of human faecal microbiota in pH-controlled batch cultures. *International Journal of Food Microbiology*, 135(3), 260–267.  
<https://doi.org/10.1016/j.ijfoodmicro.2009.08.017>

Sali, W., Patoli, D., Pais de Barros, J.-P., Labbé, J., Deckert, V., Duhéron, V., Le Guern, N., Blache, D., Chaumont, D., Lesniewska, E., Gasquet, B., Paul, C., Moreau, M., Denat, F., Masson, D., Lagrost, L., & Gautier, T. (2019). Polysaccharide Chain Length of Lipopolysaccharides From Salmonella Minnesota Is a Determinant of Aggregate Stability, Plasma Residence Time and Proinflammatory Propensity in vivo. *Frontiers in Microbiology*, 10. <https://doi.org/10.3389/fmicb.2019.01774>

Sameer, A. S., & Nissar, S. (2021). Toll-Like Receptors (TLRs): Structure, Functions, Signaling, and Role of Their Polymorphisms in Colorectal Cancer Susceptibility. In *BioMed Research International* (Vol. 2021). Hindawi Limited.  
<https://doi.org/10.1155/2021/1157023>

Sancho, E., Batlle, E., & Clevers, H. (2003). Live and let die in the intestinal epithelium. In *Current Opinion in Cell Biology* (Vol. 15, Issue 6, pp. 763–770). Elsevier Ltd.  
<https://doi.org/10.1016/j.ceb.2003.10.012>

Sano, H., Kuroki, Y., Honma, T., Ogasawara, Y., Sohma, H., Voelker, D. R., & Akino, T. (1998). Analysis of chimeric proteins identifies the regions in the carbohydrate recognition domains of rat lung collectins that are essential for interactions with phospholipids, glycolipids, and alveolar type II cells. *Journal of Biological Chemistry*, 273(8), 4783–4789. <https://doi.org/10.1074/jbc.273.8.4783>

Sathaliyawala, T., Kubota, M., Yudanin, N., Turner, D., Camp, P., Thome, J. J. C., Bickham, K. L., Lerner, H., Goldstein, M., Sykes, M., Kato, T., & Farber, D. L. (2013). Distribution and Compartmentalization of Human Circulating and Tissue-Resident Memory T Cell Subsets. *Immunity*, 38(1), 187–197. <https://doi.org/10.1016/j.immuni.2012.09.020>

- Sato, K., Yang, X. L., Yudate, T., Chung, J. S., Wu, J., Luby-Phelps, K., Kimberly, R. P., Underhill, D., Cruz, P. D., & Ariizumi, K. (2006). Dectin-2 is a pattern recognition receptor for fungi that couples with the Fc receptor  $\gamma$  chain to induce innate immune responses. *Journal of Biological Chemistry*, *281*(50), 38854–38866. <https://doi.org/10.1074/jbc.M606542200>
- Schade, J., & Weidenmaier, C. (2016). Cell wall glycopolymers of Firmicutes and their role as nonprotein adhesins. *FEBS Letters*, *590*(21), 3758–3771. <https://doi.org/10.1002/1873-3468.12288>
- Schlee, M., Wehkamp, J., Altenhoefer, A., Oelschlaeger, T. A., Stange, E. F., & Fellermann, K. (2007). Induction of human  $\beta$ -defensin 2 by the probiotic *Escherichia coli* Nissle 1917 is mediated through flagellin. *Infection and Immunity*, *75*(5), 2399–2407. <https://doi.org/10.1128/IAI.01563-06>
- Sender, R., Fuchs, S., & Milo, R. (2016). Revised Estimates for the Number of Human and Bacteria Cells in the Body. *PLoS Biology*, *14*(8). <https://doi.org/10.1371/journal.pbio.1002533>
- Shao, Y., Forster, S. C., Tsaliki, E., Vervier, K., Strang, A., Simpson, N., Kumar, N., Stares, M. D., Rodger, A., Brocklehurst, P., Field, N., & Lawley, T. D. (2019). Stunted microbiota and opportunistic pathogen colonization in caesarean-section birth. *Nature*, *574*(7776), 117–121. <https://doi.org/10.1038/s41586-019-1560-1>
- Silhavy, T. J., Kahne, D., & Walker, S. (2010). The Bacterial Cell Envelope. *Cold Spring Harbor Perspectives in Biology*, *2*(5), a000414–a000414. <https://doi.org/10.1101/cshperspect.a000414>
- Silva, C. A. de M. e, Rojony, R., Bermudez, L. E., & Danelishvili, L. (2020). Short-Chain Fatty Acids Promote *Mycobacterium avium* subsp. *hominissuis* Growth in Nutrient-Limited Environments and Influence Susceptibility to Antibiotics. *Pathogens*, *9*(9), 700. <https://doi.org/10.3390/pathogens9090700>
- Silverman, G. J., Deng, J., & Azzouz, D. F. (2022). Sex-dependent *Lupus Blautia* (Ruminococcus) *gnavus* strain induction of zonulin-mediated intestinal permeability and autoimmunity. *Frontiers in Immunology*, *13*. <https://doi.org/10.3389/fimmu.2022.897971>
- Singh, A. P., & Aijaz, S. (2016). Enteropathogenic *E. coli*: breaking the intestinal tight junction barrier. *F1000Research*, *4*, 231. <https://doi.org/10.12688/f1000research.6778.2>
- Sitarik, A. R., Kasmikha, N. S., Kim, H., Wegienka, G., Havstad, S., Ownby, D., Zoratti, E., & Johnson, C. C. (2018). Breast-feeding and delivery mode modify the association

- between maternal atopy and childhood allergic outcomes. *Journal of Allergy and Clinical Immunology*, 142(6), 2002-2004.e2. <https://doi.org/10.1016/j.jaci.2018.08.012>
- Sittipo, P., Lobionda, S., Choi, K., Sari, I. N., Kwon, H. Y., & Lee, Y. K. (2018). Toll-like receptor 2-mediated suppression of colorectal cancer pathogenesis by polysaccharide A from *Bacteroides fragilis*. *Frontiers in Microbiology*, 9(JUL), 1–11. <https://doi.org/10.3389/fmicb.2018.01588>
- Speciale, I., Verma, R., Di Lorenzo, F., Molinaro, A., Im, S. H., & De Castro, C. (2019). Bifidobacterium bifidum presents on the cell surface a complex mixture of glucans and galactans with different immunological properties. *Carbohydrate Polymers*, 218, 269–278. <https://doi.org/10.1016/j.carbpol.2019.05.006>
- Spinler, J. K., Sontakke, A., Hollister, E. B., Venable, S. F., Oh, P. L., Balderas, M. A., Saulnier, D. M. A., Mistretta, T.-A., Devaraj, S., Walter, J., Versalovic, J., & Highlander, S. K. (2014). From Prediction to Function Using Evolutionary Genomics: Human-Specific Ecotypes of *Lactobacillus reuteri* Have Diverse Probiotic Functions. *Genome Biology and Evolution*, 6(7), 1772–1789. <https://doi.org/10.1093/gbe/evu137>
- Srutkova, D., Schwarzer, M., Hudcovic, T., Zakostelska, Z., Drab, V., Spanova, A., Rittich, B., Kozakova, H., & Schabussova, I. (2015). Bifidobacterium longum CCM 7952 promotes epithelial barrier function and prevents acute dss-induced colitis in strictly strain-specific manner. *PLoS ONE*, 10(7). <https://doi.org/10.1371/journal.pone.0134050>
- Strandwitz, P. (2018). Neurotransmitter modulation by the gut microbiota. In *Brain Research* (Vol. 1693, pp. 128–133). Elsevier B.V. <https://doi.org/10.1016/j.brainres.2018.03.015>
- Strandwitz, P., Kim, K. H., Terekhova, D., Liu, J. K., Sharma, A., Levering, J., McDonald, D., Dietrich, D., Ramadhar, T. R., Lekbua, A., Mroue, N., Liston, C., Stewart, E. J., Dubin, M. J., Zengler, K., Knight, R., Gilbert, J. A., Clardy, J., & Lewis, K. (2019). GABA-modulating bacteria of the human gut microbiota. *Nature Microbiology*, 4(3), 396–403. <https://doi.org/10.1038/s41564-018-0307-3>
- Subramanian, S., Huq, S., Yatsunenkov, T., Haque, R., Mahfuz, M., Alam, M. A., Benezra, A., Destefano, J., Meier, M. F., Muegge, B. D., Barratt, M. J., VanArendonk, L. G., Zhang, Q., Province, M. A., Petri, W. A., Ahmed, T., & Gordon, J. I. (2014). Persistent gut microbiota immaturity in malnourished Bangladeshi children. *Nature*, 510(7505), 417–421. <https://doi.org/10.1038/nature13421>
- Sun, H., Xu, X. yong, Tian, X. li, Shao, H. tao, Wu, X. dong, Wang, Q., Su, X., & Shi, Y. (2014). Activation of NF- $\kappa$ B and respiratory burst following *Aspergillus fumigatus* stimulation of macrophages. *Immunobiology*, 219(1), 25–36. <https://doi.org/10.1016/j.imbio.2013.06.013>

- Sundin, J., Rangel, I., Repsilber, D., & Brummer, R. J. (2015). Cytokine response after stimulation with key commensal bacteria differ in post-infectious irritable bowel syndrome (PI-IBS) patients compared to healthy controls. *PLoS ONE*, *10*(9). <https://doi.org/10.1371/journal.pone.0134836>
- Surana, N. K., & Kasper, D. L. (2017). Moving beyond microbiome-wide associations to causal microbe identification. *Nature*, *552*(7684), 244–247. <https://doi.org/10.1038/nature25019>
- Swiatczak, B., & Cohen, I. R. (2015). Gut feelings of safety: tolerance to the microbiota mediated by innate immune receptors. *Microbiology and Immunology*, *59*(10), 573–585. <https://doi.org/10.1111/1348-0421.12318>
- Tahoun, A., Masutani, H., El-Sharkawy, H., Gillespie, T., Honda, R. P., Kuwata, K., Inagaki, M., Yabe, T., Nomura, I., & Suzuki, T. (2017). Capsular polysaccharide inhibits adhesion of *Bifidobacterium longum* 105-A to enterocyte-like Caco-2 cells and phagocytosis by macrophages. *Gut Pathogens*, *9*(1). <https://doi.org/10.1186/s13099-017-0177-x>
- Tailford, L. E., Crost, E. H., Kavanaugh, D., & Juge, N. (2015). Mucin glycan foraging in the human gut microbiome. *Frontiers in Genetics*, *5*(FEB). <https://doi.org/10.3389/fgene.2015.00081>
- Takahara, K., Tokieda, S., Nagaoka, K., & Inaba, K. (2012). Efficient capture of *Candida albicans* and zymosan by SIGNR1 augments TLR2-dependent TNF- $\alpha$  production. *International Immunology*, *24*(2), 89–96. <https://doi.org/10.1093/intimm/dxr103>
- Takayama, K., Qureshi, N., Hyver, K., Honovich, J., Cotter, R. J., Mascagni, P., & Schneider, H. (1986). Characterization of a structural series of lipid A obtained from the lipopolysaccharides of *Neisseria gonorrhoeae*. Combined laser desorption and fast atom bombardment mass spectral analysis of high performance liquid chromatography-purified dimethyl deriv. *Journal of Biological Chemistry*, *261*(23), 10624–10631. [https://doi.org/10.1016/s0021-9258\(18\)67431-9](https://doi.org/10.1016/s0021-9258(18)67431-9)
- Takeuchi, O., & Akira, S. (2010). Pattern Recognition Receptors and Inflammation. In *Cell* (Vol. 140, Issue 6, pp. 805–820). Elsevier B.V. <https://doi.org/10.1016/j.cell.2010.01.022>
- Tang, J., Lin, G., Langdon, W. Y., Tao, L., & Zhang, J. (2018). Regulation of C-type lectin receptor-mediated antifungal immunity. In *Frontiers in Immunology* (Vol. 9, Issue FEB). Frontiers Media S.A. <https://doi.org/10.3389/fimmu.2018.00123>
- Taylor, P. R., Tsoni, S. V., Willment, J. A., Dennehy, K. M., Rosas, M., Findon, H., Haynes, K., Steele, C., Botto, M., Gordon, S., & Brown, G. D. (2007). Dectin-1 is required for  $\beta$ -

- glucan recognition and control of fungal infection. *Nature Immunology*, 8(1), 31–38. <https://doi.org/10.1038/ni1408>
- ten Oever, J., Kox, M., van de Veerdonk, F. L., Mothapo, K. M., Slavcovic, A., Jansen, T. L., Tweehuysen, L., Giamarellos-Bourboulis, E. J., Schneeberger, P. M., Wever, P. C., Stoffels, M., Simon, A., Simon, A., Johnson, M. D., Kullberg, B. J., Pickkers, P., Pachot, A., Pachot, A., & Netea, M. G. (2014). The discriminative capacity of soluble Toll-like receptor (sTLR)2 and sTLR4 in inflammatory diseases. *BMC Immunology*, 15(1). <https://doi.org/10.1186/s12865-014-0055-y>
- Thomsson, K. A., Holmén-Larsson, J. M., Ångström, J., Johansson, M. E., Xia, L., & Hansson, G. C. (2012). Detailed O-glycomics of the Muc2 mucin from colon of wild-type, core 1- and core 3-transferase-deficient mice highlights differences compared with human MUC2. *Glycobiology*, 22(8), 1128–1139. <https://doi.org/10.1093/glycob/cws083>
- Thursby, E., & Juge, N. (2017). Introduction to the human gut microbiota. *Biochemical Journal*, 474(11), 1823–1836. <https://doi.org/10.1042/BCJ20160510>
- Tian, H., Li, B., Xu, T., Yu, H., Chen, J., Yu, H., Li, S., Zeng, L., Huang, X., & Liua, Q. (2021). Outer Membrane Vesicles Derived From Salmonella Enterica Serotype Typhimurium Can Deliver Shigella Flexneri 2a O-Polysaccharide Antigen To Prevent Shigella Flexneri 2a Infection In Mice. *Applied and Environmental Microbiology*, 87(19), 1–18. <https://doi.org/10.1128/AEM.00968-21>
- Tramontano, M., Andrejev, S., Pruteanu, M., Klünemann, M., Kuhn, M., Galardini, M., Jouhten, P., Zelezniak, A., Zeller, G., Bork, P., Typas, A., & Patil, K. R. (2018). Nutritional preferences of human gut bacteria reveal their metabolic idiosyncrasies. *Nature Microbiology*, 3(4), 514–522. <https://doi.org/10.1038/s41564-018-0123-9>
- Traweger, A., Toepfer, S., Wagner, R. N., Zweimueller-Mayer, J., Gehwolf, R., Lehner, C., Tempfer, H., Krizbai, I., Wilhelm, I., Bauer, H.-C., & Bauer, H. (2013). Beyond cell-cell adhesion. *Tissue Barriers*, 1(2), e25039. <https://doi.org/10.4161/tisb.25039>
- Turner, J. R. (2009). Intestinal mucosal barrier function in health and disease. In *Nature Reviews Immunology* (Vol. 9, Issue 11, pp. 799–809). <https://doi.org/10.1038/nri2653>
- Tytgat, H. L. P., & Lebeer, S. (2014). The Sweet Tooth of Bacteria: Common Themes in Bacterial Glycoconjugates. *Microbiology and Molecular Biology Reviews*, 78(3), 372–417. <https://doi.org/10.1128/mnbr.00007-14>
- Udayan, S., Buttó, L. F., Rossini, V., Velmurugan, J., Martinez-Lopez, M., Sancho, D., Melgar, S., O’Toole, P. W., & Nally, K. (2021). Macrophage cytokine responses to commensal Gram-positive Lactobacillus salivarius strains are TLR2-independent and Myd88-dependent. *Scientific Reports*, 11(1). <https://doi.org/10.1038/s41598-021-85347-7>

- Vaga, S., Lee, S., Ji, B., Andreasson, A., Talley, N. J., Agréus, L., Bidkhorji, G., Kovatcheva-Datchary, P., Park, J., Lee, D., Proctor, G., Ehrlich, S. D., Nielsen, J., Engstrand, L., & Shoaie, S. (2020). Compositional and functional differences of the mucosal microbiota along the intestine of healthy individuals. *Scientific Reports*, *10*(1). <https://doi.org/10.1038/s41598-020-71939-2>
- Vaishnava, S., Yamamoto, M., Severson, K. M., Ruhn, K. A., Yu, X., Koren, O., Ley, R., Wakeland, E. K., & Hooper, L. v. (2011). The antibacterial lectin RegIII $\gamma$  promotes the spatial segregation of microbiota and host in the intestine. *Science*, *334*(6053), 255–258. <https://doi.org/10.1126/science.1209791>
- Valueva, O. A., Shashkov, A. S., Zdrovenko, E. L., Chizhov, A. O., Kiseleva, E., Novik, G., & Knirel, Y. A. (2013). Structures of cell-wall phosphate-containing glycopolymers of *Bifidobacterium longum* BIM B-476-D. *Carbohydrate Research*, *373*, 22–27. <https://doi.org/10.1016/j.carres.2013.03.006>
- Van Herreweghen, F., De Paepe, K., Marzorati, M., & Van De Wiele, T. (2021). *Mucin as a Functional Niche Is a More Important Driver of In Vitro Gut Microbiota Composition and Functionality than Akkermansia muciniphila Supplementation*. <https://doi.org/10.1128/AEM>
- van Klinken, B. J.-W., Oussoren, E., Weenink, J.-J., Strous, G. J., Büller, H. A., Dekker, J., & Einerhand, A. W. C. (1996). The human intestinal cell lines Caco-2 and LS174T as models to study cell-type specific mucin expression. *Glycoconjugate Journal*, *13*(5), 757–768. <https://doi.org/10.1007/BF00702340>
- Van Nhieu, G. T., & Romero, S. (2016). *Common Themes in Cytoskeletal Remodeling by Intracellular Bacterial Effectors* (pp. 207–235). [https://doi.org/10.1007/164\\_2016\\_42](https://doi.org/10.1007/164_2016_42)
- Venturini, C., Ben Zakour, N. L., Bowring, B., Morales, S., Cole, R., Kovach, Z., Branston, S., Kettle, E., Thomson, N., & Iredell, J. R. (2020). Fine capsule variation affects bacteriophage susceptibility in *Klebsiella pneumoniae* ST258. *FASEB Journal*, *34*(8), 10801–10817. <https://doi.org/10.1096/fj.201902735R>
- Verma, R., Lee, C., Jeun, E.-J., Yi, J., Kim, K. S., Ghosh, A., Byun, S., Lee, C.-G., Kang, H.-J., Kim, G.-C., Jun, C.-D., Jan, G., Suh, C.-H., Jung, J.-Y., Sprent, J., Rudra, D., De Castro, C., Molinaro, A., Surh, C. D., & Im, S.-H. (2018). Cell surface polysaccharides of *Bifidobacterium bifidum* induce the generation of Foxp3 + regulatory T cells. In *Sci. Immunol* (Vol. 3). <https://www.science.org>
- Wan, C., Qian, W. W., Liu, W., Pi, X., Tang, M. T., Wang, X. L., Gu, Q., Li, P., & Zhou, T. (2022). Exopolysaccharide from *Lactobacillus rhamnosus* ZFM231 alleviates DSS-induced colitis in mice by regulating gut microbiota. *Journal of the Science of Food and Agriculture*, *102*(15), 7087–7097. <https://doi.org/10.1002/jsfa.12070>

- Wan, L., Ge, W. R., Zhang, S., Sun, Y. L., Wang, B., & Yang, G. (2020). Case-Control Study of the Effects of Gut Microbiota Composition on Neurotransmitter Metabolic Pathways in Children With Attention Deficit Hyperactivity Disorder. *Frontiers in Neuroscience, 14*. <https://doi.org/10.3389/fnins.2020.00127>
- Wang, X., Xu, M., Xu, D., Ma, K., Zhang, C., Wang, G., Dong, M., & Li, W. (2022). Structural and prebiotic activity analysis of the polysaccharide produced by *Lactobacillus helveticus* SNA12. *Carbohydrate Polymers, 296*. <https://doi.org/10.1016/j.carbpol.2022.119971>
- Wang, Y., Spatz, M., da Costa, G., Michaudel, C., Lapiere, A., Danne, C., Agus, A., Michel, M. L., Netea, M. G., Langella, P., Sokol, H., & Richard, M. L. (2022). Deletion of both Dectin-1 and Dectin-2 affects the bacterial but not fungal gut microbiota and susceptibility to colitis in mice. *Microbiome, 10*(1). <https://doi.org/10.1186/s40168-022-01273-4>
- Weis, W. I., Taylor, M. E., & Drickamer, K. (1998). The C-type lectin superfamily in the immune system. *Immunological Reviews, 163*, 19–34. <https://doi.org/10.1111/j.1600-065X.1998.tb01185.x>
- Wells, J. M., Rossia, O., Meijerink, M., & Van Baarlen, P. (2011). Epithelial crosstalk at the microbiota-mucosal interface. *Proceedings of the National Academy of Sciences of the United States of America, 108*(SUPPL. 1), 4607–4614. <https://doi.org/10.1073/pnas.1000092107>
- Wheeler, R., Bastos, P. A. D., Disson, O., Rifflet, A., Gabanyi, I., Spielbauer, J., Bérard, M., Lecuit, M., & Boneca, I. G. (2023). Microbiota-induced active translocation of peptidoglycan across the intestinal barrier dictates its within-host dissemination. *Proceedings of the National Academy of Sciences of the United States of America, 120*(4). <https://doi.org/10.1073/pnas.2209936120>
- Wicherska-pawłowska, K., Wróbel, T., & Rybka, J. (2021). Toll-like receptors (TLrs), nod-like receptors (nlrs) and rig-i-like receptors (rlrs) in innate immunity. tlrs, nlrs and rlrs ligands as immunotherapeutic agents for hematopoietic diseases. In *International Journal of Molecular Sciences* (Vol. 22, Issue 24). MDPI. <https://doi.org/10.3390/ijms222413397>
- Williams, B. B., Van Benschoten, A. H., Cimermancic, P., Donia, M. S., Zimmermann, M., Taketani, M., Ishihara, A., Kashyap, P. C., Fraser, J. S., & Fischbach, M. A. (2014). Discovery and characterization of gut microbiota decarboxylases that can produce the neurotransmitter tryptamine. *Cell Host and Microbe, 16*(4), 495–503. <https://doi.org/10.1016/j.chom.2014.09.001>
- Wirbel, J., Pyl, P. T., Kartal, E., Zych, K., Kashani, A., Milanese, A., Fleck, J. S., Voigt, A. Y., Palleja, A., Ponnudurai, R., Sunagawa, S., Coelho, L. P., Schrotz-King, P., Vogtmann, E.,

- Habermann, N., Niméus, E., Thomas, A. M., Manghi, P., Gandini, S., ... Zeller, G. (2019). Meta-analysis of fecal metagenomes reveals global microbial signatures that are specific for colorectal cancer. *Nature Medicine*, *25*(4), 679–689. <https://doi.org/10.1038/s41591-019-0406-6>
- Wittmann, A., Lamprinaki, D., Bowles, K. M., Katzenellenbogen, E., Knirel, Y. A., Whitfield, C., Nishimura, T., Matsumoto, N., Yamamoto, K., Iwakura, Y., Saijo, S., & Kawasaki, N. (2016). Dectin-2 recognizes mannosylated O-antigens of human opportunistic pathogens and augments lipopolysaccharide activation of myeloid cells. *Journal of Biological Chemistry*, *291*(34), 17629–17638. <https://doi.org/10.1074/jbc.M116.741256>
- Wu, C. M., Wheeler, K. M., Cárcamo-Oyarce, G., Aoki, K., McShane, A., Datta, S. S., Mark Welch, J. L., Tiemeyer, M., Griffen, A. L., & Ribbeck, K. (2023). Mucin glycans drive oral microbial community composition and function. *Npj Biofilms and Microbiomes*, *9*(1), 11. <https://doi.org/10.1038/s41522-023-00378-4>
- Wu, H., Crost, E. H., David Owen, C., van Bakel, W., Gascueña, A. M., Latousakis, D., Hicks, T., Walpole, S., Urbanowicz, P. A., Ndeh, D., Monaco, S., Salom, L. S., Griffiths, R., Reynolds, R. S., Colvile, A., Spencer, D. I. R., Walsh, M., Angulo, J., & Juge, N. (2021). The human gut symbiont *Ruminococcus gnavus* shows specificity to blood group A antigen during mucin glycan foraging: Implication for niche colonisation in the gastrointestinal tract. *PLoS Biology*, *19*(12). <https://doi.org/10.1371/journal.pbio.3001498>
- Wu, H., Rebello, O., Crost, E. H., Owen, C. D., Walpole, S., Bennati-Granier, C., Ndeh, D., Monaco, S., Hicks, T., Colvile, A., Urbanowicz, P. A., Walsh, M. A., Angulo, J., Spencer, D. I. R., & Juge, N. (2021). Fucosidases from the human gut symbiont *Ruminococcus gnavus*. *Cellular and Molecular Life Sciences*, *78*(2), 675–693. <https://doi.org/10.1007/s00018-020-03514-x>
- Wu, J., He, C., Bu, J., Luo, Y., Yang, S., Ye, C., Yu, S., He, B., Yin, Y., & Yang, X. (2020). Betaine attenuates LPS-induced downregulation of Occludin and Claudin-1 and restores intestinal barrier function. *BMC Veterinary Research*, *16*(1), 1–8. <https://doi.org/10.1186/s12917-020-02298-3>
- Wu, M. H., Pan, T. M., Wu, Y. J., Chang, S. J., Chang, M. S., & Hu, C. Y. (2010). Exopolysaccharide activities from probiotic bifidobacterium: Immunomodulatory effects (on J774A.1 macrophages) and antimicrobial properties. *International Journal of Food Microbiology*, *144*(1), 104–110. <https://doi.org/10.1016/j.ijfoodmicro.2010.09.003>
- Yang, K., He, Y., Park, C. G., Kang, Y. S., Zhang, P., Han, Y., Cui, Y., Bulgheresi, S., Anisimov, A. P., Dentovskaya, S. V., Ying, X., Jiang, L., Ding, H., Njiri, O. A., Zhang, S., Zheng, G., Xia, L., Kan, B., Wang, X., ... Chen, T. (2019). *Yersinia pestis* interacts with SIGNR1 (CD209b) for

- promoting host dissemination and infection. *Frontiers in Immunology*, 10(MAR).  
<https://doi.org/10.3389/fimmu.2019.00096>
- Yonekawa, A., Saijo, S., Hoshino, Y., Miyake, Y., Ishikawa, E., Suzukawa, M., Inoue, H., Tanaka, M., Yoneyama, M., Oh-hora, M., Akashi, K., & Yamasaki, S. (2014). Dectin-2 is a direct receptor for mannose-capped lipoarabinomannan of mycobacteria. *Immunity*, 41(3), 402–413. <https://doi.org/10.1016/j.immuni.2014.08.005>
- Yu, S., Balasubramanian, I., Laubitz, D., Tong, K., Bandyopadhyay, S., Lin, X., Flores, J., Singh, R., Liu, Y., Macazana, C., Zhao, Y., Béguet-Crespel, F., Patil, K., Midura-Kiela, M. T., Wang, D., Yap, G. S., Ferraris, R. P., Wei, Z., Bonder, E. M., ... Gao, N. (2020). Paneth Cell-Derived Lysozyme Defines the Composition of Mucolytic Microbiota and the Inflammatory Tone of the Intestine. *Immunity*, 53(2), 398-416.e8.  
<https://doi.org/10.1016/j.immuni.2020.07.010>
- Yu, Z. T., Chen, C., Kling, D. E., Liu, B., McCoy, J. M., Merighi, M., Heidtman, M., & Newburg, D. S. (2013). The principal fucosylated oligosaccharides of human milk exhibit prebiotic properties on cultured infant microbiota. *Glycobiology*, 23(2), 169–177.  
<https://doi.org/10.1093/glycob/cws138>
- Zelensky, A. N., & Gready, J. E. (2005). The C-type lectin-like domain superfamily. *FEBS Journal*, 272(24), 6179–6217. <https://doi.org/10.1111/j.1742-4658.2005.05031.x>
- Zerbib, D. (2016). Handbook of Electroporation. *Handbook of Electroporation*, 1–20.  
<https://doi.org/10.1007/978-3-319-26779-1>
- Zhai, L., Huang, C., Ning, Z., Zhang, Y., Zhuang, M., Yang, W., Wang, X., Wang, J., Zhang, L., Xiao, H., Zhao, L., Asthana, P., Lam, Y. Y., Chow, C. F. W., Huang, J. dong, Yuan, S., Chan, K. M., Yuan, C. S., Lau, J. Y. N., ... Bian, Z. xiang. (2023). Ruminococcus gnavus plays a pathogenic role in diarrhea-predominant irritable bowel syndrome by increasing serotonin biosynthesis. *Cell Host and Microbe*, 31(1), 33-44.e5.  
<https://doi.org/10.1016/j.chom.2022.11.006>
- Zhang, L., Mou, L., Chen, X., Yang, Y., Hu, M., Li, X., Suo, X., Zhu, X. Q., & Du, A. (2018). Identification and preliminary characterization of Hc-clec-160, a novel C-type lectin domain-containing gene of the strongylid nematode Haemonchus contortus. *Parasites and Vectors*, 11(1), 1–8. <https://doi.org/10.1186/s13071-018-3005-3>
- Zhang, Y., Zhang, S., He, Y., Sun, Z., Cai, W., Lv, Y., Jiang, L., Li, Q., Zhu, S., Li, W., Ye, C., Wu, B., Xue, Y., Chen, H., Cai, H., & Chen, T. (2020). Murine SIGNR1 (CD209b) Contributes to the Clearance of Uropathogenic Escherichia coli During Urinary Tract Infections. *Frontiers in Cellular and Infection Microbiology*, 9.  
<https://doi.org/10.3389/fcimb.2019.00457>

- Zheng, D., Liwinski, T., & Elinav, E. (2020). Interaction between microbiota and immunity in health and disease. In *Cell Research* (Vol. 30, Issue 6, pp. 492–506). Springer Nature. <https://doi.org/10.1038/s41422-020-0332-7>
- Zheng, L., Kelly, C. J., Battista, K. D., Schaefer, R., Lanis, J. M., Alexeev, E. E., Wang, R. X., Onyiah, J. C., Kominsky, D. J., & Colgan, S. P. (2017). Microbial-Derived Butyrate Promotes Epithelial Barrier Function through IL-10 Receptor–Dependent Repression of Claudin-2. *The Journal of Immunology*, *199*(8), 2976–2984. <https://doi.org/10.4049/jimmunol.1700105>
- Zimmermann, P., & Curtis, N. (2019). The effect of antibiotics on the composition of the intestinal microbiota - a systematic review. In *Journal of Infection* (Vol. 79, Issue 6, pp. 471–489). W.B. Saunders Ltd. <https://doi.org/10.1016/j.jinf.2019.10.008>
- Zuliani-Alvarez, L., Piccinini, A., & Midwood, K. (2017). Screening for Novel Endogenous Inflammatory Stimuli Using the Secreted Embryonic Alkaline Phosphatase NF-κB Reporter Assay. *BIO-PROTOCOL*, *7*(7). <https://doi.org/10.21769/bioprotoc.2220>
- Zyrek, A. A., Cichon, C., Helms, S., Enders, C., Sonnenborn, U., & Schmidt, M. A. (2007a). Molecular mechanisms underlying the probiotic effects of *Escherichia coli* Nissle 1917 involve ZO-2 and PKCζ redistribution resulting in tight junction and epithelial barrier repair. *Cellular Microbiology*, *9*(3), 804–816. <https://doi.org/10.1111/j.1462-5822.2006.00836.x>
- Zyrek, A. A., Cichon, C., Helms, S., Enders, C., Sonnenborn, U., & Schmidt, M. A. (2007b). Molecular mechanisms underlying the probiotic effects of *Escherichia coli* Nissle 1917 involve ZO-2 and PKCζ redistribution resulting in tight junction and epithelial barrier repair. *Cellular Microbiology*, *9*(3), 804–816. <https://doi.org/10.1111/j.1462-5822.2006.00836.x>

## Supplementary data

### Supplementary data 1: Composition of stock solutions used for the preparation of LAB medium

| Amino acid 10x  |      |
|-----------------|------|
| Ingredients:    | g/L  |
| I-Histidine     | 1.7  |
| I-Isoleucine    | 2.4  |
| I-Leucine       | 10   |
| I-Methionine    | 1.25 |
| I-Valine        | 7    |
| I-Arginine      | 7.2  |
| I-Cysteine      | 2    |
| I-Glutamic acid | 6    |
| I-Phenylalanine | 4    |
| I-Proline       | 7    |
| I-Asparagine    | 5    |
| I-Aspartic acid | 0.5  |
| I-Glutamine     | 6    |
| I-Serine        | 5    |
| I-Threonine     | 5    |
| I-Alanine       | 4    |
| Glycine         | 3    |
| I-Lysine        | 5    |
| I-Tryptophan    | 2    |
| I-Tyrosine      | 3    |

| Nucleotides 100x |      |
|------------------|------|
| Ingredients:     | g/L  |
| Adenine          | 1.1  |
| Guanine          | 0.56 |
| Uracil           | 2.3  |
| Xanthine         | 0.38 |

| Salt & minerals 1 1000x              |      |
|--------------------------------------|------|
| Ingredients:                         | g/L  |
| ZnSO <sub>4</sub> ·7H <sub>2</sub> O | 5    |
| CoCl <sub>2</sub> ·6H <sub>2</sub> O | 0.19 |
| CuSO <sub>4</sub> (anhydrous)        | 0.12 |
| H <sub>3</sub> BO <sub>3</sub>       | 0.75 |
| KI                                   | 0.11 |
| MnSO <sub>4</sub> ·H <sub>2</sub> O  | 0.11 |

|  |      |
|--|------|
| (NH <sub>4</sub> ) <sub>6</sub> Mo <sub>7</sub> O <sub>24</sub> ·4H <sub>2</sub> O | 0.19 |
| FeCl <sub>3</sub>  | 3    |
| FeSO <sub>4</sub> ·7H <sub>2</sub> O   | 4    |
| EDTA   | 7.34 |
| Nitrilotriacetic acid  | 7.34 |

| Salt & minerals 2 10x                                |       |
|--|-------|
| Ingredients:   | g/L   |
| KCH <sub>3</sub> CO <sub>2</sub> (Potassium acetate) | 9     |
| Ammonium citrate dibasic                             | 17    |
| MgCl <sub>2</sub>                                    | 3.86  |
| NaCl   | 30    |
| CaCl <sub>2</sub> (anhydrous)                        | 0.302 |
| K <sub>2</sub> SO <sub>4</sub>                       | 0.23  |

| Vitamins & Antioxidants 1000x |       |
|-------------------------------|-------|
| Ingredients:                  | g/L   |
| myo-Inositol                  | 2     |
| L-Glutathione reduced         | 15    |
| Biotin                        | 6     |
| Thiamine HCl                  | 0.56  |
| Riboflavin                    | 0.9   |
| Pyridoxamine . 2 HCl          | 5     |
| Niacin                        | 0.9   |
| Pyridoxine HCl                | 4.8   |
| Calcium Pantothenate          | 1.2   |
| Folic acid                    | 0.56  |
| p-Aminobenzoic acid           | 0.056 |
| Lipoic acid                   | 1     |

| Ascorbic acid 100x |     |
|--------------------|-----|
| Ingredients:       | g/L |
| Ascorbic acid      | 50  |

**Supplementary data 2: Proteins encoded by the glucorhamnan biosynthetic gene cluster in *R. gnavus* ATCC 29149, E1 and ATCC 35913 strains.**

Homologous proteins are represented on the same rows with percentage of identity and coverage (into brackets) . The proteins are colour-coded based on their predicted function: glycosyltransferase (dark blue), rhamnose biosynthesis (green), cell wall remodelling (light blue), transporter (purple), regulatory genes (magenta), glucose priming (red), 2-O-( $\alpha$ -D-glucopyranosyl)-D-glycerate synthesis (light green), rhamnose synthesis (dark green), and oligosaccharide polymerisation (yellow). Uncharacterised proteins or proteins not associated with a function are depicted in orange. The predicted function of each gene is shown next to each gene of the cluster.

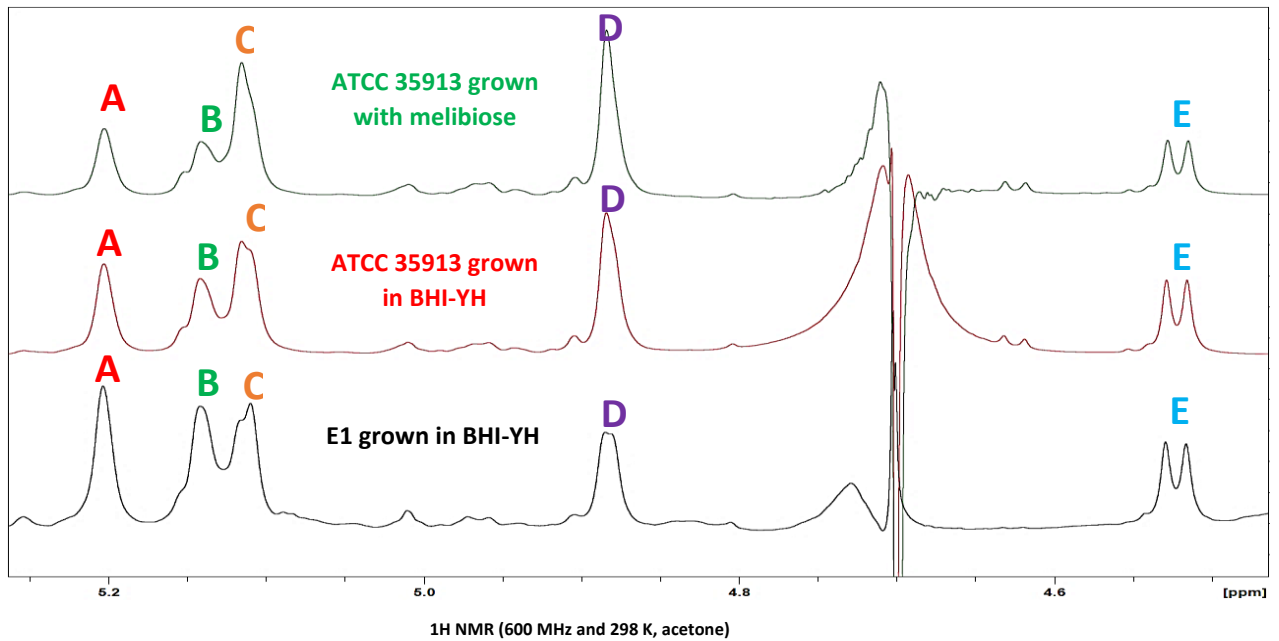
| Label | ATCC 29149    |           | E1             |           |                                    | ATCC 35913       |           |                                    |                            | Function predicted  |
|-------|---------------|-----------|----------------|-----------|------------------------------------|------------------|-----------|------------------------------------|----------------------------|---|
|       | Protein name  | Size (aa) | Protein name   | Size (aa) | % identity with ATCC 29149 protein | Protein name     | Size (aa) | % identity with ATCC 29149 protein | % identity with E1 protein |   |
| 1     | RUMGNA_03_512 | 516       | RUGNEv3_61_015 | 515       | 99,42 % (99%)                      | RGNV35913_02_504 | 514       | 100% (99%)                         | 99,42 % (99%)              | Cohesin domain  |
| 2     | RUMGNA_03_513 | 529       | RUGNEv3_61_016 | 520       | 97,69 % (98%)                      | RGNV35913_02_505 | 529       | 99,05 % (100 %)                    | 98,27 % (99%)              | polyisoprenyl-teichoic acid--peptidoglycan teichoic acid transferase TagV |
| 3     | RUMGNA_03_514 | 308       | RUGNEv3_61_017 | 309       | 98,05 % (100 %)                    | RGNV35913_02_506 | 308       | 98,38 % (100 %)                    | 99,03 % (99%)              | rhamnosyltransferase GT2  |
| 4     | RUMGNA_03_515 | 443       | RUGNEv3_61_018 | 440       | 97,72 % (99%)                      | RGNV35913_02_507 | 443       | 99,10 % (100 %)                    | 97,72 % (99%)              | oligosaccharide repeat unit polymerase                                    |
| 5     | RUMGNA_03_516 | 360       | RUGNEv3_61_019 | 334       | 99,70 % (92%)                      | RGNV35913_02_508 | 360       | 99,78 % (100 %)                    | 99,7 % (99%)               | LCP family protein  |
| 6     | RUMGNA_03_517 | 468       | RUGNEv3_61_020 | 469       | 99,57 % (100 %)                    | RGNV35913_02_509 | 468       | 100% (100 %)                       | 99,57 % (99%)              | undecaprenyl-phosphate glucose phosphotransferase                         |
| 7     |               |           | RUGNEv3_61_021 | 362       |                                    |                  |           |                                    |                            | Transposase   |
| 8     | RUMGNA_03_518 | 326       | RUGNEv3_61_022 | 327       | 99,39 % (100 %)                    | RGNV35913_02_510 | 326       | 99,39 % (100 %)                    | 99,39 % (99%)              | N-acetylglucosaminyl-diphospho-decaprenol L-rhamnosyltransferase          |
| 9     | RUMGNA_03_519 | 901       |                |           |                                    |                  |           |                                    |                            | polysaccharide pyruvyl transferase family protein                         |
| 10    | RUMGNA_03_520 | 203       | RUGNEv3_61_023 | 204       | 99,1 %                             | RGNV35913_02_511 | 203       | 100% (100 %)                       | 99,01 % (99%)              | Spore germination protein   |

|    |                                  |          |                |          |                 |                                       |              |                 |                                     |  |
|----|----------------------------------|----------|----------------|----------|-----------------|---------------------------------------|--------------|-----------------|-------------------------------------|--|
|    |                                  |          |                |          | (100 %)         |                                       |              |                 |                                     |  |
| 11 | RUMGNA_03_521                    | 282      | strL           | 283      | 99,29 % (100 %) | RGNV35913_02_512                      | 282          | 98,23 % (100 %) | 98,94 % (99%)                       | dTDP-4-dehydrorhamnose reductase   |
| 12 | RUMGNA_03_522                    | 508      |                |          |                 |                                       |              |                 |                                     | conserved hypothetical integral membrane protein                                     |
| 13 | RUMGNA_03_523                    | 484      |                |          |                 |                                       |              |                 |                                     | Uncharacterised  |
| 14 |                                  |          | RUGNEv3_61_025 | 318      |                 | RGNV35913_02_513                      | 307          |                 | 99,67 % (96%)                       | bifunctional apolipoprotein N-acyltransferase/polyprenol monophosphomannose synthase |
| 15 |                                  |          | RUGNEv3_61_026 | 707      |                 | RGNV35913_02_514;<br>RGNV35913_02_515 | 42;<br>666   |                 | 5% (100 %);<br>98,31 % (92%)        | putative membrane protein  |
| 16 | RUMGNA_03_524                    | 814      | RUGNEv3_61_027 | 834      | 48,43 % (83%)   | RGNV35913_02_516;<br>RGNV35913_02_517 | 511<br>; 322 | 56,16 % (62%)   | 99,41 % (61%)<br>;<br>97,67 % (35%) | Hyaluronan synthase  |
| 17 | RUMGNA_03_525                    | 202      | RUGNEv3_61_028 | 202      | 29,21 % (100 %) | RGNV35913_02_518                      | 201          | 29,70 % (100 %) | 99% (99%)                           | Uncharacterised  |
| 18 | RUMGNA_03_526                    | 244      | rfbB           | 247      | 67,22 % (98%)   | TagGH                                 | 246          | 67,22 % (98%)   | 99,59 % (99%)                       | teichoic acids export ATP-binding protein  |
| 19 | RUMGNA_03_527                    | 258      | RUGNEv3_61_030 | 261      | 58,46 % (100 %) | RfbD                                  | 260          | 58,85 % (100 %) | 99,62 % (99%)                       | teichoic acid translocation permease protein TagG                                    |
| 20 | RUMGNA_03_528 (also called rfbC) | 183      | rfbC           | 184      | 97,81 % (100 %) | RGNV35913_02_521                      | 183          | 97,27 % (100 %) | 99,45 % (99%)                       | dTDP-4-dehydrorhamnose 3,5-epimerase   |
| 21 | RUMGNA_03_529 (also called rfbA) | 294      | rmlA           | 295      | 97,27 % (99%)   | RGNV35913_02_522                      | 294          | 97,27 % (99%)   | 100% (99%)                          | glucose-1-phosphate thymidyltransferase  |
| 22 | RUMGNA_03_530 (also called rfbB) | 358      | rfbB           | 361      | 99,16 % (100 %) | RGNV35913_02_523                      | 360          | 99,16 % (100 %) | 100% (99%)                          | dTDP-glucose 4,6-dehydratase   |
| 23 |                                  |          | RUGNEv3_61_034 | 391      |                 | RGNV35913_02_524                      | 381          |                 | 99,21 % (97%)                       | N-acetylgalactosaminyl-diphosphoundecaprenol glucuronosyltransferase                 |
| 24 | RUMGNA_03_531                    | 131<br>2 | RUGNEv3_61_035 | 131<br>6 | 76,85 % (100 %) | RGNV35913_02_525                      | 130<br>1     | 75,36 % (100 %) | 97,57 % (99%)                       | N-acetylmuramoyl-L-alanine amidase   |
| 25 | RUMGNA_03_532                    | 311      |                |          |                 |                                       |              |                 |                                     | Bactoprenol glucosyl transferase   |

|    |                  |     |                   |     |                     |                     |     |                     |                     |   |
|----|------------------|-----|-------------------|-----|---------------------|---------------------|-----|---------------------|---------------------|---|
| 26 | RUMGNA_03<br>533 | 550 | RUGNEv3_61<br>037 | 549 | 93,61<br>%<br>(99%) | RGNV35913_02<br>526 | 548 | 93,61<br>%<br>(99%) | 98,91<br>%<br>(99%) | sulfatase-like<br>hydrolase/transferase   |
| 27 | RUMGNA_03<br>534 | 317 | RUGNEv3_61<br>038 | 304 | 98,68<br>%<br>(95%) | RGNV35913_02<br>527 | 303 | 99,34<br>%<br>(95%) | 99,34<br>%<br>(99%) | dTDP-glucose<br>pyrophosphorylase;<br>UDP- <i>N</i> -<br>acetylglucosamine<br>diphosphorylase/glucos<br>amine-1-phosphate <i>N</i> -<br>acetyltransferase |

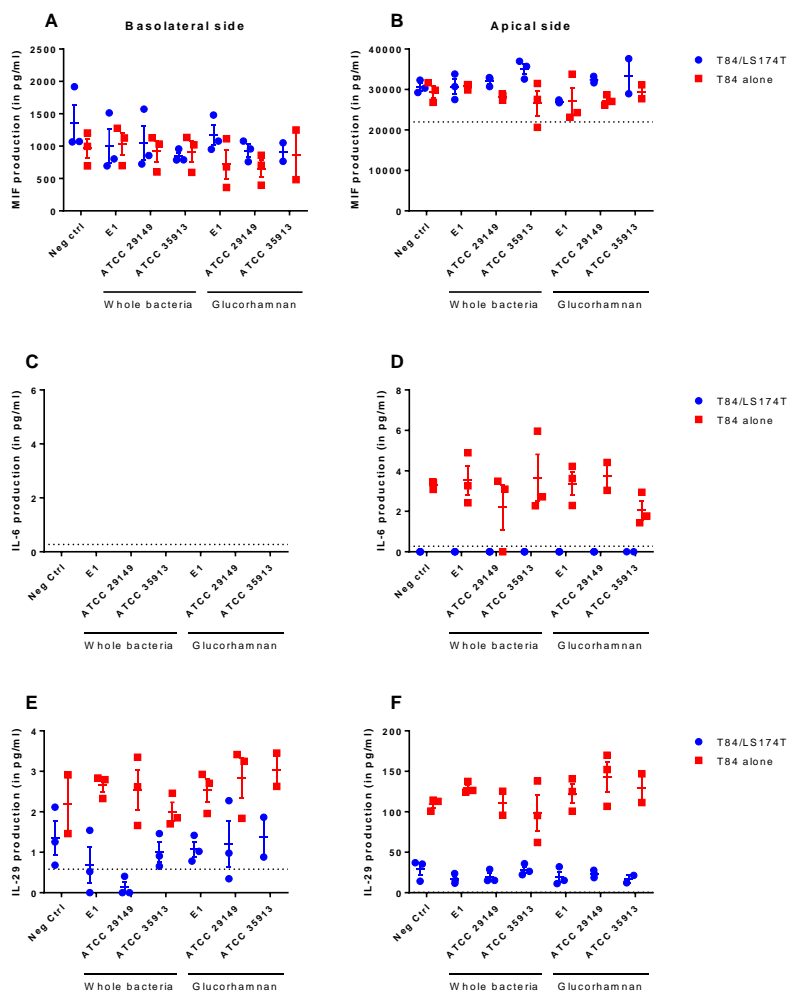
**Supplementary data 3: <sup>1</sup>H NMR spectra of glucorhamnan purified from *R. gnavus* strains.**

Glucorhamnan was extracted and purified from *R. gnavus* ATCC 35913 grown with melibiose (top), from ATCC 35913 grown in BHI-YH (middle), and from E1 grown in BHI-YH (bottom). Each letter corresponds to a monosaccharide of the glucorhamnan repeating unit (A, B C and D corresponding to rhamnose-associated peaks and E to glucose-associated peak).



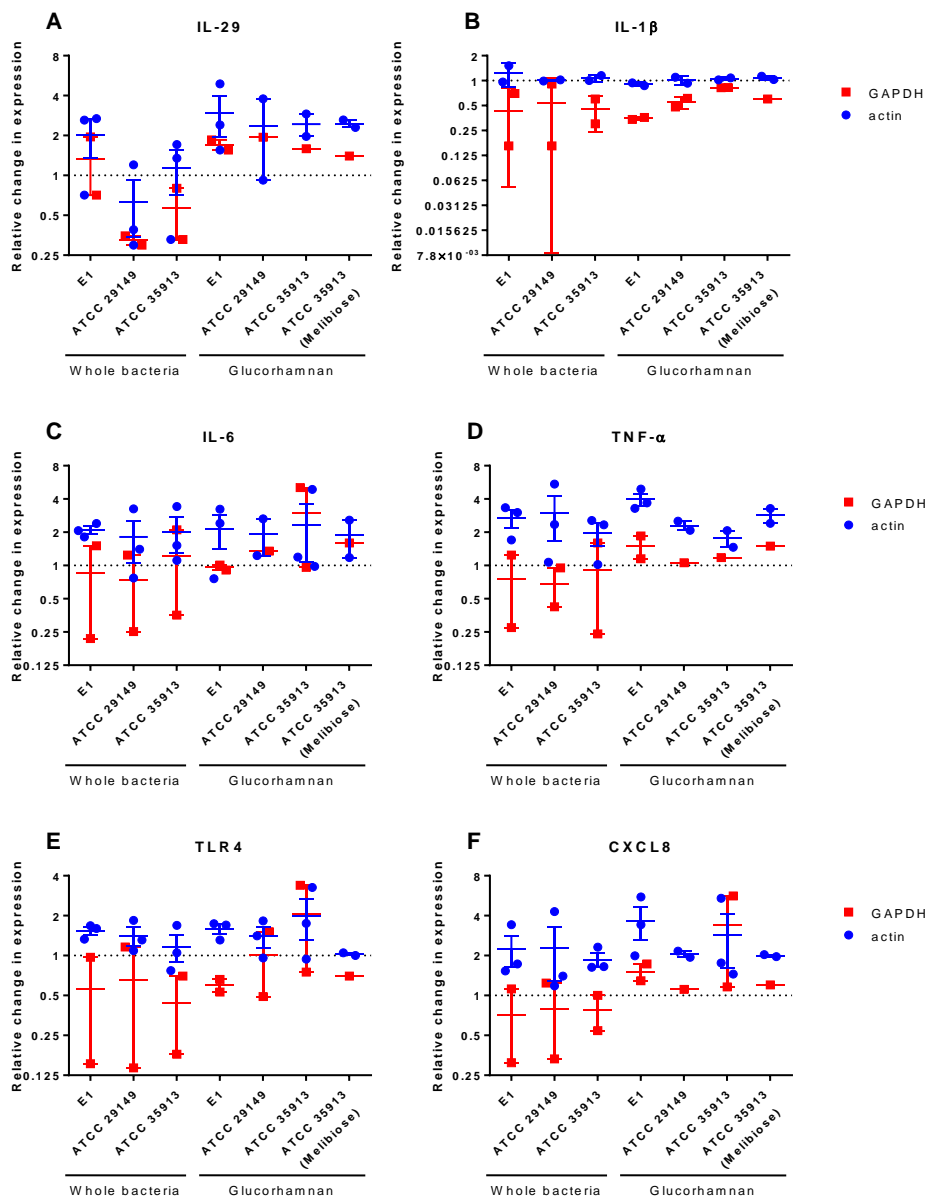
**Supplementary data 4: Effect of *R. gnavus* strains and purified glucorhamnans on cytokine production by intestinal cells in the apical side of the T84/LS174T model.**

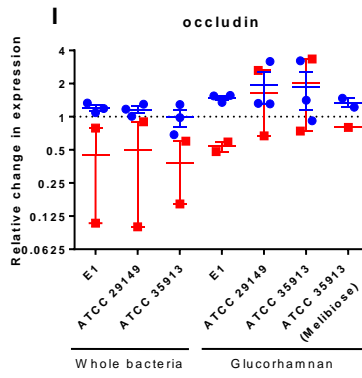
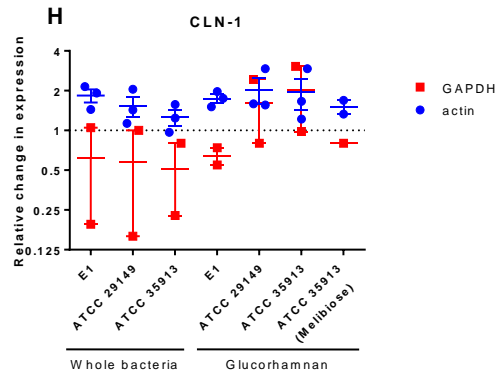
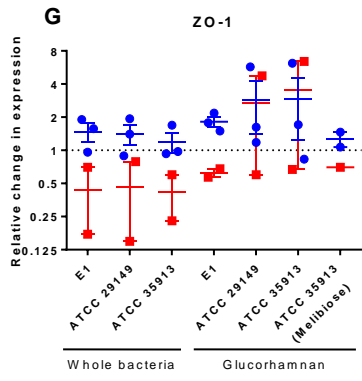
*R. gnavus* ATCC 29149, ATCC 35913 and E1 (MOI of 20:1) (A, C and E) and purified glucorhamnan (200 µg/ml) from these strains (B, D and F) were incubated with T84/LS174T cells for 18 h. Neg ctrl refers to T84/LS174T cells cultured without bacteria or glucorhamnan. The relative cytokine production of MIF (A and B), IL-6 (C and D) and IL-29 (E and F) by T84/LS174T cells was determined in the apical side of the transwells with the U-plex kit. The experiment was carried out in 3 biological replicates. Horizontal line on each graph indicates the lower limit of detection (expect for MIF, where it indicates upper limit of detection). Empty bars indicate when no cytokine was detected. One way ANOVA was used for comparison with the negative control (\* for p<0.05, \*\* for p<0.01, \*\*\* for p<0.001).



**Supplementary data 5: Effect of *R. gnavus* strains and purified glucorhamnans on tight junction gene expression in the T84 model.**

T84 cells were grown on transwells and treated with *R. gnavus* E1, ATCC 29149 or ATCC 35913 (MOI of 20:1) or with associated glucorhamnans (200 µg/ml) and incubated for 18 h. The gene expression level of IL-29 (A), IL-1β (B), IL-6 (C), TNF-α (D), TLR4 (E), CXCL8 (F), ZO-1 (G), CLN-1 (H) and occludin (I) was determined by qPCR. GAPDH and actin were used as house-keeping gene to normalise the data. The relative changes were calculated using 3 biological replicates. The dotted line indicates the level of expression in the untreated control T84 cells. Statistics were determined using the ΔCt values.





**Supplementary data 6: Set of methods used for the structural analysis of *R. gnavus* ATCC 35913 cell surface polysaccharide.**

Chemical reactions are shown framed, in blue are represented the acetylated alditols products and in red the analysis that can be done from those.

